

**JAK/STAT SIGNALLING IN THE  
INDUCTION OF THE L-ARGININE-NITRIC  
OXIDE PATHWAY IN MACROPHAGES  
AND VASCULAR SMOOTH MUSCLE  
CELLS**

**EDMUND DZIGBORDI GARR**

Submitted to the University of Hertfordshire in partial  
fulfilment of the requirements of the degree of PhD  
September 2013



# DECLARATION

I declare that:

All the work described in this report has been carried out by myself and all the results (including any survey findings, etc.) given herein were first obtained by myself - except where I may have given due acknowledgement to others.

All the prose in this report has been written by me in my own words, except where I may have given due acknowledgement to others and used quotation marks, and except also for occasional brief phrases of no special significance which may be taken from other people's work without such acknowledgement and use of quotation marks;

All the figures and diagrams in this report have been devised and produced by me, except where I may have given due acknowledgement to others.

I understand that if I have not complied with the above statements, I may be deemed to have failed this PhD, and/or I may have some other penalty imposed upon me by the Board of examiners.

Signed: *E GARR*.....

Name: Edmund Dzigbordi Garr

## ABBREVIATIONS

AG490:	Tyrphostin B42.
B2M:	Beta-2-microglobulin
BCA:	Bicinchoninic acid
BH4:	(6R)-5, 6, 7, 8-tetrahydrobiopterin.
BIM:	Bisindolylmaleimide
BSA:	Bovine Serum Albumin
CAA:	Cationic Amino Acid
CaM:	Calmodulin
CAT:	Cationic Amino Acid Transporter
CCD;	Coil-coil domain
CEBP:	CCAAT/enhancer binding protein
cGMP:	Cyclic guanosine monophosphate.
COSHH:	Control of Substance Hazardous to Health
CREB	cAMP responsive element binding protein
DAG:	Diacylglycerol
DMEM:	Dulbecco's Modified Eagle's Medium
DNA:	Deoxyribonucleic Acid
DPM:	Desintegrations per minute
ECL:	Enhanced chemiluminescence
ECM:	Extra Cellular Matrix
EDRF:	Endothelium-derived relaxing factor
eNOS:	Endothelial Nitric Oxide Synthase
ERK:	Extracellular signal regulated kinase
ERK:	Extracellular signal Regulated Kinases
ERKs:	Extracellular signal-regulated kinases
FAD:	Flavin Adenine Dinucleotide
FERM:	Four point-one ezrin, radixin, moesin
FMN:	Flavine mononucleotide
FPP:	farnesylpyrophosphates
GAPDH:	Glyceraldehyde-3-phosphate dehydrogenase
GAS:	gamma-activated site
GEF:	Guanine-nucleotide exchange factors

GFP:	Green fluorescent protein
GGPP:	Geranylgeranylpyrophosphate
GPCR:	G-protein coupled receptors
GPI:	Glucophosphatidylinositol
GTPases:	Guanosine Triphosphate enzymes
HDL:	High Density Lipoproteins
HEPES:	4-(2-hydroxyethyl)-1-piperazine ethanesulphonic acid
HMG-CoA:	3-Hydroxy-3-methylglutaryl CoA
IFN:	Interferon
IFN- $\gamma$ :	Interferon-gamma
Ig:	Immunoglobulin (an antibody isotype)
IL:	Interleukin
iNOS:	Inducible Nitric Oxide
IRF:	IFN- $\gamma$ regulatory factor
ISRE:	Interferon –alpha stimulated response element
JAK:	Janus Kinase
JH:	JAK homology
LDL:	Low density lipoproteins
LPS:	Lipopolysaccharide
MAPKs:	Mitogen activated protein kinase
mRNA:	Messenger RNA
Na <sub>3</sub> VO <sub>4</sub> :	Sodium Orthovanadate
NF <sub><math>\kappa</math></sub> B:	Nuclear Factor kappa B
nNOS:	Neuronal Nitric Oxide
NO:	Nitric oxide
NOS:	Nitric oxide synthase
O <sub>2</sub> <sup>-</sup> :	Superoxide anion
OD:	Optical Density
ONOO <sup>-</sup> :	Peroxynitrite
OS:	Oxidative stress
PAMP:	Pathogen-Associated Molecular Pattern
PBS:	Phosphate Buffered Saline
PC:	Phosphatidilcholine

PI:	Phosphatidilinositol
PI3K:	Phosphatidylinositol-3-kinase
PIP <sub>2</sub> :	Phosphatidyl Inositol Diphosphate
PKB:	Protein kinase B
PKC:	Protein kinase C
PTK:	Protein Tyrosine Kinase
PVDF:	Polyvinylidene difluoride
RASMCs:	Rat Smooth muscle cells
RNA:	Ribonucleic acid
SAPKs;	Stress-activated protein kinases
sCD14:	Soluble CD14
SDS:	Sodium dodecyl sulphate
Ser-727:	Serine-727
sGC:	Soluble Guanyl Cyclase
SMC	Smooth Muscle Cells
SH2:	Src-homology 2 domain
siRNA:	Small interference RNA (also called short or silencing RNA)
SOD:	Superoxide Dismutase
STAT:	Signal transducers and activators of transcription
TAD:	Transcription activator domain
TBS:	Tris Buffered Saline
Tris Base	Tris (Hydroxymethyl) aminoethane
TLR-4:	Toll-like Receptor-4
TNF:	Tumour necrosis factor
Tyr-701:	Tyrosine-701

## **ACKNOWLEDGEMENT**

This research thesis has been possible with the support of so many people. I take this opportunity to especially express my gratitude and indebtedness to Prof Anwar Baydoun, without who's persistent and invaluable guidance, this thesis would not have been possible. He greatly inspired me to work on this project and his willingness to motivate and assist in whichever way possible enabled me to develop an independent understanding of this thesis. His knowledge combined with enthusiasm and passion for science research contributed to the successful completion of this thesis. I also wish to express my gratitude to Dr Shori Thakur for her assistance and insightful discussions during this project until its final completion.

The success of this thesis has without doubt been the joint encouragement from so many other people. My deepest gratitude is therefore also extended to members of the supervisory committee. I will also like to acknowledge and extend my heartfelt thanks to Prof Robert Slater and members of the faculty of Life Sciences.

In addition, I also extend my special thanks to my postgraduate and graduate friends, Dr Peter Humphrey, Dr Alex Nunes, Marziah Zamani, Iffat Malik, Yogesh Kamara, Kumar, Hema, Sanil, Ashish and Nok who through their helpful suggestions and encouragements made my stay in the lab, a very pleasant, stimulating and memorable experience. Needless to say a special thanks to the technical staff, Sue, Di and respective teams for their technical assistance and advice with equipment and chemical supplies as well as support and guidance. Also my great appreciation and thanks to Claire and members of the animal house team for the supply of animal tissues and guidance towards this thesis.

Special thanks to my brothers William and Seth for their prayers and sacrifices made on my behalf. Last but not least my very special thanks to my beloved wife, Delphine and to Stephen, my son for their understanding and patience during those difficult times. Most especially, my admiration of their endless love, encouragement and steadfastness throughout the duration of my studies is most humbly acknowledged and greatly appreciated. To my departed parents I say thank you for the devotion and nurturing of a son and of the fond memories I hold dear.

Finally my praise and thanks to God for his constant companionship guidance, strength and will to achieve my heartfelt ambition and made all things possible in the end.

## 1 Table of Contents

### **JAK/STAT SIGNALLING IN THE INDUCTION OF THE L-ARGININE-NITRIC OXIDE PATHWAY IN MACROPHAGES AND VASCULAR SMOOTH MUSCLE CELLS ....1**

Chapter 1. INTRODUCTION.....	18
1.1 NITRIC OXIDE.....	19
1.1.1 Physical, chemical and biochemical properties of nitric oxide .....	19
1.1.2 Historical perspectives of mammalian NO .....	23
1.1.3 Industrial/Commercial production and uses of nitric oxide .....	23
1.1.4 Biosynthesis of Nitric Oxide .....	25
1.1.5 Nitric oxide synthase isoforms .....	27
1.1.6 Structure and molecular characteristics of Nitric Oxide Synthase .....	29
1.1.7 Physiological properties of Nitric oxide .....	32
1.1.8 Pathological properties of Nitric oxide.....	33
1.1.9 Atherosclerosis and inflammation.....	37
1.1.10 Sepsis and septic shock; an inflammatory disease .....	39
1.2 L-ARGININE.....	40
1.2.1 L-arginine: characteristics and metabolism.....	40
1.2.2 L-arginine transporter system.....	44
1.2.3 Characteristics of members of system $\gamma^+$ : CATs.....	46
1.2.4 Requirements of L-arginine transport in NO synthesis .....	49
1.2.5 Regulation of the inducible L-arginine-NO pathway .....	51
1.2.6 Regulation of CAT expression.....	56
1.2.7 The JAK/STAT pathway .....	58
1.2.8 GTPase Inhibitors as potential regulators of induced nitric oxide production.....	70
Chapter 2. MATERIALS AND METHODS.....	72
2.1 Preparation of cell culture medium .....	73
2.2 Culture of J774 macrophages .....	73
2.3 Isolation of Rat Aortic Smooth Muscle Cells (RASMCs).....	73
2.4 Sub-culturing of RASMCs .....	74
2.5 Characterisation of RASMCs.....	74
2.6 Cell counting.....	77

2.7	Plating of cells for experimentation.....	78
2.8	Treating of plated cells with inhibitors .....	78
2.9	Measurement of nitrite as an indicator of NO production .....	81
2.10	Measurement of L-[ <sup>3</sup> H] arginine transport .....	83
2.11	Measurement of total cell protein using bicinchoninic acid assay .....	84
2.12	Determination of changes in cell viability.....	87
2.13	Western Blot analysis .....	89
2.14	Gene silencing using small interference RNA (siRNA) .....	95
2.14.1	siRNA knockdown of GAPDH .....	95
2.14.2	siRNA knockdown of JAK2 .....	96
2.15	Total RNA Isolation .....	97
	Spectrophotometric quantification of isolated RNA .....	98
	Determination of RNA integrity by gel electrophoresis.....	99
2.16	PCR Primer design .....	99
2.17	Reverse Transcription.....	104
2.18	Polymerase Chain Reaction .....	105
	Quantitative PCR analysis of Cationic amino acid transporters in both RASMCs and J774 macrophages.....	106
2.19	Normalization of Housekeeping genes .....	108
2.20	STATISTICAL ANALYSIS.....	111
Chapter 3.	The effects of JAK inhibitors on the induction of nitric oxide synthesis and L-arginine transport.....	112
3.1	INTRODUCTION .....	113
3.2	METHOD .....	115
3.2.1	Experimental conditions .....	115
3.2.2	Determination of drug effects on nitrite production .....	115
3.2.3	Drug effects on L-arginine transport.....	115
3.2.4	Drug effects on iNOS expression by western blotting .....	116
3.2.5	Determination of drug cytotoxicity.....	116
3.3	STATISTICAL ANALYSIS.....	116
3.4	RESULTS .....	117
3.4.1	Morphological characterization of J774 macrophage cells.....	117

3.4.2 Morphological and biochemical characterization of rat cultured aortic smooth muscle cells (RASMCs).....	118
3.4.3 Nitrite production following activation of both J774 macrophages and RASMCs 121	
3.4.4 Inducible Nitric Oxide Synthase expression in J774 macrophages and RASMCs following activation.....	124
3.4.5 Time course induction of iNOS and NO production in activated RASMCs and J774 macrophages.....	127
3.4.6 Effects of JAK inhibitor I and AG490 on nitrite production in both RASMCs and J774 macrophages.....	130
3.4.7 Effects of JAK inhibitor I and AG490 on iNOS expression in RASMCs and J774 macrophages.....	135
3.4.8 Effects of JAK inhibitor I and AG490 on L-arginine transport in RASMCs and J774 macrophages.....	145
3.4.9 Cell viability assays on inhibitors in both RASMCs and J774 macrophages..	150
3.4.10 Expression of JAK2, Tyk-2 and their phosphorylated proteins in RASMCs and J774 macrophages.....	153
3.5 DISCUSSION.....	160
Chapter 4. Confirmation of the role of JAK2 in the induction of iNOS, NO and L-arginine transport in RASMCs using JAK2 selective siRNA .....	166
4.1 INTRODUCTION.....	167
4.2 AIM.....	168
4.3 METHOD .....	168
4.3.1 Cell culture.....	168
4.3.2 Transfection Studies; Optimization of siRNA knockdown in RASMCs .....	168
4.3.3 Effect of JAK2 siRNA on JAK2 expression in RASMCs .....	171
4.3.4 Effect of JAK2 knockdown on nitrite production in RASMCs .....	171
4.4 STATISTICAL ANALYSIS.....	171
4.5 RESULTS .....	172
4.5.1 Effect of different culture media on nitrite production in RASMCs .....	172
4.5.2 Effects of the transfection reagents on nitrite production in RASMCs.....	172
4.5.3 Optimization of siRNA delivery in RASMCs.....	176

4.5.4	Assessment of knockdown of JAK2 following JAK2 siRNA treatment .....	176
4.5.5	NO production in JAK2 knockdown RASMCs following siRNA treatment. ....	181
4.6	DISCUSSION.....	183
Chapter 5. Expression of phosphorylated STAT-1 and role of GTPases in the induction of the inducible L-arginine-NO pathway in J774 macrophages and rat cultured aortic smooth muscle cells.....		
		190
5.1	INTRODUCTION.....	191
5.2	METHODS.....	193
5.2.1	Experimental conditions .....	193
5.2.2	Treating of cells with Rho-inhibitors .....	193
5.2.3	Determination of nitric oxide production .....	194
5.2.4	Protein assay .....	194
5.2.5	Western blot analysis.....	194
5.2.6	Cell cytotoxicity assay.....	194
5.3	STATISTICAL ANALYSIS.....	195
5.4	RESULTS .....	196
5.4.1	Detection of phosphorylated STAT-1 protein in both RASMC and J774 macrophage cultures .....	196
5.4.2	Time-dependent phosphorylation of STAT-1 in RASMCs and J774 macrophages .....	199
5.4.3	Effect of AG490 and JAK inhibitor I on STAT-1 phosphorylation.....	202
5.4.4	Role of small GTPases in the induction of iNOS.....	207
5.4.5	Effect of atorvastatin on nitrite production and inducible nitric oxide expression in RASMCs and J774 macrophages .....	207
5.4.6	Effects of atorvastatin on iNOS protein expression in both RASMCs and J774 macrophages .....	211
5.4.7	Effects of atorvastatin on L-arginine transport in both RASMCs and J774 macrophages .....	214
5.4.8	Effects of atorvastatin on cell viability .....	217
5.4.9	Effects of Y-27632 on nitrite production in RASMCs and J774 macrophages	

5.4.10 Effect of Y-27632-inhibitor on L-arginine transport in both RASMCs and J774 macrophages .....	223
5.4.11 Effect of Y-27632 inhibitor on cell viability.....	226
5.5 DISCUSSION.....	229
Chapter 6. Expression profile of Transporters in RASMCs and J774 macrophages	234
6.1 INTRODUCTION.....	235
6.2 METHODS.....	237
6.2.1 cDNA synthesis from extracted RNA .....	237
6.2.2 Primer Design .....	238
6.2.3 Reference gene Normalization.....	238
6.2.4 Complementary DNA (cDNA) synthesis and real time; PCR analysis .....	242
6.3 STATISTICAL ANALYSIS.....	242
6.3.1 GeNORM Analysis .....	242
6.4 RESULTS .....	244
6.5 DISCUSSION.....	265
CONCLUSION.....	271
FUTURE WORK .....	281
REFERENCES .....	283

## **ABSTRACT**

The production of Nitric Oxide (NO) under physiological conditions has beneficial roles in acting as a key signaling component of many biological processes as well as having an anti-microbial effect. However its effects following excess production by the inducible NO pathway is potentially detrimental in the pathogenesis of chronic inflammation including sepsis and several other inflammatory diseases. Understanding the mechanisms that regulate the expression of the inducible nitric oxide synthase (iNOS) responsible for producing the excessive amounts of NO in disease states is therefore critical. In this regards, experiments were carried out to identify the signaling pathways that may mediate this process, focusing specifically on the JAK/STAT cascade. The reason for selecting the latter is because our research group, amongst others, has carried out extensive work investigating other signaling pathways, including the mitogen activated kinases (MAPK). Moreover, studies have also been carried out in an attempt to identify the critical role of JAK/STAT signaling for iNOS induction. These studies however failed to conclusively demonstrate whether, as with the MAPKs, the JAK/STATs may also play an essential role. Furthermore there is indeed controversy in the literature with researchers unable to agree whether expression of iNOS does require JAK/STAT activation. Thus, the aim of the project described in this thesis was to establish unequivocally whether activation of the JAK/STATs precedes induction of iNOS. The studies were extended to L-arginine transport as well because the latter is widely reported to be induced in parallel with iNOS and substrate supply to iNOS may be critical for sustained NO production. Changes in transporter activity as well as their expression profiles were assessed.

All experiments were carried out in either rat aortic smooth muscle cells (RASMCs) or in the J774 macrophage cell line. These cell types were selected because RASMCs are one of the prime targets for induced NO production in vascular inflammation and the macrophages are involved in host defence, acting in part through NO production. To establish the role of JAK/STATs, pharmacological and molecular approaches were used. Pharmacologically, two inhibitors were used and these were AG490 and JAK inhibitor I. The former is reported to be a selective JAK2 inhibitor and the other blocks all known JAK proteins. The potential of the GTPases to regulate the induction of iNOS was also examined using selective inhibitor known to regulate these proteins. In

addition to these drugs, siRNA targeting JAK2 was also exploited and western blotting was extensively used to detect expression of various proteins including iNOS, native and phosphorylated JAK2 and TYK2. Changes in iNOS activity was monitored by determining nitrite production using the Griess assay and L-arginine transport was monitored using tritiated arginine (L-[<sup>3</sup>H]arginine). RASMCs were treated with a combination of LPS (100 µg/ml) and IFN-γ (100 U/ml) and the macrophages with LPS (1 µg/ml) to induce iNOS and transporter activity.

Consistent with previous reports, the above treatment of both cell types resulted in the expression of iNOS, production of NO and enhanced transport of L-arginine. These effects were not affected by AG490 but blocked by JAK inhibitor I. Furthermore, although both cell types expressed the key JAKs (JAK2 and TYK2), neither of these proteins were phosphorylated under conditions of induced NO production. Moreover, siRNA experiments showed that JAK2 expression could be abolished without any significant change in NO production, confirming that at least JAK2 may not be required for this process. Whether TYK2 is involved still remains to be resolved as the phosphor-protein could not be detected. However the conclusive siRNA knockdown studies could not be carried out due to time and cost constraints. Apart from iNOS and NO production, changes in induced L-arginine transport were also not significantly affected under the experimental conditions described above suggesting that like with iNOS, induction of L-arginine transport is independent of at least JAK2. Interestingly however, STAT-1 was phosphorylated and this was blocked by JAK inhibitor I but not AG490. Thus, STAT-1 activation may be essential but its activation may be independent of the JAKs. One possible alternate upstream activator of STAT-1 may be the GTPases. Indeed these proteins have been indicated to phosphorylate STAT-1 independent of the JAKs. However, in this project, inhibition of the GTPase pathway enhanced NO production and L-arginine transport suggesting that the GTPases downregulate these processes.

In conclusion, the studies carried out in this thesis have shown that induction of iNOS, NO production and L-arginine transport in both RASMCs and J774 macrophages are independent of JAK2 but require STAT-1 activation which may be phosphorylated

independently of the JAKs. The role of other JAKs such as TYK2 although unlikely, will need to be resolved using a more specific approach such as siRNA.



## **Chapter 1. INTRODUCTION**

## 1.1 NITRIC OXIDE

### 1.1.1 Physical, chemical and biochemical properties of nitric oxide

Nitric oxide (NO) is a seamlessly simple (30 Da) diatomic, colourless but very reactive molecule implicated in a myriad of cellular and physiological processes in mammals including humans. Nitric oxide, also called nitrogen monoxide, is basically two molecules consisting of nitrogen and oxygen (see Figure 1.1) combining together to form NO. It is a gaseous and hence a diffusible substance, which is generated in biological systems by a family of enzymes collectively known as nitric oxide synthases (NOS). Under gaseous conditions NO reacts with molecular oxygen forming NO<sub>2</sub> gas. This molecule is able to spontaneously dimerize, forming N<sub>2</sub>O<sub>4</sub> which can yield equimolar quantities of both NO<sub>2</sub><sup>-</sup> and NO<sub>3</sub><sup>-</sup> by spontaneous dismutation in water. However, in pure oxygen-containing aqueous solution, NO displays a longer half-life of 500 seconds or more (Wink *et al.*, 1993) and yields significant quantities of NO<sub>2</sub><sup>-</sup> without much NO<sub>3</sub><sup>-</sup> production. These reactions are outlined in Figure 1.2 and other properties of NO are summarized in Table 1.1.

The biological actions of NO are fairly diverse and widespread while its' fate is significantly dependent on the physiological environment. The often complex nature of atherosclerosis and associated inflammation are now considered one of the prime underlying pathologies of cardiovascular disease (CVD). The structural elements of the vascular endothelium wall are the principal targets. At the center of these myriad of events are circulating components including inflammatory cells (such monocytes and macrophages) platelets and leukocytes. Evidence from experiments involving intact animals, tissues or cells suggest that the excess NO produced is the cause of the pathophysiological processes of CVD such as in atherosclerosis (Cooke *et al.*, 1997) and associated complications such as in sepsis and septic shock. (Kirkeboen *et al.*, 1999) In this thesis we shall aim to investigate the regulation of iNOS expression in both RASMCs and J774 macrophages.

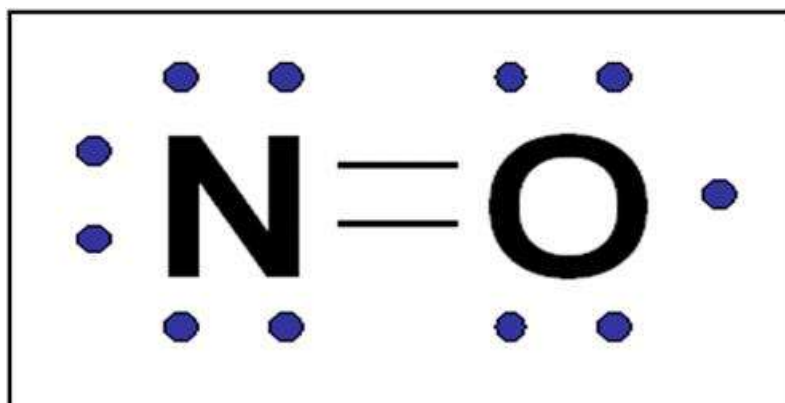
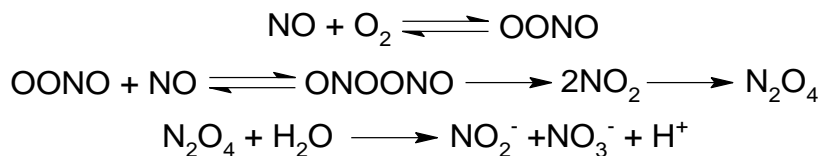


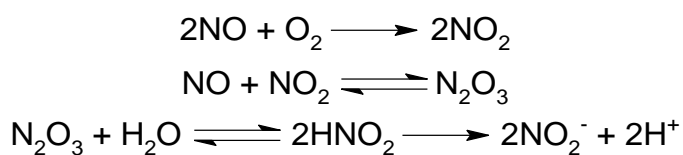
**Figure 1.1** Lewis structure of Nitric oxide.

The unpaired electron on the oxygen atom makes this molecule highly reactive.

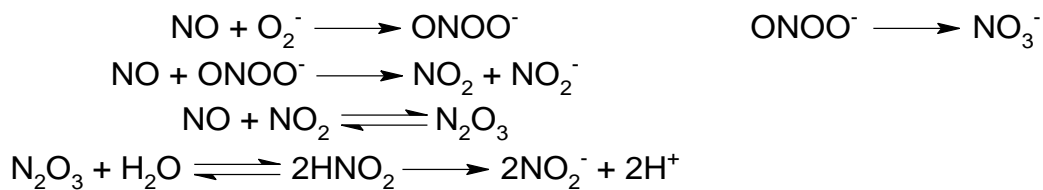
### Gaseous conditions



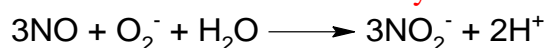
### Aqueous conditions



### Cell systems



#### Overall stoichiometry



### In the presence of oxyhemoproteins

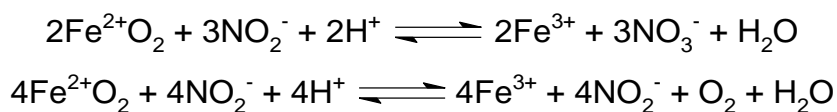


Figure 1.2 Reactivity of NO under different conditions

**Table 2.1 Summary of the physical properties of nitric oxide**

<b>PROPERTIES</b>	
<b>Molecular formula</b>	<b>NO</b>
<b>Molar Mass</b>	<b>30.0061 g/mol</b>
<b>Appearance</b>	<b>Colourless gas</b>
<b>Density</b>	<b>1.3 × 10<sup>3</sup> kg m<sup>-3</sup> (liquid)</b> <b>1.34 g dm<sup>-3</sup> (vapour)</b>
<b>Melting point</b>	<b>-163.6°C (109.6 K)</b>
<b>Boiling point</b>	<b>-151.7 °C (121.4 K)</b>
<b>EU classification</b>	<b>Toxic (T), corrosive (C)</b>
<p><b>NFPA 704</b></p>	<b>FIRE - 0</b> <b>HEALTH - 3</b> <b>REACTIVITY - 1</b>

### 1.1.2 Historical perspectives of mammalian NO

Nitric oxide was originally identified as endothelium-derived relaxing factor (EDRF) by Furchgott and Zawadzki in 1980. Later, other independent investigators identified NO as EDRF (Palmer et al. 1987), which is produced by endothelial cells and induce smooth muscle cell relaxation in response to agonists such as acetylcholine (Furchgott *et al.*, 1980). This discovery suggested for the first time a physiological role for NO, which has since been shown to be the principal target in cardiovascular and immune systems. It also has an important role in protein interactions and is a key target in normal cellular metabolism.

### 1.1.3 Industrial/Commercial production and uses of nitric oxide

The inception of NO research goes back as far as 1772 when it was first described as an air pollutant. Up until the last century, NO has been an important intermediate raw material in the chemical industry and was produced on a massive scale as an intermediate in the Ostwald process for the synthesis of nitric acid from ammonia (<http://chemed.chem.purdue.edu/genchem/topicreview/bp/ch10/group5.php>). One of the leading industrial uses during the first world war was the production of explosives in artillery shells and fairly later on, its applications in the semiconductor industry where it is used in combination with nitrous oxide to form oxynitride gates in Complementary metal–oxide–semiconductor (CMOS) devices; a major class of integrated circuits. In the electronic industry, detection of surface radicals on polymers is made possible by the use of nitric oxide and the subsequent incorporation of nitrogen. A quantitative measure is undertaken by means of X-ray photoelectron spectroscopy (Carley *et al.*, 1979)

It is estimated that about 80% of emitted NO worldwide is primarily from human activities such as in farming and its' associated practises. As an environmental pollutant, NO or nitrogen oxides is commonly found in gasoline engine emission (Brooks *et al.*, 1993; Wallace *et al.*, 1981) and in cigarette smoke where is it reported to significantly affect the expression or activity of eNOS (or type III NOS) (Nadler *et al.*, 1983; Yang *et al.*, 2007). It is also produced as a result of fossil fuel combustion and from other industrial processes (Cao *et al.*, 2008; Frey *et al.*, 2008). In addition, NO is

the active compound released under acidic conditions from many meat preservation techniques using nitrites and nitrates (Benjamin *et al.*, 1994; Reddy *et al.*, 1983).

In agriculture, the production of nitric acid is closely linked to the manufacture and demand for nitrogenous fertilizers. At present fertilizers are sourced as solid urea rather than as ammonium nitrate. The influence on plant growth and activities of soil microbes maintains a fine balance between microbial mineralization, nitrification, nitrogen fixation, and denitrification processes. This consequently is a major factor in determining soil nitrogen availability in the natural ecosystem. In plants, NO is released into the soil by denitrifying bacteria as a free intermediate between nitrite and N<sub>2</sub>O (Carr *et al.*, 1990; Heiss *et al.*, 1989; Zafiriou *et al.*, 1989) in the roots of leguminous plants whose main role is providing plants and the surrounding soil ecosystem with a rich and available source of nitrates and nitrites. In addition NO is obtained from dietary intake of fresh foods such as lettuce, spinach and beetroot which has a natural abundance of nitrates.

In mammals, NO is produced by the NOS enzymes which are described in more detail below (Section 1.1.4 and 1.1.5). In addition, NO is also obtained either from dietary intake when accumulated salivary nitrites are acidified in the stomach (Benjamin *et al.*, 1994; Dykhuizen *et al.*, 1996) or from biosynthesis by the NOS enzymes using the amino acid L-arginine as a substrate (see below).

#### 1.1.4 Biosynthesis of Nitric Oxide

All NOS enzymes catalyse a multi-electron oxidation of the terminal guanidine-nitrogen of the cationic amino acid L-arginine by performing two separate oxidation cycles (Marletta *et al.*, 1988; Palmer *et al.*, 1988b) as illustrated in Figure 1.3. The first of these reaction steps (Monooxygenase I) catalyses the oxidation of L-arginine to N<sup>ω</sup>-hydroxy-L-arginine (NHA), whereas the second step (monooxygenase II) catalyses the oxidation of NHA to citrulline and NO (as shown in Figure 1.4) (Marletta *et al.*, 1988; Pufahl *et al.*, 1992; Zembowicz *et al.*, 1991).

During the first monooxygenation, binding of BH<sub>4</sub> and L-arginine to the oxygenase domain increases haem redox potential forming a ferric haem. On the reductase domain, electrons are donated from NADPH and flow via FAD and FMN to the oxygenase domain, where they reduce the ferric haem to ferrous haem. Binding of an oxygen molecule forms a ferrous-oxy complex which equilibrates with a ferric-superoxide complex. Simultaneous addition of an electron and a proton from BH<sub>4</sub> reduces the superoxide bound to hydroperoxide. Further protonation induces the irreversible breaking of the oxygen-oxygen bond, resulting in a ferryl iron with a protein-bound cation radical and H<sub>2</sub>O. This highly oxidizing species rapidly oxygenates L-arginine to NHA, and the enzyme resting state is regenerated.

Throughout the second monooxygenation reaction, a single electron from the reductase domain reduces the ferric haem iron to ferrous-oxy complex allowing binding of molecular oxygen and thus generating the ferrous-oxy complex. Finally, this ferrous-oxy complex catalyses the NHA oxidation to NO, citrulline and water, and regenerates the ferric haem protein again (Andrew *et al.*, 1999).

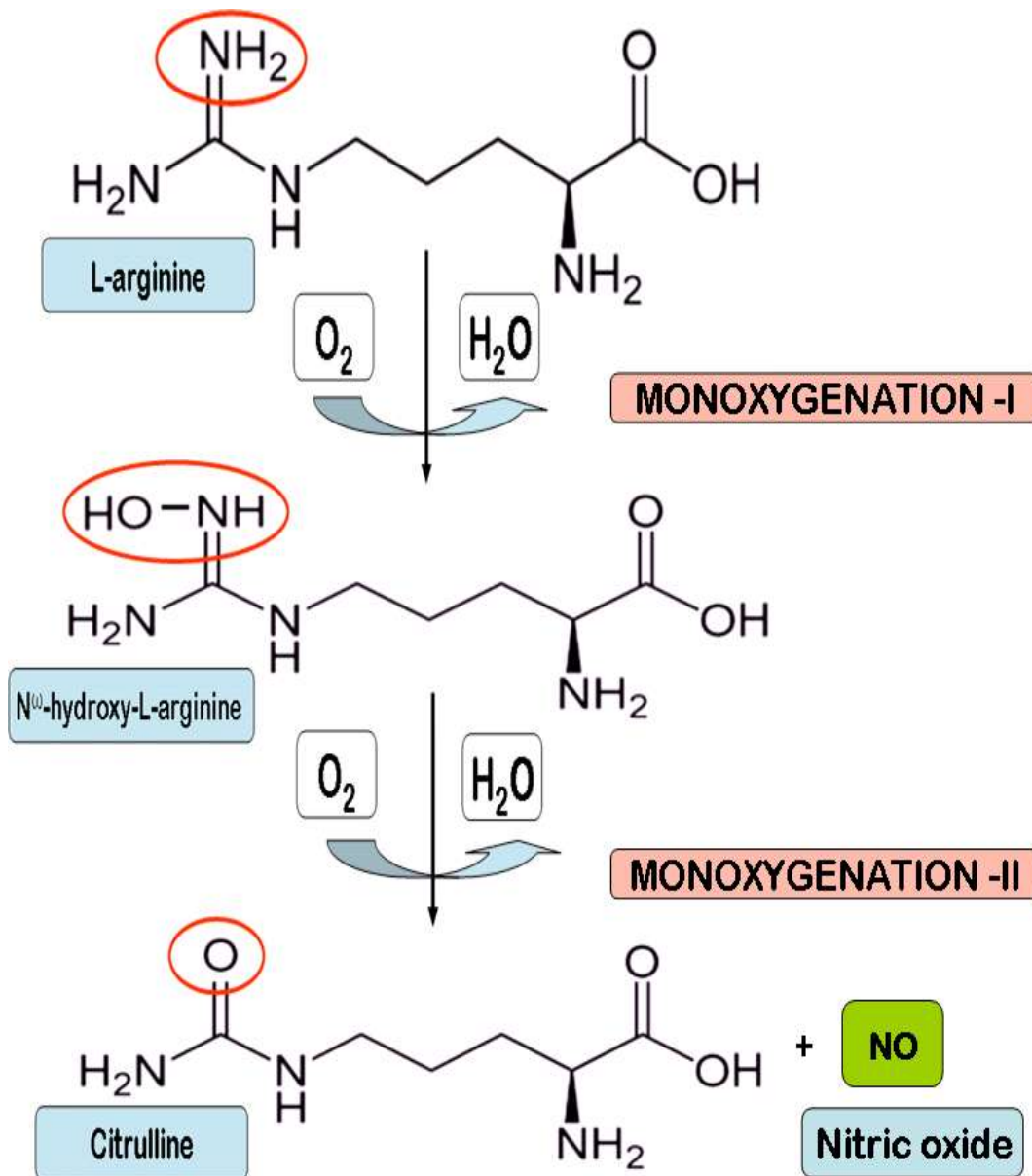


**Figure 1.3** The two step consecutive hydroxylation reactions of NOS enzyme on L-arginine with N<sup>ω</sup>-hydroxy-L-arginine (NHA) as the intermediate and NO and L-citrulline as the products. Adapted from (Abramson *et al.*, 2001)

### 1.1.5 Nitric oxide synthase isoforms

As already highlighted, NO is synthesized by the NOS family of enzymes (NOSs, EC 1.14.13.39) of which there are three different isoforms; endothelial NOS (eNOS, NOS1 or NOSI), neuronal NOS (nNOS or NOS3 or NOSIII) and inducible NOS (iNOS or NOS2 or NOSII). These are products of three different genes with a homology between isoforms of 50-58% (Janssens *et al.*, 1992; Lamas *et al.*, 1992; Nishida *et al.*, 1992; Sessa *et al.*, 1992). The enzymes also show differences in localization, regulation, catalytic properties and inhibitor sensitivity (Bredt *et al.*, 1991; Geller *et al.*, 1998; Janssens *et al.*, 1992; Lamas *et al.*, 1992; Lowenstein *et al.*, 1992; Lyons *et al.*, 1992; Nishida *et al.*, 1992; Sessa *et al.*, 1992; Yui *et al.*, 1991). They were firstly classified by their expression pattern as constitutive and inducible isoforms, but are now classified according to their expression profile in neuronal, endothelial and inducible tissues (Alderton *et al.*, 2001; Andrew *et al.*, 1999; Forstermann *et al.*, 1994; Forstermann *et al.*, 1995a; Forstermann *et al.*, 1995b; Papapetropoulos *et al.*, 1999). All three isoforms, though structurally related, differ in their dependence on Ca<sup>+</sup> for activity, genetic origin, anatomic distribution and physiological role in disease (Wu *et al.*, 2002).

Neuronal NOS (nNOS or NOS1) (Bredt *et al.*, 1991) and endothelial NOS (eNOS or NOS3) (Janssens *et al.*, 1992; Lamas *et al.*, 1992) are constitutively expressed, and thus known as constitutive NOS (cNOS). While nNOS was first identified in neuronal cells from the central and peripheral nervous systems, eNOS was initially discovered in endothelial cells. Nonetheless, they are both known to be expressed in various other tissues and cell types (Alderton *et al.*, 2001; Anderson, 2003; Forstermann *et al.*, 1995a; Forstermann *et al.*, 1995b; Papapetropoulos *et al.*, 1999). Both isoforms have expression patterns that are quite complex (Boissel *et al.*, 1998). In nNOS, however regulation of expression in specific physiological conditions are under promoter control. This is reported to involve different transcriptional units containing alternative promoters. Both isoforms constitutively produce NO within the low picomolar range and participate in the regulation of physiological processes in the neuronal and cardiovascular system respectively. Production of NO by these isoforms is regulated mainly at the enzymatic level, where changes in the concentration of intracellular calcium (Ca<sup>2+</sup>) play a central role in their regulation by stabilizing calmoduline (CaM) binding to its binding site and thereby inducing NO synthesis (Busse *et al.*, 1990).

Inducible NOS, in contrast to its constitutive isoforms, is mainly regulated at the expressional level and is entirely  $\text{Ca}^{2+}$  insensitive probably due to its peculiar non-covalent association with calmodulin. In particular, expression of iNOS in resting cells is usually very low or absent, although it can be induced by hypoxia (Iadecola *et al.*, 1996; Nagafuji *et al.*, 1992). Additionally it can be induced by LPS and/or proinflammatory cytokines (IL-1, IL-2, IL-6, and TNF- $\alpha$  and IFN- $\gamma$ ) in almost every cell type including macrophages, lymphocytes (Kirk *et al.*, 1990), neutrophils (Rimele *et al.*, 1988; Schmidt *et al.*, 1989), smooth muscle cells (Beasley *et al.*, 1991) hepatocytes (Mellouk *et al.*, 1994) and cardiac myocytes (Szabo *et al.*, 1993). Once induced, iNOS expression requires a delay of several hours for de novo protein synthesis before the onset of NO production. Moreover, once expressed, iNOS produces NO in the high nanomolar range (1000-fold larger quantities than the constitutive isoforms) over several hours or even days. In addition, iNOS activity is not changed by modulation of calcium [ $\text{Ca}^{2+}$ ] probably due to the tight binding of CaM to the enzyme (Cho *et al.*, 1992), thus suggesting that iNOS regulation occurs at the transcriptional level (see figure 1.3). Nonetheless, limited evidence suggest that regulation of iNOS may also occur at the functional level by post-translational modification through phosphorylation (Panaro *et al.*, 1999; Salh *et al.*, 1998).

Evidence has been put forward for a fourth NOS isoform, distinct from those described above which appears to be of relevance in mitochondrial bioenergetics. This novel isoform is referred to as mitochondrial NOS (mtNOS) (Elfering *et al.*, 2002; Ghafourifar *et al.*, 1997; Ghafourifar *et al.*, 1999; Giulivi *et al.*, 1998). However, its relationship with other isoforms and its regulation is not clearly understood as yet (Adcock *et al.*, 1994; Kanai *et al.*, 2004).

### 1.1.6 Structure and molecular characteristics of Nitric Oxide Synthase

The active NOS enzyme is dimeric and presumed to function as a homodimer during activation. It is made up a calmodulin-dependent hemoprotein (homologous to cytochrome P450) with both a reductase and oxygenase domains. The presence of flavin adenine dinucleotide (FAD) and flavin mononucleotide aids in its ability to carry out a 5-electron oxidation of non-aromatic amino acid arginine with the aid of tetrahydrobiopterin (BH<sub>4</sub>). Calmodulin acts as a molecular switch to enable electron flow from FAD to heme thereby facilitating the conversion of oxygen and L-arginine to NO and citrulline.

The NOS enzymes consists of two domains: an oxygenase and a reductase domain (Chen *et al.*, 1996; Ghosh *et al.*, 1995; Sheta *et al.*, 1994) with a CaM binding domain in between (Figure 1.4) (Ghosh *et al.*, 1995; Klatt *et al.*, 1995; Maciejewski *et al.*, 1995; Marrero *et al.*, 1998) (see Figure 1.4) in one dimer. The reductase or C-terminal domain contains binding sites for one molecule of nicotinamide adenine dinucleotide phosphate (NADPH), flavin adenine dinucleotide (FAD), and flavin mononucleotide (FMN) (Bredt *et al.*, 1992; Cho *et al.*, 1992; Geller *et al.*, 1998; Lowenstein *et al.*, 1992; Nishida *et al.*, 1992; Sessa *et al.*, 1992). The oxygenase or N-terminal domain binds iron protoporphyrin IX (haem, Fe), and (6R)-5, 6, 7, 8-tetrahydrobiopterin (BH<sub>4</sub>) together with the substrate L-Arginine (Bredt *et al.*, 1992; Cho *et al.*, 1992; Geller *et al.*, 1998; Lowenstein *et al.*, 1992; McMillan *et al.*, 1992; Nishida *et al.*, 1992; Sessa *et al.*, 1992). Both NOS monomers interact by their oxygenase domains leaving the reductase domains still attached as independent extensions in a head-to-head manner (Figure 1.4) (Ghosh *et al.*, 1995; Klatt *et al.*, 1995; Maciejewski *et al.*, 1995; Marrero *et al.*, 1998). This association requires a large interface, which includes the binding site for BH<sub>4</sub> and helps to structure the active-site pocket containing the haem and the L-Arginine binding site (Crane *et al.*, 1998; Fischmann *et al.*, 1999; Ghosh *et al.*, 1995; Klatt *et al.*, 1995; Maciejewski *et al.*, 1995; Sahin-Toth *et al.*, 1997). In addition, this dimer is further stabilised by two cysteine residues forming either disulphide bridges or ligating a zinc ion between monomers (Hemmens *et al.*, 2000; Li *et al.*, 1999), and an N-terminal hook swapping between the two monomers (Alderton *et al.*, 2001; Andrew *et al.*, 1999; Crane *et al.*, 1999). However, binding of BH<sub>4</sub> (Reif *et al.*, 1999; Sahin-Toth *et al.*, 1997; Saura *et al.*, 1996), haem and L-Arginine have also been suggested to

promote and/or stabilize the active dimeric form, although the different NOS isoforms present distinct dimer interaction (Panda *et al.*, 2002).

Nitric oxide could through a negative feedback mechanism involving s-nitrosation (or s-nitrosylation), regulate NOS expression. There is however substantial evidence implicating the rate limiting steps in NO production in some cell to the availability of extracellular L-arginine. Both NOS1 and NOS2 can be inactivated by forming ferrous-nitrosyl complexes in their heme prosthetic groups (Abu-Soud *et al.*, 1995; Buga *et al.*, 1993).

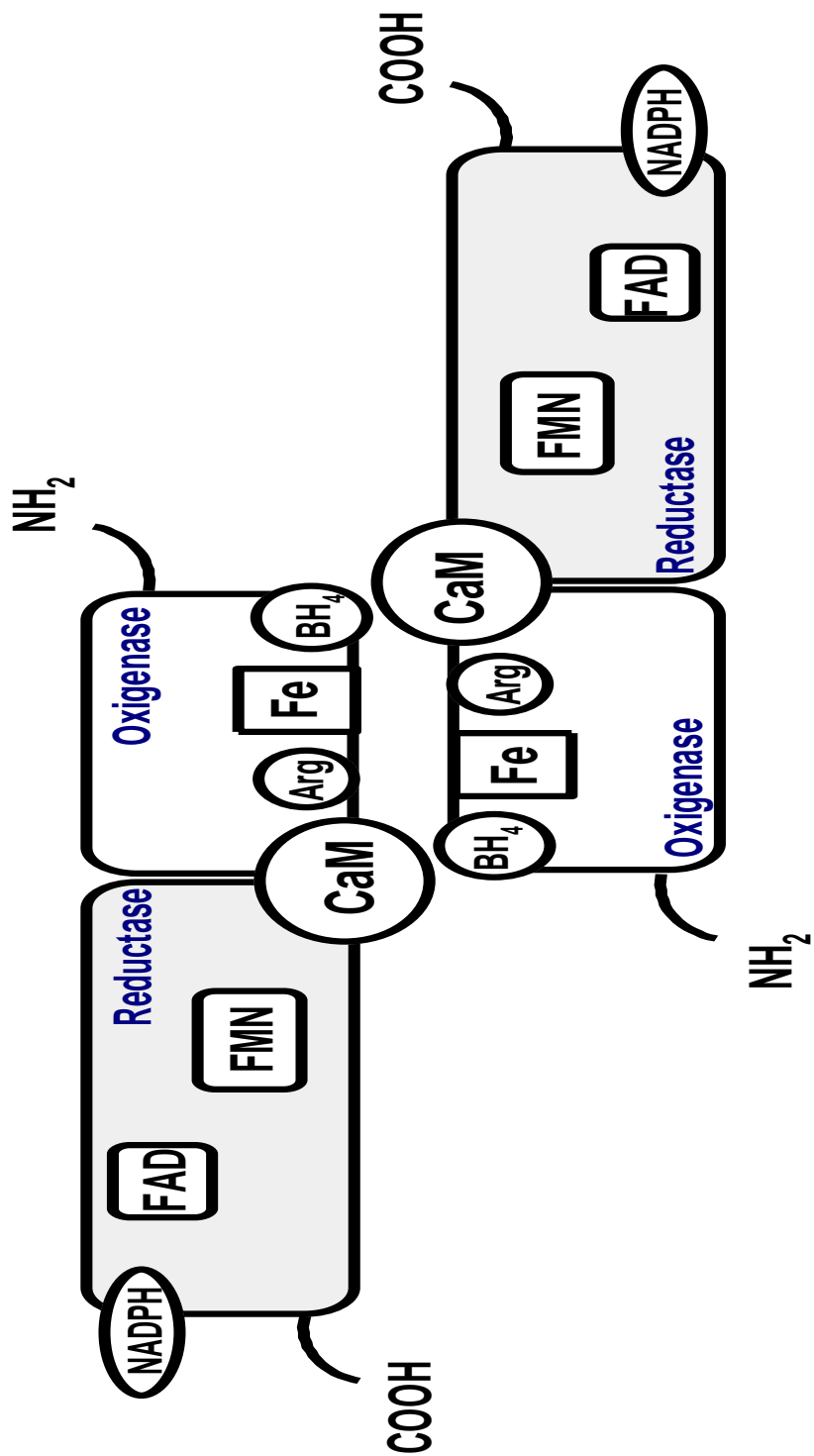


Figure 1.4 Schematic domain structure of the NOS dimer.

An illustration showing the main cofactors and substrate binding sites of the NOS dimer

### 1.1.7 Physiological properties of Nitric oxide

The endogenous production of NO as well as its effects on the surrounding tissues have led some investigators to hypothesize its role as a secondary mediator. One of the principal actions of NO is its role as a biological messenger, targeting soluble guanylyl cyclase (sGC) which catalyses the conversion of guanosine triphosphate (GTP) to cyclic 3', 5' guanosine monophosphate (cGMP) (Ignarro *et al.*, 1982). Once produced, cGMP is able to cause vascular smooth muscle relaxation thus mediating NO-induced vascular relaxation (Furchgott *et al.*, 1980; Moncada *et al.*, 1993; Palmer *et al.*, 1988a; Radomski *et al.*, 1987). This stems from the slightly faster diffusion coefficient of NO [approx. 3800  $\mu\text{m}^2/\text{s}$ ] (Vanderkooi *et al.*, 1994) compared to that of oxygen [2000  $\mu\text{m}^2/\text{s}$  at 25 °C or 3240  $\mu\text{m}^2/\text{s}$  at 40 °C] or carbon dioxide [1600  $\mu\text{m}^2/\text{s}$  at 25 °C], and its hydrophobicity thus allowing it an accelerated diffusion through cells relatively quickly (Lancaster, 1994).

Physiological concentrations of NO has also been shown to have anti-platelet actions, inhibiting platelet aggregation (Alheid *et al.*, 1987; Furlong *et al.*, 1987; Glusa *et al.*, 1974; Mellion *et al.*, 1981) and adhesion to vascular endothelium (Benjamin *et al.*, 1991; Kubes *et al.*, 1991; Radomski *et al.*, 1987; Sneddon *et al.*, 1988), thus avoiding blockage of the vasculature through a similar action on sGC (Radomski *et al.*, 1987; Yamakado *et al.*, 1982).

Nitric oxide has also been implicated in neuronal signalling, mediating the ability of the excitatory neurotransmitter glutamate to stimulate cGMP levels via N-methyl-D-aspartate (NMDA) receptors in the brain (Bredt *et al.*, 1989; Garthwaite *et al.*, 1989). This has led to the implication of NO in long term potentiation (a model of memory and learning), where NMDA induces changes in synaptic transmission (Bohme *et al.*, 1991; O'Dell *et al.*, 1991; Schumann *et al.*, 1996). Similarly, in the cerebellum, NO may act as a messenger in long term depression (a model of motor learning) (Shibuki *et al.*, 1991). Furthermore, NO in the peripheral nervous system regulates relaxation of the gastrointestinal tract (Bult *et al.*, 1990; Gibson *et al.*, 1990; Gillespie *et al.*, 1989; Ramagopal *et al.*, 1989), penile erection (Bowman *et al.*, 1986; Ignarro *et al.*, 1990), and blood flow to the adrenal medulla (Breslow *et al.*, 1992) by acting as a non-adrenergic non-cholinergic (NANC) neurotransmitter. Within the immune system, NO

produced by macrophages may mediate host response immunity to invading organisms (Hibbs *et al.*, 1988).

### **1.1.8 Pathological properties of Nitric oxide**

The characteristically high NO output from iNOS following induction means that the associated unshared electron(s), mediating cell-to-cell communication, signaling and a growing list of biological processes, can often result into pathological events inspite of fulfilling some physiological objectives. In some studies however low NO may stimulate cell growth and be protective of cells from apoptosis (Kim *et al.*, 2001). To date, evidence suggest that the effects of NO overproduction is dependent on concentration ( $\mu\text{M}$ ), tissue type and duration of exposure (overs days to weeks) (Abramson *et al.*, 2001). These parameters have all been implicated in the pathogenesis of various diseases including cancer (Hibbs *et al.*, 1992; Xu *et al.*, 2002), atherosclerosis (Chin *et al.*, 1992; Napoli *et al.*, 2006) and in endotoxin (Andoh *et al.*, 2013; Westenberger *et al.*, 1990), hemorrhagic (Andoh *et al.*, 2013; Thiemermann *et al.*, 1993) and anaphylactic shocks (Amir *et al.*, 1991; Evora *et al.*, 2007) or even in the hyperdynamic state such as cirrhosis (Benjamin *et al.*, 1994). Similarly, several other immune-associated pathologies such as acute (Ialenti *et al.*, 1992) and chronic inflammation (Laroux *et al.*, 2001), rheumatoid arthritis (Farrell *et al.*, 1992; McCartney-Francis *et al.*, 1993), ulcerative colitis (Middleton *et al.*, 1993), inflammatory bowel disease (Singer *et al.*, 1996), asthma (Kharitonov *et al.*, 1994; Zhou *et al.*, 2006) and diabetes (Kleemann *et al.*, 1993; Kroncke *et al.*, 1993) have also been linked to abnormal overproduction of NO. These deleterious actions of NO have also been implicated in pathologies within the CNS such as cerebral ischemia (Beckman, 1991; Nowicki *et al.*, 1991), epilepsy (Beckman, 1991), Huntington's disease (Dawson *et al.*, 1991; Norris *et al.*, 1996), multiple sclerosis (Sherman *et al.*, 1992), and the dementia found in acquired immunodeficiency syndrome patients.

With iNOS, for instance, its expression in various tissues is associated with pathological conditions where overproduction of NO is believed to contribute to the initiation and/or progression of the disease. This is particularly true for septic shock which is an

inflammatory condition within the vasculature that is mediated, potentially, by excessive iNOS-derived NO (Enkhbaatar *et al.*, 2006; Thiernemann *et al.*, 1993; Vallance *et al.*, 1993) as one of its principal causes. Indeed, studies in animal models have shown that the induction of iNOS within the blood vessel wall (especially the smooth muscle layer) contributes to vascular collapse caused by NO-induced vasodilatation resulting in severe hypotension, poor perfusion of tissues and thus multi organ failure and subsequent death (Enkhbaatar *et al.*, 2006; Thiernemann *et al.*, 1993). In addition, some patients in intensive care with severe sepsis do suffer from severe hypotension with associated cardiovascular collapse and multiple organ dysfunction syndrome (MODS) (Vallance *et al.*, 1993).

The expression of iNOS is also only restricted to some tissues where expression remains low under normal physiological conditions and only expressed when induced by certain factors. Evidence suggests that transcription of iNOS gene is often up-regulated by pro-inflammatory stimuli including cytokines (TNF- $\alpha$ , IL-1, IFN- $\gamma$ ), growth factors and endotoxin (LPS) (Moncada *et al.*, 1991; Nathan *et al.*, 1994). This is evident from the variety of inflammatory diseases mentioned previously. Expression is also upregulated in certain stressful conditions (Fang, 2004) or even, following an infection by microbial products such as LPS. Irrespective of the source of trigger, the very high levels of NO generated has often been associated with an uncontrolled tissue injury. At other times, the high NO output could prove too cytotoxic to the bacteria and thereby either contribute to abrogation of the bacteria itself or restriction in its rate of growth. In summary, there is overwhelming evidence to suggest that inflammation within the vasculature together with high NO production are major contributory factors in the pathogenesis of diseases such as atherosclerosis (Ross, 1999).

A major factor that mediates these unwanted effects of NO has been the result of its free diffusible and highly reactive nature. In addition, the principle determinant of the wellbeing of the vasculature is its redox state and NO is a key mediator of endothelial function. Both L-arginine and BH4 are very important in maintaining both adequate (healthy) vascular function and an active NOS dimer in order to function at its optimum level. L-arginine is an absolute substrate for NO production whiles BH4 functions both as allosteric enzyme by improving the binding affinity to L-arginine and as redox cofactor by

providing electrons to the heme of eNOS (Gao *et al.*, 2007; Wei *et al.*, 2008). In a state of limited L-arginine and BH<sub>4</sub> supply, NOS becomes 'uncoupled' and the NADPH derived electrons instead of being channelled to L-arginine for citrulline and O<sub>2</sub> production are rather added to the latter with subsequent production of ROS. A vicious cycle results in further increases in peroxynitrite production with subsequent restrictions in NO production by oxidizing tetrahydrobiopterin (BH<sub>4</sub>) (Kohnen *et al.*, 2001) to levels below physiological levels for optimum eNOS function. Under these circumstances eNOS reverts from a NO producing enzyme to superoxide generating one (Xu *et al.*, 2006).

The high level of NO (at micromolar range) is less often associated with rapid blood delivery, glucose uptake, contractility and other exercise associated beneficial effects than to the deleterious effects of its chemical reactivity with reactive oxygen species, ROS or more specifically, superoxide anion reacts with NO to form the highly reactive peroxynitrite. The latter is reported to result in the oxidation of cellular components such as proteins (enzymes) in the cell. These effects ultimately lead to altered protein structure, especially of enzymes and therefore compromise on protein function, and/or catalytic capacity. In addition, it seriously compromises on important physiological and biochemical events in cell regulation and function. To this end, various species of ROS have been implicated. These include production of high level of NO which reacts with reactive oxygen species such as O<sub>2</sub><sup>-</sup> to generate peroxynitrites (ONOO<sup>-</sup>) anion in the presence of NADPH oxidase (Beckman *et al.*, 1990). In alkaline solutions the peroxynitrite becomes stable and rapidly decays once protonated by hydrogen anions. However in very acidic environments further reactions of peroxynitrite with ROS species and/ or hydrogen peroxides results in further cytotoxic reactions.

The highly reactive peroxynitrite has been implicated in apoptosis of cardiomyocytes (Arstall *et al.*, 1999; Dickhout *et al.*, 2005), endothelial (Dickhout *et al.*, 2005; Mihm *et al.*, 2000) and vascular smooth muscle cells (Li *et al.*, 2004; Li *et al.*, 2003). It is therefore of little surprise that NO under induced conditions is symptomatic of pathologies such as sepsis and other associated inflammatory disorders including cerebral infarction, diabetes mellitus and neurodegenerative disorders and multiple organ dysfunctions. However for the purpose of this thesis, it is the impact of NO

overproduction on inflammatory states and septic shock that will be the focus of our investigations.

### 1.1.9 Atherosclerosis and inflammation

There is at present, substantial evidence from clinical trials, laboratory studies and through pharmacological interventions to implicate inflammation in the pathophysiology of atherosclerosis. The current concept regards both inflammation and immune responses as contributory factors to atherogenesis (Lobo *et al.*, 2010). The inciting targets for such a remodeling process involve mainly the intima layer, composed mainly of SMC and tissue macrophages. Under inflammatory conditions endothelial cells undergo activation with the subsequent expression of various adhesion molecules (i.e. VCAM-1). The first observable signs leading to atherosclerotic plaque occurs when monocyte derived macrophages are recruited and in presence of oxidized lipids (oxLDL), chemokines and other inflammatory mediators including NO, ROS and peroxynitrites, arterial foam cells, the hallmarks of arterial lesion, are formed.

The clinical manifestations of a cardiovascular disease (CVD) or events are often elicited in the form of a heart attack and/ or stroke. In the early stages of disease progression, the reported appearance of a 'fatty' or yellow streak normally restricted to the inner layer of the artery with cholesterol impregnated smooth muscle cells, macrophages and lymphocytes are the typical hallmarks of CVD development. Recent findings of attenuation in lesion progression in animal models of familial hypercholesterolemia following a dietary intake of L-arginine supplements (Javanmard *et al.*, 2009; Khazaei *et al.*, 2012) does indicate a direct effect of iNOS. In addition the use of NOS inhibitors to reverse this protective effect of L-arginine (Vasdev *et al.*, 2008) further reinforces the assertion of a direct involvement of NOS. The events of plaque rupture, acute thrombosis and necrosis are also regarded as key events in the natural progression of atherosclerosis (Falk *et al.*, 1995) and substantial evidence suggests that macrophages might be directly implicated (Woolf, 1990). The high NO production following macrophage activation then acts as a source of oxygen free radicals and with the aid of powerful proteases, could trigger necrosis and rupture of the plaques (Woolf, 1990). The associated inflammation has been suggested as the key mediator that drives the formation, progression and rupture of the atherosclerotic plaque (van der Wal *et al.*, 1994).

In summary, the development of atherosclerosis requires several distinct events including enhanced cytokines production including interleukin (IL) 1 $\beta$ , tumour necrosis factor- $\alpha$  (TNF)- $\alpha$ . These cytokines in turn upregulate the induction of adhesion molecule VCAM-1, ICAM-1 and E- and P-selectin expression on endothelial cells (Harari *et al.*, 1999; McHale *et al.*, 1999). The latter, are responsible for the firm attachment of inflammatory cells to the vascular surface, particularly, at the sites of inflammation (O'Brien *et al.*, 1996). Presently, various lines of evidence suggest human atherosclerotic lesions contain these pro-inflammatory cytokines (Blake *et al.*, 2002; Libby, 2002; Ross, 1999) and these findings may well link the high LDL cholesterol levels to VCAM-1 expression.

At present, CVD contributes significantly to the proportion of morbidity and mortality in the developed world (Murray *et al.*, 1997). Apart from age and family history the causes are often associated with development of atherosclerotic lesion, smooth muscle cell proliferation and infection by microorganism. In addition, events such as vascular remodeling are often initiated by a number of clinical conditions such as excess low density lipid (LDL), cholesterol, diabetes mellitus and life style changes. In particular, the high LDL levels under the cytotoxic environment in the vasculature results in the modification of the lipoprotein and the induction of transcription of adhesion molecules.

### **1.1.10 Sepsis and septic shock; an inflammatory disease**

Despite the use of antibiotics and other associated therapies, severe infection and sepsis still remain a leading cause of death in most intensive care units worldwide. The generation of NO by iNOS has been implicated in several inflammatory disease states with detrimental consequences. Due to the very variable and non-specific nature of the signs and symptoms of the septic response following an infection, unraveling the complex chain of events associated with this abnormality remains a major goal. Currently, endotoxins, certain growth factors and a variety of cytokines, which are rapidly produced following sepsis, remain important mediators in the pathophysiology of sepsis (Akira *et al.*, 2004; Schulte *et al.*, 2013).

In addition, Toll-like receptors (TLRS) are the principal mediators of LPS mediated signaling and act through the nuclear factor kappa B (NF- $\kappa$ B) resulting in the upregulation of proinflammatory mediators such as TNF- $\alpha$ , NO and IL-1 $\beta$  (Knuefermann *et al.*, 2002; Ullrich *et al.*, 2000). Further studies have however identified that the sustained activity of the iNOS enzyme, and thus NO production, is critically dependent on the availability and supply of exogenous L-arginine into the cells (Mori, 2007; Wileman *et al.*, 2003). As a result, transport of L-arginine may be a crucial novel target for regulating NO synthesis by iNOS in disease states.

The symptoms that accompany septic shock are often high fever following an induction by endotoxin and/or cytokines. The actions of these mediators are reported to trigger production of proinflammatory mediators, including TNF and IL-1, Chemokines, prostaglandins and ROS. Consequently these compounds induce vasodilation and vascular leakage, myocardial suppression, respiratory failure and hyperdynamic shock as a result of increased cardiac output (Hirschfeld *et al.*, 1999; Karima *et al.*, 1999; Poussin *et al.*, 1998; Romero-Bermejo *et al.*, 2011). These effects result in physiological alterations within the vasculature which impacts severely on the normal functioning of the vessel.

## 1.2 L-ARGININE

### 1.2.1 L-arginine: characteristics and metabolism

L-arginine has been described as the physiological precursor for NO production by NOS (Palmer *et al.*, 1988a; Palmer *et al.*, 1988b), hence its relevance in our studies. It is an alpha-amino acid and basic with regard to its properties due to the long hydrophobic carbon chain nearest the backbone (Figure 1.4). L-arginine was first isolated from lupin seedlings in 1886 by Ernst Schulze, a Swiss chemist and later identified as a component of animal proteins by Hedin (1895). This cationic amino acid was originally classified as being dispensable (non-essential) in healthy adult humans (Rose *et al.*, 1954) but has since been shown to be essential for young, growing mammals (Ha *et al.*, 1978; Mertz *et al.*, 1952) and for carnivores (Deshmukh *et al.*, 1983; Morris *et al.*, 1978). As a result L-arginine is now considered to be a semi-essential amino acid (Barbul, 1986).

The majority of endogenous synthesis of L-arginine in adults involves an interorgan pathway (due to high restriction in the expression of some enzymes) known as the intestinal-renal axis. Endogenous L-arginine is synthesized by the sequential action of the cytosolic enzymes argininosuccinate synthetase (ASS) and argininosuccinate lyase (ASL) from citrulline primarily (a coproduct of the NOS-catalyzed reaction) within the epithelial cells of the small intestine. Biosynthesis of citrulline on the other hand is derived from multiple sources; from arginine via NOS; ornithine via catabolism of proline or glutamine/glutamate; or from asymmetric dimethylarginine (ADMA) via dimethylarginine dimethylaminohydrolase (DDAH) into the blood circulation which is then primarily extracted by the kidney for conversion into arginine (Dhanakoti *et al.*, 1990; Featherston *et al.*, 1973). Pathways linking all three sources are bidirectional.

Interestingly, de novo L-arginine synthesis only accounts for 5-15% of endogenous arginine flux in adults, and the major contributor to endogenous arginine flux is whole-body protein turnover (Chu *et al.*, 1998a). The highest rates of L-arginine synthesis occurs within the hepatic urea cycle, although the high levels of arginase expressed in hepatocytes results in little or no net production of arginine by the liver (Chu *et al.*, 1998a; Rabier *et al.*, 1991). The complete urea cycle is only expressed in hepatic

tissue, although other tissues present a truncated urea cycle known as the arginine-citrulline cycle (Figure 1.5). This cycle allows recycling of citrulline to arginine by the combined action of argininosuccinate synthase (ASS; EC6.3.4.5) and argininosuccinate lyase (ASL; EC 4.3.2.1) (MacMicking *et al.*, 1997).

Both ASS and ASL are expressed to some degree in nearly all cell types and seem to be co-induced with iNOS (Chu *et al.*, 1998a; Flodstrom *et al.*, 1995; Hattori *et al.*, 1994; Mellouk *et al.*, 1994). This co-induction led to the proposition of a citrulline-NO cycle in which citrulline is generated as a co-product with NO and in turn converted to L-arginine for further NO synthesis (McDonald *et al.*, 1997). Citrulline can therefore at least in part, replace arginine in supporting NO synthesis (Flodstrom *et al.*, 1996; Norris *et al.*, 1995; Raghavan *et al.*, 2001; Wu *et al.*, 1992). This proposal is however refuted by key publications from our group (Baydoun *et al.*, 1994a; Wileman *et al.*, 2003). The findings from both showed that citrulline could not sustain maximal production of NO when compared to L-arginine. Moreover, other studies have suggested that L-arginine recycled from L-citrulline represent half of that used by eNOS and is much less than that required by iNOS (Hrabak *et al.*, 1994). In addition, sustained NO production by iNOS has been shown to require extracellular L-arginine (Beasley *et al.*, 1991; Granger *et al.*, 1990; Granger *et al.*, 1988; Hibbs *et al.*, 1987; Jorens *et al.*, 1991; Schott *et al.*, 1993b) which appears to be supplied by L-arginine transport since it is co-induced by pro-inflammatory mediators (Bogle *et al.*, 1992a; Closs *et al.*, 2000; Sato *et al.*, 1992; Schmidlin *et al.*, 1995; Simmons *et al.*, 1996; Wileman *et al.*, 1995). Also, inhibition of L-arginine entry into cells by blocking transport inhibits NO synthesis (Beasley *et al.*, 1991; Granger *et al.*, 1990; Granger *et al.*, 1988; Hibbs *et al.*, 1987; Jorens *et al.*, 1991; Schott *et al.*, 1993b). This apparent lack of NO and associated endothelial dysfunction in some diseases despite the significantly higher (25 to 30 fold) saturating intracellular L-arginine within the cells has thus been reported as the L-arginine paradox. Despite these, further support has documented substantial improvement in endothelium-dependent vasomotor response following the administration of L-arginine supplements (Tentolouris *et al.*, 2004). Possible mechanism to explain this impasse has been the reported likely antagonism between L-arginine and the endogenously produced NOS inhibitor, ADMA (Bode-Boger *et al.*, 2007). In addition, inactivation of NO in certain disease states with associated high ROS production have been reported as likely causes.

The recycling of L-arginine in the cytosol is coupled to the mitochondrial citric acid cycle. Fumarate, which is produced in the cytosol, (Figure 1.5) enters the citric acid cycle in the mitochondria, where it is converted into L-malate by the enzyme, fumarase. L-malate is then metabolised to oxaloacetate by the enzyme malate dehydrogenase enzyme. Transamination of oxaloacetate by the enzyme aspartate aminotransferase forms aspartate, which is transported back to the cytosol. Once in the cytosol, aspartate is implicated in the conversion of L-citrulline to L-argininosuccinate, a reaction catalyzed by argininosuccinate synthase. Argininosuccinate is then metabolized by argininosuccinate ligase to give L-arginine (Chu *et al.*, 1998a).

In summary, L-arginine has a number of physiological roles in addition to NO production as illustrated in Figure 1.5. Significant metabolites produced in this cycle include citrulline, urea, creatine, ornithine and methylarginine derivatives. Regulation of L-arginine availability may be controlled by the degree of uptake of the latter by transporters into the various cells (McDonald *et al.*, 1997).

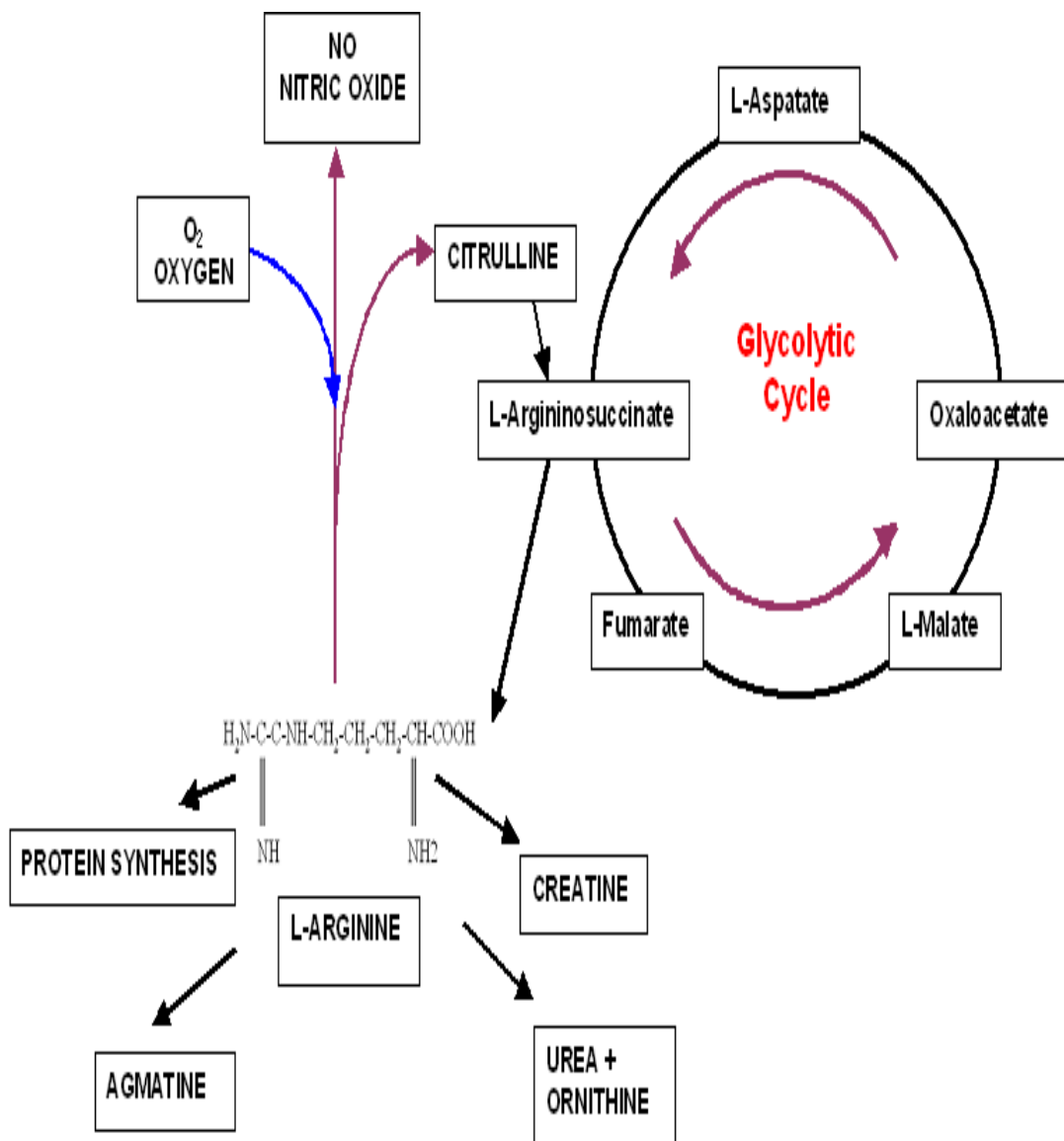


**Figure 1.5** The metabolic fate of L-arginine.

Arginine also serves as a metabolic precursor for several metabolites.

### 1.2.2 L-arginine transporter system

Our current understanding of the pivotal role of substrate availability in controlling NO production does provide opportunities in NO modulation and therapy from the effects of excessive NO production. Evidence of a substantial increase in iNOS-derived NO and elevated nitrates in plasma of patients with chronic heart failure (Habib *et al.*, 1994; Toda *et al.*, 2011; Winlaw *et al.*, 1994) or renal failure (Noris *et al.*, 1993; Qian *et al.*, 2013) together with elevated L-arginine in red blood cells (Mendes Ribeiro *et al.*, 1997; Schuster *et al.*, 2012) suggest the involvement of a transport system mediating these adaptive changes.

In most mammalian cells, arginine requirements are primarily met by uptake of extracellular arginine via specific transporters. These transporter families include the widely expressed system  $y^+$  and the tissue specific systems  $b^{0+}$ ,  $B^{0+}$ ,  $y^+L$  and  $b^+$  (Deves *et al.*, 1998c; Kilberg *et al.*, 1993; Palacin *et al.*, 1998). These transporters are a member of the solute carrier family 7 (SLC7) which consist of two subfamilies, the SLC7A1-4 which is made up of the cationic amino acid transporters (CAT-1, CAT-2A, CAT-2B, CAT-3, and CAT-4) family and the SLC7A5-11 ( $y^+LAT1$ ,  $y^+LAT2$ ,  $b^{0,+}$ ) transporter family. The latter are glycoprotein associated amino acid transporters comprising of seven proteins (the gpaAT family; also called L (light) chains amino acid transporters (LATs). They are characterized as high affinity, broad scope amino acid transporters of specifically two homologous proteins, rBAT (Bertran *et al.*, 1992b; Tate *et al.*, 1992) and 4F2hc (Bertran *et al.*, 1992a; Wells *et al.*, 1992). On the available evidence to date, the gpaAT family which is made up  $y^+LAT1$  (SLC7A7),  $y^+LAT2$  (SLC7A6),  $b^{0,+}$  (SLC7A9) and  $B^{0,+}$  (SLC7A11) genes are implicated in the transport of cationic amino acids (Verrey *et al.*, 2004).

Apart from the SLC7A family of transporters the SLC6A14 transporter ( $B^{0+}AT$ ) is also known to mediate in L-arginine transport via a sodium and chloride dependent mechanism (Sloan *et al.*, 1999). Interestingly, of all these transporters, only system  $y^+$  has been shown to be co-induced with iNOS by proinflammatory mediators in macrophages (Bogle *et al.*, 1992b), smooth muscle cells (Durante *et al.*, 1995; Wileman *et al.*, 1995), astrocytes (Heid *et al.*, 1996) and cardiac myocytes (Simmons *et al.*, 1996) amongst others. It has therefore been suggested that enhanced transporter

activity may provide a mechanism for increasing substrate supply during sustained synthesis of NO by iNOS. Thus, transport of L-arginine through system  $y^+$  may play a crucial and relevant role in regulating NO synthesis. In support of this hypothesis is the evidence already stated above that inhibition of L-arginine transport by other cationic amino acids inhibits NO synthesis in cells expressing iNOS (Bogle *et al.*, 1992a; Marletta *et al.*, 1988; Wileman *et al.*, 1995). Furthermore, NO synthesis is dramatically impaired in mice deficient in system  $y^+$  transporters (Nicholson *et al.*, 2001a). Nonetheless, new evidence suggests that the broad scope system  $y^+L$  can also be induced by IFN- $\gamma$  in human monocytes (Rotoli *et al.*, 2004), although synthesis of NO in these cells appear to be independent of L-arginine transport (Rotoli B.M., unpublished data). Since evidence from other studies show that other L-arginine transport systems may be implicated in NO production particularly via systems  $y^+$ ,  $y^+L$  and  $b^{0+}$  this study did not exclude their possible involvement in L-arginine-transport systems. Nonetheless, the discussion below will focus on system  $y^+$  as this appears to be the predominant carrier system for cationic amino acids in smooth muscle cells, the cells of choice for this thesis.

### 1.2.3 Characteristics of members of system $y^+$ : CATs

System  $y^+$  catalyses the high affinity  $\text{Na}^+$ -independent transport of cationic amino acids, in addition to its reaction involving neutral amino acids in the presence of  $\text{Na}^+$  (Christensen *et al.*, 1969; Christensen *et al.*, 1968; White *et al.*, 1982). Members of this system share a common but unique mode of transport by acquiring substrates through coupling their transport mechanism with the with the plasma membrane potential (Deves *et al.*, 1998c; Palacin *et al.*, 1998). System  $y^+$  is made up of a family of five different Cationic Amino acid Transporters (CATs) referred to as CAT-1 (Kim *et al.*, 1991), CAT2A (Closs *et al.*, 1993a), CAT2B (MacLeod *et al.*, 1990), CAT-3 (Hosokawa *et al.*, 1997; Nishiya *et al.*, 1997) and CAT-4. The latter however lacks cationic amino acid transport activity (Hammermann *et al.*, 2001; Verrey *et al.*, 2004; Wolf *et al.*, 2002).

The CATs are classified as a glycosylated solute carrier family 7 (SLC7 member) and displays the characteristic 14 putative transmembrane segments for surface expression. Their proteins essentially mediate  $\text{Na}^+$ -independent transport of cationic L-amino acids such as L-arginine, L-lysine and L-ornithine. In addition, all CATs exhibit the characteristic  $y^+$  system of trans-stimulation, i.e. concentration dependent stimulation of transport by substrate at the opposite site of the membrane. Amongst the CATs, CAT-1 has the most pronounced trans-stimulation in contrast to CAT2A, which is the least stimulated or is relatively insensitive to trans-stimulation (Closs *et al.*, 1993c).

CAT-1 was first identified (Albritton *et al.*, 1989) as the ecotropic murine leukaemia virus receptor (ecoR) (Kim *et al.*, 1991; Wang *et al.*, 1991) and was later renamed as CAT-1 (Closs *et al.*, 1993a). The rat member exhibits 95% homology with the murine (Aulak *et al.*, 1996; Wu *et al.*, 1994) and over 85 % with the human homologue. Described as a constitutive and widely distributed cationic amino acid transporter, it is formed by a 622 amino acids (aa) single polypeptide with 12 (Kavanaugh *et al.*, 1994a) to 14 transmembrane spanning domains (Albritton *et al.*, 1989; Woodard *et al.*, 1994). Transport of L-arginine, L-ornithine, and L-lysine by CAT-1 is  $\text{Na}^+$ -independent and saturable ( $K_m$  values 70–100 mM) (Kim *et al.*, 1991; Wang *et al.*, 1991). Neutral amino acids (such as glutamine, serine, homoserine, and 2-methylaminoisobutyric acid) can only induce currents at very high concentrations and only in the presence of  $\text{Na}^+$  (Wang *et al.*, 1991). Its expression has been shown in all tissues investigated except normal

liver, although it is expressed during liver regeneration (Deves *et al.*, 1998c; Kim *et al.*, 1991; Palacin *et al.*, 1998). Evidence to date suggest that in different cell types depletion of their substrate availability results in a coordinated increase in CAT-1 mRNA level and  $\gamma^+$  mediated transport (Fernandez *et al.*, 2001). In other words there is synergistic adaptive regulation of cationic amino acid transport and protein synthesis to changes in their substrate availability.

Studies on transcriptional control by amino acid availability depend on the modulation in both transcription and mRNA stability. The transcription of two key genes, present on the first exon in CAT-1 gene; an amino acid response element (AARE) and CCAAT/enhancer binding protein (CEBP) homologous gene (GTGATGCAAT) are prime targets. These two genes are induced by amino acid depletion, potential transcription factors and their target cis-DNA elements.

A second member of the CAT family, CAT2, has been identified in different mammalian species for which two main splice variants have been characterized in the  $\gamma^+$  transport system. The two variants, referred to as CAT2A and CAT2B have been described to be structurally homologous to CAT-1 but different in kinetic properties, tissue distribution and expression patterns in the body. Both transporters are products of the same gene generated by alternative splicing (Finley *et al.*, 1995) although they produce two distinct proteins. These proteins have a 97% homology, only differing in 20 amino acids within a stretch of 41 base pairs (Closs *et al.*, 1997). This difference in their sequences may account for the differences in affinity and kinetic properties of these two proteins.

CAT2B, described as an inducible carrier, is usually co-expressed with CAT-1, and its expression has been documented in lung, brain (Deves *et al.*, 1998b; Palacin *et al.*, 1998), activated cells such as macrophages (Closs *et al.*, 2000), astrocytes (Heid *et al.*, 1996) and aortic vascular smooth muscle cells (Baydoun *et al.*, 1999). It is also normally induced together with iNOS (Hattori *et al.*, 1999; Heid *et al.*, 1996; Schwartz *et al.*, 2002; Simmons *et al.*, 1996), and it has been suggested that it may have a specific role in delivering substrate to iNOS (Closs *et al.*, 2000; Hammermann *et al.*, 2001; Manner *et al.*, 2003; Nicholson *et al.*, 2001a; Schwartz *et al.*, 2002). However, other studies suggests that CAT2B is not essential for NO production by iNOS (Cui *et al.*, 2005). In contrast to CAT2B, CAT2A is a low affinity carrier of cationic substrates ( $K_m =$

2-5 mM) and appear to be less sensitive to trans-stimulation (Closs *et al.*, 1993a). The tissue distribution pattern of this carrier is also different from CAT2B, being found mainly in liver, skeletal muscle, skin, ovary, stomach (Deves *et al.*, 1998c; Palacin *et al.*, 1998) and smooth muscle cells (Baydoun *et al.*, 1999).

CAT-3 is another sodium-independent carrier for L-arginine that has been described to be expressed exclusively in the brain (Hosokawa *et al.*, 1997; Nishiya *et al.*, 1997). The 619 aa peptide CAT-3 is a Na<sup>+</sup>-independent L-arginine transporter ( $K_m = 103 \mu\text{M}$ ), which is not affected by neutral amino acids and can be inhibited by K<sup>+</sup>-induced depolarization (Hosokawa *et al.*, 1997; Nishiya *et al.*, 1997).

Several other amino acid transport systems with differing amino acid specificity, cell type and sodium ion-dependence have been characterised so far (Christensen, 1990; Collarini *et al.*, 1987). There is substantial evidence to implicate CAT transporters in the transport of L-arginine following NO synthesis which will partly form our focus on this thesis.

#### 1.2.4 Requirements of L-arginine transport in NO synthesis

To understand the close association between L-arginine and NO, one needs to recall the requirements for NO production. As previously stated (in section 1.1.2) NO is formed from the N-guanido terminal of L-arginine and oxygen by NOS enzymes of which various isoforms exist. Various lines of evidence to date have pointed to the requirement of an external L-arginine (the precursor of nitric oxide) for nitric oxide production. In particular, evidence from clinical studies does suggest that intravenous administration of L-arginine can improve endothelium-dependent vasodilatation in coronary artery disease (Dubois-Randé *et al.*, 1992) and in patients with septic shock (Reade *et al.*, 2002). Also in a double-blind randomized crossover trial of ten men (41 +/- 2 years), oral administration of L-arginine has been found to improve endothelium-dependent dilatation and a reduction in monocyte/endothelial cell adhesion (Adams *et al.*, 1997). Patients with various pathologies have been observed to have a dysfunction in L-arginine transport where the entry of L-arginine into cells is impaired (Chin-Dusting *et al.*, 2007).

In animal models, similar observations show that inhibition of transport attenuates NO synthesis in blood vessels of endotoxemic rats (Schott *et al.*, 1993c) and in SMCs exposed to pro-inflammatory stimuli (Hattori *et al.*, 1999; Wileman *et al.*, 2003). Similarly, knockout studies in mice have indicated that limitation in L-arginine through blockade of CAT-2B results in a marked attenuation in NO production (Nicholson *et al.*, 2001a). These observations have also been demonstrated in *in vitro* cultured cells systems such SMCs (Durante *et al.*, 1995; Hattori *et al.*, 1999; Wileman *et al.*, 1995) and in experimental models of endotoxin-induced shock *in vivo* (Hattori *et al.*, 1999; Huang *et al.*, 2004a; Yang *et al.*, 2005).

All available evidence to date does point to an absolute stereo-specificity in the requirements of an exogenous arginine. When L- and D-arginine intracoronary infusions were administered to patients, there was significant dilatation of stenosis of the proximal segments of both normal and diseased arteries with L-arginine (Schott *et al.*, 1993a) compared to D-arginine (Tousoulis *et al.*, 1999) which remained largely unaffected. However, extracellular L-arginine had no effect on nitrite production by eNOS in the absence iNOS induction or any cardiovascular disease (Schott *et al.*, 1993a). In

diseased coronary arteries, evidence also suggests that administration of L-arginine reversed the effects of the non selective NOS inhibitor L-NG-monomethyl arginine (LNMMA) which in addition achieved a greater degree of dilatation in diseased hearts (Tousoulis *et al.*, 1999).

Taken together, these findings strongly indicate an important functional link between L-arginine transport and iNOS mediated NO synthesis. Since the supply of arginine is rate-limiting for NO production, there is substantial support for the cooperative existence of both processes during inflammatory disease states. Selectively modulating this process can therefore provide the therapeutic means of controlling the excessive NO production in the various inflammatory disease phenotypes so far mentioned.

## 1.2.5 Regulation of the inducible L-arginine-NO pathway

### 1.2.5.1 Regulation of iNOS gene expression

In view of the central role of iNOS in disease states and the close coupling between iNOS-induced NO production and L-arginine transport, several groups including ours have focused on understanding the mechanisms that mediate the induction of these processes in various cell systems. These studies should shed light on the cellular/molecular mechanisms that regulate induction of the enzyme and upregulation of L-arginine transport into cells. The findings may provide alternative mechanisms for regulating over production of NO and potentially regulating disease states associated with the latter.

There have been many challenges in designing specific iNOS inhibitors to target their active sites in order to block their function. While all three isoforms produce nitric oxide from L-arginine and possess a common modular architecture with a conserved active site, it is of particular significance that iNOS is primarily responsible for the high NO output attributed to diseases such as rheumatoid arthritis, cancer, sepsis and associated cardiovascular complications as earlier discussed. Despite their intricate regulation, attempts to limit iNOS induced nitrite production without affecting the beneficial aspects of NO from the other isoforms have been a major challenge for years. Previous attempts on the use of amino acid precursor to nitric oxide, arginine or nitric oxide pro-drug, nitroglycerin have resulted in associated peroxynitrites (Axelsen *et al.*, 2011; Smith *et al.*, 1997) and its accompanying byproduct with long term harmful effects.

One alternative approach that has been intensely investigated was in the use of pharmacological inhibitors of the enzyme to achieve therapeutic outcomes. Several small molecule inhibitors have been identified including L-arginine analogues such as the endogenous (N (G)-monomethyl-L-arginine (L-NMMA)) (de Meirelles *et al.*, 2007) and the highly selective N-iminoethyl-L-ornithine and L-N (6)-(1-iminoethyl)-lysine (L-NIL) (Budzinski *et al.*, 2000; Ulhaq *et al.*, 1999). Another highly selective inhibitor with added attributes of time, concentration and NADP-dependent irreversible inactivator of

iNOS is N-(3-(Aminomethyl) benzyl) acetamidine (1400W) has been reported (Zhu *et al.*, 2005).

Other non-amino acid-based inhibitors include the guanidines, benzoxazolones, 2-amino-pyridines and isothioureas of which various levels of selectivity and potency have also been developed (Cochran *et al.*, 1996; Nakane *et al.*, 1995). The uses of some of these molecules in various animal studies have indicated some benefit. For instance, aminoguanidine provides beneficial effects in a rodent model of endotoxic shock (Pedoto *et al.*, 1998) and protects against brain injury after cerebral ischemia (Iadecola *et al.*, 1997; Zhang *et al.*, 1998a). Similarly, selective inhibition of iNOS using L-NIL improved survival in sepsis-induced renal dysfunction in rats (Asakura *et al.*, 2005). There is however concern over the specificity of these inhibitors for other NOS isoforms, their potential cytotoxic effects and also about the high concentrations required for these drugs to be effective *in vivo*. Additionally, effective therapies in man targeting iNOS overproduction with pharmacological interventions are yet to be developed. Thus, looking at alternative targets such as the cellular/molecular pathways that regulate the expression of iNOS and the accompanying increase in L-arginine transport are required.

Regulation of iNOS is mainly achieved at the expressional level. Studies on the 5'-upstream sequence of iNOS (considered as the promoter region) have shown that this region contains a number of transcription factor binding sites including copies for IFN- $\gamma$  regulatory factor (IRF), gamma-activated site (GAS), nuclear factor- $\kappa$ B (NF- $\kappa$ B), IFN-stimulated response element (ISRE), activating protein-1 (AP-1), tumor necrosis factor (TNF) response element and CAAT box element (Beck *et al.*, 1998; Chu *et al.*, 1998b; Lowenstein *et al.*, 1993; Niwa *et al.*, 1997; Xie *et al.*, 1993; Yang *et al.*, 1998; Zhang *et al.*, 1996). Studies investigating the role of these nuclear factors have revealed that binding of STAT-1 $\alpha$  and IRF-1 to GAS and ISRE binding sites, respectively, was required for optimal induction of the iNOS gene (Kamijo *et al.*, 1994; Kleinert *et al.*, 1998; Martin *et al.*, 1994). Additional studies reported NF- $\kappa$ B as an essential element for iNOS expression (Forstermann *et al.*, 1995a; Martin *et al.*, 1994; Xie *et al.*, 1994; Xie *et al.*, 1993; Yang *et al.*, 1998), although it has been suggested that NF- $\kappa$ B and AP-1 are not sufficient for iNOS expression (Adcock *et al.*, 1994; Beck *et al.*, 1998; Chu *et al.*,

1998a; Nathan *et al.*, 2005; Taylor *et al.*, 1998; Xie *et al.*, 1994; Yang *et al.*, 1998). In addition, other studies have suggested that AP-1 could act as an inhibitory regulator of iNOS expression (Kleinert *et al.*, 1998). Other alternative studies have suggested that CAAT box/enhancer binding protein (C/EBP) and cAMP responsive element binding protein (CREB) may have synergistic effects on iNOS induction via the CAAT box (Kinugawa *et al.*, 1997).

Activation of these nuclear factors are frequently associated with exposure of tissues or cells to proinflammatory mediators including LPS and/or cytokines (Beasley *et al.*, 1991; Kirk *et al.*, 1990; Mellouk *et al.*, 1994; Rimele *et al.*, 1988; Schmidt *et al.*, 1989; Szabo *et al.*, 1993). These proinflammatory mediators often act synergistically, by activating a substantial array of signalling pathways that feed into the activation of nuclear factors essential for iNOS gene transcription. In addition, several protein kinases have also been identified as being critical for activation of iNOS gene transcription. Amongst these proteins, tyrosine kinase (PTK) inhibition with pharmacological inhibitors has been consistently shown to inhibit LPS and/or cytokine induced iNOS expression (Baydoun *et al.*, 1999; Hellendall *et al.*, 1997; Kong *et al.*, 1996; Lee *et al.*, 1997; Marczin *et al.*, 1993; Paul *et al.*, 1995). Thus, indicating that activation of these proteins may be essential. In contrast, the specific role of protein kinase C (PKC) is less convincing with some reports suggesting that activation of this family of serine/threonine kinases either potentiates (Hellendall *et al.*, 1997; Hortelano *et al.*, 1993; Oda *et al.*, 2003; Paul *et al.*, 1997; Scott-Burden *et al.*, 1994), inhibits (Zhou *et al.*, 2006) or is of no consequence (Baydoun *et al.*, 1999; Lee *et al.*, 1997; Marczin *et al.*, 1993; Yoon *et al.*, 1994). Similarly, studies on phosphatidylinositol 3-kinase (PI3K) and protein kinase B (PKB or Akt) appear controversial with reports suggesting an exclusive role in iNOS post-translational modifications (Salh *et al.*, 1998) and others suggesting both a negative and positive regulation of iNOS induction (Diaz-Guerra *et al.*, 1999; Park *et al.*, 1997). Furthermore, previous studies on protein kinase A (PKA) do suggest that although it may not be involved in iNOS signalling transduction (Hellendall *et al.*, 1997; Lee *et al.*, 1997), it may have a role in iNOS mRNA stability.

Several reports (Doi *et al.*, 2000) have also implicated the mitogen activated protein kinases (MAPKs) as a critical signalling cascade activated by cytokine in inducing iNOS

expression. The MAPK family includes several members which are grouped into three subfamilies:

1. Extracellular signal-regulated kinases (ERKs): p44 MAPK (ERK1) and p42 MAPK (ERK2)
2. Stress-activated protein kinases (SAPKs), also referred to as c-Jun N-terminal kinases (JNKs), which include p54 SAPK (SAPK  $\alpha$  /  $\beta$  JNK2) and p45 SAPK (SAPK  $\gamma$ , JNK1)
3. p38 MAPKS ( $\alpha$ ,  $\beta$ ,  $\gamma$  and  $\delta$ )

In addition, reports in the literature have provided evidence implicating one or more of these pathways in the induction of iNOS but this seem to be dependent on the cell system being examined (Bellmann *et al.*, 2000; Blanchette *et al.*, 2003a; Caivano, 1998; Chan *et al.*, 1998; Chan *et al.*, 2001c; Ignarro *et al.*, 1982; Morikawa *et al.*, 2000). In smooth muscle cells, for instance, the p38 MAPKs may be more relevant as its inhibition by SB203580, a potent inhibitor of this enzyme activity, abolished iNOS production while ERK1/2 seems to have little effect (Baydoun *et al.*, 1999). On the contrary, ERK1/2 appears to play a partial role in the induction of iNOS in J774 macrophages where p38 was found not to be involved (Feng *et al.*, 1999).

Another signalling pathway that may be involved but as yet not unequivocally implicated in the induction of iNOS is that associated with JAK-STAT signalling. This is the main focus of this thesis and is discussed further in the sections below. The interest in these proteins have come from evidence suggesting that induction of iNOS and indeed CATs in vascular smooth muscle cells requires their exposure to IFN- $\gamma$ , which is a potent activator of JAK signalling.

In addition to the above events, several reports have also implicated the JAK/STATs in supporting cytokine induction of iNOS expression as summarised in Figure 1.6.

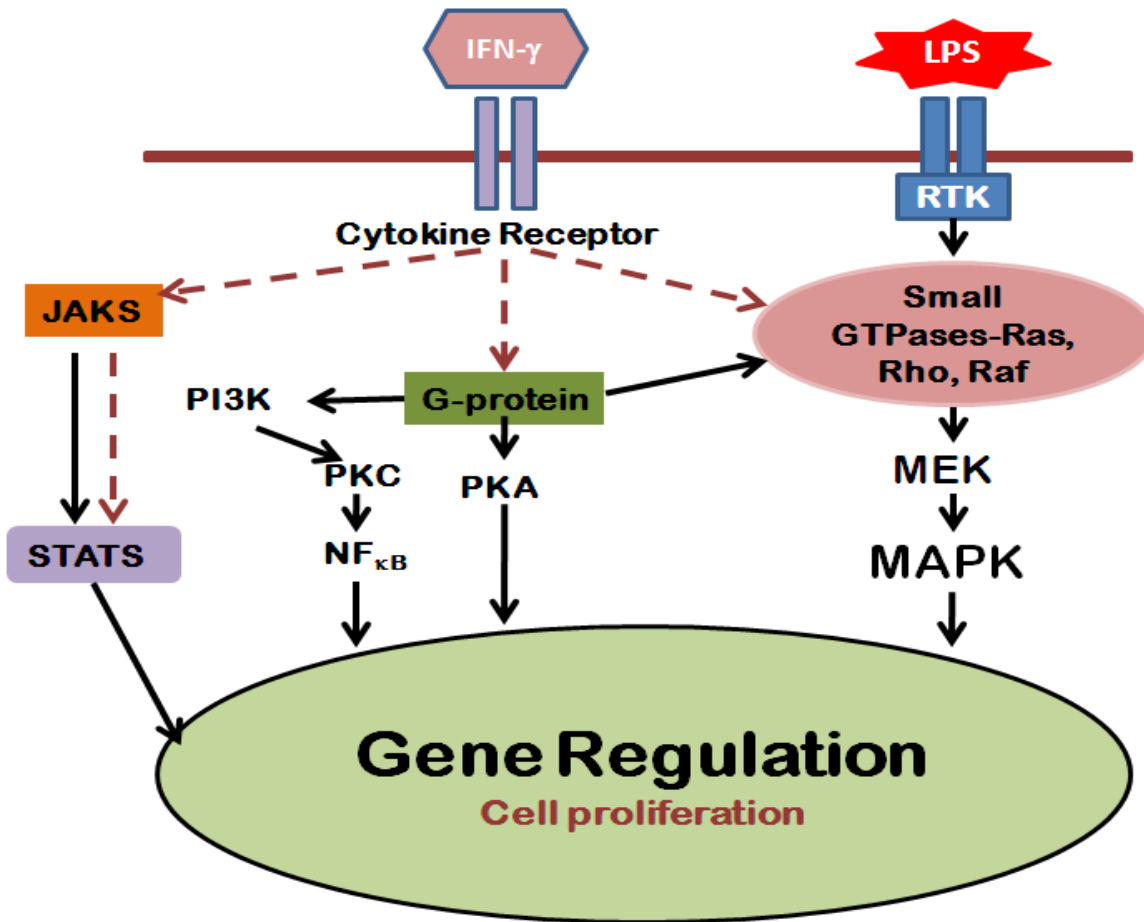


**Figure 1.6 Schematic representation of the regulation of iNOS production**

Illustration showing proposed (shown by broken lines) activation via the JAK/STAT and other pathways. Plausible cross-talk between the signaling pathways is also indicated.

### 1.2.6 Regulation of CAT expression

In contrast to iNOS, the mechanisms that regulate the induction of CATs are still poorly understood with limited data implicating the p38 MAPKs as perhaps being critical for this process (Baydoun *et al.*, 1999). Moreover, very little work has been carried out on cloning the promoter regions of CATs and as a result there is limited data available in the literature on the regulatory elements that may be present. Studies looking at the regulation of iNOS expression would clearly benefit from exploring the mechanisms that regulate the CATs in parallel and this is one of the focused areas of this thesis. There is at present a myriad of potential targets that could be investigated as potential regulators of the induction of not only iNOS but the CATs as well. Some attempts have therefore been made in this thesis to establish what role the JAK/STAT signalling plays in regulating CAT expression and function in parallel with iNOS expression.

Earlier studies have looked at the impact of proinflammatory compounds such as LPS and IFN- $\gamma$  in different cell systems on CAT2A or CAT2B transporter expressions. However such studies have not addressed the relative impact of other comparable forms of CAA transport under these same conditions or in comparison with different cell systems under the same conditions. In fact there is evidence to suggest that transport contribution from system  $y^+$  is marginal compared to  $y^+L$  under normal conditions (Reade *et al.*, 2002). In addition most studies have concentrated their investigations on murine macrophages only. However reports suggest that CAA transport is species specific as demonstrated in an earlier investigation between murine and human models (Deves *et al.*, 1998b). In this thesis, we examined the effect of such proinflammatory compounds in both RASMCs and macrophages.

We also investigated transport in relation to NO production as evidence suggest that in several cell systems so far examined that produce excess NO there was co-induction of CAA transport (Bogle *et al.*, 1992b; Closs *et al.*, 1993b; Nicholson *et al.*, 2001b; Rothenberg *et al.*, 2006). Examination of the regulation in CAT2B and iNOS induction in rat astrocytes and mouse microglia cells have demonstrated that both iNOS and CAT-2B were co-induced either with LPS in combination with IFN- $\gamma$  (Kawahara *et al.*, 2001; Stevens *et al.*, 1996) or with LPS alone (Hammermann *et al.*, 2000) respectively. However earlier investigations have shown conflicting reports on the latter assertion

demonstrating different induction patterns when both J774 macrophages and RAW264.7 murine macrophages were stimulated with LPS alone (Closs *et al.*, 2000).

Various reports have also shown that presences of certain mediators are contributory to the difference in induction patterns. In particular the plasma concentrations of TNF- $\alpha$  (Stathopoulos *et al.*, 2001), treatment with apolipoprotein E (Colton *et al.*, 2001), tetrahydrobiopterin (Schwartz *et al.*, 2001) or treatment with rapamycin, an inhibitor of mTOR kinase (Visigalli *et al.*, 2007) have all been associated with increased induction in CAT2B expression. Signaling via NF- $\kappa$ B and p38 MAPK have been reported to be essential for both CAT2B and iNOS induction (Baydoun *et al.*, 1999; Hammermann *et al.*, 2000). However, requirement for protein kinase C (PKC) mediated signaling has also been reported to be essential for iNOS induction in RASMCs (Baydoun *et al.*, 1999).

### 1.2.7 The JAK/STAT pathway

The Janus kinase (JAK)/ signal transducers and activators of transcription (STATs) pathway is a very widely used transduction pathway by vertebrates including mammals to relay responses from extracellular ligands to targets within the cells.

This pathway is expressed in a wide variety of cells and tissues specific to hematopoietic cell development such as in stem cells as well as in other cellular developmental processes undergoing cell proliferation migration and differentiation. These processes are carried out by a vast array of cells including SMCs (Madamanchi *et al.*, 2005), embryonic fibroblasts (Zheng *et al.*, 2011), bone marrow cells (Li, 2013), immune cells such as in macrophages (Hu *et al.*, 2007), in order to mediate various immunological responses. Perhaps the greatest burden on cells of hematopoietic lineage is manifested in the wide range of disorders associated with JAK/STAT dysfunction or dysregulation. These responses are important for normal cell function and physiology and in certain pathological conditions. They include response by cytokines and growth factors on apoptosis, cell growth, proliferation and differentiation.

The classical JAK/STAT pathway is activated by cytokines (IFNs), endotoxin (LPS), growth factors, hormones and other polypeptide ligands. Much characterization has been undertaken over the years with respect to cytokines (see Figure 1.7). Cytokines receptors inherently do not have any intrinsic tyrosine kinase activity but do constitutively associate with the JAKs. Evidence suggest that the resulting bond is via the presence of common receptor subunits called the src homology 2 (SH-2) domains which induces a conformational change with the subsequent activation of the JAKs. The Janus kinase (JAKs) family which include JAK1, JAK2, JAK3 and TYK2, have a molecular weight of between 120-140 kDa (Pellegrini *et al.*, 1997; Schindler, 2002). The family consists of a group of intracellular protein-tyrosine kinases (PTK) that are constitutively associated with the cytokine receptors on the membrane following cytokine stimulation.

With the exception of JAK3 which is mainly confined to hematopoietic cells, the rest of the JAKs are widely expressed in most tissues. The JAKs have also been implicated in signal transduction mechanisms involving growth hormones (Argetsinger *et al.*, 1993;

Herrington et al., 2000) and interferons (Silvennoinen *et al.*, 1993b). Consequently, they are said to form a critical component of the cytokine signaling system. The signaling cascade involves interacting with receptor components to undergo intracellular phosphorylation and enzymatic activation upon ligand binding (Darnell, 1997). However the signaling aspects of the reaction components and cascade tiers are yet to be fully understood despite the role played by a multitude of components whose nature or character have to a large extent been well defined. Evidence to date acknowledged that these reactions are principally mediated via STAT proteins which through either homo or heterodimerization generate docking sites via their respective SH2 domains.

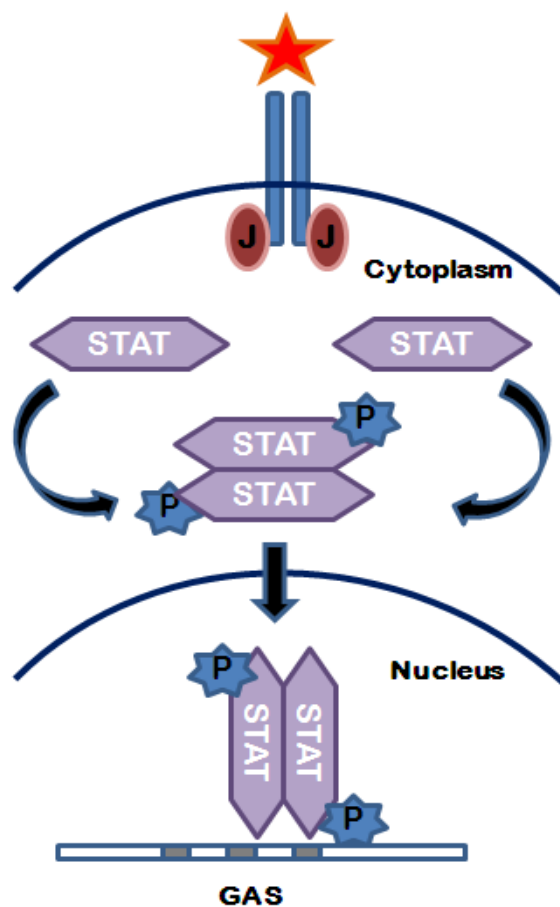


**Figure 1.7 Schematic representation of the classical JAK/STAT pathway**

This is an illustration of the main components and the cascade of events linking extracellular ligands (LPS and cytokines) to intracellular events in the cell.

The JAKs undergo either autophosphorylation or transphosphorylation at specific tyrosine (or serine/threonine) residues at the carboxyl end of the molecule. A complex is formed which acts as a docking site to further recruit STAT proteins via their SH-2 domains. STATs then in turn become phosphorylated, dimerize, move into the nucleus and bind to specific DNA sequences (GAS) in the promoter region of designated genes to activate transcription (Schindler et al., 1995).

It is significant to note that other pathways are indirectly involved in STAT phosphorylation. Evidence suggest that dephosphorylation of the JAKs (Starr et al., 1999) could also trigger the activation of the MAPK pathway to modulate STAT activity via serine-phosphorylation.

Despite their vast reviews in many publications, it is still unclear as to the role of this family of signalling molecules referred to as the JAKs. The interest in these proteins is due to the fact that induction of iNOS and indeed CATs in vascular smooth muscle cells requires the exposure of these cells to IFN, a potent activator of JAKs.

Interferons in general exert pleiotropic effects in key cellular functions such as induction of differentiation, modulation of the immune system and inhibition of both angiogenesis and cell proliferation via multiple signaling pathways (Pestka *et al.*, 1987; Pfeffer *et al.*, 1998; Stark *et al.*, 1998). As cytokines, they play a complex and central role in mammalian resistance to pathogens (Boehm *et al.*, 1997). There are two major groups of interferons that share very different homologies with very unique receptors (Pestka *et al.*, 1987; Stark *et al.*, 1998); type I (made up of IFN- $\alpha$ , - $\beta$  and  $\omega$ ) and type II (IFN  $\gamma$ ) interferons.

Type I interferons are derived from virus-infected cells and bind to the Type I IFN receptor. They consist of two distinct structural subunits; IFNAR1 (110 kDa protein) and IFNAR2 (occurs in two splice variant – a long 100 kDa IFNAR2c and a short 51kDa IFNAR2b) (Uze *et al.*, 1995).

Type II interferons (IFN- $\gamma$ ) are from thymus-derived (T) cells and natural killer (NK) cells. In addition, IFN- $\gamma$  transmit signals to the cell interior through a distinct Type II IFN

receptor which is made up of two subunits, IFNGRI (110 kDa) and IFNGRII (62 kDa) (Bach *et al.*, 1997; Pestka *et al.*, 2004).

The effects of IFN- $\gamma$  signaling are extensive and diverse and include nearly all aspects on host defense, inflammation and autoimmunity. In order to mediate signaling the IFN receptor subunits need to associate with members of the JAK family at some stage in the cascade of signaling reactions. What is uncertain at this stage is how far downstream that stage is.

#### **1.2.5.2 Structure and functional role of the JAKs in cytokine induced nitric oxide signaling**

A recent review (Ivashkiv *et al.*, 2004) suggest that following ligand induced stimulation of the IFN receptors at the cell surface, there is activation of the receptor associated JAKs by phosphorylation. In addition, the target receptor associated with Tyk2 is the 100-kDa longer splice variant of interferon receptor-2 (IFNAR2c) subunit (Bach *et al.*, 1997). Of the four members of the mammalian JAKS (JAK-1, -2, -3 and TYK2) only three (JAK-1, JAK-2 and TYK2) are reported to undergo tyrosine phosphorylation of receptors and thereby creating binding sites for specialized domain sites on STAT proteins called SH domains. Both Tyk2 and JAK2 share with other members of the JAK family, a unique structural framework made up of seven conserved JAK homology (JH) regions (Wilks *et al.*, 1991) as shown in Figure 1.8 below. In addition reports suggest that JAK2 kinase is implicated in cross-talk of the JAK/STAT pathway (Argetsinger *et al.*, 1993; McWhinney *et al.*, 1998).

Src homology 2 (SH2) domains are specialized motif regions, containing approximately about 100 amino acids (Moran *et al.*, 1990) which are found in a variety of proteins including JAKs and STATs. They are intricately linked to signal transduction which involves cell surface signal initiators on the membrane to changes in gene expression. In addition SH2 contain unique binding sites for phosphotyrosine residues (Tyr-P) and a binding specificity with the associated SH2 motif domain. The association between the SH2 domain with the phosphotyrosine binding sites provides the framework for signal

transducer complex formation. To effect the changes in gene expression they convert the changes in protein-tyrosine phosphorylation into altered protein-serine/ threonine phosphorylation.

From the above, we can surmise that the Janus kinase/signal transducers and activators of transcription (JAK/STAT) pathway play an essential intracellular mechanism that controls expression of certain target genes.

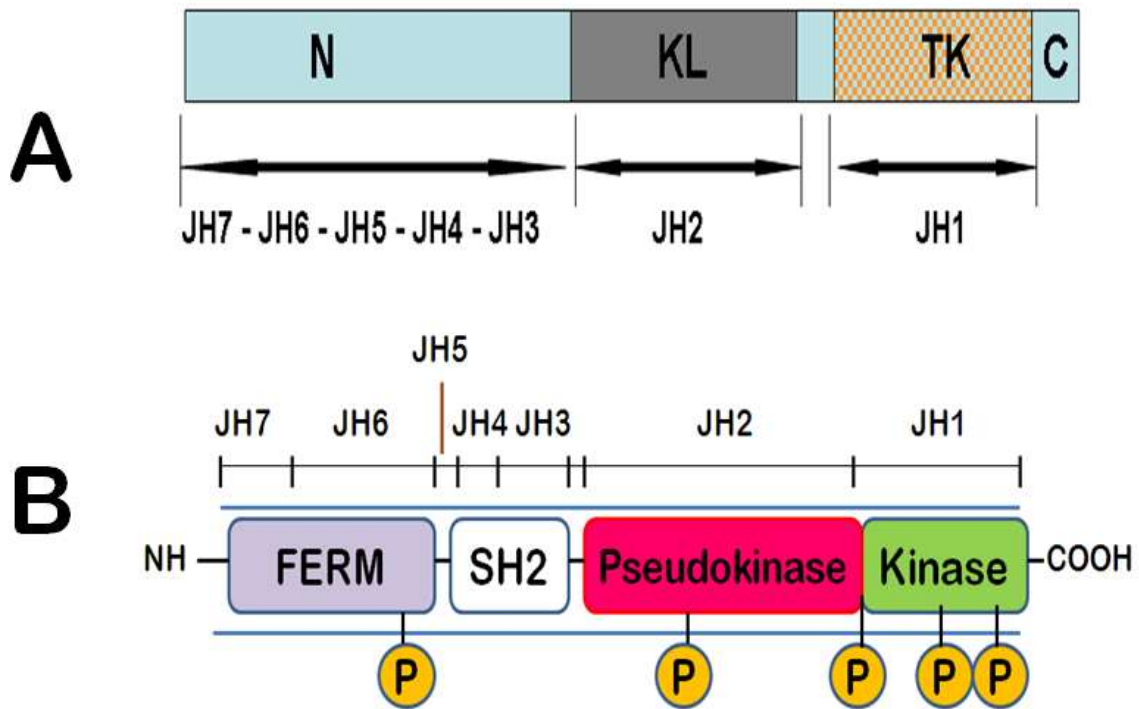


**Figure 1.8 A schematic structural representation of the JAK structure.**

An illustration of the comparative domains (Figure A) and the relative positions of the different JAK Homology (JH) domains (Figure B).

JAKs share 7 regions of high homology JH1 to JH7. JH2 represents a pseudokinase domain and appears to regulate JH1, the kinase domain that has catalytic activities. JH3 to JH7 region mediates receptor association. (**N** represents receptor mediator region or amino terminal region; **KL**, pseudokinase or kinase-like domain; **TK**, tyrosine kinase domain; **C**, carboxyl terminal tail). Figure **B** is a more detailed representation of JAK and comprise FERM, SH2, pseudokinase, and kinase domains. The FERM domain mediates receptor interactions. Both the FERM and pseudokinase domains regulate catalytic activity.

### 1.2.5.3 Structure and functional role of the STATs proteins in nitric oxide signaling

STATs are latent cytoplasmic transcription factors which following receptor activation dimerizes and translocates into the nucleus. They are induced by a variety of growth factors and cytokines (Ihle, 1996). They are activated by tyrosine phosphorylation though an additional serine phosphorylation in some STATs appears to enhance transcription of some target genes (Decker *et al.*, 2000).

They are approximately 80 – 95 kDa in size. In mammals, seven genes encoding different STAT proteins (STAT-1, STAT2, STAT3, STAT4, STAT5a, STAT5b and STAT6) have so far been identified (Aaronson *et al.*, 2002). Just as in the JAKs, the STATs share a highly conserved structural and functional domain as shown in Figure 1.9

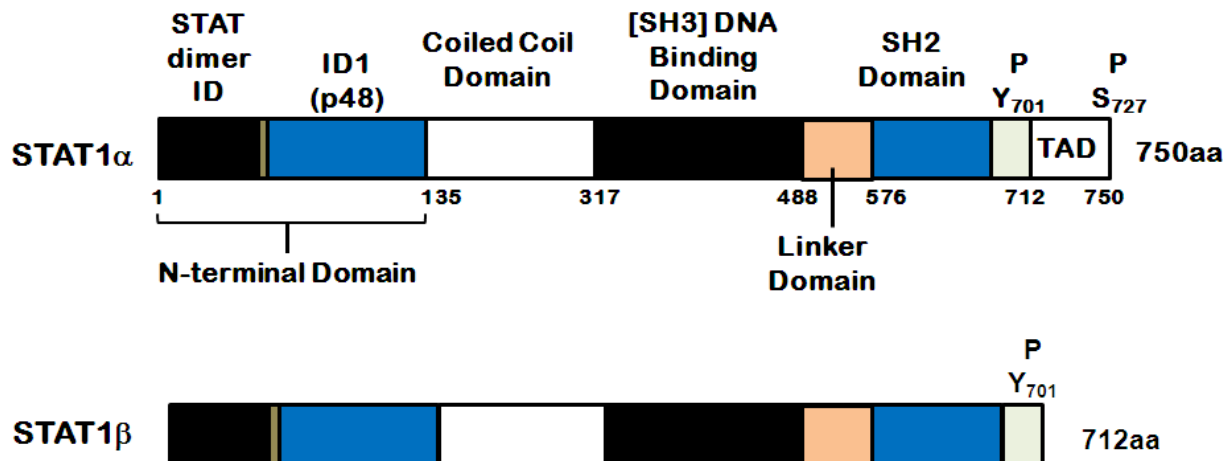


**Figure 1.9 Schematic structural representation of STAT-1**

An illustration of the homologies between STAT-1 $\alpha$  and STAT-1  $\beta$  and the relative positions of the respective STAT-1 domains (TAD is Transactivation domain).

These domains include an amino-terminal domain (NH<sub>2</sub>), the coil-coil domain (CCD), a DNA binding domain (DBA), the linker domain and the SH<sub>2</sub>/tyrosine activation domain. All the STATs do however share a divergent but unique carboxy-terminal domain called the carboxy-terminal transcriptional activation domain (TAD). There are two isoforms of STAT-1, STAT-1 $\alpha$  and STAT-1 $\beta$ . The latter lacks a 38 amino acid residue at the carboxy-terminal end compared to the STAT-1 $\alpha$  (as shown in Figure 1.9).

The JAK/STAT pathway plays an essential role in vascular smooth muscle cell proliferation following cytokine activation (Darnell *et al.*, 1994; Ihle, 1995). The classical transduction mechanism involving the JAKs and STATs involves the homo- and heterodimerization via their src homology 2 (SH<sub>2</sub>) domains. In support of this concept, evidence suggest that reductions in JAK/STAT activity either through mutations or mutations that constitutively activate or fail to regulate its associated JAK signaling properly can lead to inflammatory and other associated diseases (Igaz *et al.*, 2001; O'Shea *et al.*, 2002). In general, phosphorylation of the STATs enable them to then undergo homo- and or heterodimerization and translocate into the nucleus, to activate IFN-stimulated response elements (ISREs, AGTTTCNNTTTCNC/T) in order to transcribe the appropriate genes associated with this signalling cascade (Chen *et al.*, 2004).

STATs activate transcription by binding to a DNA motif, TTCNNGAA, in the promoter region of target gene. This motif represents a specific response element within the gene promoter. One of their well-characterized response element GAS is expressed in the iNOS gene promoter and may be essential for iNOS gene induction (Schindler *et al.*, 1995). Of the STAT proteins thus far investigated, STAT-1 is known to undergo homodimerization of phosphorylated STAT-1.

#### **1.2.5.4 Activation of STATs independent of JAKs; Role of the GTPases**

Most of the responses to cytokines in cells result in the activation of JAKs through tyrosine phosphorylation of STAT-1 (Ihle, 1995; Yeh *et al.*, 1999) on tyrosine-701 (Tyr-701) residue. This may also be achieved independently of JAKs with other upstream signaling molecules directly phosphorylating STAT1 and thus initiate iNOS gene transcription. In this regard, protein tyrosine kinases (PTK) as well as serine and threonine kinases with much broader substrate specificity have also been implicated. Other cell surface receptors such as G-protein coupled receptors (GPCR) have also been shown to activate the STATs through tyrosine phosphorylation and induce STAT DNA binding in cells (Bhat *et al.*, 1994; Marrero *et al.*, 1995; Rodriguez-Linares *et al.*, 1994). However the cascade of events by which G-proteins activate the JAK/STAT pathway are far from certain.

During iNOS mediated expression the majority of the signal cascades by kinases are orchestrated mainly by protein tyrosine kinases (PTK) though serine and threonine kinases with much broader substrate specificity have also been implicated. In addition, many of the cytokine (IFN- $\gamma$ ) or endotoxin (LPS) mediated stimuli do activate multiple signal transduction cascades. For example, PTK receptors are reported to activate both PI3K-Akt and MAPK pathways, following induction by cell proliferation associated stimuli (Muto *et al.*, 2007). The phosphorylated PTK receptor activates PI3K via cytokines and other extracellular ligands. Consequently considerable overlap and cross-talk between many of these cytokine mediated signaling pathways have been reported (Tachado *et al.*, 2005; Wang *et al.*, 2006). We envisage that these interactions may provide the cooperation and coordinated interactions that are important in STAT-1 activation via the GTPases and independent of the JAKs.

Many extracellular ligands including endotoxins (LPS) cytokines (IFN- $\gamma$ ) are reported to activate multiple signal transduction cascades. For example, PTK receptors have been reported to activate the PI3K-Akt pathway in addition to the MAPK pathway, when stimulated by signals that induce cell proliferation and cell survival. What has been

clearly defined is the extent and diversity in the IFN- $\gamma$  mediated interaction across distinct but synergistic pathways. In macrophages IFN- $\gamma$  mediated NO production has been evident not only in the JAK/STAT pathway but also reported in the ERK1/2 and MAPK pathways. Further downstream of the JAK/STAT cascade, IFN- $\gamma$  is also reported to activate class II trans-activator (CIITA) CCAAT enhancer-binding protein (Roy *et al.*, 2000), and interferon-responsive factors (IRFs).

Other cell surface receptors such as G-protein coupled receptors (GPCR) have been shown to also activate the STATs through tyrosine phosphorylation and induce STAT DNA binding in cells (Bhat *et al.*, 1994; Marrero *et al.*, 1995; Pelletier *et al.*, 2003; Rodriguez-Linares *et al.*, 1994). However the cascade of events through which G-proteins activate the JAK/STAT pathway are far from certain but G-proteins such as Rho GTPases can activate STAT-1 and induce its transcriptional activity (Pelletier *et al.*, 2003). These G-proteins may also induce expression of cytokines through parallel pathways involving the transcription factor, nuclear factor (NF)- $\kappa$ B (Goodman *et al.*, 1982; Okusawa *et al.*, 1987; Okusawa *et al.*, 1988) suggesting a multiple cascade of effects of which some may be STAT-dependent.

Small GTPases comprises a functionally diverse group of proteins (G proteins) responsible for a range of cellular processes important in almost all organisms including prokaryotes and eukaryotes. They regulate processes by functioning as molecular switch from GDP bound form (inactive or off position) to GTP bound form (active or on position) as shown in Figure 1.10 below.

Of particular importance is their involvement in the regulation of a diverse range of processes including cell proliferation, cell migration, transport inflammation (Laufs *et al.*, 1998; Muniyappa *et al.*, 2000) amongst others. In addition, at least one other report suggest that most of the inflammatory cytokines and extracellular stimuli which induce iNOS are also implicated in the activation of G-proteins associated with the Ras/Rho family (Kjoller *et al.*, 1999). In particular, there is evidence supporting this concept demonstrated that Rho signaling down regulated iNOS expression in RASMCs (Muniyappa *et al.*, 2000). In view of these findings, our examination of iNOS regulation will also take into account components of the of the Rho GTPase pathway.

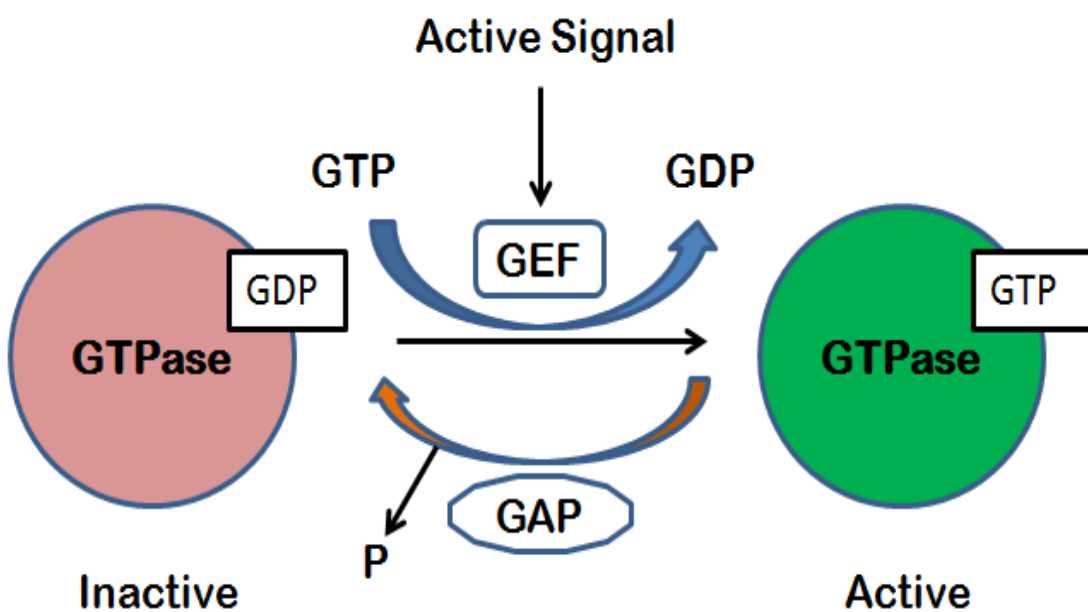


**Figure 1.10 Regulation of small G protein activity.**

Schematic representation of the molecular switching role of the small GTPases showing the GTP bound (active state) and GDP bound (inactive state).

GTPases control many aspects of cell activities by cycling between an inactive (GDP-bound) to an active (GTP-bound) conformational state following hydrolysis of guanine triphosphate (GTP) (Boguski *et al.*, 1993). It is only in the latter conformational state that GTPases are able to interact with effector molecules (GEF) in order to mediate in cellular processes.

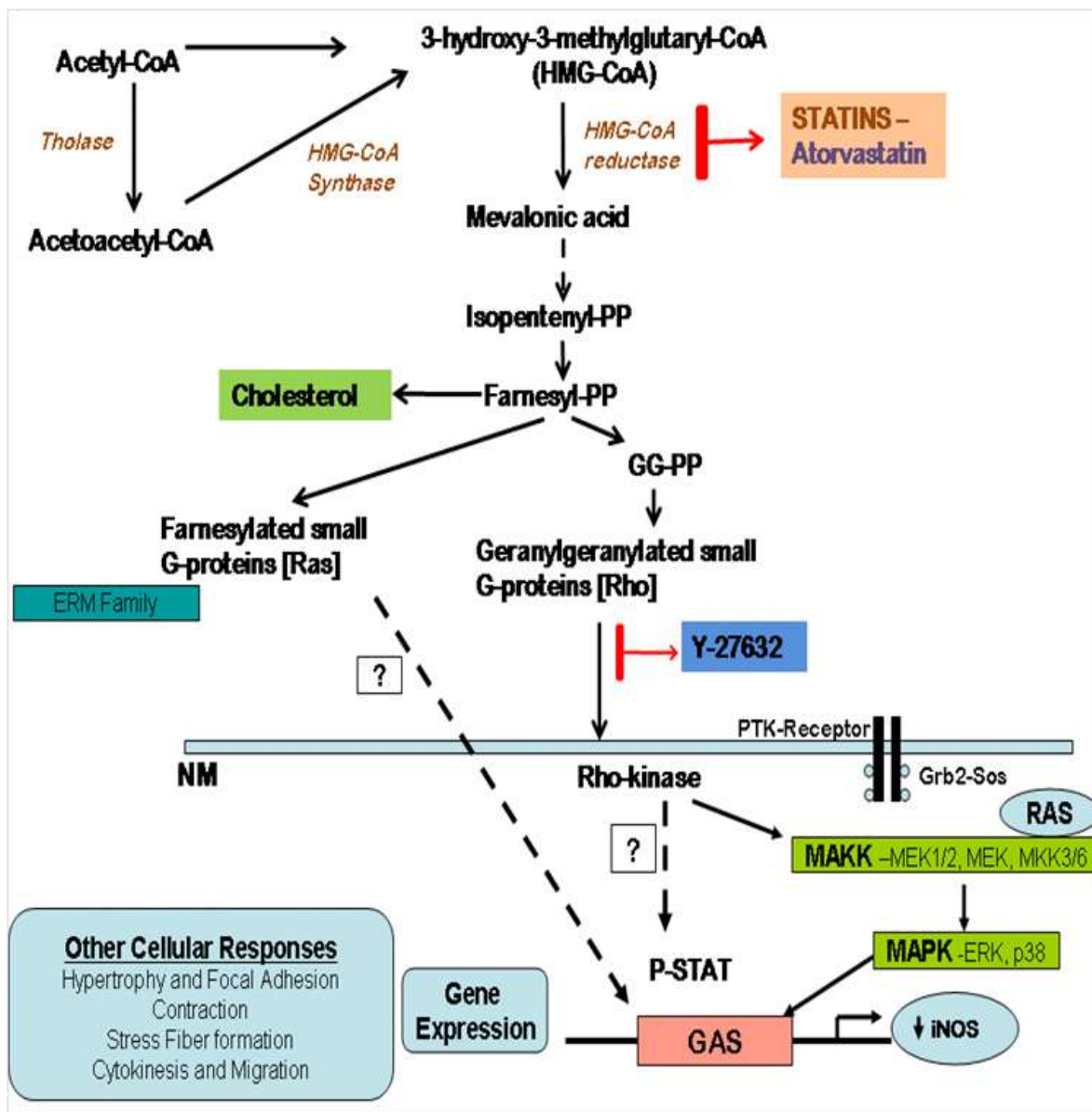


**Figure 1.11 Schematic representation of the Mevalonate pathway and its downstream signalling**

The figure illustrates the main intermediates in the mevalonate pathway and highlights key targets for some of the pharmacological inhibitors used in this study. The convergence of the different pathways is proposed to link JAK/STATs to GTPases and transcription factors further downstream. (Broken lines are plausible links that are yet to be determined).

### **1.2.8 GTPase Inhibitors as potential regulators of induced nitric oxide production**

The compound Y27632 ((+)-(R) trans-4-(1-aminoethyl)-N-(4-pyridyl) cyclohexanecarboxamide dihydrochloride) is a synthetic compound reported to inhibit the ROCK family of kinases. Y-27632 is used to investigate the possible involvement of small GTPases in the signaling transduction upstream of the JAKs. This compound has been reported to inhibit agonist-induced contraction of both vascular and bronchial SMCs through blocking the calcium sensitized SMC contractions (Bai *et al.*, 2006; Lazaar, 2002). The main targets are the Rho-associated coiled-coil forming protein serine/threonine kinase (ROCK) family, which acts on downstream effector targets in small GTPases. The ROCK family consists of p160ROCK (ROCK-I) (Ishizaki *et al.*, 1996) and ROK $\alpha$ /Rho-kinase/ROCK-II (Leung *et al.*, 1995).

The potency of its reaction is reported to be over 100 times more when compared to other naturally occurring kinases including protein kinase C, cAMP-dependent kinase and myosin light chain kinase. These targets are implicated in Rho-induced formation of actin stress fibers and focal adhesions (Amano *et al.*, 1997; Ishizaki *et al.*, 1997; Leung *et al.*, 1996) and the down regulation of myosin phosphatases (Kimura *et al.*, 1996).

In our experimental setup, the inhibitor, Y-27632 was used, to assess the role of Rho pathway in the induction iNOS with LPS and IFN- $\gamma$  in RASMCs and LPS alone in J774 macrophages.

## **AIM**

The main aim of this thesis was to confirm unequivocally whether JAK/STAT signalling play a critical role in the induction of the inducible L-arginine-NO pathway in either smooth muscle cells or J774 macrophages. Furthermore, the project was also aimed at identifying changes in the profile of expression of CATs in induced cells with a view to establishing the critical role played by each transporter in sustaining substrate supply into cells for sustained NO synthesis. To achieve these aims, studies were carried out using both pharmacological and molecular approaches to dissect the specific JAK and/or STAT signalling that may be associated with the expression of iNOS and/or CATs. Gene silencing using siRNA knockdown was also attempted to establish the role of JAK2 as this has been the most studied and often the most implicated JAK protein for iNOS induction, but with inconclusive outcomes.

## **Chapter 2. MATERIALS AND METHODS**

All substances used in cell culture experiments were handled in accordance with the regulation for the Control of Substances Hazardous to Health (COSHH) guidelines. Solutions and apparatuses were autoclaved and experiments were carried out in a laminar flow cabinet using aseptic techniques when required.

## **2.1 Preparation of cell culture medium**

Dulbecco's Modified Eagle's Medium (DMEM; without sodium pyruvate, with 1000 mg-1 glucose, and with pyridoxine HCl) was used throughout these studies as the culture medium. The media was supplemented with penicillin (100 Uml-1) and streptomycin (100 µg ml-1) plus 10% foetal bovine serum (FBS). Once prepared, the complete growth medium (referred to here on as complete DMEM) was stored at 4°C and used within a period of no more than 2 weeks.

## **2.2 Culture of J774 macrophages**

The murine monocyte/macrophage cell line J774 macrophage was a generous gift from Neil Foxwell (Wolfson Institute for Biomedical Research, University College London-The Cruciform Building). J774 macrophages cells were maintained in continuous culture in T75 tissue culture flasks containing complete DMEM. Cells were harvested by gentle scraping and passaged every 3-6 days by dilution of a suspension of the cells in media in a ratio of 1:4. Once every two months, old cells were discarded and new cells were defrosted and brought to confluence for use.

## **2.3 Isolation of Rat Aortic Smooth Muscle Cells (RASMCs)**

Vascular smooth muscle cells were obtained from rat aortic explants as described previously by Wileman et al (Wileman *et al.*, 1995). Essentially, male Wistar rats (from Charles Rivers) were asphyxiated by CO<sub>2</sub> and the thoracic aorta dissected out into a Petri dish containing complete DMEM. Following removal of the connective tissue on the adventitia, the aorta was cut open and the monolayer of endothelial cells removed by gentle scraping. Each aorta was cut into approximately 2 mm<sup>2</sup> segments and placed in a T-25 Falcon flask containing 5 ml of complete media with the intimae facing the flask surface. Flasks were placed upright in a tissue culture incubator (100% humidity

and 5% CO<sub>2</sub>) overnight to allow adherence of the explants to the plastic surface. After 24 hours, flasks were gently placed flat and explants were left in culture for 14 days. Over this period, rapidly dividing and migrating cells were harvested and cultured to confluence in a T-75 Falcon flask.

## **2.4 Sub-culturing of RASMCs**

Proliferating cells that had migrated from the explants were harvested with trypsin-EDTA (0.01/0.02 %) diluted in phosphate buffered saline (PBS; mM: NaCl, 140; KCl, 2.7; Na<sub>2</sub>HPO<sub>4</sub>, 8.1; KH<sub>2</sub>PO<sub>4</sub>, 1.5; pH 7.4). Following aspiration of the growth medium, cells were washed at least twice with pre-warm (37°C) PBS (X1) in order to remove any trace of protease inhibitors present in the serum from the complete media. The pre-warm (37°C) trypsin-EDTA solution was added (1 ml per 25 cm<sup>2</sup> of surface area) to the cell monolayer and distributed uniformly. Detachment of SMC was monitored under an inverted light microscope at 2 minutes intervals. When most of the cells acquired a round shape the flask was gently tapped to help cell detachment and 13 ml of complete DMEM was added to re-suspend the cells and inactivate trypsin. Cells were then gently dispersed with a Pasteur pipette before being transferred into a sterile T-75 tissue culture flask. RASMCs were passaged weekly and only cells between passages 3 to 5 were used in the experiments described in this report.

## **2.5 Characterisation of RASMCs**

Cells extracted from the Wistar rat aorta were routinely identified and characterised as smooth muscle cells by immunostaining of smooth-muscle  $\alpha$ -actin (Skalli *et al.*, 1986) as described by Wileman and co-workers (Wileman *et al.*, 1995). Briefly, cells at passages 2 to 5 were plated at sub-confluent density in a culture chamber slide and grown in complete DMEM. All cultures were grown in a 100% humidified incubator at 37°C under 5% CO<sub>2</sub> in air. After 2 days of growth, cells were washed twice with PBS to eliminate serum contamination prior to being fixed with ice-cold methanol for 45 seconds. Fixed cells were blocked with 5% bovine serum albumin (BSA) in PBS for 20 minutes before incubation with an anti- $\alpha$ -actin antibody (1:50 dilution) for 1 hour. Excess primary antibody was eliminated following several wash cycles (four times) with PBS for

5 minutes each wash. Cells were then incubated with an anti-mouse IgG-FITC conjugated secondary antibody (1:50 dilution) for 1 hour in the dark. Subsequently, cells were treated with increasing dilutions of glycerol (30%, 50%, and 80%) in PBS for 15 seconds each time. Cells were finally mounted in 100% glycerol prior to placing a cover slip over the cells and sealing with standard nail varnish. Cells were visualized under UV light using a Nikon EFD3, LABOPHOT-2 Light Microscope at 400X magnification. An example of routine cultures stained with  $\alpha$ -actin is shown in Figure 2.1.

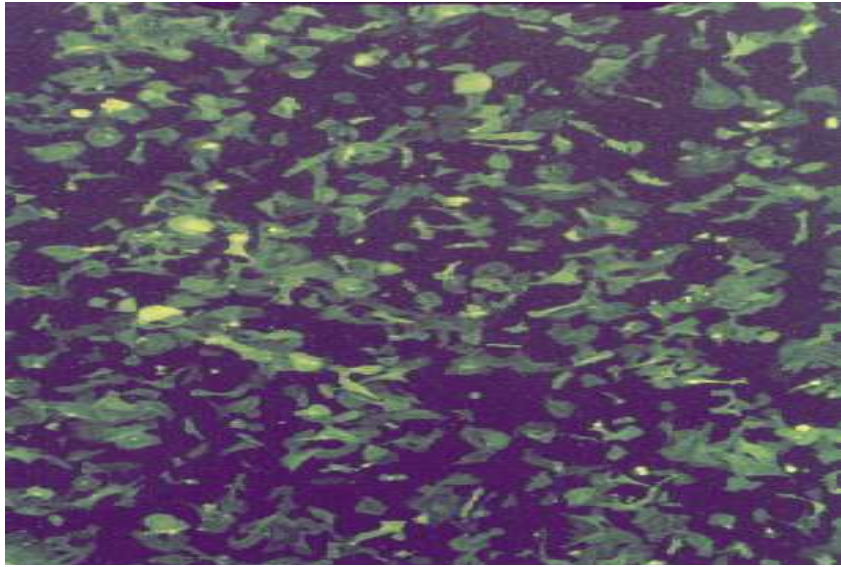


**Figure 2.1 Representative photograph showing positive immunostaining of smooth muscle  $\alpha$ -actin in cells extracted from rat aortas**

Sub-confluent cultures of RASMCs, extracted from rat aorta were immunostained with  $\alpha$ -actin antibodies (Sigma, UK). Cells were viewed under UV-light using a Nikon EFD3, LABOPHOT-2 Light Microscope at 400X magnification. The characteristic elongated shape of RASMCs is not observed in this picture but rather they adopt a star shape or polyhedral conformation under sub-confluent culture conditions due to the lowconfluent nature of the cells.

## 2.6 Cell counting

Cell density was estimated using a haemocytometer. Briefly, cell suspensions were obtained as previously described. Cell suspension was mixed with 0.4% trypan blue solution in a 1:1 ratio and 10  $\mu\text{l}$  of thoroughly mixed cell suspension loaded into each chamber. The haemocytometer was then placed on the microscope stage and the total number of cells was determined by counting the cells inside each large square, ensuring that only cells touching the top and left borders were counted. The average cell count was estimated and used to determine total cell number. Therefore, the number of cells per ml was determined by multiplying the number of cells obtained by 10000. The final number of cells in each suspension was then obtained using equation 3.1.

$$\text{Cells/ml} = \frac{\text{number of cells counted}}{\text{squares counted}} \times \text{conversion factor}$$
$$\text{Total cells} = \text{cells ml}^{-1} \times \text{total volume of cell suspension}$$

Where:

**Number of cells** is the total number of cell counted.

**Square counted** is the number of squares counted in order to get an average.

**Conversion factor** corresponds to  $10^4$  as explained above.

To get the total number of cells harvested the number of cells determined per ml was multiplied by the original volume of medium in which the cells were suspended in.

## 2.7 Plating of cells for experimentation

Confluent monolayer of J774 macrophages were gently scraped and counted as described above. Cells were then diluted to the required concentration and plated at a seeding density of  $2.5 \times 10^4$  cells  $\text{ml}^{-1}$ . Plates were incubated overnight in a tissue culture incubator to allow cell adherence and growth. For RASMCs, confluent monolayer in T-75 flasks were trypsinised and counted as described above. Cells were then seeded at  $3 \times 10^4$  cells  $\text{ml}^{-1}$  and allowed to grow to confluence for approximately three days in a tissue culture incubator at  $37^\circ\text{C}$  under 5%  $\text{CO}_2$  in air.

## 2.8 Treating of plated cells with inhibitors

In order to characterize the role of JAK/STAT signalling in iNOS induction and nitrite production as well as L-arginine transport we used a pharmacological approach. In this thesis, the two main pharmacological inhibitors of JAKs used were JAK inhibitor I and AG490 inhibitor:

**JAK inhibitor I:** [2-(1,1-Dimethylethyl)-9-fluoro-3,6 dihydro-7H-benz[h]-imidaz[4,5-f]isoquinolin-7-one P6 Pyridone 6].

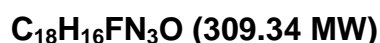
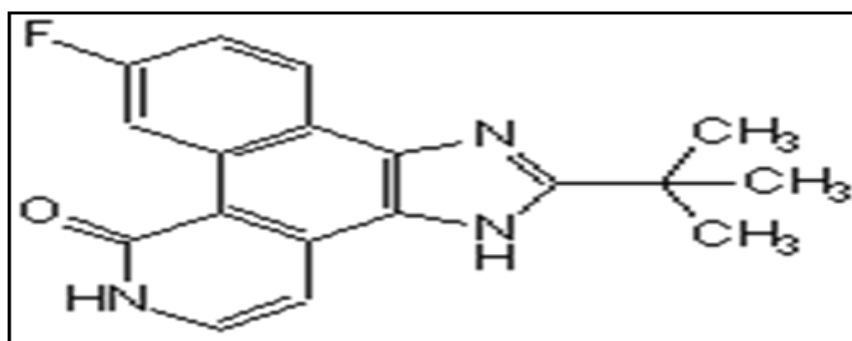
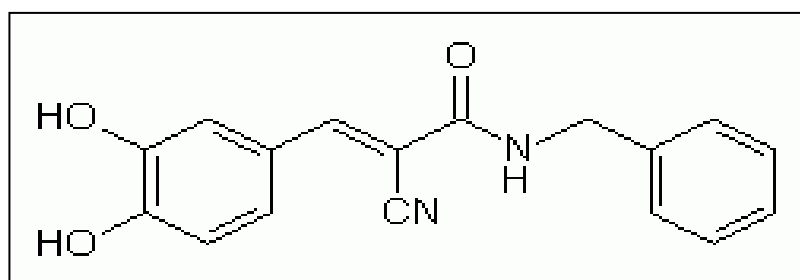


Figure 2.2 Chemical structure of JAK inhibitor I

JAK inhibitor I is a clear, colourless but potent inhibitor of the JAKs. It is prepared from the photochemical cyclization of Pyridone 5 to 6. The resulting product under steady state conditions is a reversible inhibitor that is competitive with respect to ATP and non-competitive with respect to the peptide substrate. It displays potent inhibitory activity against JAK1 (IC<sub>50</sub> = 15 nM for murine JAK1), JAK2 IC<sub>50</sub> = 1 nM), JAK3 (K<sub>i</sub> = 5 nM), and Tyk2 (IC<sub>50</sub> = 1 nM). It inhibits other kinases only at much higher concentrations and shows specificity for the JAK family of Protein Tyrosine Kinase (PTK) over other kinases. JAK inhibitor I however has limited selectivity amongst the JAKs. Both JAK2 and TYK2 (IC<sub>50</sub>=1 nM) are inhibited slightly more potently than JAK3 and JAK1 (IC<sub>50</sub>=5 and 15 nM, respectively) (Thompson et al., 2002).

Tyrphostin B42 (AG490): [ $\alpha$ -Cyano-(3, 4-dihydroxy)-N-benzylcinnamide]



**C<sub>17</sub>H<sub>14</sub>N<sub>2</sub>O<sub>3</sub>; (Mol. Wt., 294.3)**

**Figure 2.3 Chemical structure of Tyrphostin B42 (AG490)**

Tyrphostin B42 (AG490) is a specific synthetically derived member of the class of drugs collectively called Tyrphostins which are derived from benzylidenemalononitrile nucleus. Erbstatin, which is the smallest competitive PTK inhibitor together with other small tyrosine-containing peptides have provided the structural backbone from which all other tyrphostins have been developed. AG490 is regarded as a protein PTK inhibitor or blocker. It is also regarded as potential antiproliferative agent and therefore a potential therapeutic agent for diseases caused by the hyperactivity of PTK. AG490 is reported to selectively block JAK2 thus making it's a specific inhibitor of the protein over the others in the group (Levitzki, 1992; Meydan et al., 1996). When used, each inhibitor was incubated with cells at the appropriate concentration for 30 min prior to activation with the respective stimuli. The cell culture medium was collected for nitrite measurement and the cell monolayer used for either L-arginine transport studies or for western blotting.

## 2.9 Measurement of nitrite as an indicator of NO production

As nitrite is a major breakdown product of NO in both mouse and rat (Ignarro *et al.*, 1993; Marletta *et al.*, 1988) we used the Griess assay to measure nitrite in solution as an indicator of NO production as described by (Seguin *et al.*, 1994; Wileman *et al.*, 1995). In these studies, RASMC or J774 macrophage cells were seeded at  $3.0 \times 10^4$  cells ml<sup>-1</sup> and  $2.5 \times 10^4$  cells ml<sup>-1</sup> respectively in 96 well plates and cultured in a humidified cell culture incubator at 37°C until they reached confluence. Confluent monolayer of RASMCs were activated for a further 24 hours with LPS (100 µg/ml) and IFN-γ (100 U/ml) while macrophages were activated with LPS (1.0 µg/ml) alone. As indicated above, drugs were added to cells 30 min prior induction with the respective stimulus.

A stock of Griess reagent **A** (2% sulfanilamide amine) and Griess reagent **B** (0.2% naphthylethylenediamine plus 10% phosphoric acid) were prepared and stored at 4°C. When required, both reagents were mixed in a 1 to 1 ratio before performing the assay on the bench at room temperature. The inner wells of a non sterile 96-well plate were used to transfer 100 µl of medium from the cell cultures and the outer wells were used to add standards of sodium nitrite in a final volume of 100 µl. Both samples and standards in the wells were incubated with 100 µl of Griess reagent and incubated at room temperature for 10 minutes.

Absorbances were measured using a Multiskan II plate reader (Ascent, Nitrite protocol) set at a wavelength of 540 nm. Sodium nitrite standard concentrations were used to produce a standard curve (as shown in Figure 3.2) from which the concentrations of nitrite in samples were determined.

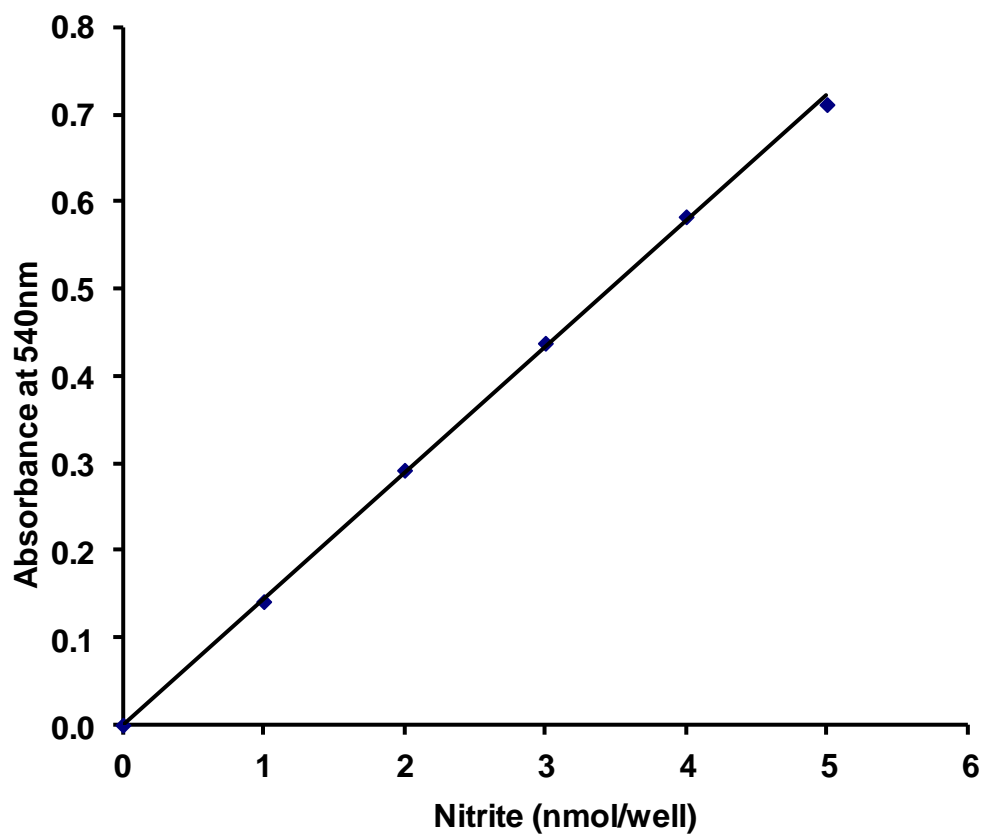


**Figure 2.4 Nitrite Standard Curve**

The standard curve was constructed as described above using serially diluted solutions of sodium nitrite made up in complete DMEM at the concentrations shown on the graph. The graphs often show linearity over the concentration ranges of 1 to 10 nmole nitrite  $100 \mu\text{l}^{-1}$  (equivalent to 0.01 to 0.1 mM nitrite).

## 2.10 Measurement of L-[<sup>3</sup>H] arginine transport

Both RASMCs and J774 macrophages were seeded at  $3.0 \times 10^4$  and  $2.5 \times 10^4$  cells/ ml respectively. Transport studies were carried out on the cell monolayer after removing the culture medium for analysis of nitrite concentrations. Prior to initiating transport of L-arginine, cells were washed three times with warm HEPES-buffered Krebs solution. Special care was taken to ensure complete removal of buffer at the end of each wash cycle. Cells were then incubated in a 'Hot Box' at 37°C with 50 µl of transport buffer containing 1 µCi/ ml L-[<sup>3</sup>H] arginine plus 100 µM of unlabelled (non-radioactive) L-arginine. Incubations were terminated after 2 min by placing the 96-well plates on ice and immediately washing three times with 200 µl of ice-cold Na<sup>+</sup>-free Kreb's buffer containing 10 mM excess unlabelled L-arginine. Cells were subsequently lysed using 50 µl of distilled water and protein content assessed using BCA assay as described earlier. Full content of each well was then transferred into scintillation vials containing 4 ml of scintillation fluid. The β-vials were sealed and transferred onto a scintillation counter (Beckman Coulter™ LS6500 β-Scintillation counter). The levels of radioactivity in samples were determined by scintillation counting and the disintegrations per minute (DPM) converted to pmol µg protein<sup>-1</sup> min<sup>-1</sup> using the following equation:

$$\frac{[(5000 \times D_c)/M]}{Y} = R$$

Where:

**R** is the amount of L-arginine in cell lysates expressed in pmole

**5000** is the amount of cold L-arginine in pmole present in 50 µl of a 100 µM solution used in the transport studies

**D<sub>c</sub>** is the DPM in the cell lysates

**M** is the DPM in 50 µl of 100 µM L-arginine solution + 1 µCi ml<sup>-1</sup> L-[<sup>3</sup>H] arginine

Y is the total protein content of the cell lysates counted.

## 2.11 Measurement of total cell protein using bicinchoninic acid assay

The bicinchoninic acid protein assay is based on the two step process of an initial, biuret reaction involving a reduction of copper (Cu) to cupric ions ( $\text{Cu}^{2+}$ ) in alkaline environment containing sodium potassium tartrate when bound to a peptide containing at least 3 amino acid residues. The resulting structure is a light blue to violet colouration. The intensity of the colouration is directly proportional to the amount of protein. This is subsequently followed by a second step involving formation of a complex with the reduced cupric ions. The resulting complex can then be colorimetrically determined by measuring absorbance at 640 nm.

Cell protein was determined using the commercially available Bicinchoninic Acid (BCA) protein assay reagent kit from Pierce (Smith et al., 1985). The monolayer of cells was rinsed twice with PBS in order to eliminate any contamination from extracellular proteins (e.g. serum proteins contained in the culture media). Cells were subsequently lysed by the addition of X 1 lysis buffer solution (10 mM TRIS, 10 % sodium dodecyl sulphate (SDS), pH 7.4) containing 200  $\mu\text{M}$  sodium orthovanadate ( $\text{Na}_3\text{VO}_4$ ), 200  $\mu\text{M}$  phenyl methyl sulfonyl fluoride (PMSF) and 1 mM sodium fluoride (NaF). BSA standard concentrations were prepared from a bovine serum albumin (BSA) stock solution (1 mg/ml) in double distilled water (DDW). Preparation of BSA standards is as shown in Table 2.1:

**TABLE 2.1 PREPARATION OF BSA STANDARDS**

Volume ( $\mu$ l) 1 mg/ml BCA Working stock	Volume of Lysis Buffer ( $\mu$ l)	Final BSA CONC. ( $\mu$ g/ $\mu$ l)
0	1000	0
10	990	0.01
20	980	0.02
40	960	0.04
100	900	0.1
250	750	0.25
500	500	0.5
750	250	0.75

A 96-well plate format was used to measure the absorbance of our protein lysates and BSA standards. Standard wells were filled with 10  $\mu$ l BSA standard to give the concentration range (0.0 to 0.75 g/ $\mu$ l) shown in Table 2.1. 10  $\mu$ l of lysate from each sample was added in triplicate to the inner sixty wells. BCA stock reagent A (containing sodium carbonate, sodium bicarbonate, Bicinchoninic acid and sodium tartrate in 0.1M sodium bicarbonate) and B (containing 4%[w/v] Copper(II)sulphate pentahydrate ( $\text{CuSO}_4 \cdot 5\text{H}_2\text{O}$ )) were mixed in 1:50 dilution, according to manufacturer's instructions (200  $\mu$ l BCA reagent B in 9.8 ml BCA reagent A). Each well was then incubated with 100  $\mu$ l of the mixture for 30 minutes at room temperature. Absorbance readings were measured by using a Multiskan II plate reader (Ascent, BCA protocol) set at a wavelength of 620 nm. Protein concentration of each sample was determined from the standard curve. A representative standard curve is shown in Figure 2.5 below.

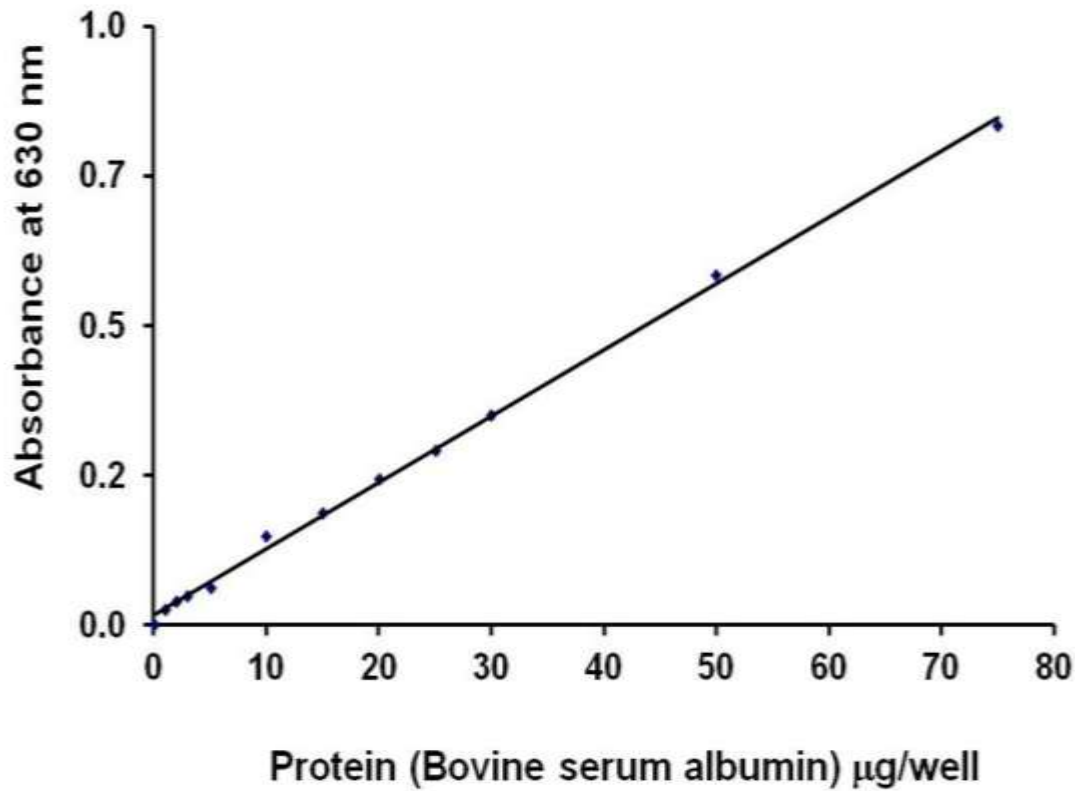


**Figure 2.5 Protein Standard Curve**

An example of a BSA standard curve used to determine protein concentration. Protein levels in samples were determined by using a standard curve with increasing concentrations of BSA (from 1 to 1000 µg well<sup>-1</sup>) prepared in distilled water. The graph is linear from 1 to 1000 µg well<sup>-1</sup>.

## 2.12 Determination of changes in cell viability

The MTT cell cytotoxicity assay is based on the reduction of 3-[4, 5-Dimethylthiazol-2yl]-2, 5-diphenyl tetrazolium bromide (MTT), a tetrazole by the mitochondrial enzyme, succinate reductase (EC 1.3.99.1) in the respiratory chain of metabolically active cells as shown in Figure 2.4.

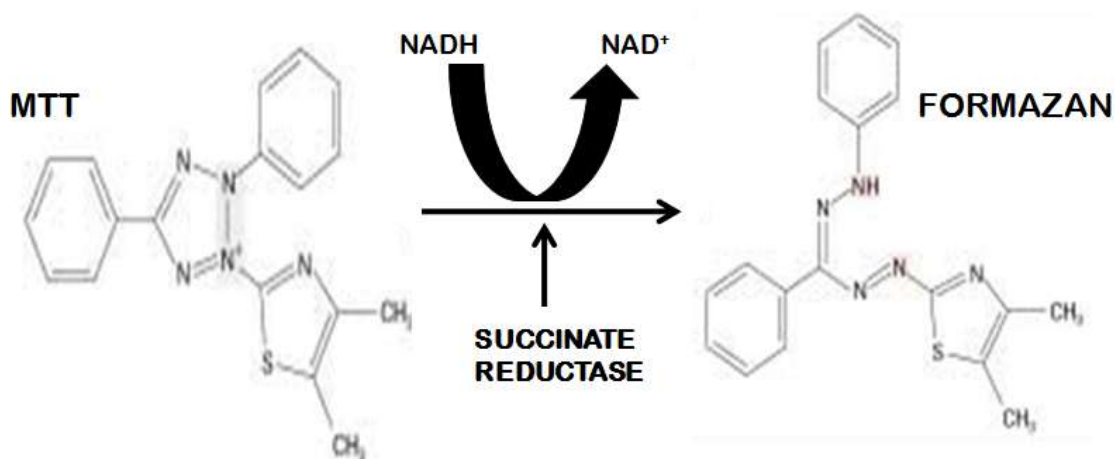


**Figure 2.6** Reduction reaction of MTT to Formazan by mitochondrial reductase enzymes.

The principle behind this action is that when viable cells are incubated in media containing the yellow tetrazolium compound, MTT is reduced by mitochondrial reductase enzymes in metabolically active cells to an insoluble purple formazan in the mitochondria. This reduction is thus directly related to the number of viable active cells. The insoluble formazan crystals are subsequently dissolved by the addition of an organic solvent such as isopropanol (Slater *et al.*, 1963). Briefly, 5.0 mg of MTT was weighed and made up to a volume of 10 ml with PBS (final concentration, 0.5 mg ml<sup>-1</sup>) in a laminar flow cabinet under sterile conditions. After a 24 hour treatment of confluent cells in 96-well plates with activation media and/or compounds of interest, 100 µl of media was removed from each well and used to determine nitrate production. 10 µl of MTT stock solution was added to the remaining 100 µl of medium in each well and cells incubated for 4 hours at 37°C in a cell culture incubator at 5% CO<sub>2</sub>. The medium was

subsequently removed by aspiration, cells lysed and formazan crystals solubilized by the addition of 100  $\mu$ l of isopropanol to each well and allowed to incubate for 1 hour. The extent of reduction of MTT to formazan was quantified by measuring the absorbance at 540 nm in a Multiskan II plate reader (Ascent, MTT protocol).

The cell viability in the untreated control was taken as 100% and the viability under other conditions was calculated as a percentage of the control (untreated) cells. Viability was expressed using the following equation:

$$\% \text{ Cell Viability} = \frac{\text{Ab}_{540} \text{ Drug treated cells}}{\text{Ab}_{540} \text{ Control cells}} \times 100$$

## 2.13 Western Blot analysis

Confluent monolayers of J774 macrophages or RASMCs in 6-well culture plates were pre-incubated for 30 min with media alone or media containing inhibitor prior to activation. Incubations were terminated after 24 hours by rapid aspiration of the media followed by several washes in ice cold phosphate buffered solution (PBS) supplemented with sodium orthovanadate (2 mM). For the detection of non-phosphorylated protein, cells were lysed in hot lysis buffer containing 20 mM Tris-HCL (pH 7.4), 1% sodium dodecyl sulphate (SDS) and 150 mM NaCl.

For phospho-protein detection, cells were lysed in ice cold lysis buffer consisting of: 1% Triton X, 150 mM NaCl, 50 mM Tris pH 7.5, 1 mM EDTA, 1 mM 4-(2-Aminoethyl) benzenesulfonyl fluoride hydrochloride (AEBSF), 2 mM sodium orthovanadate, 80  $\mu$ M leupeptin, 1  $\mu$ g/mL aprotinin, 1.0 mM Sodium Fluoride (NaF), 2.0 mM sodium pyrophosphate and 0.25% sodium deoxycholate.

The resulting cell lysates were transferred into microcentrifuge tube heated at 95 °C for 5 minutes and then sonicated for 2-3 minutes and followed by further centrifugation at 10,000 RPM at 4 °C. The upper clear supernatant was transferred into fresh clean microcentrifuge tubes for storage at -20 °C. Total protein in lysates was determined by the BCA assay as previously described (see Section 2.11). Cell lysates were prepared with sample buffer as previously described (see Section 2.12) and Western blotting carried out immediately or samples stored at -20 °C for future western blot analysis.

### 1. Sample Preparation

An equal volume of cell lysates containing 20  $\mu$ g of total proteins was added to an equal volume of 2X concentrated sample buffer containing Tris-HCl, pH 6.8 (120mM), SDS (4%), Glycerol (10%),  $\beta$ -mercaptoethanol (2%) and bromophenol blue 0.006%). Lysates in eppendorf tubes were boiled at 95 °C for 3 to 5 minutes, centrifuged and loaded onto the polyacrylamide gels.

## **2. SDS Gel Electrophoresis**

Two types of gels were prepared: a resolving gel followed by a stacking gel. The resolving gel was prepared by mixing 5 ml of the 8.0% acrylamide gel (enough for one mini blot) with the following components: double distilled water (2.34ml), 30% acrylamide/bisacrylamide 37.5:1 (1.30ml), 1.5M Tris, pH8.8 (1.25ml), 10% SDS (0.050ml), 10% APS (0.025ml) and TEMED (0.005ml).

After completion of polymerization of the above gel, 5% stacking gel was prepared with the following components: water (2.84ml), 30% acrylamide/bisacrylamide 37.5:1 (0.83ml), 0.5M Tris-HCl pH6.8 (1.25ml), 10% SDS (0.050ml), 10% APS (0.025ml) and TEMED (0.005ml). The stacking gel was poured on top of the resolving gel and this was allowed to polymerize completely.

The gel cast containing the gel was transferred into an electrophoresis tank and a X1 electrophoretic buffer was prepared from a 10X stock solution containing the following components: 30.28 g/L of Tris base (0.25M), 144.0 g/L of glycine (1.92M), 100ml of 10% SDS (1%) with the pH adjusted to 8.3. Electrophoresis buffer was added to the gel tank and allowed to cover the top of the gel. The samples and biotinylated molecular weight protein ladder (NEB, UK) were heated at 95°C for 5 minutes and then loaded onto the gel. The gel was run at a constant voltage of 100V until the bromophenol blue dye reached the bottom of the gel.

## **3. Protein Transfer from Gel to PVDF Membrane**

Following SDS-PAGE, a PVDF membrane (Amersham, UK) was cut to the size of the gel and soaked in methanol for up to 15 - 30 seconds, washed with distilled water and then equilibrated in 1X transfer buffer for a further 15 minutes. The transfer Buffer was prepared from a 10X concentrated stock containing: 58.2 g/L of Tris base (0.48M; pH 8.3), 29.3 g/L of glycine (0.39M), and 3.75 ml of 10% SDS (0.038%). Briefly, 100 ml of the above was diluted down ten fold with 200ml methanol (20%) and 700ml dH<sub>2</sub>O. Precut extra thick blotting paper (Bio-Rad) was soaked in the diluted transfer buffer and two of the blot papers were placed on the semi-dry transfer system. The PVDF membrane was then laid on top of the soaked blot paper on the blotter. A reference for

the protein side of membrane was made by cutting a small notch in one corner of the membrane. The gel was removed from the gel cast and laid on top of the membrane followed by 2 pieces of soaked blot papers placed on top of the gel. An illustration of the transfer setup of gels, PVDF membrane and blotting paper is shown in Figure 2.7 below. Air bubbles between the gel and the blot papers were removed by gently rolling a clean 25ml pipette over the surface of the membrane. To initiate protein transfer, a constant current of  $0.8\text{mA}/\text{cm}^2$  was applied to the gel for 60 minutes.

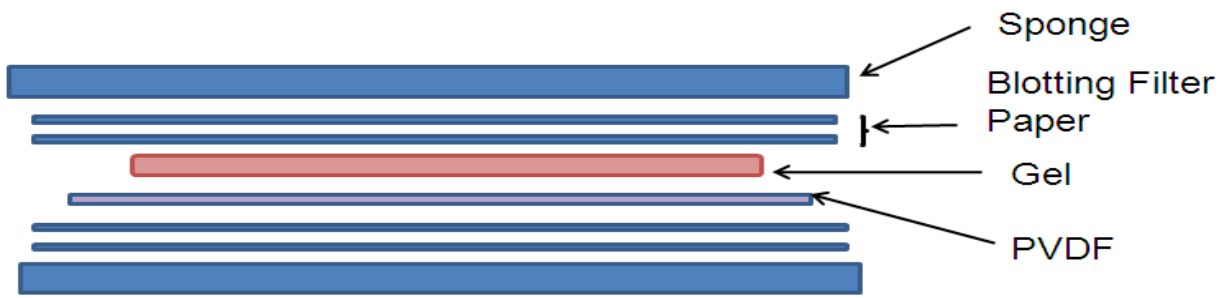


**Figure 2.7** Transfer of proteins to PVDF membrane

The diagram illustrate the construction of the gel 'sandwich' with the membrane at the anode or bottom side relative to the gel.

#### **4. Membrane Blocking**

The PVDF membrane was incubated in 5% non fat milk (Marvel Brand) in 1x TBS (Tris-buffered saline; TBS) containing 0.1% Tween-20 (Sigma, UK) for 1 hour at room temperature or overnight at 4°C. The TBS (1litre) was prepared prior to use by making a 1:10 dilution of a 10X stock solution with the following components: 24.2 g/L of Tris base (20 mM; pH 7.5) and 87.7 g/L of NaCl (150mM). For phosphorylated protein detection the PVDF membrane was blocked in 5% BSA instead of non-fat milk. The incubation in the blocking buffer blocks hydrophobic binding sites on the membrane. Blocking also reduces background and prevents binding of the primary antibody to the non-specific areas or sites of the membrane itself.

#### **5. Primary antibody incubation**

After blocking, the membranes were incubated, using gentle agitation on a shaker, with the primary antibody in a sealed plastic bag. The primary antibody used to probe the blots were rabbit monoclonal antibody to TYK2, phospho-TYK2 (1:2500), phospho-JAK2 or JAK2 (1:2500) in blocking buffer (All antibodies were purchased from InSight Biotechnology, UK).

Following primary antibody incubation, the blot were washed three times (each wash lasting for 5 minutes on a shaker) in wash buffer (TBS containing 0.1% Tween 20). The incubations and post incubation washes as detailed for the primary antibody were repeated goat anti-rabbit IgG conjugated to horseradish peroxidase secondary antibody (1:5000) (New England Biolabs, UK). An anti-biotin antibody (1:2000) (New England Biolabs, UK) also conjugated to horseradish peroxidase was added in order to detect the molecular weight ladder.

## **6. Detection of protein bands by Enhanced Chemiluminescence (ECL) detection**

Protein band detection was carried using the enhanced chemiluminescence (ECL) detection system. Equal volumes of reagent 1 (5 ml) and 2 ( 5 ml) in the ECL Western Blotting Detection kit (Amersham, UK) were mixed and added to the blot as per manufacturer's instructions and incubated for 1 minute at room temperature. The excess detection reagent was drained from the membrane using a folded tissue paper. The blot was covered with cling film, ensuring all trapped air bubbles were gently smoothed out. A sheet of autoradiographic film, Hyperfilm ECL (Amersham, UK) was placed on top of the wrapped blot in an x-ray cassette holder and the film was exposed for 5 minutes, developed, fixed, rinsed under running tap water and then dried in air at room temperature.

## **7. Quantification of Proteins on ECL Western Blots**

The developed protein bands on the film were scanned and the intensities of the scanned image were measured using the densitometry software, Syngene Gene Tools (version 3.00).

## 2.14 Gene silencing using small interference RNA (siRNA)

### 2.14.1 siRNA knockdown of GAPDH

Small interference RNA (siRNA) was intended as a tool to knock down targeted genes including that for JAK2 in order to determine unequivocally the role played by these proteins in the induction of iNOS. The protocol for using siRNA was optimized in J774 macrophages using the lipid-based siPORT NeoFX transfection agent (Ambion, UK), GAPDH siRNA including negative control siRNA mixtures (CAT #: AM4624 Silencer® GAPDH siRNA (Human, Mouse, Rat) and 5 nmol + 2 nmol Negative Control 50 µM). Confluent monolayer of J774 macrophages in T25 flasks were resuspended by scrapping cells in 10 ml, complete DMEM. A 15µl of siPORT NeoFX transfection agent was diluted in 300 µl of OPTI-MEM I medium and incubated for 10 minutes at room temperature. Pre-designed GAPDH siRNA (RefSeq NM\_002046 (human), NM\_001001303 (mouse), and NM\_017008 (rat)) and negative control siRNA (Ambion's validated scrambled sequence siRNA) which has limited sequence similarity to the human, mouse, or rat genomes were both separately diluted in OPTI-MEM I medium to achieve a final concentration of 1 µM. The reaction mixtures of media and target siRNA were subsequently combined and incubated for 10 min to allow transfection complexes to form. The transfection complex (200µl/well) was then dispensed into a clean 6-well culture plate. The re-suspended J774 macrophages (2300 µl) cells were gently overlaid over the transfection complex mixture, a procedure referred to as reverse transfection. Culture plates were then gently tilted back and forth to achieve a uniform distribution of the transfection complex and cells in the plate.

Culture plates were eventually transferred into an incubator at 37°C and maintained under normal cell culture conditions for 24 hour. The existing media was replaced after 24 hrs with fresh complete DMEM and the cultures incubated for a further 24 hours. Cells from respective wells were harvested and total RNA extracted as previously described. Extracted RNA was treated with RNase-free DNase (Ambion) to get rid of residual DNA prior to RT assay. In addition a no "RT" and "water control" was included in the RT reaction. The resulting cDNAs were then subjected to real time PCR as previously described.

### 2.14.2 siRNA knockdown of JAK2

To investigate the effect of JAK2 knockdown in RASMCs were initially cultivated at passage 2 or 3 in a T-75 flask at 37°C, 5% CO<sub>2</sub> until confluent. Cell were then trypsinized and plated out at three plating densities (5 x 10<sup>3</sup>, 1 x 10<sup>4</sup>, 2.5 x 10<sup>4</sup> cells per well) so as to determine the optimal seeding density for the most efficient delivery of siRNA into cell. Within this parameter, we also investigated the concentration of DhF-2 that will achieve the most effective delivery of siRNA into each cell. All the cells were serum starved (1%FBS) in Opti-MEM (Invitrogen) media and cultured in both 96-well and 12-well plate formats. These cells were used to optimize conditions for siRNA delivery into cell in the complete absence of penicillin/streptomycin. After day two when cells had achieved 70-90 % confluency, media was changed and cells were transfected with 0.125 nM DharmaFECT (DhF) transfection reagent-2 in Opti-MEM containing 1%FBS.

Prior to the transfection studies, the MTT assay was carried out to determine the toxicity of DharmaFECT transfection reagent-2 on RASMCs. This was to establish the most appropriate concentration that could be used in the transfection experiments without resulting in cytotoxicity.

Using the forward transfection (FT) approach for gene silencing, RASMCs were seeded at 2.5x10<sup>4</sup> cells/L for 48 hours in cell culture incubator. On day 3, transfection complex were prepared as per manufacturer's instructions. Briefly, the following transfection mixes were prepared:

Tube A containing diluted 0.125 nM DharmaFECT (DhF) transfection reagent-2 in Opti-MEM with 1%FBS.

Tube B containing JAK2 siRNA (100 nM) diluted in Opti-MEM with 1%FBS.

Cells were incubated at 37 °C in 5% CO<sub>2</sub> for 24 hours and the transfection media replaced with fresh complete media for a further 24 hours prior to protein analysis. Lysates were prepared for western blotting as described in section 2.14 and JAK2

protein expression was assessed using a selective anti-JAK2 primary antibody (Santa Cruz Biotechnology, UK).

## **2.15 Total RNA Isolation**

Total RNA was prepared from confluent monolayers of cells using the RNA STAT60 reagent (AMC Biotechnology) as per manufacturers' instructions. This involved adding 2 ml of RNA STAT-60 to each T25 plate and incubating at room temperature for 10 min to allow lysis and complete dissociation of nucleoprotein complexes. Cell lysates were transferred into eppendorf tubes and 200 µl of chloroform per ml of RNA STAT-60 added to each tube. The mixture was then incubated for a further 5 min at room temperature. Each tube was vortexed for 15-20 sec, incubated for 10 min at room temperature and centrifuged at 4°C for 25 min at 12,000 rpm. The upper clear aqueous phase containing RNA was carefully removed and transferred into a new eppendorf tube. Total RNA was precipitated by adding 500 µl of isopropyl alcohol per ml of RNA STAT-60 to the clear supernatant and samples incubated at room temperature for 10 min before centrifuging at 4°C for 20 min at 10,000 rpm. The RNA pellet was washed three times with 75% ethanol, briefly air dried in the fume cupboard and re-dissolved in 50 to 100 µl of DNase free treated water depending on size of pellet. The quantity of RNA concentration was assessed using a UV spectrophotometer (Eppendorf Biophotometer, Germany) as described below.

## Spectrophotometric quantification of isolated RNA

RNA quantity and purity was determined using a spectrophotometer by determining the ratio of absorbance at 260 nm and at 280 nm ( $A_{260}/A_{280}$ ) in DDW. Absorbances were determined using a UV spectrophotometer (Eppendorf Biophotometer, Germany) at 260 (OD260) and 280 (OD280) nm and concentrations of RNA determined using the following equation:

$$\text{RNA concentration } (\mu\text{g}) = A_{\lambda 260} \times 40 \times \text{Dilution Factor}$$

Where

$A_{\lambda 260}$  is Absorbance of RNA

**40** represent the concentration in  $\mu\text{g ml}^{-1}$  of RNA in a solution with an **OD**<sub>λ260</sub> Of 1.

Measurements were carried out in triplicate, and had an average Coefficient Variation (CV) of less than 10%. The average purity (OD260/ OD280) of the samples was consistently above 1.75. RNA integrity was verified by electrophoresis in a 1% agarose gel in TAE buffer containing ethidium bromide. Each sample containing RNA was warmed up to 70° C for one minute and immediately placed on ice. RNA sample was then carefully loaded into designated wells. Gel electrophoresis was carried out at 10 V/cm to avoid RNA degradation during electrophoresis. The gel slab was then placed in a UV Gel Scan apparatus and examined for the presence of clear bands of 4.5 and 2.0 kb which represent 28S and 18S rRNA.

## **Determination of RNA integrity by gel electrophoresis**

Aliquots of extracted total RNA (1 to 2.5 µg) were run on a 1% non-denaturing agarose gel in Tris Borate EDTA buffer (TBE) (89 mM Tris-HCl pH 7.8, 89 mM borate, 2 mM EDTA) for 60 min at 80 volts. The gel was then stained with 0.5 µg/ml ethidium bromide to visualise the 28S and 18S ribosomal bands. RNA bands were visualized under UV light and image captured using a Syngene (Cambridge, UK) Gel Documentation Unit system which incorporates Syngene's software (GeneTools) for analysing the band quantities in 1D gel images.

### **2.16 PCR Primer design**

Primers for use in PCR analysis of iNOS and CATs were designed together with those for the house keeping genes including glyceraldehyde-3- phosphate dehydrogenase, (GAPDH) and Beta-2-microglobulin (B2M). These were all designed from respective published sequences obtained from the murine database with cross-reference to the National Center for Biotechnology Information (NCBI). The sequences retrieved are shown in Table 6.3:

**TABLE 2.2 Source of primers designed from NCBI database with GenBank Accession references.**

GENES	GenBank Accession (MURINE)	GenBank Accession (RATTUS)
CAT-1 [Slc7a1]	NM_007513.3	NM_013111
CAT2A & B [Slc7a2]	NM_007514.3	NM_022619
iNOS [NOS2]	NM_010927.2	NM_012611
y+LAT-1 [Slc7a7]	NM_011405	NM_031341
y+LAT-2 [Slc7a6]	NM_178798	NM_001107424
b+0 [Slc7a9]	NM_021291	NM_053929
GAPDH	NM_008084.2	NM_017008
B2M	NM_009735.3	NM_012512

Primers were designed with a melting temperature ( $T_m$ ) of  $60^\circ\text{C} \pm 2^\circ\text{C}$  using the FASTPCR and Molecular Beacon programs, ensuring the GC content of all primers was within the range of 40 – 60% and the primer length was no more than 18 -23 base pairs. Sequences generated (see Tables 6.4 and 6.5) were checked for hairpins, maximum permissible local alignment score between primer pairs or the primer itself (3' complementarity and self-complementarity) using the Oligonucleotide Properties calculator software. In addition the specificity of primers was assessed using BLAST and/or ClustaW.

The designed primer sequences used in both mouse and rat gene expressions are shown in Tables 6.4 and 6.5 respectively. Except for GAPDH and  $\beta$ -2-microglobulin all other housekeeping genes used in this thesis were purchased from PrimerDesign (UK).

**TABLE 2.3 Mouse primer sequence used in PCR analysis**

GENES	FORWARD PRIMER 5'-sequence-3'	FINAL CONC. (nM)	REVERSE PRIMERS 5'-sequence-3'	FINAL CONC. (nM)	ANNEALING TEMP (° C)
CAT1 (SLC7A1)	CTTCTTGATTGCTGCTCTC	250	AAGTACCGATGATGTAGGAG	250	61.0
CAT2A (SLC7A2A)	GCGTTTGAGTATGTCAGATGGAG	250	GCATAGATTACACGAGGCATTG G	250	59.0
CAT2B (SLC7A2B)	CCCGCCAAATATGTTGTCTCG	250	GACTGCCTCTTACTCACTCTTGC	250	59.8
iNOS (NOSII)	AACCAGTATTATGGCTCCTT	400	TCCTGTTGTTTCTATTTCCCTT	300	60.0
γ-LAT1	CCTTCTACTTCTTCATCATCAG	250	ACAACCTCCATCTTCCAA	250	60.0
γ-LAT2	ACACGAGTACAAGACACAT	250	CCAACCTGAGTAAGAGAAGA	250	60.0
b <sup>0</sup>	CCTCCTGCTGTGGTAGTGAAAC	250	AGTCCGCTGATGATGATGATGG	250	60.0
GAPDH	CTCCACTCACGGCAAATCAAC	250	GTAGACTCCACGACATACTCAG C	250	61.0
Beta-2- microglobulin	CTGGTCTTTCTGGTCTTGCTC	250	GCAGTTCAGTATGTTCCGGCTTCC	250	60.0

**Note:** All other Housekeeping primers used in this thesis were purchased from PrimerDesign (UK).

**TABLE 2.4 Rat primer sequences used in PCR analysis**

GENES	FORWARD PRIMER 5'-sequence-3'	FINAL CONC. (nM)	REVERSE PRIMERS 5'-sequence-3'	FINAL CONC. (nM)	ANNEALIN G TEMP. (° C)
CAT1 (SLC7A1)	TACTCTCCTGGCTTACTCT	250	CATCTCATTCTGGTCTACCT	250	61.0
CAT2A (SLC7A2A)	AGTCTTCTGGGTTCTATGTT	250	CTGCCTCTTACTCACTCTT	250	59.0
CAT2B (SLC7A2B)	CAATGCCTCGTGTAATCTATG	250	AGTAGCAATTATTGGTGTCTTC	250	59.8
iNOS (NOSII)	GGAAGAGGAACAACACTACTG	400	AAATACCGCATACCTGAAG	300	60.0
γ-LAT1	TAGCGATACCATCAACTCC	250	TCCATCTTCCAAGTCCATT	250	60.0
γ-LAT2	TCTTCTTACTCAGGTTGG	250	CTGCGTCACTCTTATGGA	250	60.0
bO+	AAGTGCTATCCTACATCAGT	250	CTCATCACAACGAGTCCTA	250	60.0
GAPDH	CAAGTTCAACGGCACAGTCAAG	250	ACATACTCAGCACCAGCATCAC	250	61.0
Beta-2- microglobulin	GCCGTCGTGCTTGCCATTC	250	CTGAGGTGGGTGGAACCTGAGAC	250	60.0

**Note:** All other Housekeeping primers used in this thesis were purchased from PrimerDesign (UK).

## 2.17 Reverse Transcription

Reverse transcription in combination with polymerase chain reaction is a powerful method currently used to quantify the level of gene expression (Bustin *et al.*, 2013; Horikoshi *et al.*, 1992; Murphy *et al.*, 1990). Ribonucleases are ubiquitous and are often the leading cause of RNA degradation during RNA isolation. Before the resulting RNA could be converted to cDNA we had to ensure that the extracted RNA is of high quality, intact and free of DNA contamination. To achieve this, the extracted RNA was initially treated with (2 U) RNase-free DNase 1 and 0.1 volumes of 10X DNase I Buffer to eliminate DNA from the RNA sample. Reverse transcription was then carried out using the ImProm-II Reverse Transcription System (Applied Biosystems). The first-strand was synthesised in 20 µl total reaction mixture in the presence of 1 U/µl recombinant RNasin ribonuclease inhibitor (20 U), although the addition of this enzyme is optional.

The RT reaction master mix was prepared by combining the following:

Reaction buffer (10X concentration) -	<b>2.0 µl</b>
ImProm-II™ Reverse transcriptase -	<b>2.0 µl</b>
Magnesium chloride -	<b>3.5 µl</b>
dNTPs	<b>2.0 µl</b>
Nuclease-free water -	<b>5.5 µl</b>

The mixture was carefully mixed with a pipette and briefly spun at 9000 rpm. A working stock of RNA was also generated by diluting RNA with nuclease-free water to create a working concentration of 0.1 mg/ml to 1 µg RNA. Transcription was first initiated by heating the template RNA (2.5 µl) and random hexamers (2.5 µl) for 5 minutes at 70°C to facilitate annealing of the random hexamers to the template. Each tube was quickly chilled on ice after a brief spin at 9000 rpm. This was then added to the RT master mix and subjected to 60 min incubation at 42 °C, followed by denaturing at 72°C for 10 min in order to deactivate the transcriptase enzyme.

## 2.18 Polymerase Chain Reaction

Polymerase Chain Reaction (PCR) was carried out after reverse transcription using the fluorogenic minor groove binding dye, Sybr green, in a reaction mixture (20  $\mu$ l) consisting of 10  $\mu$ l Power Sybr green master mix, 2  $\mu$ l each of both sense and antisense primers, 2  $\mu$ l of template cDNA (from 1 in 5 dilution of original stock cDNA generated) together with 4  $\mu$ l of DNA free water.

PCRs were performed on a Quantica real time machine (Techne. UK) using the 'hot-start' approach as follows:

AmpliTaq Gold polymerase activation at 95°C for 10 min

Template cDNA denaturing at 95°C for 15 sec

Annealing for 30 sec between 59 to 61°C (mean  $T_M$  used was 60 °C) depending on the primer used

Extension at 72°C for 10 sec

The annealing/extensions were allowed to progress through a maximum of 45 cycles, followed by dissociation at 58°C to 95°C and a final hold at 4°C

## Quantitative PCR analysis of Cationic amino acid transporters in both RASMCs and J774 macrophages

To investigate changes in target gene expression levels we used the relative quantification strategy to analyze the data generated from our PCR results. In these studies, it was mandatory to relate the changes in gene expression of the target gene to changes in control or non-treated cells. In addition both target gene in treated cells (activated cells) and control are normalized to a housekeeping (or Reference) gene (HKG). These HKGs are normally cellular maintenance genes selected from a panel using a procedure called normalization and is commonly used to normalize for the variability between samples. The relative quantities can thus be compared across multiple real time PCR experiments (Orlando *et al.*, 1998).

Analysis of the Q-PCR results was carried out by the comparative Threshold cycle (CT) method, also called the Delta-Delta CT method ( $2^{-\Delta\Delta CT}$ ) where

$$\Delta\Delta C_t = \Delta C_t (\text{sample}) - \Delta C_t (\text{reference})$$

Where

$\Delta C_t (\text{sample})$  is Ct values of test sample which has been normalized to the endogenous HKG or reference gene

$\Delta C_t (\text{reference})$  is Ct values of non-treated (control) sample which has been normalized to the endogenous HKG or reference gene

To ensure validity to the above equation both amplification efficiencies of the target gene and the HKG must be very similar.

The threshold cycle value represents the cycle at which there is an observable fluorescence emission far in excess of the background emission (Higuchi *et al.*, 1993). The threshold cycle analysis involves comparing threshold cycle (Ct) values of both the

target gene and the housekeeping gene. The threshold cycle value represents the cycle at which there is an observable fluorescence emission far in excess of the background emission (Higuchi *et al.*, 1993). By comparison, the Delta-Delta CT method assumes that PCR amplification is the same in both control and activated cells. In addition it is assumed that both have the same amplification profile. To further improve our amplification profile, we incorporate a mathematical model and analysed our data by adjusting for PCR efficiency differences as described by Pfaffl (Pfaffl, 2001).

## 2.19 Normalization of Housekeeping genes

At present real time RT-PCR is the most sensitive, precise and reproducible means of measuring target gene expression by using specific mRNA sequences (Bustin, 2000). It is also imperative in normalizing target gene expression that the housekeeping genes used for normalization shows minimal variation in its expression profile irrespective of the treatment or experimental conditions being employed. In effect, expression of the housekeeping gene must be stable and free from any form of influence from the existing experimental conditions. To determine which housekeeping gene was suitable for use in our studies, we investigated the expression pattern of nine commonly used housekeeping genes in both RASMCs and J774 macrophages. As shown in Table 2.5, these included  $\beta$ -2-microglobulin, glyceraldehyde-3-phosphate dehydrogenase, cyclophilin- $\beta$ , hypoxanthine ribosyltransferase, tyrosine 3-monooxygenase /tryptophan 5-monooxygenase activation protein zeta, calnexin, alpha Actin, ribosomal protein L13A, and Ubiquitin C. All except for the first two, HKGs were designed in house.

In this thesis, monolayer of cells with varying treatment conditions were subjected to RNA extraction and DNase I treatment (Ambion, UK) following manufacturer's instructions. Briefly, extracted total RNA samples from RASMCs were initially diluted in 0.2  $\mu$ g/ $\mu$ l of nuclease-free water. Prior to treatment, 50  $\mu$ l of resuspended RNA solution (0.2  $\mu$ g/ $\mu$ l) was aliquoted into a 0.5 ml reaction microcentrifuge tube and initially treated with 5  $\mu$ l of DNase I Buffer (0.1 volume) and 1  $\mu$ l of rDNase. The solution was mixed thoroughly and incubated a 37 °C for 30 minutes. For rigorous DNase treatment a further 1  $\mu$ l of rDNase was added, mixed and the incubation step repeated. Resuspended DNase Inactivation Reagent (0.1 volume) was added to resulting solution, gently mixed and incubated at room temperature for 2 minutes. Finally, the mixture was centrifuged at 10, 000 x g for 1.5 minutes and the upper layer containing pure RNA transferred into a fresh tube.

The RNA was quantified spectrophotometrically at 260 nm and its purity assessed using the 260/280 ratio. The integrity was determined by 1% agarose gel electrophoresis. Reverse transcription of DNase treated RNA samples followed by q-PCR analysis were subsequently carried out. Generated CT values of respective genes were analysed using Quansoft system software and the resulting data transformed

using their delta CT ( $\Delta$ CT) values into relative quantification data using geNORM analysis procedures. Real time reactions of the different products were assessed by dissociation curve or melting point analysis after each reaction.

**TABLE 2.5 Housekeeping genes used for normalisation in both murine J774 macrophages and RASMCs and their respective functions**

	<b>MOUSE</b>	<b>RAT</b>	<b>FUNCTION</b>
1	β2-Microglobulin (B2M)	β2-Microglobulin (B2M)	Component of Major histocompatibility complex
2	Cyclophilin (CYC)	Cyclophilin (CYC)	Protein folding-serine-threonine phosphatase inhibitor
3	Glyceraldehyde-3-phosphate dehydrogenase (GAPDH)	Glyceraldehyde-3-phosphate dehydrogenase (GAPDH)	Glycolytic pathway
4	Hypoxanthine ribosyltransferase (HPRT):	Hypoxanthine ribosyltransferase (HPRT):	metabolic salvage of nucleotides-translational control
5	Tyrosine 3-monooxygenase /tryptophan 5-monooxygenase activation protein, zeta (YWHAZ)	Tyrosine 3-monooxygenase /tryptophan 5-monooxygenase activation protein, zeta (YWHAZ)	Role in regulating insulin sensitivity
6	Calnexin (CANX)	Calnexin [CANX]	MHC binding protein [p88]
7	Alpha Actin (α-Actin)	Alpha Actin (α-Actin)	Major component of the cell cytoskeleton
8	Ribosomal protein L13A (RPL13A)	Ribosomal protein L13A (RPL13A)	Translational control in eukaryotic cells
9	Ubiquitin C (UBC)	Ubiquitin C (UBC)	Cell metabolism

## **2.20 STATISTICAL ANALYSIS**

All experiments were performed at least three times and data expressed as means  $\pm$  SEM as indicated. For data with multiple comparisons, data were analyzed by one-way ANOVA followed by Dunnett's test (in order to compare each treatment to control value). Where required, Student's t-tests were used for single comparisons between treatment and control. A difference was considered to be statistically significant when the P value was less than 0.05 ( $P < 0.05$ ).

**Chapter 3.        The effects of JAK inhibitors on the induction of nitric oxide synthesis and L-arginine transport**

### 3.1 INTRODUCTION

As highlighted in our main introduction (section 1.1.7 & 1.1.8), NO is an important mediator, widely involved in both the physiology and pathophysiology of the cardiovascular, nervous and immune systems (Moncada *et al.*, 1993; Nathan, 1992). Under normal physiological conditions NO production is at basal level but increase significantly in different pathophysiological states such as during local inflammation (i.e. atherosclerosis) or in systemic inflammation (sepsis and septic shock) (Titheradge, 1999). The main enzymes responsible for NO production include the constitutive isoforms, eNOS and nNOS, and the inducible isoform, iNOS. The former two are predominantly regulated through intracellular calcium/calmodulin following stimulation by various agents. The inducible NOS which is expressed and regulated following induction by cytokines, LPS or other pro-inflammatory mediators and its regulation seems to be predominantly transcriptional, involving an ever growing list of signaling kinases since it is not constitutively expressed in tissues except when induced. It is implicated in lethal and often very debilitating diseases including chronic Inflammation, sepsis, stroke, diabetes, arthritis and therefore a key therapeutic target. Unravelling the cascade of reactions leading to its expression and subsequent NO production could prove essential in developing strategies for treating disease states associated with this enzyme.

In this regard, considerable progress has been made in identifying key signaling molecules such as the MAPKs (Bhat *et al.*, 1999; Bhat *et al.*, 1998; Da Silva *et al.*, 1997), PKC (Bhatt *et al.*, 2010; Nakai *et al.*, 1998; Yoon *et al.*, 1994) and P13Ks (Guha *et al.*, 2002; Park *et al.*, 1997). Another pathway which may be important but as yet inconclusive is that involving the JAK/STAT pathway.

The JAK/STATs may be considered essential molecules through which cytokine induce iNOS expression. However, at present it is still unclear as to whether activation of the JAK/STAT pathway is critical for the induction of iNOS or indeed L-arginine transport which is co-induced with the enzymes in different cell systems. Although there is evidence that activation of JAK/STATs may be essential in LPS and IFN- $\gamma$  induced astroglial cells (Dell'Albani *et al.*, 2001) and in IL-1 $\beta$  and TNF- $\alpha$  induced rat VSMCs (Doi *et al.*, 2002) the extent and main components in the intracellular signals mediating iNOS

expression is far from being fully characterized. Moreover, preliminary studies in our group have demonstrated that AG490, a selective inhibitor of JAK2 (Meydan *et al.*, 1996) was without effect in activated smooth muscle cells. This indicates, at least in our hands, that JAK2 may not be essential for iNOS induction. This is however not in agreement with the studies highlighted above where a case for JAK2 involvement has been made. There are however three other JAK proteins and whilst JAK-1 or JAK-3 may not be required for iNOS expression the fourth, Tyk-2, remains a candidate which is yet to be implicated. To explore this, previous studies with AG490 have been extended using another pharmacological inhibitor, JAK inhibitor I which inhibits all four JAK proteins including Tyk-2 (Thompson *et al.*, 2002).

To establish unambiguously the role of the JAK/STAT pathway in our system, studies were conducted repeating those carried out previously using AG490 and in addition by using JAK inhibitor I which is a potent inhibitor of all four JAK family members. Furthermore, the activated status of JAK2 and Tyk-2, the two most likely kinases of this family likely to mediate the induction of iNOS, were also examined under different experimental conditions.

## **3.2 METHOD**

### **3.2.1 Experimental conditions**

Both RASMCs and J774 macrophages were cultured and maintained in complete DMEM as described in Chapter 2. When needed, cells were plated at the appropriate seeding densities and allowed to grow to confluence in either 96-or 6-well plates for nitrite measurement and L-arginine transport studies or for Western blotting respectively.

Each plate was pre-treated with either AG490 (0 to 10  $\mu$ M) or JAK inhibitor-I (0 to 10  $\mu$ M) for 30 minutes prior to stimulation with 100  $\mu$ g/ml LPS and 100 U/ml IFN- $\gamma$  (RASMCs) or 1  $\mu$ g/ml LPS alone (J774 macrophages) for a further 24 hours.

### **3.2.2 Determination of drug effects on nitrite production**

The effects of AG490 or JAK inhibitor I on induced NO production was assessed by determining changes in accumulated nitrite levels at the end of each incubation period using the Griess assay described in Section 2.9 (Chapter 2).

### **3.2.3 Drug effects on L-arginine transport**

Changes in L-arginine transport were assessed on the cell monolayer as described in Section 2.10 (Chapter 2). These studies were carried out after removing the culture medium for nitrite measurements and further investigations were carried out in parallel with those aimed at determining the effects of AG490 and JAK inhibitor I on NO synthesis.

### 3.2.4 Drug effects on iNOS expression by western blotting

At indicated time points, cells were rapidly washed with ice-cold phosphate-buffered saline (PBS) containing 2 mM sodium orthovanadate. For Phospho-JAK2 and Phospho-TYK2 western blot, the cells were solubilized in cold lysis buffer containing 1% Triton X-100, 150 mM NaCl, 50 mM Tris pH 7.5, 1.0 mM EDTA, 1.0 mM phenylmethylsulfonylfluoride, 2 mM sodium orthovanadate, 80  $\mu$ M leupeptin, 1  $\mu$ g/mL aprotinin, 1 mM NaF, 2 mM sodium pyrophosphate, 0.25% sodium deoxycholate. Lysates generated were processed and subjected to western blotting as described in Section 2.13 (Chapter 2)

### 3.2.5 Determination of drug cytotoxicity

In these studies, cells were incubated at the end of the 24 hour activation period with 0.5 mg/ml MTT diluted in complete DMEM. Cell viability was subsequently determined by the MTT assay as described in Section 2.12 (Chapter 2).

## 3.3 STATISTICAL ANALYSIS

All experiments were performed three times and data expressed as **means  $\pm$  SEM** as indicated. For data with multiple comparisons, statistical analysis was carried out with Graph Pad Prism (Graph Pad software, USA) and analyzed by using one-way ANOVA followed by Dunnett's test (in order to compare each treatment to control value). Where required, Student's t-tests were used for single comparisons between treated and control groups. Statistical significance was established at  $P < 0.05$ .

## 3.4 RESULTS

### 3.4.1 Morphological characterization of J774 macrophage cells

The characterization of the J774 macrophages was through identification of their characteristic rounded shape, their pattern of growth and general morphology. Following initial plating of cells in T-75 Flask, cells quickly attached within 1-2 hours and started to divide within 12-24 hours especially in areas where they formed clusters (Figure 3.1). This growth pattern was observed in all cultures and cells reached 60-70% confluency within 2-3 days.



**Figure 3.1 Inverted phase contrast micrograph showing the morphology of murine J774 macrophage cells cultured in complete DMEM.**

J774 macrophage cells were cultured in DMEM supplemented with 10% FBS, 100 U/ml penicillin and 100 µg/ml streptomycin in T-75 tissue culture flask. Cultures were viewed using a Nikon TMS inverted microscope at 200X magnification and the figure above represents the morphology of the cells in culture.

### **3.4.2 Morphological and biochemical characterization of rat cultured aortic smooth muscle cells (RASMCs)**

Rat smooth muscle cells were identified on the basis of their growth pattern and morphological characteristics. Cells attached within 1-3 hrs following initial plating and started to divide within 18-24 hours especially in areas where they formed clusters and reaching between 60 to 70% confluent within 2-3 days. In terms of their morphology, the cells looked spindle shaped and showed the characteristic 'hill and valley'-like pattern with increasing density. These were observed in all cultures of RASMCs. Further biochemical characterization was carried out to ensure specificity of the cell type. Cells were characterized by immunoassaying for  $\alpha$ -actin. As shown in Figure 3.3, cultures routinely isolated stained positively for  $\alpha$ -actin confirming these cells as being smooth muscle. Cross staining of the cells with Dil-labelled acetylated low density lipoproteins (Dil-Ac-LDL) proved negative, discounting any possible cross contamination with endothelial cells and thus confirmed isolated pure populations of smooth muscle cells in our experiments.

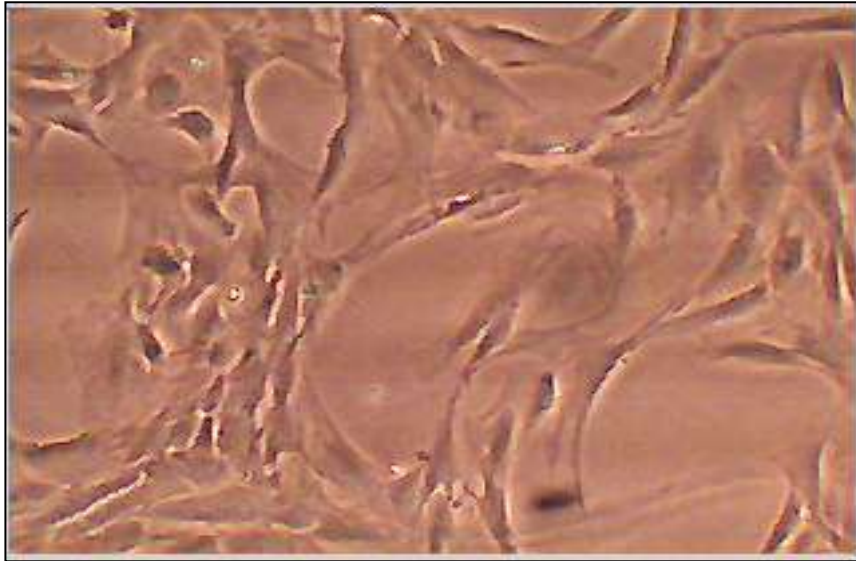


**Figure 3.2 Inverted phase contrast micrograph showing the morphological characteristics of rat smooth muscle cells cultured in complete DMEM.**

Isolated cells were cultured in DMEM supplemented with 5% FBS, 100 U/ml penicillin and 100 $\mu$ g/ml streptomycin in T-75 tissue culture flask. Cultures were examined using a Nikon TMS inverted microscope at 200X magnification and the figure above represents the morphology of the cells in culture.

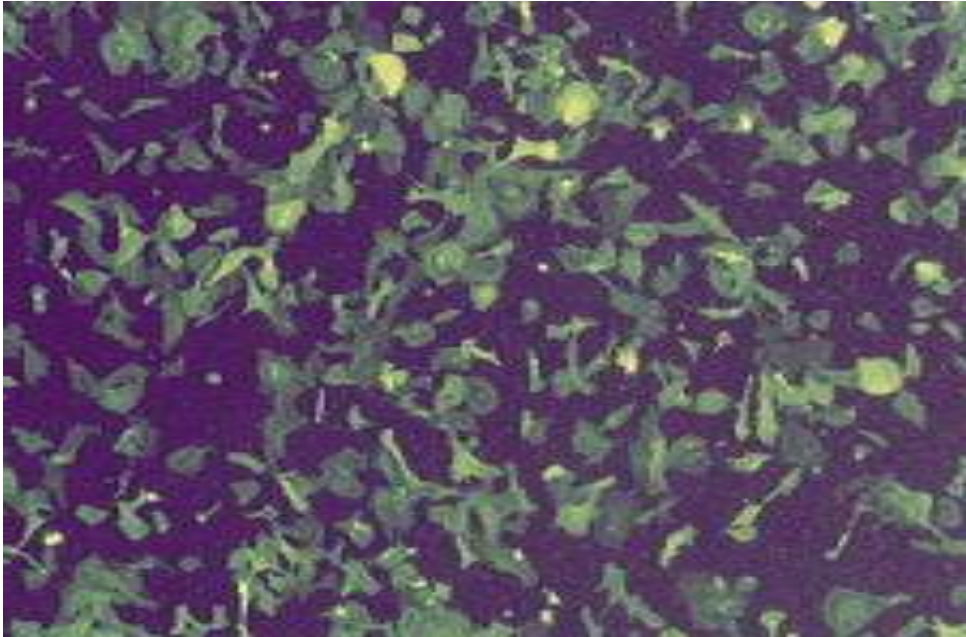


**Figure 3.3 Positive identification of rat cultured smooth muscle cells by staining for alpha-actin.**

Cultures of rat aortic smooth muscle cell routinely isolated were stained for  $\alpha$ -actin expression using the FITC labelled  $\alpha$ -actin monoclonal antibody as previously described in Methods (Section 2.6). The above figure was taken using a Nikon Quadfluor Episcopic Fluorescence EFD-3 microscope under UV with a FITC Filter at 400X magnification. The picture is representative of at least four experiments carried out randomly over the period of the studies.

### **3.4.3 Nitrite production following activation of both J774 macrophages and RASMCs**

The effects of IFN- $\gamma$  and/or LPS or LPS alone on nitrite production in RASMCs and J774 macrophages were assessed respectively. Nitrite accumulation in the cell culture media was used as an indication of NO production. Treatment of RASMCs with LPS and IFN- $\gamma$  or J774 macrophages with LPS alone resulted in significant increases despite marked differences in levels of nitrite production. The results obtained in Figure 3.4 showed that stimulation of RASMCs with LPS (100  $\mu\text{g/ml}$ ) together with IFN- $\gamma$  (100 U/ml) resulted in a significant increase in nitrite levels ( $p < 0.05$ ) with peak levels of about 55.0 nM after a 24-hour incubation period. Basal levels of nitrite under control experimental conditions average not more than 5.0 nM. By comparison, activation of RASMCs with either LPS (100  $\mu\text{g/ml}$ ) or IFN- $\gamma$  (100 U/ml) alone caused a small but statistically non-significant increase in nitrite production ( $p > 0.05$ ) when compared to control cells. Activation of cells with either LPS or IFN- $\gamma$  alone resulted in an average nitrite production of 8.0 nM and 13 nM respectively (Figure 3.4).

Control J774 macrophages (as shown in Figure 3.5) produced, on average, 3 nM nitrite under basal conditions. Activation of these cells with 1.0  $\mu\text{g/ml}$  LPS produced a peak average nitrite of up to 85.0 nM. This represents roughly a two-fold increase in comparison with that in RASMCs. However activation of cells with IFN- $\gamma$  alone induced marginal production of nitrite which was not statistically different from the basal control levels ( $p > 0.05$ ). When macrophages were activated with 10  $\mu\text{g/ml}$  LPS there was a significant increase (90.0 nM;  $p < 0.001$ ) in nitrite production above basal. This increase was however only marginally higher than that seen with 1.0  $\mu\text{g/ml}$  LPS (as shown in Figure 3.5) and at 10  $\mu\text{g/ml}$  LPS caused significant cytotoxicity in cells. The concentrations used in further studies in this thesis were therefore limited to 1  $\mu\text{g/ml}$  in macrophages.

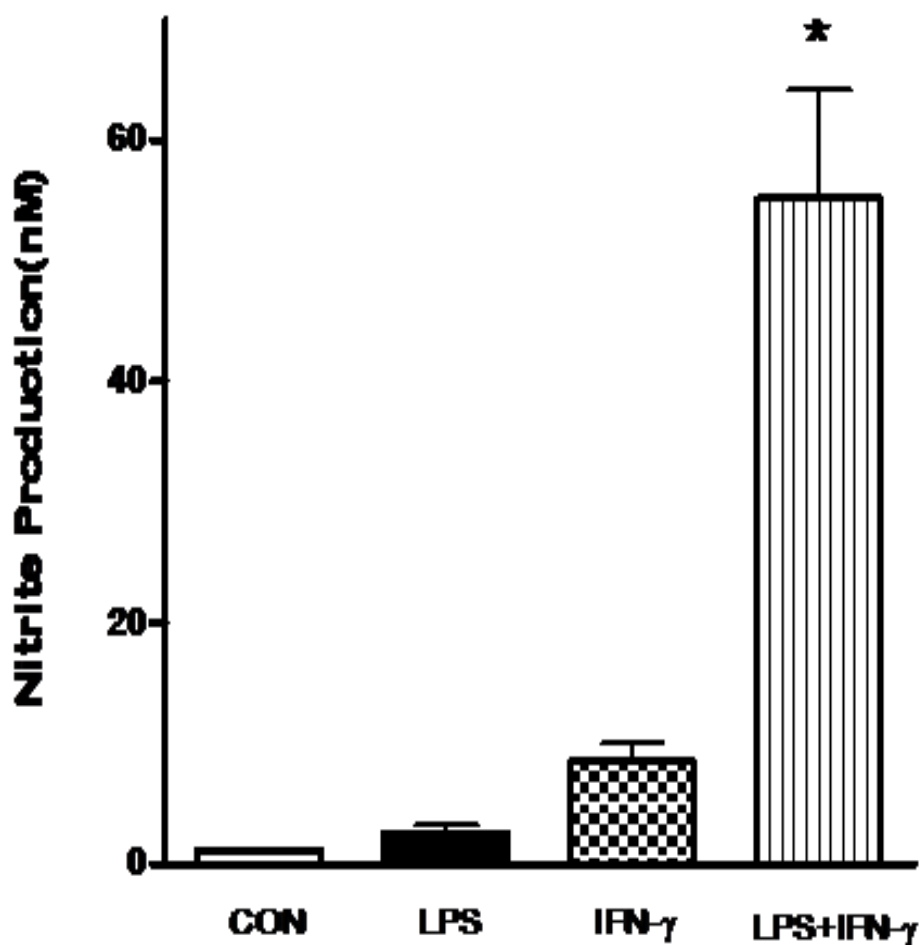


**Figure 3.4 Comparison of different activators on nitrite production in RASMCs.**

Confluent monolayer of RASMCs in complete DMEM were stimulated with LPS (100  $\mu\text{g/ml}$ ) alone, IFN- $\gamma$  alone (100 U/ml) or a combination of both LPS (100  $\mu\text{g/ml}$ ) and IFN- $\gamma$  (100 U/ml) for 24 hours. Controls were incubated in complete DMEM only. The stable NO metabolite, nitrite, present in the medium was analysed using the Greiss assay as described in Method (Section 2.9). The data represents the **mean  $\pm$  S.E.M.** obtained from three independent experiments, each with six replicates. Statistical differences between means were determined using one-way analysis of variance (ANOVA) followed by Dunnett's multiple comparisons test of the normalized data. \* denotes  $P < 0.001$  when compared to untreated control.

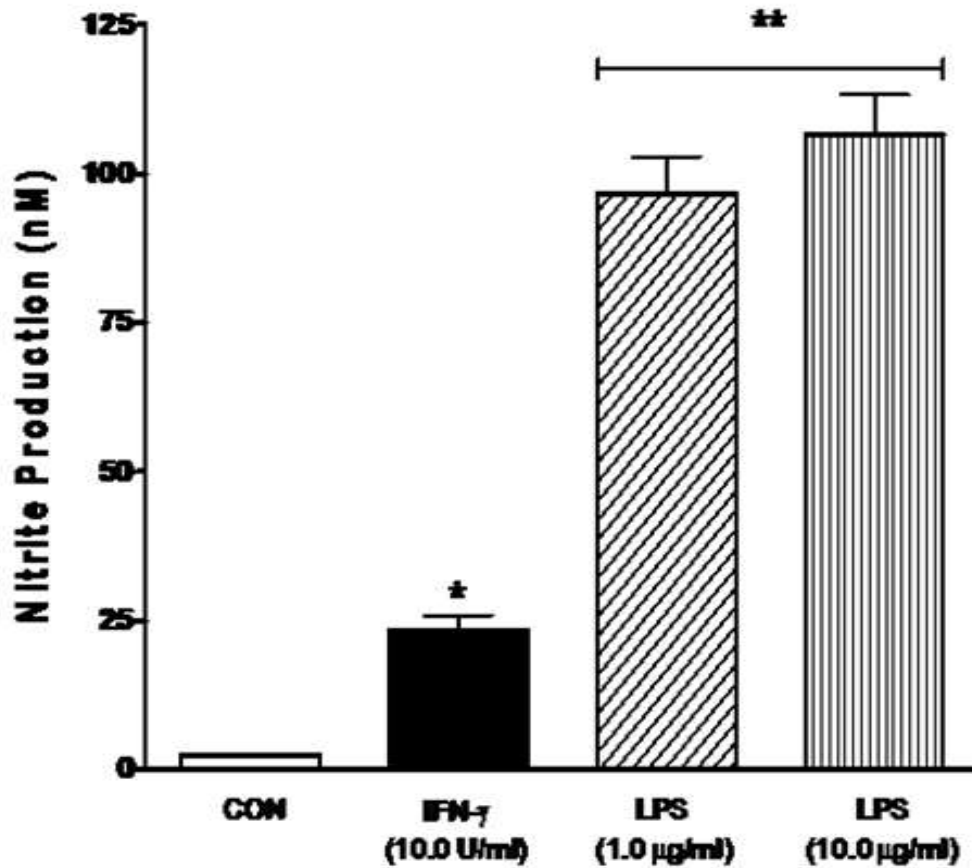


**Figure 3.5 Effects of different activators on nitrite production in J774 macrophages.**

Confluent monolayer of J774 macrophages in complete DMEM were stimulated with IFN- $\gamma$  (10.0 U/ml) or with LPS (1.0  $\mu$ g/ml or 10.0  $\mu$ g/ml) for 24 hours. Controls were incubated in complete culture medium only. The stable NO metabolite, nitrite, present in the medium was analysed using the Greiss assay as described in Method (Section 2.9). The data represents the **mean  $\pm$  S.E.M.** obtained from three independent experiments, each performed with five replicates. Statistical differences between means were determined using one-way analysis of variance (ANOVA) followed by Dunnett's multiple comparisons test of the normalized data. \* & \*\* denotes  $P < 0.05$  and  $P < 0.001$  respectively when compared to untreated controls.

#### **3.4.4 Inducible Nitric Oxide Synthase expression in J774 macrophages and RASMCs following activation**

The expression of iNOS protein increased progressively following the induction by LPS and IFN- $\gamma$  or by LPS alone. Results from western blots shown below demonstrate that iNOS expression is induced in both RASMCs (Figure 3.6) and J774 macrophages (Figure 3.7) following a 24 hours incubation with a combination of IFN- $\gamma$  (100 U/ml) and LPS (100  $\mu$ g/ml) or LPS (1.0  $\mu$ g/ml) alone respectively. As expected, there was negligible or no expression of iNOS in control cells.

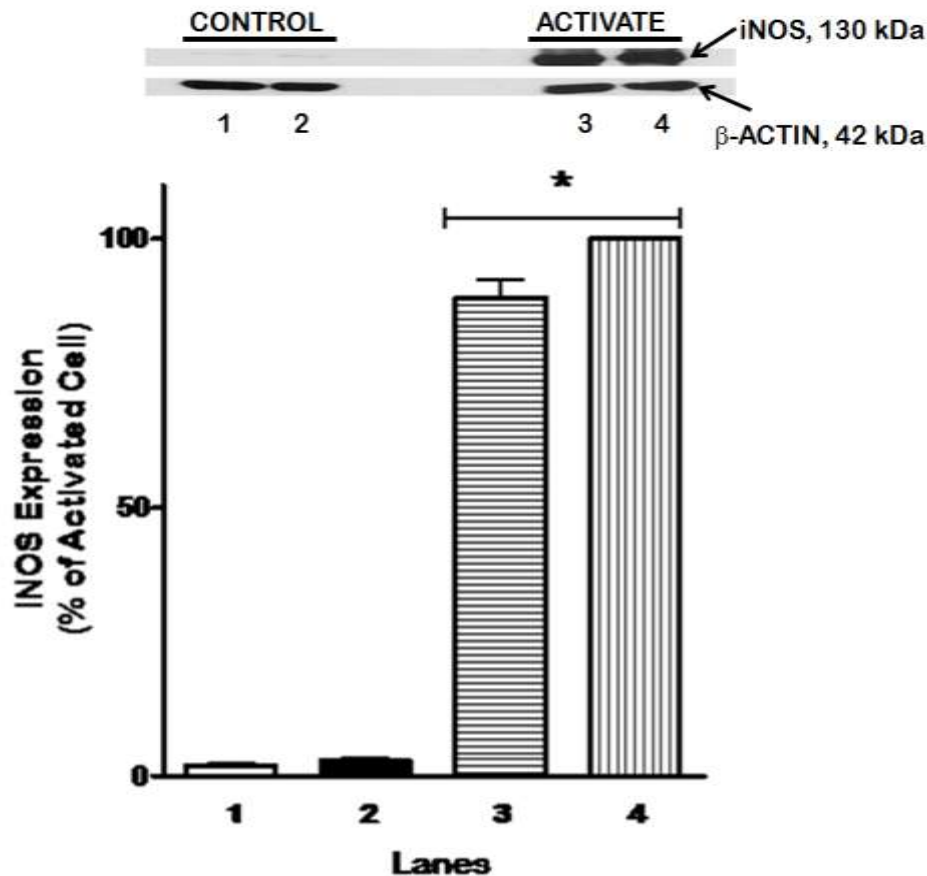


**Figure 3.6 Induction of iNOS expression in control and activated RASMCs.**

Confluent monolayer of RASMCs in 6-well plates were incubated with either complete DMEM alone (Controls=Lanes 1 and 2) or in complete DMEM with a combination of LPS (100  $\mu\text{g/ml}$ ) and IFN- $\gamma$  (100 U/ml) (Activated cells=Lanes 3 and 4) for a further 24 hours. Whole cell lysates (20  $\mu\text{g}$ ) generated were subjected to western blotting using a specific anti-iNOS antibody as described in the Methods (section 2.13). A representative western blot is shown in Figure A. Respective band intensities were quantified by densitometric analysis and normalized to  $\beta$ -actin protein (Figure B). The data is transformed and presented as percentage of relative intensity of the maximum expression of iNOS protein. Data represent the **mean  $\pm$  S.E.M.** from three independent experiments. Statistical differences between means were determined using one-way analysis of variance (ANOVA) followed by Dunnett's multiple comparisons test of the normalized data. \* denotes  $P < 0.001$  when compared to untreated controls.

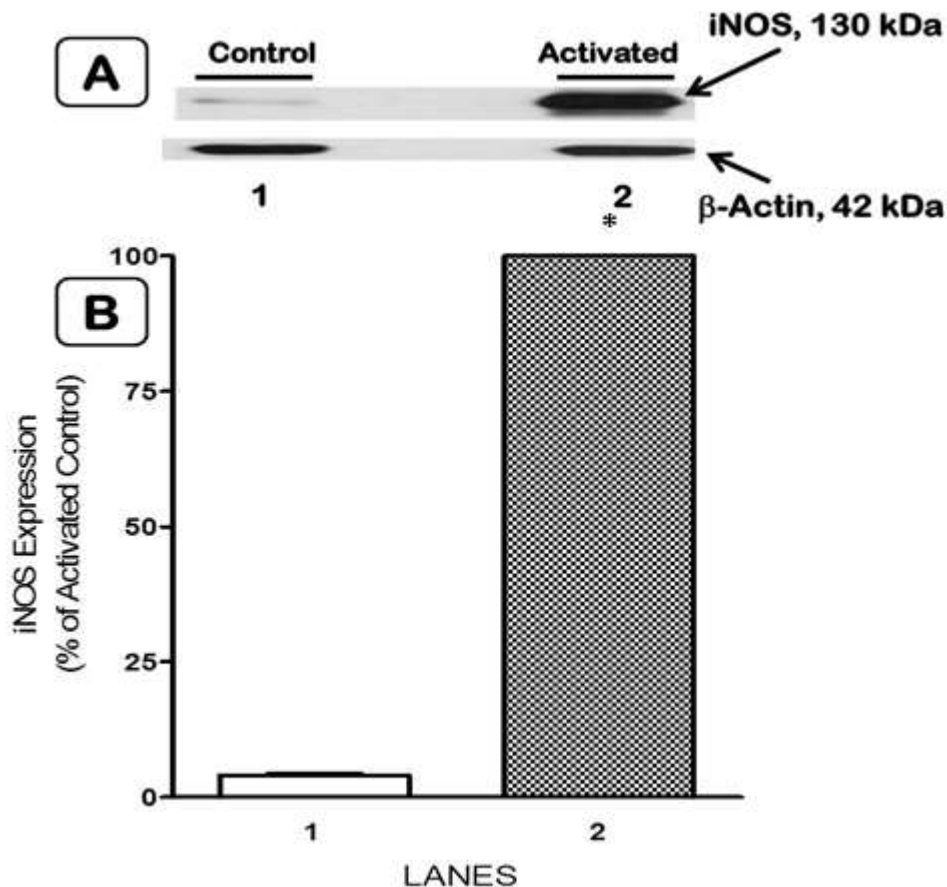


**Figure 3.7 Induction of iNOS expression in both control and activated J774 macrophages.**

Confluent monolayer of J774 macrophages in 6-well plates were incubated with either complete DMEM alone (Control=Lane 1) or in complete DMEM with LPS (1.0  $\mu\text{g/ml}$ ) (Activated=Lane 2) for further 24 hours. Whole cell lysates (20  $\mu\text{g}$ ) generated from cells with respective treatment conditions were subjected to western blotting using a specific anti-iNOS antibody as described in the Methods (section 2.13). A representative western blot is shown in Figure A. Respective band intensities were quantified by densitometric analysis and normalized to  $\beta$ -actin protein (Figure B). The data is transformed and presented as percentage of relative intensity of the maximum expression of iNOS protein. Data represent the **mean  $\pm$  S.E.M.** from three independent experiments. Statistical differences between means were determined using one-way analysis of variance (ANOVA) followed by Dunnett's multiple comparisons test of the normalized data. \* denotes  $P < 0.05$  when compared to untreated controls.

### **3.4.5 Time course induction of iNOS and NO production in activated RASMCs and J774 macrophages**

The induction of both iNOS and NO production in activated RASMCs and J774 macrophages followed a time course. As illustrated in Figures **3.8A** and **3.9A**, the time course of activation of NOS peaked after 24 hours following stimulation in both RASMCs and J774 macrophages. In J774 macrophages basal expression of iNOS following stimulation was detected after 9 hours of exposure to LPS (1.0 µg/ml). In contrast iNOS expression in RASMCs was apparent after only 6 hours following induction LPS (100 µg/ml) and IFN-γ (100 U/ml).

NO production also showed a similar trend as shown in Figures **3.8B** and **3.9B**, by increasing its production with time and peaked at 24 hours in both J774 macrophages and RASMCs. This occurred after a lag phase of about six hours and increased significantly thereafter till 24 hours after activation.

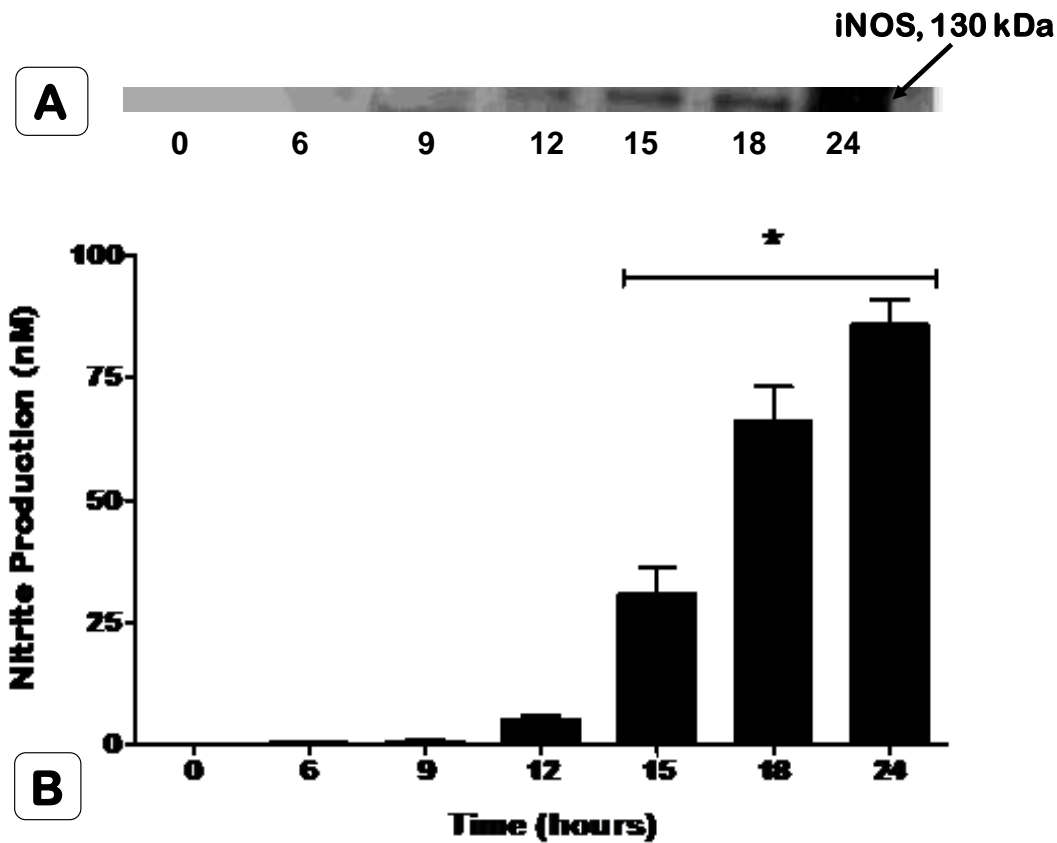


**Figure 3.8** Time dependent increase in iNOS expression [A] and nitrite production [B] in activated J774 macrophages.

Confluent monolayer of J774 macrophage in 6-well plates in complete DMEM were stimulated with LPS (1.0  $\mu\text{g/ml}$ ) alone at different time point as indicated above. Cells were lysed at the respective time points and 40  $\mu\text{g}$  of total protein subjected to western blotting as described in the Methods (section 2.13). The stable NO metabolite, nitrite, present in the medium at the indicated time points was analysed using the Greiss assay (Figure B) as described in the Method (Section 2.9). The data is presented as percentage of nitrite production by activated cells. Data represent the **mean  $\pm$  S.E.M.** from three independent experiments with five replicates in each. Statistical differences between means were determined using one-way analysis of variance (ANOVA) followed by Dunnett's multiple comparisons test of the normalized data. \* denotes  $P < 0.05$  when compared to non activated control.

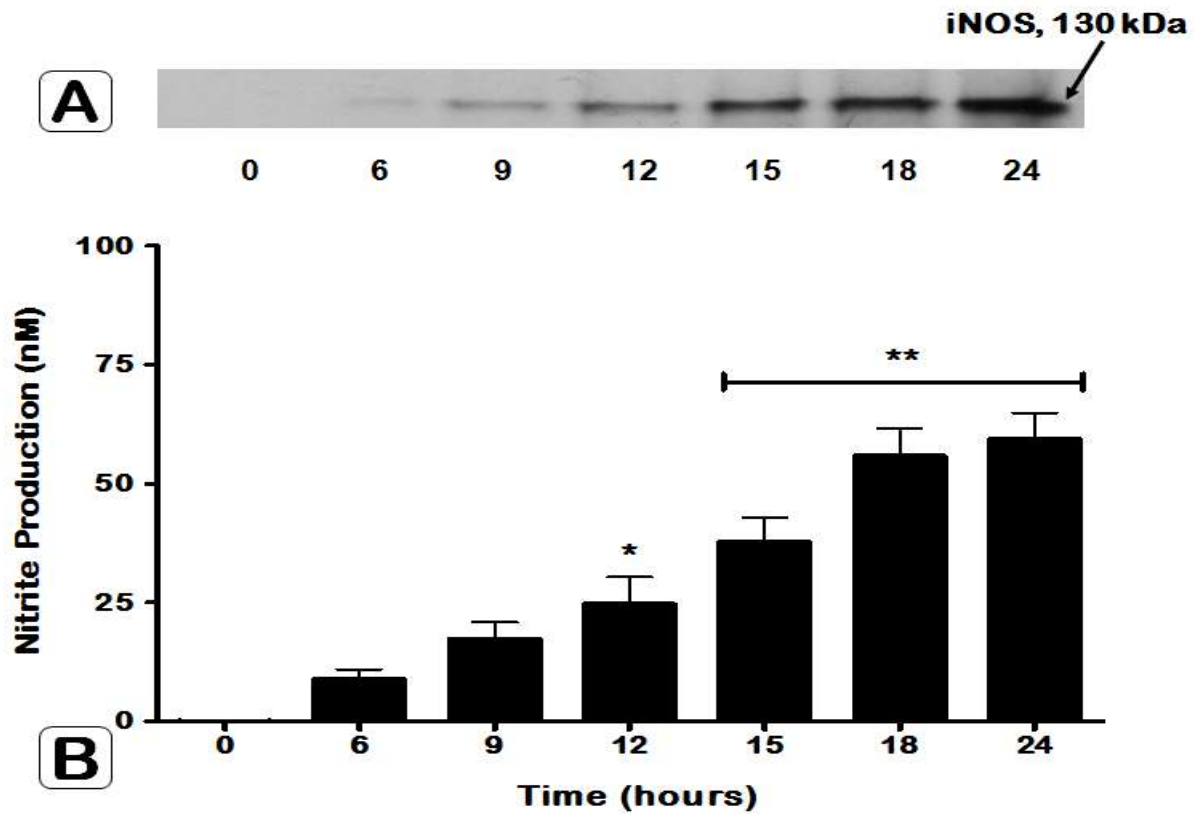


**Figure 3.9** Time dependent increase in iNOS expression [A] and nitrite production [B] in activated RASMCs.

Confluent monolayer of RASMCs in 6-well plate in complete DMEM were stimulated with a combination of LPS (100  $\mu\text{g/ml}$ ) and IFN- $\gamma$  (100 U/ml) at different time point as indicated above. Cells were lysed at the respective time points and 40  $\mu\text{g}$  protein subjected to western blotting as described in the Methods (section 2.13). The blot (Figure A) is representative of iNOS expression three independent experiments. The stable NO metabolite, nitrite, present in the medium at the indicated time points was analysed using the Greiss assay (Figure B) as described in the Methods (Section 2.9). Data represent the **mean  $\pm$  S.E.M.** from at least three independent experiments with five replicates in each. Statistical differences between means were determined using one-way analysis of variance (ANOVA) followed by Dunnett's multiple comparisons test of the normalized data. \* & \*\* denotes  $P < 0.05$  and  $P < 0.01$  respectively when compared to non activated control.

#### **3.4.6 Effects of JAK inhibitor I and AG490 on nitrite production in both RASMCs and J774 macrophages**

In order to further characterize the involvement of the JAK/STAT pathway in iNOS induction we used a pharmacological approach and investigated the effects of JAK inhibitor I or AG490 on nitrite production in both RASMCs and J774 macrophages. The results obtained indicate that treatment of RASMCs with JAK inhibitor I (0.01 to 10.0  $\mu$ M) for 30 minutes prior to activation with LPS (100  $\mu$ g/ml) and IFN- $\gamma$  (100 U/ml) resulted in a significant decrease ( $p < 0.01$ ) in nitrite production. This occurred in a concentration dependent manner and the most significant decrease (approximately down to 38.6%) was with a concentration of 10.0  $\mu$ M (Figure **3.10**). Similarly, JAK inhibitor I concentration-dependently inhibited nitrite production in LPS (1  $\mu$ g/ml) activated J774 macrophages, reducing this by 85 % at 10  $\mu$ M (Figure **3.11**). In contrast AG490 was without effect in both cell types with very marginal (15% reduction) non-concentration dependent inhibition of nitrite production in either RASMCs (Figure **3.12**) or J774 macrophages (Figure **3.13**). In addition there was no significant change in nitrite production in non-activated cells incubated with either JAK inhibitor I (Figures **3.10** and **3.11**) or with AG490 (Figures **3.12** and **3.13**) in respective cells.

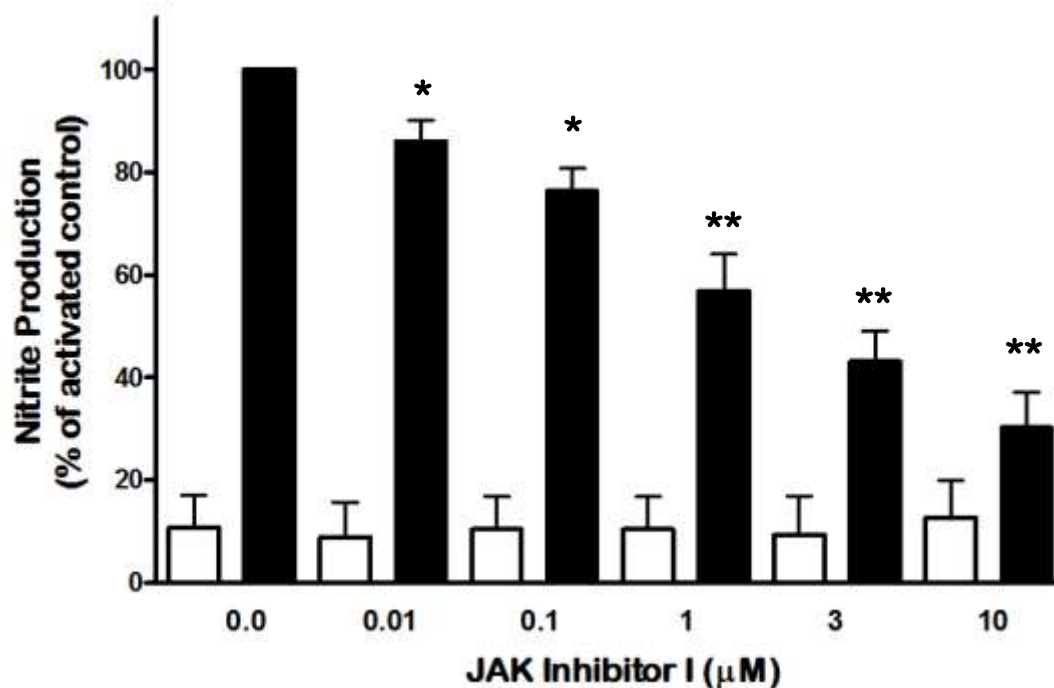


**Figure 3.10 Concentration-dependent effect of JAK Inhibitor I on nitrite production in both control and activated RASMCs.**

Confluent monolayers of RASMCs in 6-well plates in either complete DMEM alone (Controls) or in complete DMEM with different concentrations of JAK inhibitor I (0.01 to 10 µM) for 30 minutes prior to activation. Cells were activated with LPS (100 µg/ml) and IFN- $\gamma$  (100 U/ml) in the absence and continued presence of JAK inhibitor I for 24hours. The stable NO metabolite, nitrite, present in the medium was analysed using the Greiss assay as described in the Methods (section 2.9). The data is presented as percentage of nitrite production by activated cell (activated control). Data represent the **mean  $\pm$  S.E.M.** from at least three independent experiments, each with five replicates. Statistical differences between means were determined using one-way analysis of variance (ANOVA) followed by Dunnett's multiple comparisons test of the normalized data. \* & \*\* denotes  $P < 0.05$  and  $P < 0.01$  respectively when compared to untreated activated control.

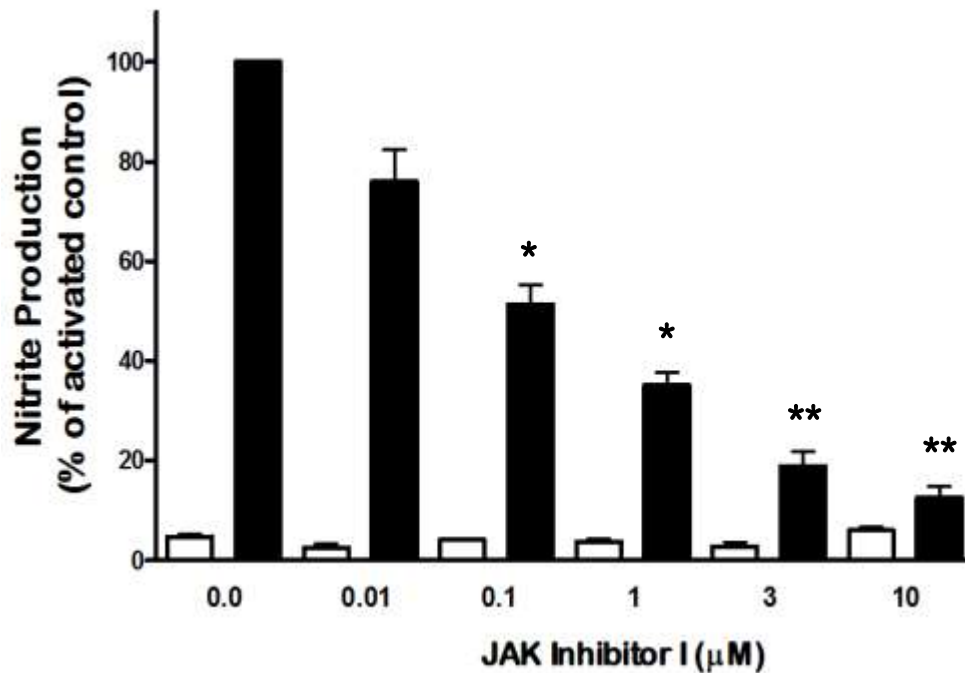


**Figure 3.11 Concentration-dependent effect of JAK-inhibitor I on nitrite production in both control and activated J774 macrophages.**

Confluent monolayers of J774 macrophages in 6 well plates in either complete DMEM alone (Controls) or in complete DMEM with different concentrations JAK inhibitor I (0.01 to 10 µM) for 30 minutes prior to activation. Cells were activated with LPS (1.0 µg/ml) in the absence and continued presence of JAK inhibitor I for 24hours. The stable NO metabolite, nitrite, present in the medium was analysed using the Greiss assay as described in the Methods (Section 2.9). The data is presented as percentage of nitrite production by activated cell (activated control). Data represent the **mean ± S.E.M.** from three independent experiments with five replicates. Statistical differences between means were determined using one-way analysis of variance (ANOVA) followed by Dunnett's multiple comparisons test of the normalized data. \* & \*\* denotes  $P < 0.05$  and  $P < 0.001$  respectively when compared to untreated activated control.

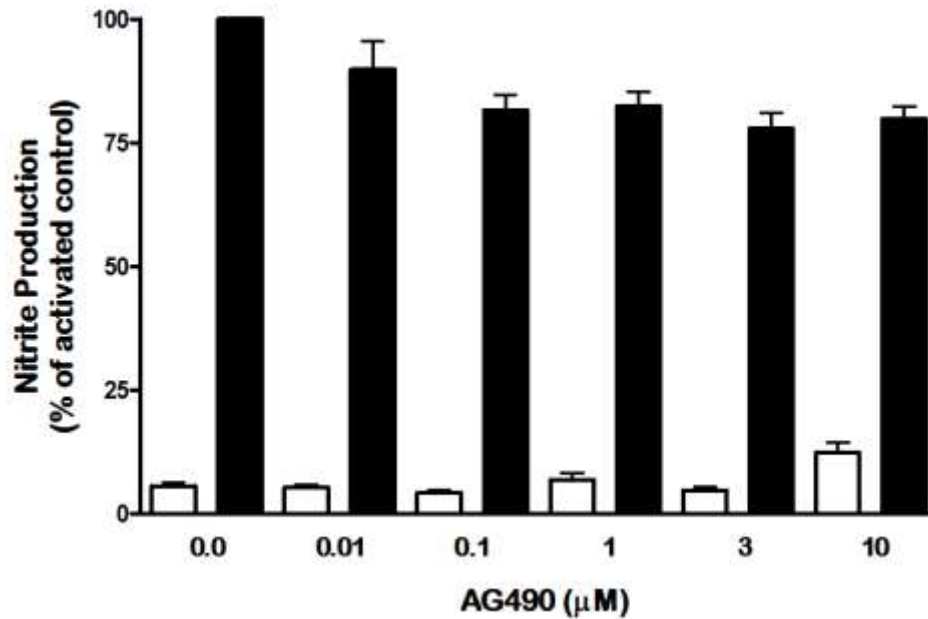


**Figure 3.12 Concentration-dependent effect of AG490 on nitrite production in both control and activated RASMCs.**

Confluent monolayer of RASMCs in 6 well plates was treated in either complete DMEM alone (Controls) or in complete DMEM with different concentrations of AG490 (0.01 to 10 μM) for 30 minutes prior to activation. Cells were activated with LPS (100.0 μg/ml) and IFN-γ 100.0 U/ml) in the absence and continued presence of AG490 for 24 hours. The stable NO metabolite, nitrite, present in the medium was analysed using the Greiss assay as described in the Methods (section 2.9). The data is presented as percentage of nitrite production by activated cell (activated control). Data represent the **mean ± S.E.M.** from three independent experiments each with 5 replicates. Statistical differences between means were determined using one-way analysis of variance (ANOVA) followed by Dunnett's multiple comparisons test of the normalized data.  $P > 0.05$  confirmed there was no significant difference when compared to untreated activated control.

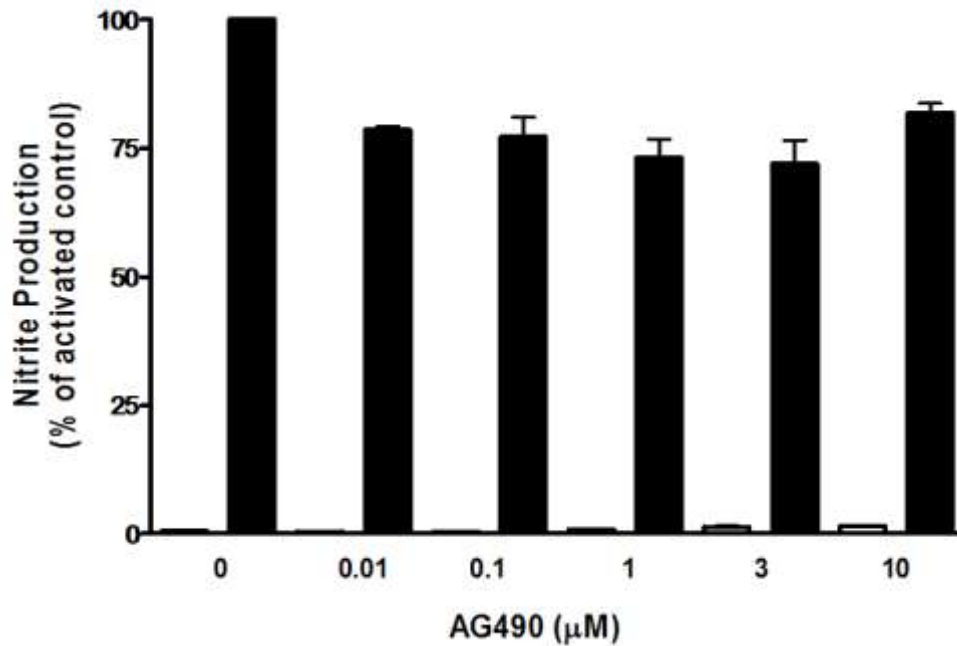


**Figure 3.13 Concentration-dependent effect of AG490 in nitrite production in both control and activated J774 macrophages.**

Confluent monolayers of J774 macrophages in 6 well plate in either complete DMEM alone (Controls) or in complete DMEM with different concentrations AG490 (0.01 to 10 μM) for 30 minutes prior to activation. Cells were activated with LPS (1.0 μg/ml) in the absence and continued presence of AG490 inhibitor for 24hours. The stable NO metabolite, nitrite, present in the medium was analysed using the Greiss assay as described in the methods. The data presented as percentage of nitrite production by activated cell without inhibitor treatment (activated control). Data represent the **mean ± S.E.M.** from three independent experiments each with five replicates. Statistical differences between means were determined using one-way analysis of variance (ANOVA) followed by Dunnett's multiple comparisons test of the normalized data.  $P > 0.05$  confirmed there was no significant difference when compared to untreated activated control.

### **3.4.7 Effects of JAK inhibitor I and AG490 on iNOS expression in RASMCs and J774 macrophages**

Western blot analysis was carried out to determine whether JAK inhibitor I or AG490 altered expression of iNOS in RASMCs. Our earlier results showed that stimulation of RASMCs with LPS (100 µg/ml) and IFN-γ (100 U/ml) resulted in the induction of iNOS protein expression (Figure 3.6) which was not detectable in control non-activated cells. Pre-treatment of cells with JAK inhibitor I prior to activation concentration dependently inhibited iNOS expression (Figure 3.14) in RASMCs and this occurred over the same concentration range that inhibited nitrite production. However in non-activated cells, pre-treatment with JAK inhibitor I (Figure 3.15) resulted in complete lack of iNOS protein expression. In contrast, pre-treatment with AG490 followed by activation with LPS (100 µg/ml) and IFN-γ (100 U/ml) caused no significant change in iNOS expression (Figure 3.16). This is also consistent with its lack of effect on nitrite production as described earlier. There was in addition no iNOS protein expression in non activated RASMCs following treatment with AG490 (as shown in Figure 3.17).

Similarly, J774 macrophages exposure to LPS (1.0 µg/ml) resulted in iNOS expression (Figure 3.18) which as in RASMCs was not detected in non-activated controls (Figure 3.19). Treatment of these cells with JAK inhibitor I prior to activation with LPS (1.0 µg/ml) resulted in a significant ( $p < 0.001$ ) concentration dependent decrease in iNOS expression (Figure 3.20). There was in addition, no significant change in iNOS expression when macrophages were treated with AG490 inhibitor, 30 min prior to activation with LPS (1.0 µg/ml) (Figure 3.24). With both inhibitors, there was no change in iNOS expression in non activated controls (Figure 3.23 and Figure 3.25).

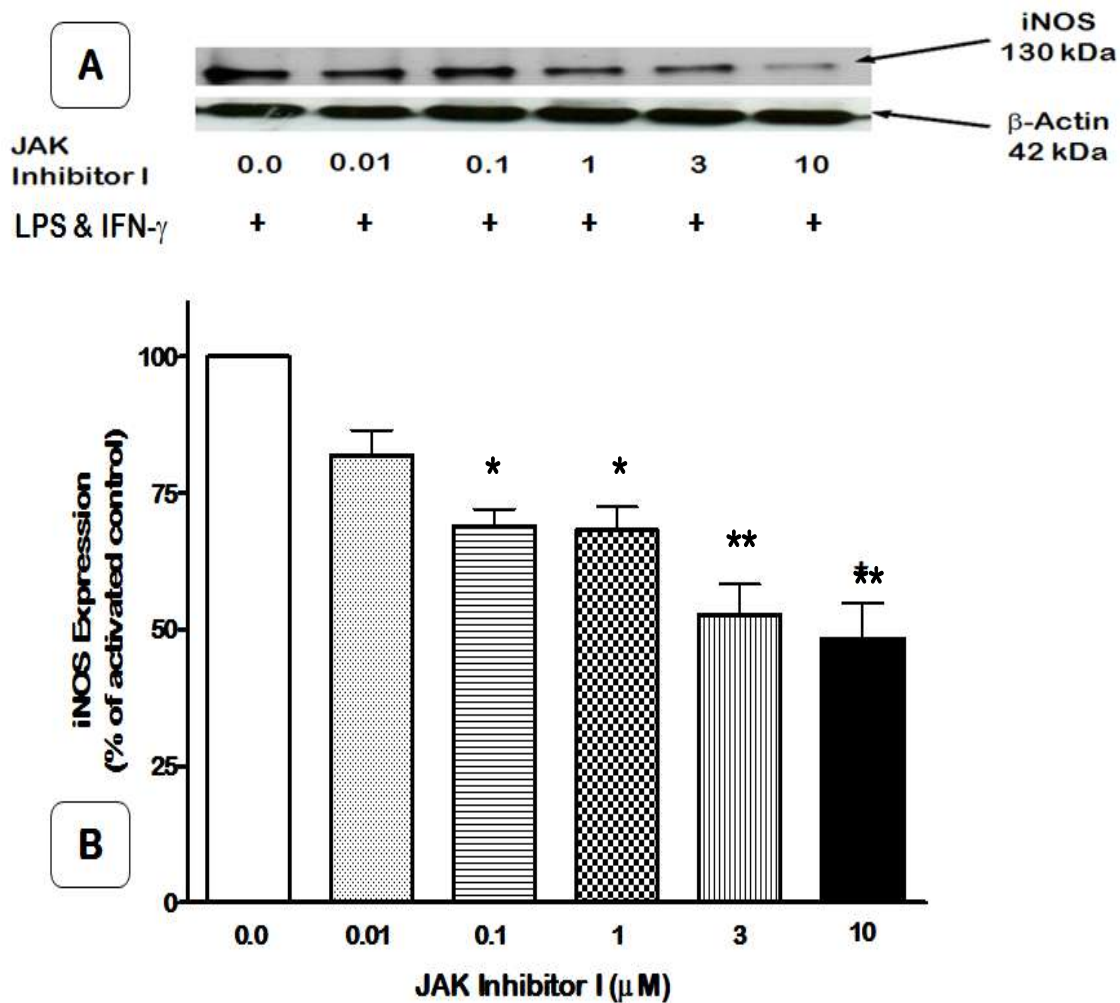


**Figure 3.14 Effects of JAK inhibitor I on iNOS expression in activated RASMCs**

Confluent monolayer of RASMCs in 6-well plate were pre-treated with complete DMEM alone (Controls) and in complete DMEM with different concentrations of JAK inhibitor I (0.01 to 10  $\mu\text{M}$ ) for 30 minutes prior to activation. Cells were activated with both LPS (100  $\mu\text{g}/\text{ml}$ ) and IFN- $\gamma$  (100 U/ml) in the absence and continued presence of JAK inhibitor I. After 24 hours, cell lysates were generated as previously described in the Methods (Section 2.13). Equal quantities of lysates (40  $\mu\text{g}$ ) were subjected to western blotting using a specific anti-iNOS antibody. The above western blot (Figure A) is representative of at least three independent experiments. Respective band intensities were quantified by densitometric analysis and normalized to  $\beta$ -actin protein (Figure B). The data is presented as a percentage of relative intensity of the maximum expression of iNOS protein. Data represent the **mean  $\pm$  S.E.M.** from three independent experiments. Statistical differences between means were determined using one-way analysis of variance (ANOVA) followed by Dunnett's multiple comparisons test of the normalized data. \* & \*\* denotes  $P < 0.05$  and  $P < 0.001$  respectively when compared to untreated activated control.

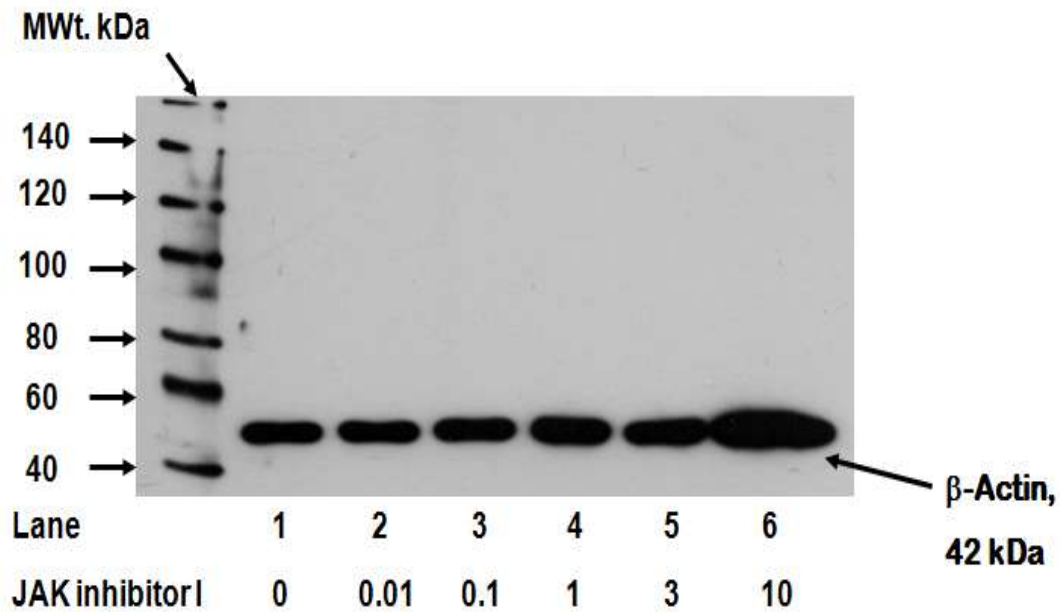


**Figure 3.15 Effects of JAK inhibitor I on iNOS expression in control RASMCs**

Confluent monolayer of RASMCs in 6-well plates were incubated in complete DMEM and pre-treated with different concentrations of JAK inhibitor I (0.01 to 10.0  $\mu\text{M}$ ) for 30 min. Cells were cultured in continued presence of JAK inhibitor I for a further 24 hours. Cell lysates were generated as previously described in the Methods (Section 2.13). Equal quantities of lysates (40  $\mu\text{g}$ ) were subjected to western blotting using a specific anti-iNOS antibody. The housekeeping protein,  $\beta$ -Actin (42 kDa) was used as a loading control. The above western blot is representative of at least three independent experiments.

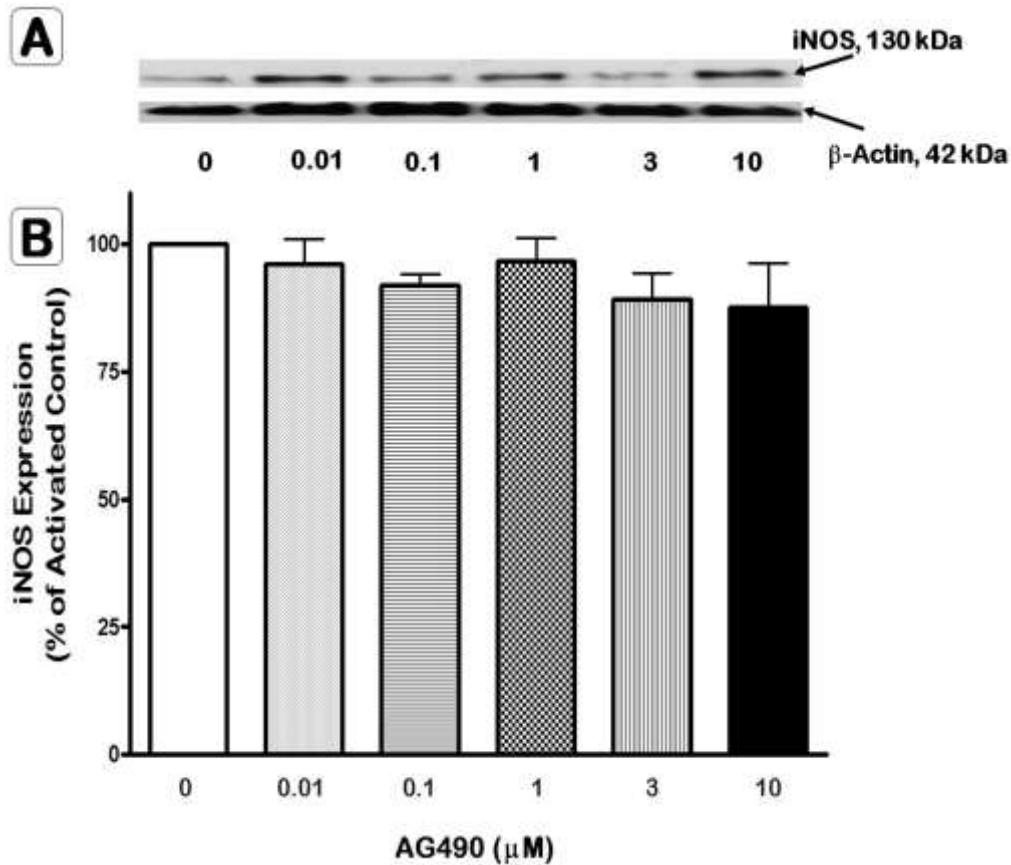


**Figure 3.16 Effects of AG490 on iNOS expression in activated RASMCs**

Confluent monolayer of RASMCs in 6-well plates were pre-treated with complete DMEM alone (Controls) and in complete DMEM with different concentrations of AG490 (0.01 to 10.0 μM: Lane 6) for 30 min prior to activation. Cells were activated with both LPS (100 μg/ml) and IFN-γ (100 U/ml) in the absence and in continued presence of AG490 inhibitor. After 24 hours cell lysates were generated as previously described in the Methods (Section 2.13). Equal quantities of lysates (40 μg) were subjected to western blotting using a specific anti-iNOS antibody. The above western blot (Figure A) is representative of at least three independent experiments. Respective band intensities were quantified by densitometric analysis and normalized to β-actin protein (Figure B). The data is presented as a percentage of relative intensity of the maximum expression of iNOS protein. Data represent the **mean ± S.E.M.** from three independent experiments. Statistical differences between means were determined using one-way analysis of variance (ANOVA) followed by Dunnett's multiple comparisons test of the normalized data.  $P > 0.05$  confirmed there was no significant difference when compared to untreated activated control.

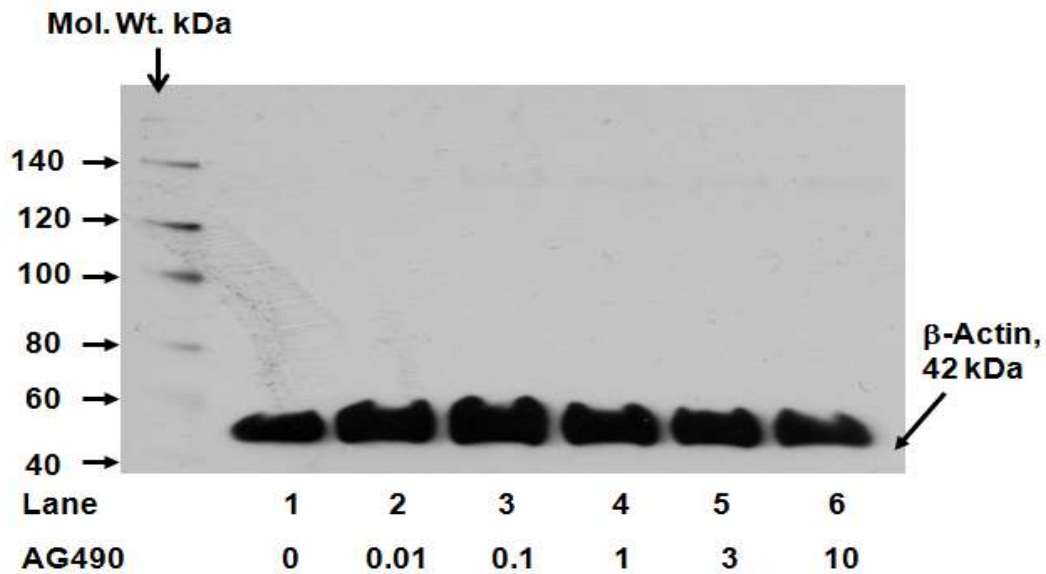


**Figure 3.17 Effects of AG490 on iNOS expression in control RASMCs**

Confluent monolayer of RASMCs in 6-well plates were incubated in complete DMEM and pre-treated with different concentrations of AG490 (0.01 to 10.0  $\mu$ M) for 30 min prior to activation. Cells were cultured in continued presence of AG490 inhibitor for a further 24 hours. Cell lysates were generated as previously described in the Methods (Section 2.13). Equal quantities of lysates (40  $\mu$ g) were subjected to western blotting using a specific anti-iNOS antibody. The housekeeping protein,  $\beta$ -Actin (42 kDa) was used as a loading control. The above western blot is representative of at least three independent experiments.

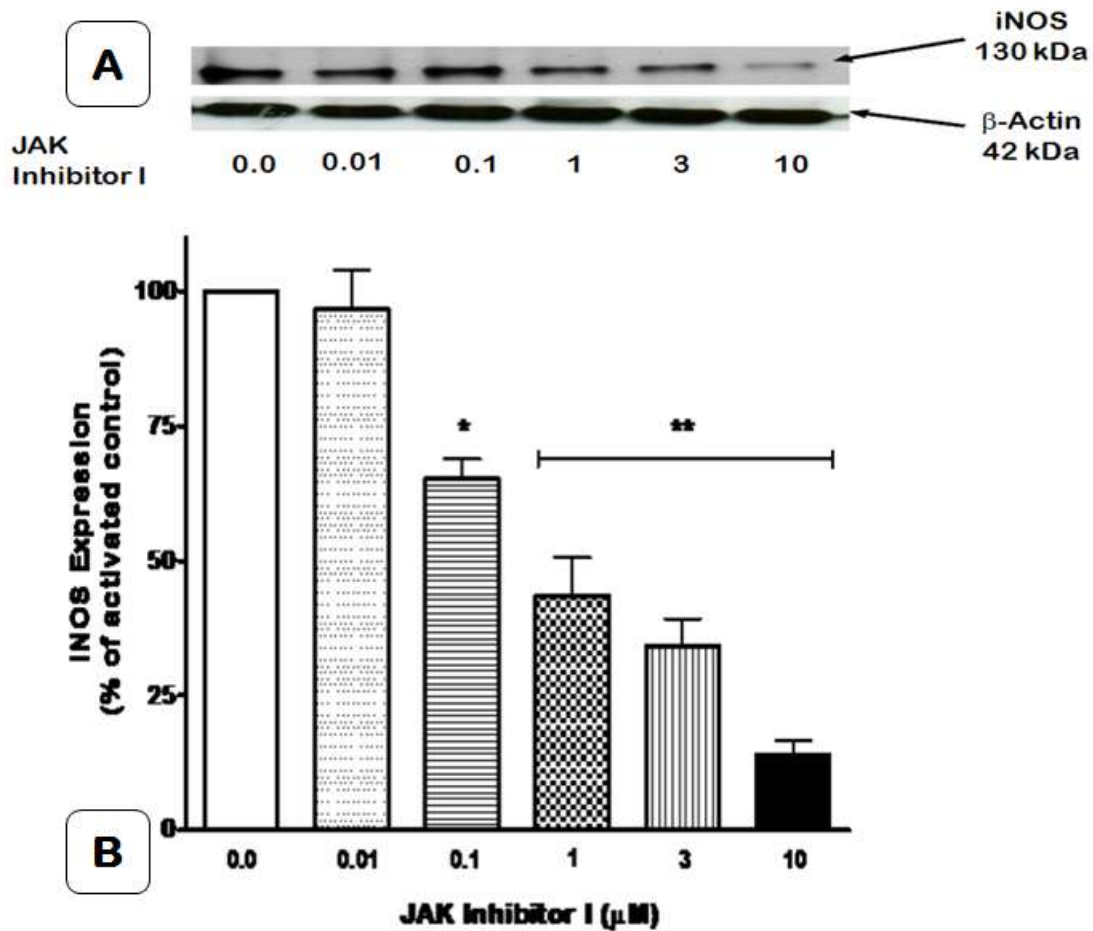


**Figure 3.18 Effects of JAK Inhibitor I on iNOS expression in control J774 macrophages.**

Confluent monolayer of J774 macrophages in 6-well plates were incubated with either DMEM alone (Control; Lane 1) or in complete DMEM with different concentrations of JAK inhibitor I (0.01 to 10.0 μM) for 30 min prior to activation. Cells were stimulated with LPS (1.0 μg/ml) for a further 24 hour incubation. Equal quantities of lysates (40 μg) were subjected to western blotting using a specific anti-iNOS antibody (Figure A) using a specific anti-iNOS antibody as described in the Methods (section 2.13). Respective band intensities were quantified by densitometric analysis and normalized to β-actin protein (Figure B). The data is transformed as a percentage of relative intensity of the maximum expression of iNOS protein. Data represents the **mean ± S.E.M.** of densitometric values obtained from three independent experiments. Statistical differences between means were determined using one-way analysis of variance (ANOVA) followed by Dunnett's multiple comparisons test of the normalized data. \* & \*\* denotes  $P < 0.05$  and  $P < 0.001$  respectively when compared to untreated activated controls.



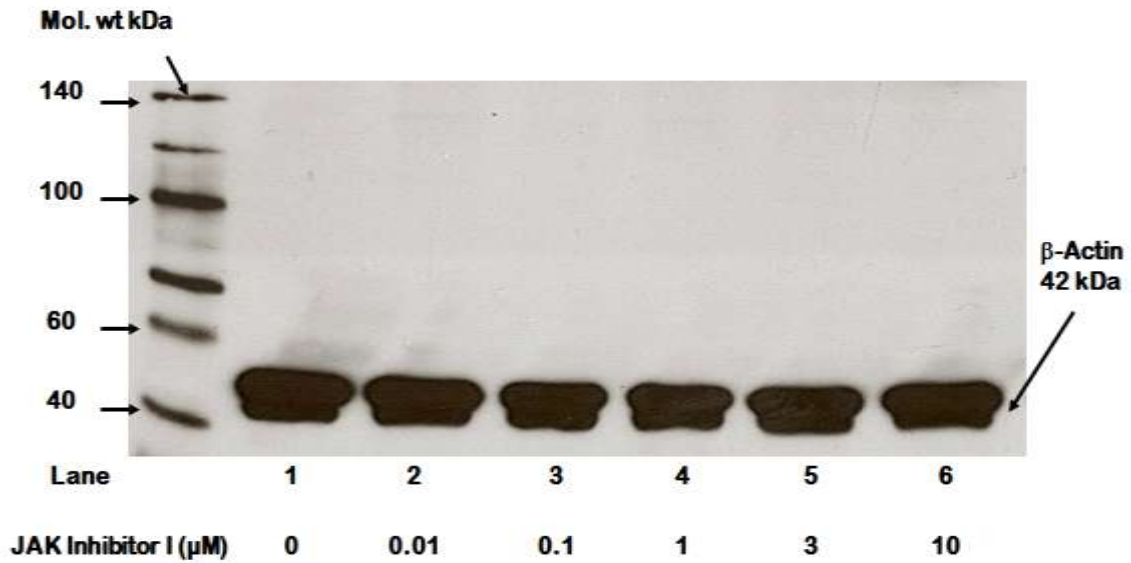


**Figure 3.19 Effects of JAK Inhibitor I on iNOS expression in control J774 macrophages**

Confluent monolayer of J774 macrophages in 6-well plates were incubated in complete DMEM and pre-treated with different concentrations of JAK inhibitor I (0.01 to 10.0 μM) for 30 min. Cells were cultured in continued presence of JAK inhibitor I for a further 24 hours. Cell lysates were generated as previously described in the Methods (Section 2.13). Equal quantities of lysates (40 μg) were subjected to western blotting using a specific anti-iNOS antibody. The housekeeping protein, β-Actin (42 kDa) was used as a loading control. The above western blot is representative of at least three independent experiments.

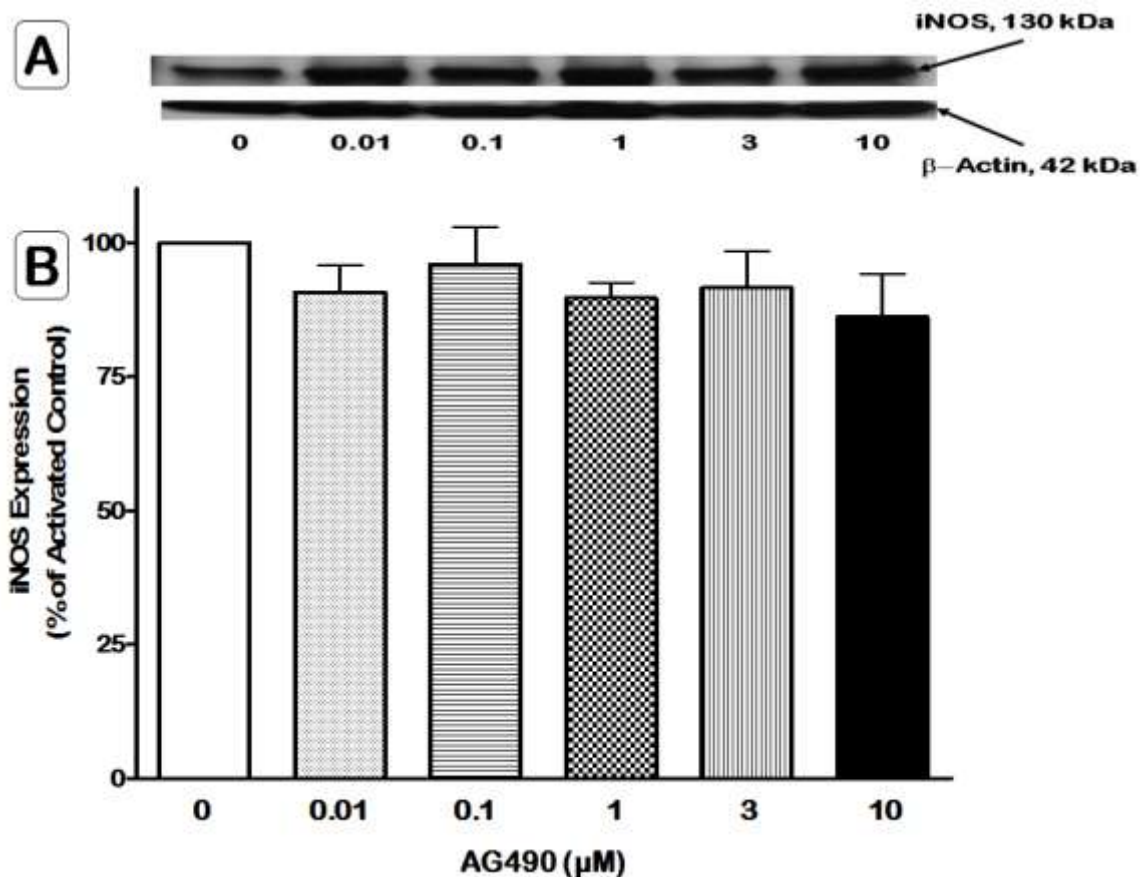


**Figure 3.20 Effects of AG490 inhibitor on iNOS expression in activated J774 macrophages**

Confluent monolayer of J774 macrophages in 6-well plates were pre-treated with either complete DMEM alone (as Control) or in complete DMEM with different concentrations of AG490 inhibitor for 30 min prior to activation. Cells were activated with LPS (1.0  $\mu$ g/ml) in the absence and in continued presence of AG490 inhibitor. After 24 hours cell lysates were generated as previously described in the Methods (Section 2.13). Equal quantities of lysates (40  $\mu$ g) were subjected to western blotting using a specific anti-iNOS antibody. The above western blot (Figure A) is representative of at least three independent experiments. Respective band intensities were quantified by densitometric analysis and normalized to  $\beta$ -actin protein (Figure B). The data is presented as a percentage of relative intensity of the maximum expression of iNOS protein. Data represent the **mean  $\pm$  S.E.M.** from three independent experiments. Statistical differences between means were determined using one-way analysis of variance (ANOVA) followed by Dunnett's multiple comparisons test of the normalized data.  $P > 0.05$  confirmed there was no significant difference when compared to untreated activated control.

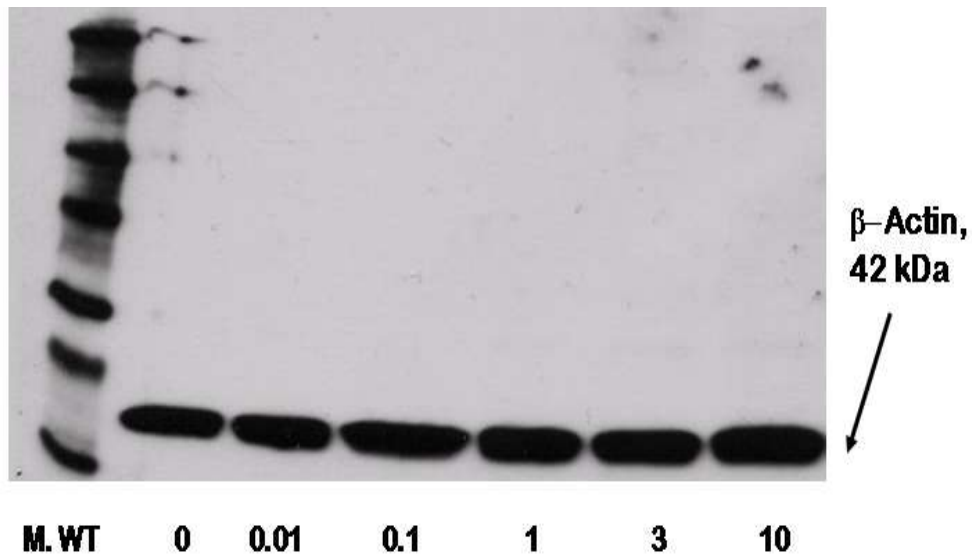


**Figure 3.21 Effects of AG490 inhibitor on iNOS expression in control J774 macrophages**

Confluent monolayer of J774 macrophages in 6-well plates were incubated in complete DMEM and pre-treated with different concentrations of AG490 (0.01 to 10.0  $\mu$ M) for 30 min. Cells were cultured in continued presence of AG490 inhibitor for a further 24 hours. Cell lysates were generated as previously described in the Methods (Section 2.13). Equal quantities of lysates (40  $\mu$ g) were subjected to western blotting using a specific anti-iNOS antibody. The housekeeping protein,  $\beta$ -Actin (42 kDa) was used as a loading control. The above western blot is representative of at least three independent experiments.

### **3.4.8 Effects of JAK inhibitor I and AG490 on L-arginine transport in RASMCs and J774 macrophages**

The dependence of NO production on L-arginine uptake in both activated RASMCs and J774 macrophages led us to characterise further the effects of JAK inhibitor I and AG490 on L-arginine transport in both cell models. Our results confirm earlier findings that activation of RASMCs with a combination of LPS (100 µg/m) and IFN-γ (100 U/ml) or J774 macrophages with LPS (1.0 µg/m) alone resulted in an increase not only in nitrite production but also in L-arginine transport. In the presence of JAK inhibitor I, L-arginine transport was inhibited in a concentration dependent manner in RASMCs but only in activated cells (Figure **3.22**).

In J774 macrophages, JAK inhibitor I showed inhibition which was concentration dependent. This was significantly evident in activated cells where induced transport was reduced back to basal levels in the presence of 0.1 µM inhibitor (Figure **3.23**). In contrast, AG490 caused no significant change in L-arginine uptake in either RASMCs (Figure **3.24**) or J774 macrophages (Figure **3.25**) under activated or control conditions.

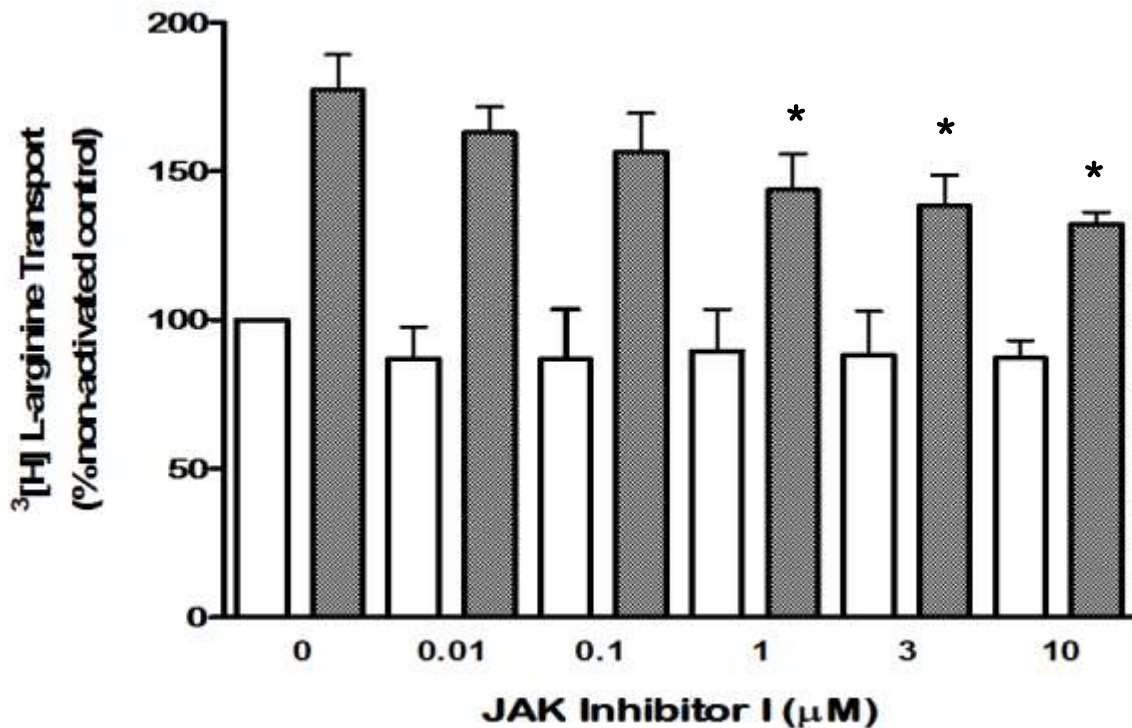


**Figure 3.22 Concentration dependent effect of JAK inhibitor I on L-arginine transport in both control and activated RASMCs**

Confluent monolayer of RASMCs in 96-well plate were pre-treated in either complete DMEM alone (Controls) or in complete DMEM with different concentrations of JAK inhibitor I (0.1 to 10 μM) for 30 min prior to activation. Cells were activated with both LPS (100 μg/ml) and IFN-γ (100 U/ml) in the absence and continued presence of JAK inhibitor I. After 24 hour incubation period, nitrite and protein content of sample wells were assessed by the Greiss and BCA assays respectively as described in the methods (Sections 2.9 and 2.11 respectively). Transport of <sup>3</sup>[H] L-arginine was assessed over 2 min in both control and activated cells as described in the Methods (Section 2.10). Open bars represent controls and closed grey bars represent activated cells. Data are presented as percentage of <sup>3</sup>[H] L-arginine transport by activated controls without inhibitor. Data represent the **mean ± S.E.M.** from at least three independent experiments with five replicates in each. Statistical differences between means were determined using one-way analysis of variance (ANOVA) followed by Dunnett's multiple comparisons test of the normalized data. \* denotes  $P < 0.05$  when compared to untreated activated controls.

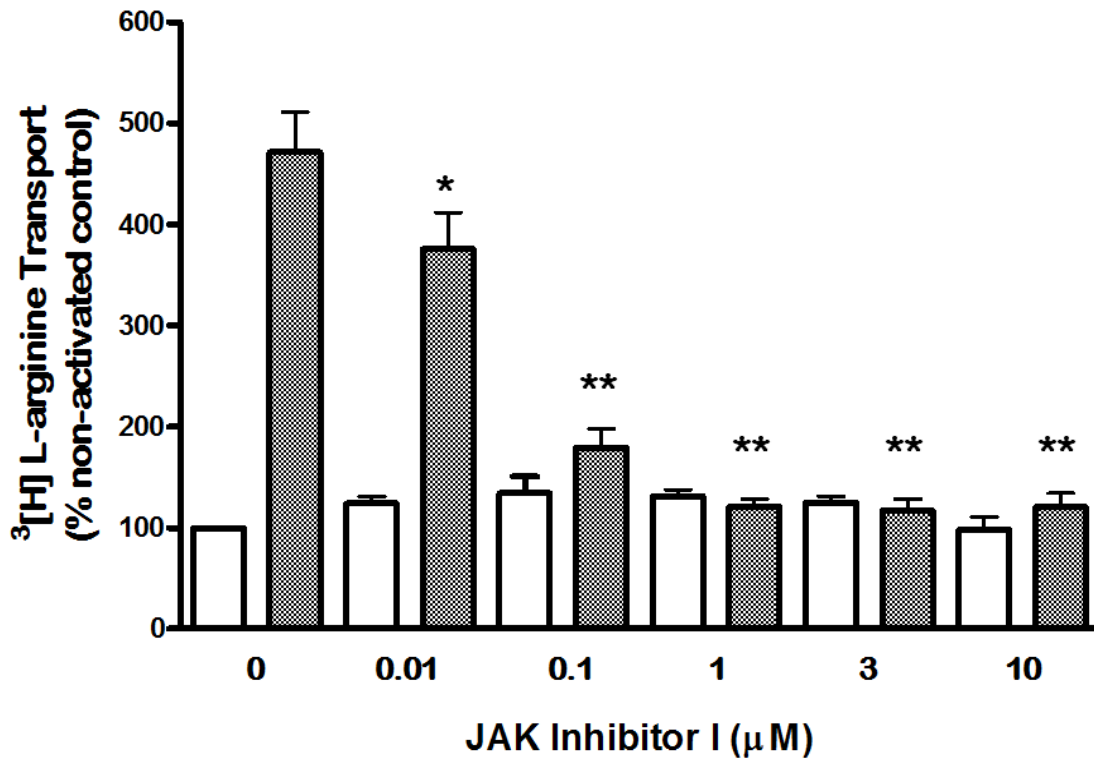


**Figure 3.23 Concentration dependent effect of JAK inhibitor I on L-arginine transport in both control and activated J774 macrophages.**

Confluent monolayer of J774 macrophages in 96-well plate were pre-treated with either complete DMEM alone (Controls) or in complete DMEM with different concentrations of JAK inhibitor I (0.1 to 10 μM) for 30 min prior to activation. Cells were activated with LPS (1.0 μg/ml) in the absence and in continued presence of JAK inhibitor I. After 24 hour incubation period, nitrite and protein content of respective wells were assessed by the Greiss and BCA assays respectively as described in the methods (Sections 2.9 and 2.11 respectively). Transport of  $^3\text{[H]}$  L-arginine was assessed over 2 min in both control and activated cells as described in the methods (Section 2.10). Open bars represent controls and closed grey bars represent activated cells. Data are presented as percentage of  $^3\text{[H]}$  L-arginine transport by activated controls without inhibitor. Data represent the **mean ± S.E.M.** from three independent experiments with five replicates in each. Statistical differences between means were determined using one-way analysis of variance (ANOVA) followed by Dunnett's multiple comparisons test of the normalized data. \* & \*\* denotes  $P < 0.05$  and  $P < 0.01$  respectively when compared to untreated activated control.

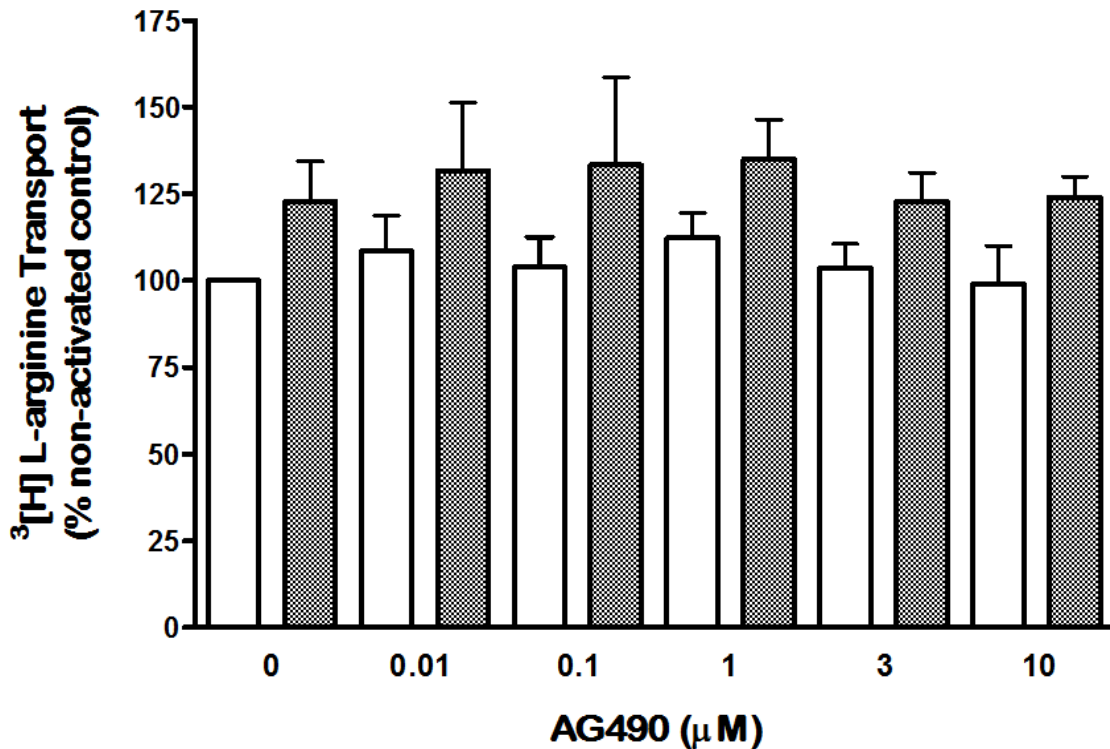


**Figure 3.24 Concentration dependent effect of AG490 on L-arginine Transport in both control and activated RASMCs.**

Confluent monolayer of RASMCs in 96-well plate were pre-incubated with either complete DMEM alone (Controls) or in complete DMEM with varying concentrations of AG490 (0.01 to 10.0 μM) for 30 min prior to activation. Cells were activated with LPS (100 μg/ml) and IFN-γ (100 U/ml). After 24 hour incubation period, nitrite and protein content of respective wells were assessed by use of Greiss and BCA assays respectively as earlier described in Methods (Sections 2.9 and 2.11 respectively). Transport of <sup>3</sup>[H] L-arginine was assessed over 2 min in both control and activated cells as described in the Methods (Section 2.10). Open bars represent controls and closed grey bars represent activated cells. Data are presented as percentage of <sup>3</sup>[H] L-arginine transport by activated controls without inhibitor. Data represent the **mean ± S.E.M.** from three independent experiments with five replicates in each. Statistical differences between means were determined using one-way analysis of variance (ANOVA) followed by Dunnett's multiple comparisons test of the normalized data.  $P > 0.05$  confirmed there was no significant difference when compared to untreated activated control.

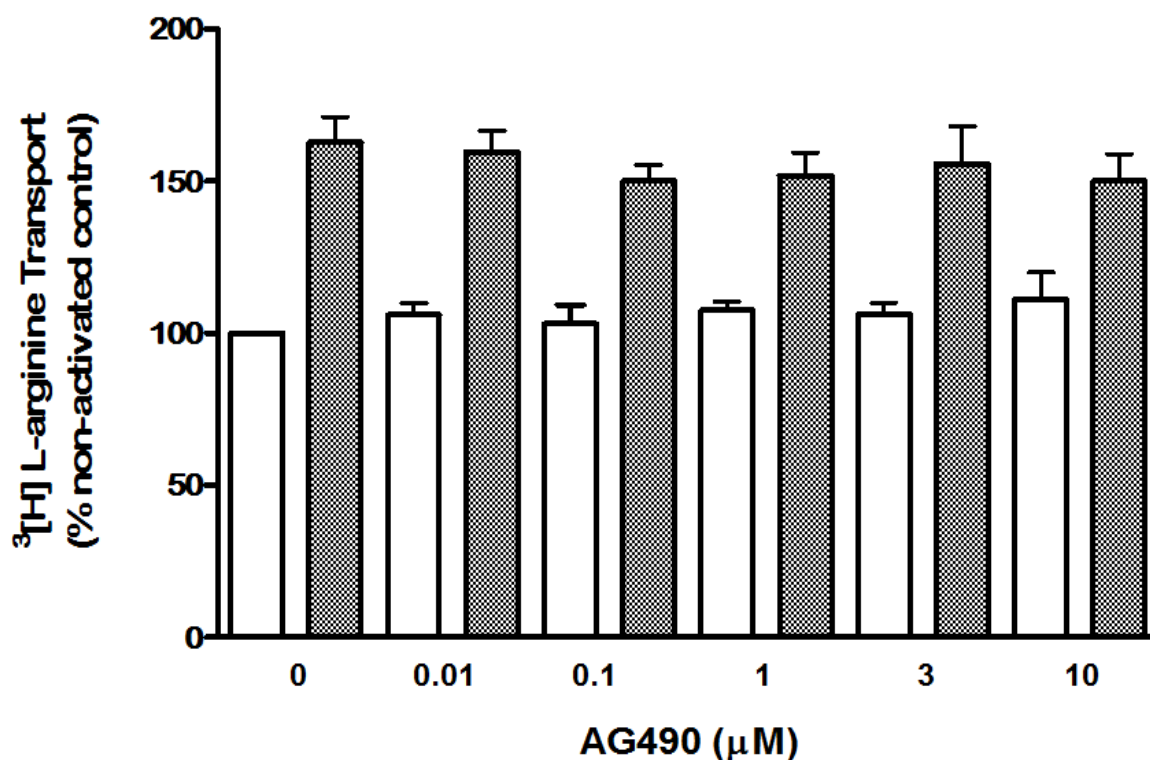


**Figure 3.25 Concentration dependent effect of AG490 on L-arginine Transport in both control and activated J774 macrophages.**

Confluent monolayer of cells were pre-treated in either complete DMEM alone (Controls) or in complete DMEM with varying concentrations of AG490 (0.01 to 10.0 μM) for 30 min prior to activation. Cells were activated with LPS (1.0 μg/ml). After 24 hour incubation period, nitrite and protein content of respective wells were assessed by use of Greiss and BCA assays respectively as earlier described in Methods (Sections 2.9 and 2.11 respectively). Transport of  $^3\text{[H]}$  L-arginine was assessed over 2 min in both control and activated cells as described in the methods (Section 2.10). Open bars represent controls and closed bars represent activated cells. Data are presented as percentage of  $^3\text{[H]}$  L-arginine transport of activated controls without inhibitor. Data represent the **mean ± S.E.M.** from three independent experiments with five replicates in each. Statistical differences between means were determined using one-way analysis of variance (ANOVA) followed by Dunnett's multiple comparisons test of the normalized data.  $P > 0.05$  confirmed there was no significant difference when compared to untreated activated control.

### **3.4.9 Cell viability assays on inhibitors in both RASMCs and J774 macrophages**

The cytotoxic effects of JAK inhibitor I and AG490 were assessed by measuring mitochondrial dependent reduction of MTT to formazan as described in the Methods (Section 2.12). The results obtained showed there was no alteration in the reduction of MTT in LPS and IFN- $\gamma$  stimulated RASMCs pre-treated with JAK inhibitor I (Figure 3.26A) when compared to control cells. Similarly, metabolism of MTT was also unaffected in both controls and LPS stimulated J774 macrophages (Figure 3.27A) when exposed to JAK inhibitor I.

Parallel investigations with AG490 showed that in RASMCs there was a slight decrease in the reduction of MTT in both LPS and IFN- $\gamma$  activated cells and controls at 10  $\mu$ M concentration (Figure 3.26B). These effects were however not statistically significant. In addition there was no apparent cytotoxic effect of AG490 in control J774 macrophages when compared to LPS activated cells (Figure 3.27B).

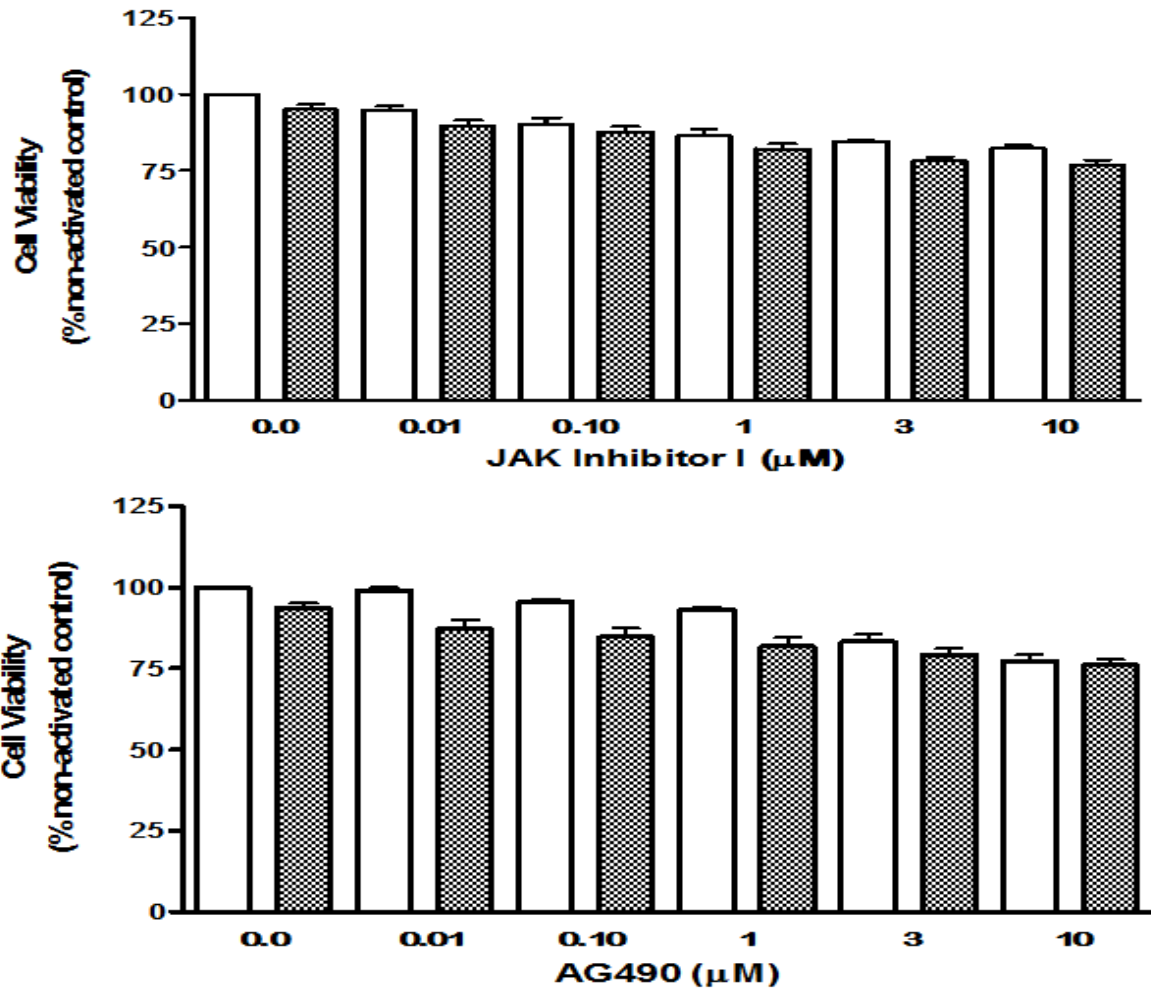


**Figure 3.26 Concentration-dependent effect of JAK inhibitor I and AG490 on RASMCs viability.**

Confluent monolayer of RASMCs in 96 well plates were pre-treated with either complete DMEM alone (Controls) or in complete DMEM with different concentrations of JAK Inhibitor I (0.01 to 10  $\mu\text{M}$ ; Figure **A**) or AG490 (0.01 to 10  $\mu\text{M}$ ; Figure **B**) for 30 minutes. Cells were then activated with LPS (100  $\mu\text{g}/\text{ml}$ ) and IFN- $\gamma$  (100 U/ml) in the absence and continued presence of JAK Inhibitor I or AG490 for 24 hours. MTT metabolism by cells was determined colorimetrically as described in the Methods Section 2.12). Open bars represent untreated non-activated cells (Controls) and closed bars represent treated activated cells. Data represent the **mean  $\pm$  S.E.M.** from three independent experiments with five replicates in each. Statistical differences between means were determined using one-way analysis of variance (ANOVA) followed by Dunnett's multiple comparisons test of the normalized data.  $P > 0.05$  confirmed there was no significant difference when compared to non activated control.

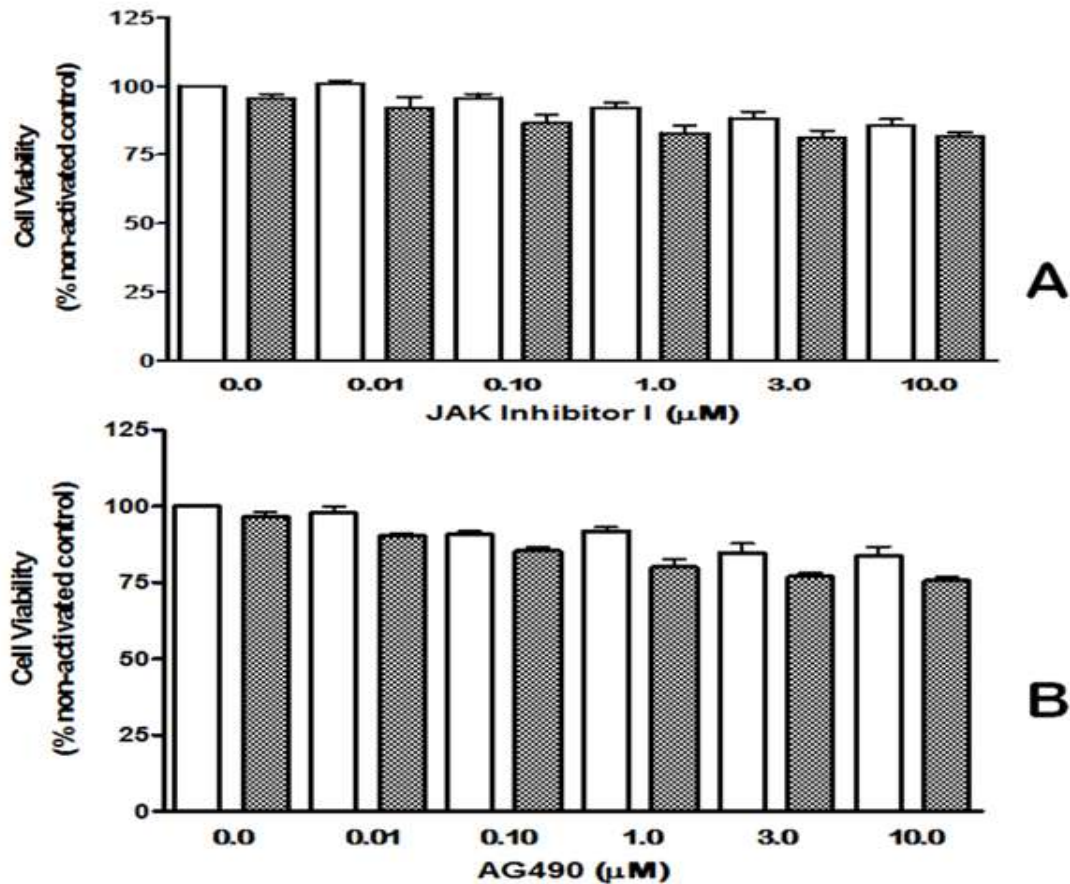


**Figure 3.27 Concentration-dependent effect of JAK inhibitor I and AG490 on viability of J774 macrophages.**

Confluent monolayers of J774 macrophages in 96 well plates were pre-treated with either complete DMEM alone (Controls) or in complete DMEM with different concentrations of JAK Inhibitor I (0.01 to 10 μM; Figure **A**) or AG490 (0.01 to 10 μM; Figure **B**) for 30 minutes. Cells were then activated with LPS (1μg/ml) in the absence and continued presence of JAK Inhibitor I or AG490 for 24 hours. MTT metabolism by cells was determined colorimetrically as described in the Methods (Section **2.12**). Open bars represent untreated non-activated cells (Controls) and closed bars represent treated activated cells. Data represent the **mean ± S.E.M.** from three independent experiments, each with five replicates. Statistical differences between means were determined using one-way analysis of variance (ANOVA) followed by Dunnett's multiple comparisons test of the normalized data.  $P > 0.05$  confirmed there was no significant difference when compared to non activated control.

#### **3.4.10 Expression of JAK2, Tyk-2 and their phosphorylated proteins in RASMCs and J774 macrophages**

In view of the lack of effect with AG490 it was essential to demonstrate whether RASMCs and J774 macrophages express JAK2, TYK2 and their phosphorylated proteins; the latter following activation of cells. As shown in Figure **3.28**, JAK2 was detectable in both cells examined but more predominant in RASMCs. By comparison, TYK2 was also detectable in both cell types but with an apparent difference in protein expression (Figure **3.29**) as determined by western blotting. Our results suggest there is a comparatively higher expression in J774 macrophages (Figure 3.29A) compared to that in RASMCs (Figure **3.29B**). Activation of RASMCs with LPS (100 µg/ml) and IFN- $\gamma$  (100 U/ml) or J774 macrophages with LPS (1.0 µg/ml) failed to show any significant change in the basal expression of either phosphorylated TYK2 (Figures **3.30** and **3.31**) or JAK2 (Figures **3.32** and **3.33**) in either suggesting that these proteins may not be phosphorylated in these cells when activated.

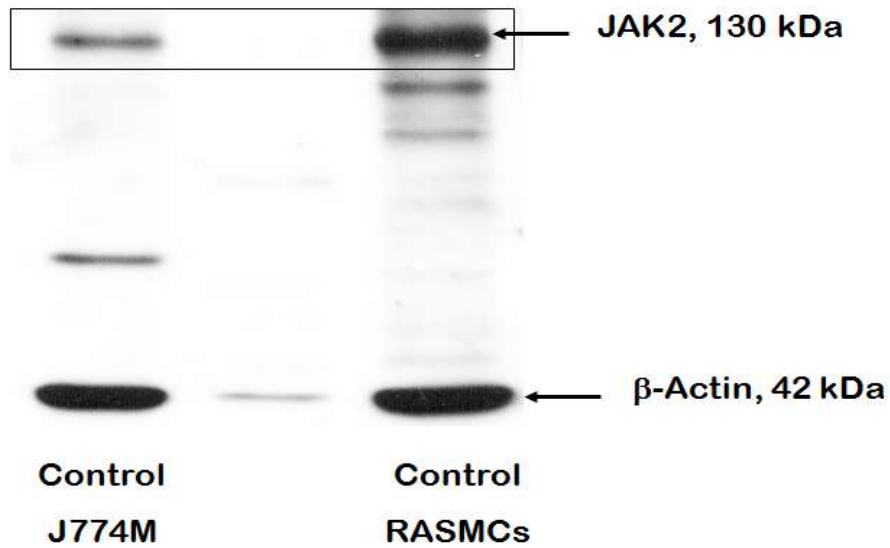


**Figure 3.28 Expression of JAK2 in control J774 macrophages and RASMCs.**

Confluent monolayer(s) of J774 macrophages or RASMCs in 6-well plates were separately cultured in complete DMEM and incubated for 24 hours. Whole cell lysates (40  $\mu$ g) generated were subjected to western blotting using a JAK2 specific antibody as described in the Methods (section 2.13). The bands at 42 kDa show expression levels of the house keeping protein,  $\beta$ -actin, which was detected using a selective antibody targeting this protein. The blot is representative of at least three independent experiments.

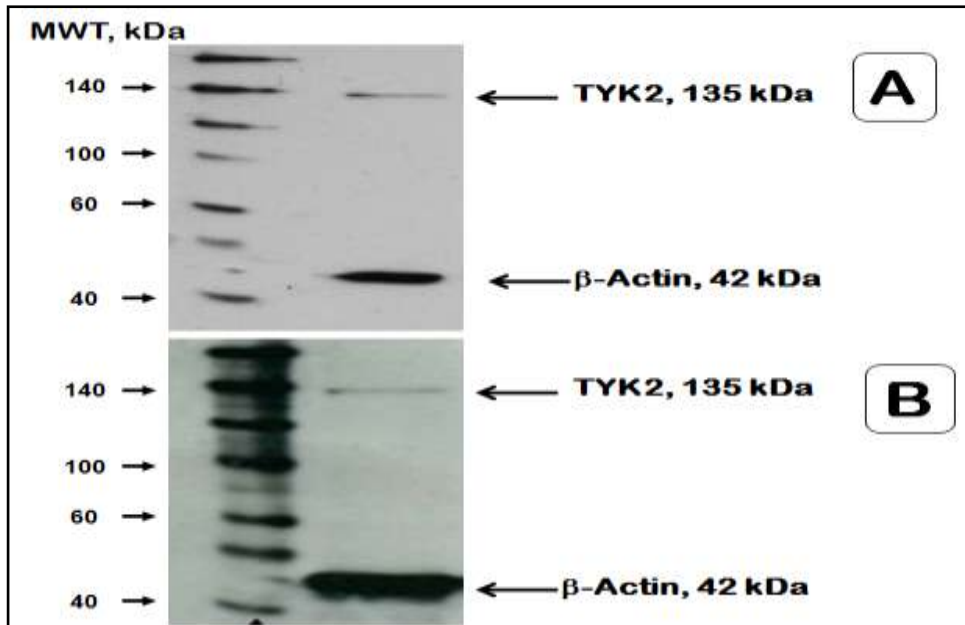


**Figure 3.29 Expression of TYK2 in control J774 macrophages (A) and RASMCs (B).**

Confluent monolayer(s) of J774 macrophages or RASMCs in 6-well plates were separately cultured in complete DMEM and incubated for 24 hours. Whole cell lysates (40  $\mu$ g) were generated from the respective wells and subjected to western blotting using a specific anti-TYK2 antibody as described in the Methods (Section 2.13). The bands at 42 kDa show expression levels of the house keeping protein,  $\beta$ -actin, which was detected using a selective antibody targeting this protein. The blot is representative of at least three independent experiments.

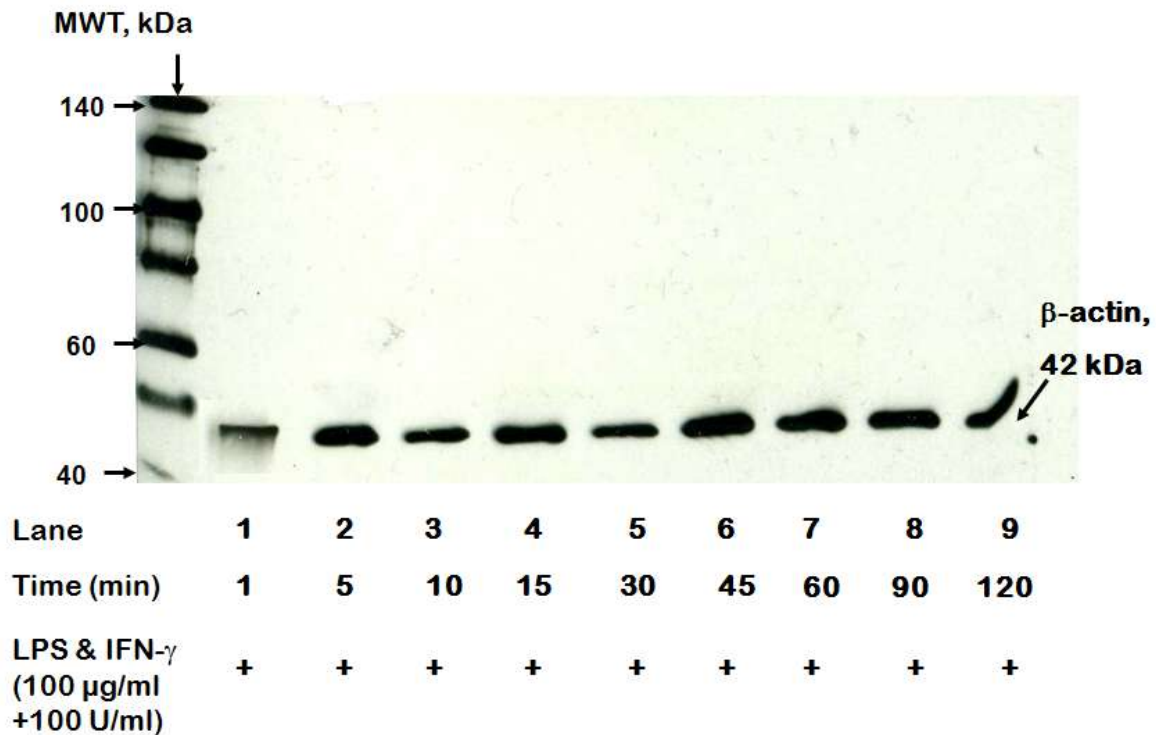


**Figure 3.30 Expression of phospho-TYK2 in control and activated RASMCs**

Confluent monolayer of RASMCs in p33 culture dishes were stimulated with both LPS (100  $\mu$ g/ml) and IFN- $\gamma$  (100 U/ml) in continued presence of complete DMEM for varying time periods as indicated. Equal quantities of lysates (containing 40  $\mu$ g of protein) were subjected to western blotting using a specific anti-phospho-TYK2 antibody as described in the Methods (**Section 2.13**). The bands at 42 kDa show expression levels of the house keeping protein,  $\beta$ -actin, which was detected using a selective antibody targeting this protein. The blot is representative of at least three independent experiments.

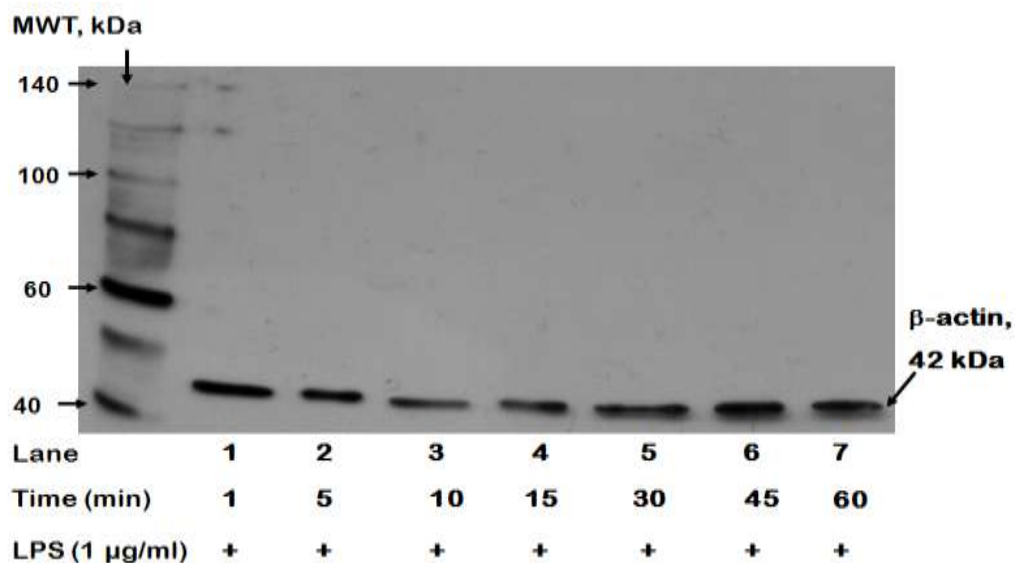


**Figure 3.31 Expression of phospho-TYK2 in control and activated J774 macrophages**

Confluent monolayer of J774 macrophages in p33 culture dishes were stimulated with LPS (1.0  $\mu$ g/ml) in continuous presence of complete DMEM for varying time periods as indicated. Equal quantities of lysates (containing 40  $\mu$ g of protein) were subjected to western blotting using a specific anti-phospho-TYK2 antibody as described in the Methods (**Section 2.13**). The bands at 42 kDa show expression levels of the house keeping protein,  $\beta$ -actin, which was detected using a selective antibody targeting this protein. The blot is representative of at least three independent experiments.

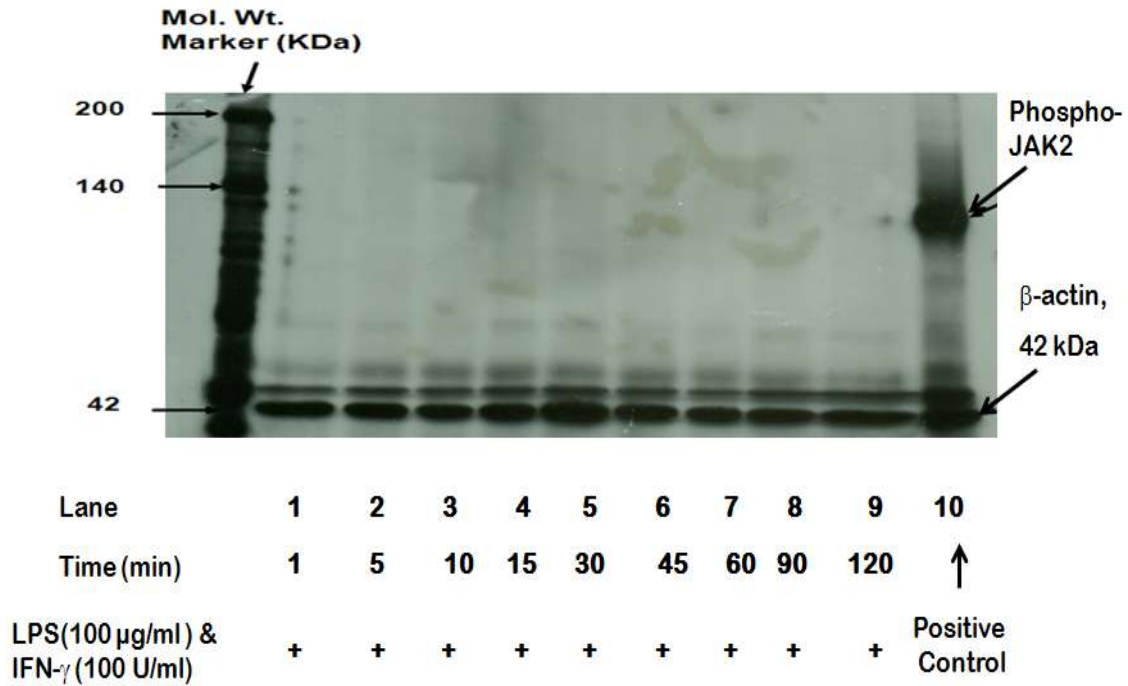


**Figure 3.32 Expression of phospho-JAK2 in control and activated RASMCs**

Confluent monolayers of RASMCs in p33 culture dishes were stimulated with activated with LPS (100 µg/ml) and IFN-γ (100 U/ml) for varying time periods as indicated. Equal quantities of lysates (containing 40 µg of protein) were subjected to western blotting using a specific anti-phospho-JAK2 antibody as described in the Methods (**Section 2.13**). Lane 10 represents a positive control for phospho-JAK2 generated from HeLa cells treated with IFN-α. The band at 42 kDa shows expression level of the house keeping protein, β-actin, which was detected using a selective antibody targeting this protein. The blot is representative of at least three independent experiments.

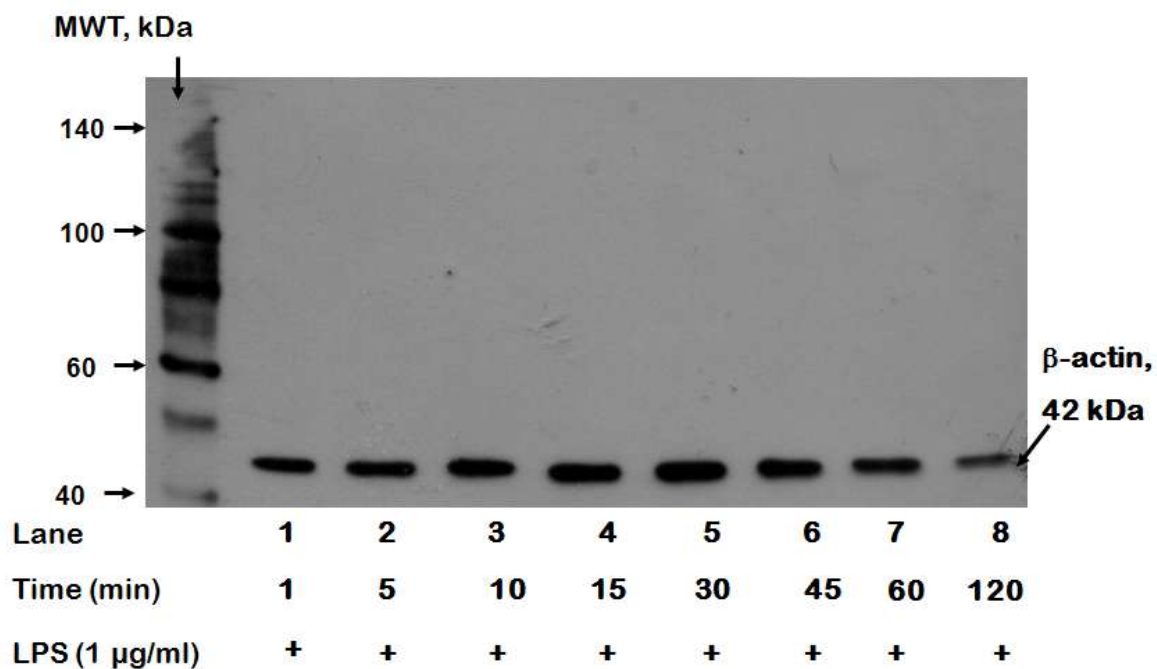


**Figure 3.33 Expression of phospho-JAK2 in control and activated J774 macrophages**

Confluent monolayers of J774 macrophages in p33 culture dishes were stimulated with activated with LPS (1.0  $\mu\text{g/ml}$ ) for varying time periods in continuous presence of complete DMEM. Equal quantities of lysates (containing 40  $\mu\text{g}$  of protein) were generated from the respective wells and subjected to western blotting using a specific anti-phospho-JAK2 antibody as described in the Methods (**Section 2.13**). The band at 42 kDa shows expression level of the house keeping protein,  $\beta$ -actin, which was detected using a selective antibody targeting this protein. The blot is representative of at least three independent experiments.

### 3.5DISCUSSION

The studies described in this chapter were aimed at establishing the role of the JAKs in the induction of iNOS expression, NO production and L-arginine transport in RASMCs and J774 macrophages. These two cell types were chosen because there is evidence to show that the induction of iNOS is predominantly localised to the smooth muscle cells within the vasculature (Cohen *et al.*, 1998). Macrophages on the other hand express high levels of iNOS as part of our host defence mechanisms (Annane *et al.*, 2000) but were used in these studies partly for comparative purposes. In any case, for both cell types, an understanding of the mechanisms that regulate iNOS gene expression is important since this would provide strategies for regulating its expression and thus overproduction of NO in disease states.

There are currently a wide range of stimuli capable of inducing iNOS expression and NO production in various cell systems. These have been reported to include, depending on the cell type, LPS (Kim *et al.*, 2007), Granulocyte macrophage colony –stimulating factor (GM-CSF) (Vital *et al.*, 2003), erythropoietin (Epo) (Genc *et al.*, 2006), growth hormone (GH) (Argetsinger *et al.*, 1993) and a range of cytokines including IFN- $\gamma$ , TNF- $\alpha$  and interleukins amongst others (Kleinert *et al.*, 2004). The induction of iNOS may subsequently result in or contribute to the pathogenesis fo inflammatory disease states such as in septic shock (Bultinck *et al.*, 2006; Mastronardi *et al.*, 2011; Thiemermann *et al.*, 1990; Titheradge, 1999; Zhang *et al.*, 1998b) and in atherosclerosis (Behr-Roussel *et al.*, 2000; Knowles *et al.*, 1994; Perrotta *et al.*, 2011).

To initiate the studies outlined in this thesis, the model for inducing iNOS in the two cell systems had to be developed and this was established using previous protocols in our laboratory. This involved using a combination of LPS and IFN- $\gamma$  for smooth muscle cells and LPS alone for macrophages at predetermined concentrations. As demonstrated in this thesis, a combined exposure to both LPS and IFN- $\gamma$  induced iNOS in RASMCs while LPS alone was sufficient to induce macrophages. This suggests cell type specificity in the induction of iNOS expression. These results are consistent with our previous findings (Baydoun *et al.*, 1998; Baydoun *et al.*, 1993a; Baydoun *et al.*, 1993b; Baydoun *et al.*, 1999; Hsiao *et al.*, 2003) and with studies in other cell types such as

astrocytes where both LPS and IFN- $\gamma$  are required for iNOS induction (Bolanos *et al.*, 1997; Nicoletti *et al.*, 1998).

In addition to the above we also demonstrated in this thesis that there was no iNOS expression in either cell types under control conditions but strongly induced following treatment of cells with the appropriate stimuli. In both cell types this was associated with a significantly distinct and elevated NO production accompanied by the parallel induction of L-arginine transport as previously demonstrated (Baydoun *et al.*, 1993a; Baydoun *et al.*, 1990). The induction of iNOS in both cell types was time-dependent though the pattern of induction in macrophages had a much longer lag time compared to RASMCs. These observations are again consistent with previous findings from our group (Baydoun *et al.*, 1998; Baydoun *et al.*, 1993b; Wileman *et al.*, 2003) as well as from other studies (Fleming *et al.*, 1991; Kang *et al.*, 1999; Kolyada *et al.*, 1996; Wileman *et al.*, 2003).

Nitrite due to its bactericidal effects on pathogenic microorganisms and in addition provide a compensatory role in maintaining vascular homeostasis (Yan *et al.*, 1996). In contrast, the high NO production has also been implicated in endothelial dysfunction, hypotension, multiple organ failure and eventual death (Cauwels *et al.*, 2011; Hon *et al.*, 1998; Thiemermann *et al.*, 1990; Titheradge, 1999) due to deleterious effects associated with high amounts of NO within biological systems.

In view of the results obtained it is likely that in RASMCs, the combined signalling mediated by LPS and IFN- $\gamma$  are a necessary pre-requisites for the optimum induction of iNOS protein expression, NO production and of L-arginine transport. Further to this, it has also been reported that cells primed by IFN- $\gamma$  become more sensitive to other stimuli such as LPS in potentiating induction of inflammatory genes such iNOS (Kamijo *et al.*, 1994; Xie *et al.*, 1993). There are other additional reports which suggest that IFN- $\gamma$  may also act to stabilize the mRNA levels for iNOS thereby prolonging its half-life (Weisz *et al.*, 1994). Thus, for prolonged and sustained expression of iNOS in smooth muscle cells both LPS and IFN- $\gamma$  are critical and the two may synergize to enhance the transcription of the iNOS gene.

In summary, in RASMCs the combined exposure to both LPS and IFN- $\gamma$  is essential for iNOS induction while in macrophages, LPS alone is required. The precise reasons for these differences in the requirements of respective stimuli are not entirely clear but it is worth noting that the promoter region of the iNOS gene for different species may vary and this could have implications in the requirements for the induction of iNOS.

Although the promoter region of both RASMCs and J774 macrophages contain common elements, the composition of NF- $\kappa$ B subunits and associated induction patterns (Spink *et al.*, 1995; Xie *et al.*, 1994) are critical factors in delineating the differences between both cell types. In murine macrophages evidence suggest that the ratio of p50:p65 was much lower in macrophages compared to RASMCs (Zhang *et al.*, 2001). In addition, the associated oxidative status of the respective cells following induction of iNOS, are possible basis for the differences in the regulation of iNOS. Also the NF- $\kappa$ B transcription element located downstream of the mouse promoter is the critical promoter propagating the responses following cytokine stimulation. In contrast in RASMCs the critical NF- $\kappa$ B promoter sequence is located further upstream of the iNOS promoter (Spink *et al.*, 1995; Xie *et al.*, 1994). Also, consistent with current evidence, our data suggest that macrophage mediated induction of iNOS is only plausible via LPS stimulation while both LPS and IFN- $\gamma$  are required for iNOS induction in RASMCs.

With regards to the stimuli used in our studies, both LPS and IFN- $\gamma$  have been extensively used for the induction of iNOS either independently or in combination in many different cell systems. Signalling via LPS is mainly mediated through binding with LPS binding protein (LBP) present in the blood and subsequent association with CD14 (Wright *et al.*, 1990) in protein complex formation. The latter, binding to TLR-4, initiates activation of a cascade of signalling pathways (see below and also highlighted in the introduction) which may vary in individual cell systems but may eventually resulting in activation of transcription factors which can induce protein synthesis including iNOS. In a recent study the cis-regulatory element, octamer within the iNOS gene promoter has also been reported to be critical for maximum iNOS transcription by LPS (Lu *et al.*, 2009). In contrast IFN- $\gamma$  signalling is mediated via IFN- $\gamma$  receptor chains  $\alpha$  and  $\beta$  (Bach *et al.*, 1997; Boehm *et al.*, 1997). Both type I IFNs (IFN- $\alpha/\beta$ ) and type II IFNs (IFN- $\gamma$ ) are important for innate and adaptive immune responses (Pestka *et al.*, 1987). As earlier

discussed in the introduction, IFN- $\gamma$  signalling which is actively secreted from activated T cells and macrophages is critical in NO production (Lorsbach *et al.*, 1993). Current evidence suggest that two of the most important signal transduction pathways by which IFN- $\gamma$  induces its inflammatory responses include the JAK/STAT pathway (Yu *et al.*, 2012) which is mostly responsible for its anti-viral and growth inhibitory properties and the NF- $\kappa$ B activation (Chang *et al.*, 2011; Stempelj *et al.*, 2007).

Within the JAK family, there are reported differences in their responses to different cytokines. For example, while the biological responses to IFN- $\gamma$  requires JAK1 and JAK2 (Muller *et al.*, 1993; Silvennoinen *et al.*, 1993a; Velazquez *et al.*, 1992; Watling *et al.*, 1993) that to IFN- $\alpha$  is mediated largely by JAK1 and TYK2. In addition, report suggests that type I IFN responses which also includes IFN- $\gamma$  amongst others is dysfunctional though not completely abrogated in TYK2<sup>-/-</sup> mice (Karaghiosoff *et al.*, 2000). Our results following JAK inhibitor treatment of both cell types clearly showed a concentration dependent decrease in responses to LPS and IFN- $\gamma$  stimulation. A modulating role for TYK2 is also further supported by the specificity of STAT-1 activation in this thesis and its subsequent downregulation following JAK inhibitor I pre-treatment.

To establish which JAK may be required in the cell systems used in this thesis, experiments were carried out using pharmacological compounds known to inhibit the JAK pathways. The compounds investigated were AG490, a synthetic tyrophostin derived from benzylidine malononitrile, and JAK inhibitor I, pyridine-containing tetracycle. Of the two, AG490 is reported to selectively block JAK2 activation (Levitzki, 1992; Meydan *et al.*, 1996) but has also been shown to inhibit JAK3 (Kirken *et al.*, 1999) while JAK inhibitor I shows potent inhibitory activity against JAK1 (IC<sub>50</sub> = 15 nM), JAK2 (IC<sub>50</sub> = 1 nM), JAK3 (K<sub>i</sub> = 5 nM), and Tyk2 (IC<sub>50</sub> = 1 nM) (Thompson *et al.*, 2002). However, in our studies, AG490 was without effect on induced iNOS expression, nitrite production or L-arginine transport, thus strongly eliminating JAK2 and indeed JAK3 as potential critical kinases for the induction of these processes. This conclusion however contradicts reports implicating a critical role for JAK2 in the induced expression of iNOS (Dell'Albani *et al.*, 2001; Doi *et al.*, 2002; Nakashima *et al.*, 1999). For instance, in a dendritic cell line AG490 is reported to inhibit LPS stimulated NF- $\kappa$ B activation and

iNOS induction (Cruz *et al.*, 2001). In addition, JAK2 has also been demonstrated to phosphorylate I $\kappa$ B subsequent to NF- $\kappa$ B activation (Steffan *et al.*, 1995) which can lead to iNOS expression. The reasons for these discrepancies with AG490 are unclear and require further investigation but could reflect in part cell type differences.

In contrast to AG490, our results with JAK inhibitor I have demonstrated a concentration-dependent inhibition of iNOS expression, NO production and L-arginine transport. These observations indicate that, potentially, a JAK family member other than JAK2 or JAK3 may be involved and of the two remaining, JAK1 can be eliminated on the grounds that kinase negative mutants are capable of sustaining IFN- $\gamma$  production and Th1 cell differentiation. This therefore leaves TYK2 as the potential candidate but TYK2 appears to be more involved with IFN- $\alpha/\beta$  rather than IFN- $\gamma$  signalling (Karaghiosoff *et al.*, 2000). However, as already noted in the introduction chapter, apart from the interferons, JAK mediated biological response can be initiated by other stimuli including LPS (Kovarik *et al.*, 1998), erythropoietin (Epo) (Witthuhn *et al.*, 1993) and growth hormone (GH) (Argetsinger *et al.*, 1993). In particular, LPS can activate JAKs including TYK2 which has been implicated in the induction of iNOS and subsequently septic shock in mice (Strobl *et al.*, 2011). Thus even if IFN- $\gamma$  does not recruit JAKs such as TYK2 their activation by LPS could indicate a potential involvement for the induction of iNOS in our cell systems. The observed effects with JAK inhibitor I would corroborate this assumption. However, the effects produced were only partial, thus suggesting that activation of additional pathways other than the JAKs may be required. Other kinases also implicated include the MAP kinases p42 (ERK2), p44 (ERK1) (Meng *et al.*, 1997), p38 (Huang *et al.*, 2004b) and c-Jun kinase (JNK) (Chan *et al.*, 2001b). These have been highlighted in the introduction chapter and a full discussion of their role is beyond the scope of this thesis.

One concern raised by the findings discussed above is whether the failure of AG490 to exert any effect in either RASMCs or J774 macrophages is due to the lack of expression or activation of JAK2 and/or TYK2 in these cells. Both these proteins are however known to be present in macrophages (Zhu *et al.*, 2013) and in smooth muscle cells (Liu *et al.*, 2012). This is indeed consistent with the western blot data obtained showing expression when lysates for the J774 macrophages and the RASMCs were

probed for JAK2 and TYK2 using selective antibodies for each. Thus, the next issue was to confirm whether these JAKs are in fact activated through phosphorylation following activation of cells with either LPS and IFN- $\gamma$  (RASMCs) or LPS alone (J774 macrophages). In these studies neither JAK2 nor TYK2 appeared to be phosphorylated in response to stimulation as the western blots produced failed to show any phospho-proteins, suggesting that neither was activated by LPS and IFN- $\gamma$  or LPS alone. This was an unexpected finding especially since there is a plethora of published data showing that JAK2 is phosphorylated in response to IFN- $\gamma$  (Bhat *et al.*, 1998; Ihle, 1995; Kakar *et al.*, 2005; Kitamura *et al.*, 1996; Silva *et al.*, 1994; Taniguchi, 1995). In addition both JAK2 and TYK2 are phosphorylated in response to LPS (Cruz *et al.*, 2001; Karaghiosoff *et al.*, 2000; Ohmori *et al.*, 2001; Okugawa *et al.*, 2003; Vadiveloo *et al.*, 2000) and especially of the later, of type one interferon response in vivo (Prchal-Murphy *et al.*, 2012; Shimoda *et al.*, 2002).. At present it is not clear why the phospho-proteins were not detected and this cannot be attributed to failed experiments since a positive control for JAK2 was picked up. The only reasonable conclusion at this stage is that neither protein is activated under our experimental conditions. This would at least account for the lack of effects with AG490 and would indicate that other signalling pathways other than the JAKs may mediate the actions of LPS and of IFN- $\gamma$ .

Apart from the effects observed on iNOS and NO production, L-arginine transport was also regulated by JAK inhibitor I but not by AG490. Transport of L-arginine is often co-induced with iNOS but very little is currently known about its regulation, especially by JAK signalling. Indeed this is the first report to show that induced uptake of L-arginine is susceptible to inhibition by JAK inhibitor I. However, from the discussions above, it is still not clear whether this might be the result of action on the JAKs, nor confirmation that the latter are required for induced transporter activity.

**Chapter 4. Confirmation of the role of JAK2 in the induction of iNOS, NO and L-arginine transport in RASMCs using JAK2 selective siRNA**

## 4.1 INTRODUCTION

The exact role of the JAKs particularly JAK2 in mediating cytokine induced iNOS expression in our cell systems still remains unclear. Our earlier approach using pharmacological inhibitors failed to confirm that JAK2 may be required for this process as its selective inhibitor, AG490, was without effect. These findings, as discussed, contrast with reports, suggesting that JAK2 activation was critical for induced iNOS expression in other cell systems. The reason for the discrepancies between our data and that published in the literature is unclear. However, to ensure that we can support the conclusions from our pharmacological experiments, we have extended our studies in this chapter using a siRNA approach by targeting JAK2 to elicit a knockdown and establish unequivocally whether induction of iNOS in RASMCs requires JAK2 activation. In these studies, specific siRNA nucleotide sequences targeting JAK2 were synthesised and transfected into cells prior to activation with LPS and IFN- $\gamma$ . In pilot studies, the efficiency of transfection of the nucleotides was initially optimised and changes in JAK2 protein expression determined by western blotting. This was then followed by monitoring changes in both iNOS expression and NO production in subsequent experiments. These studies were limited to RASMCs as it was difficult to transfect the J774 macrophages. Moreover there was only limited time available towards the end of the registered study period and there was not enough time available to conduct detailed studies in the macrophages.

## 4.2 AIM

The aim of this chapter was to confirm indisputably whether JAK2 activation is indeed essential for the induction of iNOS in RASMCs. The studies were carried out using a more specific molecular approach that exploited JAK2 selective siRNA nucleotides to knockdown JAK2 expression in the cells.

## 4.3 METHOD

### 4.3.1 Cell culture

Rat aortic smooth muscle cells were cultured to confluency as described in the methods. Prior to transfection RASMCs were trypsinized and diluted in Opti-MEM antibiotic free media and seeded at an optimal density of  $2.5 \times 10^6$  cells/ml in both 96-well (100  $\mu$ l) and in 12-well (500  $\mu$ l) plates for greiss assays and western blotting respectively. Cells were allowed to grow up to 70% confluency within 72 hours. The culture medium of each well or plate was replaced after 24 hours with fresh antibiotic free media for a further 24 hours.

### 4.3.2 Transfection Studies; Optimization of siRNA knockdown in RASMCs

For the selective suppression of JAK2 expression, RASMCs were transfected with ON-TARGET-plus small interfering RNA (siRNA) targeting JAK2 at optimal cell density and appropriate lipid mediated DharmaFect2 concentrations. To aid in this task, we used siGLO Green (Dharmacon, UK), a fluorescent oligonucleotide which when utilised, is retained in the nucleus to ensure an unambiguous visual confirmation of uptake and the optimal transfection conditions for siRNA. It however does not ensure the successful confirmation of knockdown.

Monolayer of adherent RASMCs were transfected with siRNA (100 nM final concentration) using the lipid mediated transfection reagent, DharmaFect2 as per manufacturer's instructions. Control transfection and optimization of transfection

conditions (i.e. plating density, concentration range of DharmaFect2) conditions using ON-TARGET-plus siRNAs targeting CYCLOPHILIN B with DharmaFect2 were also investigated in parallel.

Prior to transfection, a transfect mix containing 2  $\mu$ M siRNA solution diluted in 1X siRNA buffer and DharmaFect2 were separately prepared in appropriate volumes of serum free Opti-MEM media (containing deoxyribonucleosides, L-glutamine ribonucleosides, without ascorbic acid,- Invitrogen, UK) in complete absence of antibiotics as per manufacturer's instructions. Briefly in Tube 1, 17.5  $\mu$ l of 2  $\mu$ M siRNA with 17.5  $\mu$ l of serum free Opti-MEM media were incubated for 5 min at room temperature. In a separate tube (Tube-2), 1.4  $\mu$ l of DharmaFect2 with 33.6  $\mu$ l of serum free Opti-MEM were mixed and incubated for 5 min at room temperature. The contents of both tube 1 and 2 were mixed gently and further incubated for another 20 min at room temperature. Transfection mix (from combined contents from both tubes 1 and 2) were subsequently mixed gently (by pipetting up and down) with 280  $\mu$ l of complete Opti-MEM media (without antibiotics). Old media were aspirated off cells and 100  $\mu$ l of the transfection mix with complete media were added onto adherent cells (in triplicate) in 96-well plate. In a further study semi confluent 24-well plate containing RASMCs were cultured for western blotting. Transfection mix were prepared as previously described and respective volumes scaled up by a factor of 1.5 and aliquoted into designated wells.

Prior to transfection, spent media from culture plates were aspirated off and the above prepared transfection mix in combination with an appropriate volume of Opti-MEM media were added onto the monolayer of adherent RASMCs. Cells were incubated for a further 24 hours in an incubator at 37 °C in 5% CO<sub>2</sub>. Transfection media was replaced with fresh antibiotic free media (Opti-MEM) 24 hrs after signs of cell toxicity were observed in the culture flask. Lysates were subsequently generated and subjected to western blotting for JAK2 expression.

**TABLE 4.1. ON TARGET plus JAK2 siRNA nucleotide sequences**

JAK2 siRNA NUCLEOTIDES	SEQUENCE	DHARMACON CODE
JAK2 - 09	CGGAAGCGGAUAAGGU ACA	J-088340-09
JAK2 - 10	CUGUGGAAUUUAUGCG AAU	J-088340-10
JAK2 - 11	CAACAUUACAGAGGCA UAA	J-088340-11
JAK2 - 12	GAGAGUAUGUUGCCGA AGA	J-088340-12

### **4.3.3 Effect of JAK2 siRNA on JAK2 expression in RASMCs**

To assess the level of knockdown following siRNA treatment for 48 hours, media was firstly carefully aspirated off the plate and adherent cells lysed in lysis buffer (x1) followed by brief centrifugation at 12,000g for 1 min at room temperature. Protein concentrations were determined by BCA assay as previously described and equal amounts (40 µg protein/lane) were electrophoresed using 8% SDS PAGE. Separated proteins were transferred to PVDF membrane by semi-dry electroblotting and then blocked in 5% non-fat milk followed by primary incubation with a JAK2 specific antibody for an overnight incubation at 4 °C. The PVDF membrane was washed three times with wash buffer (containing 0.1% Tween-20 in Tris buffer) followed by a one hour incubation with a horseradish-peroxidase-conjugated secondary antibody at room temperature. Detection of JAK2 protein bands was by ECL chemiluminescence system.

### **4.3.4 Effect of JAK2 knockdown on nitrite production in RASMCs**

The effect of silencing JAK2 on LPS (100 µg/ml) and IFN- $\gamma$  (100 U/ml) induced NO production was assessed by determining changes in accumulated nitrite levels at the end of each incubation period using the Griess assay as described in Section 2.9 (Chapter 2).

## **4.4 STATISTICAL ANALYSIS**

All experiments were performed three times and data expressed as **means  $\pm$  SEM** as indicated. For data with multiple comparisons, statistical analysis was carried out with Graph Pad Prism (Graph Pad software, USA) and analyzed by using one-way ANOVA followed by Dunnett's test (in order to compare each treatment to control value). Where required, Student's t-tests were used for single comparisons between treated and control groups. Statistical significance was established at  $P < 0.05$ .

## 4.5 RESULTS

### 4.5.1 Effect of different culture media on nitrite production in RASMCs

Because the transfection studies had to be carried out in a different media (opti-MEM) to that used previously in activating the cells (ie DMEM) it was important to establish whether the change in media affected nitrite production or detection. Cells were therefore activated with LPS and IFN- $\gamma$  for 24 hr as in previous studies. As shown in Figure 4.1, there was comparable basal production of nitrite in the absence of any stimulation. The induction of nitrite production, although marginally low in cells cultured in opti-MEM, was not significantly different between the two conditions. Thus, the change in culture media does not alter the ability of cells to respond to LPS and IFN- $\gamma$  in expressing iNOS.

### 4.5.2 Effects of the transfection reagents on nitrite production in RASMCs

In parallel studies, the effect of the transfection agent *DharmaFect2* used in delivering siRNA into cells was investigated on nitrite production. This was to establish whether this agent on its own has the ability to regulate iNOS expression and/or function and thus nitrite production. As shown in Figure 4.2, *DharmaFect2* caused no statistically significant change in nitrite production either in controls or in activated cells over the concentration range of 0.05 to 0.125 nM subsequently used in the transfection studies. Similarly, *DharmaFect 2* did not cause any statistically significant change in cell viability except at the highest concentration of 0.5 nM (Figure 4.3).

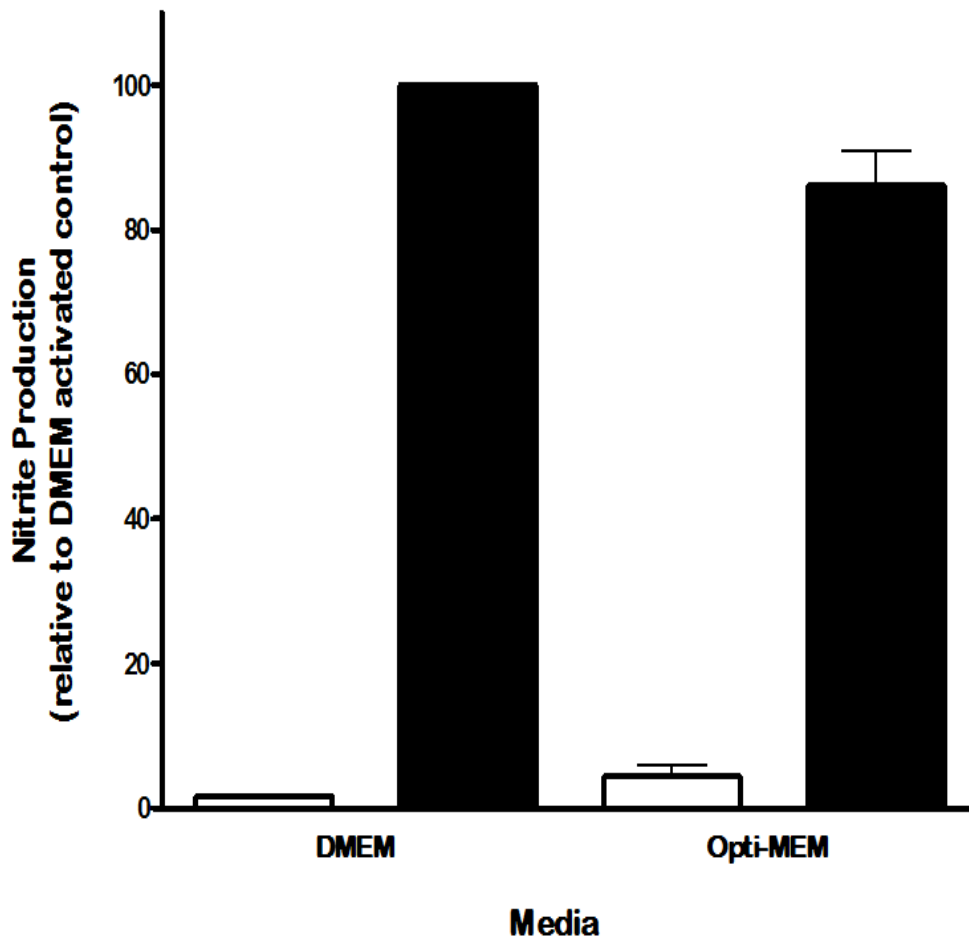


**Figure 4.1. Effects of culture media on nitrite production in RASMCs**

Confluent monolayers of RASMCs were incubated in two separate 96-well plates containing antibiotic free complete DMEM in one and Opti-MEM media in the other. Cells were stimulated with a combination of LPS (100 µg/ml) and IFN-γ (100 U/ml) for a 24-hour incubation period. Controls were incubated in complete culture medium alone. Nitrite produced in the medium was analysed using the Greiss assay as described in Method (Section 2.9). Open bars indicate control samples whilst black filled bars indicate activated samples. Data represent the **mean ± S.E.M.** from three independent experiments, each performed in triplicates. Statistical differences between means were determined using one-way analysis of variance (ANOVA) followed by Dunnett's multiple comparisons test of the normalized data.  $P > 0.05$  confirmed there was no significant difference in the levels of nitrite produced by cells cultured in DMEM compared to that in opti-MEM.

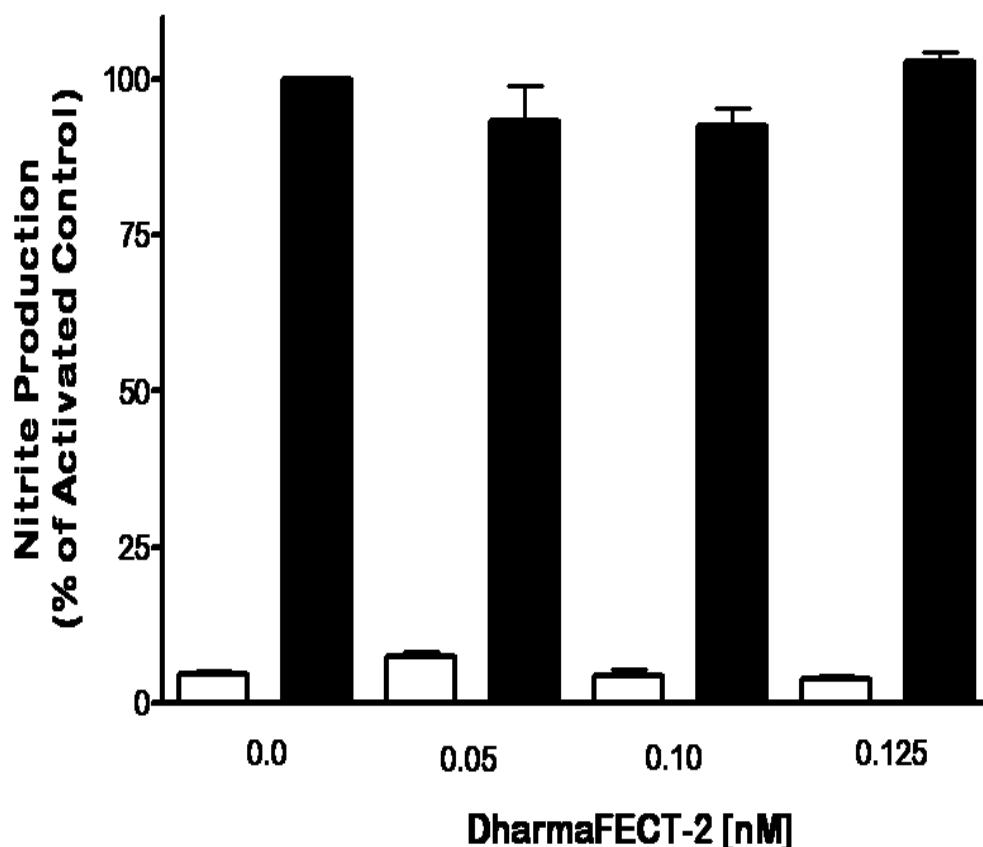


**Figure 4.2. Effects of DharmaFect 2 on nitrite production in RASMCs**

Semi-confluent (90 %) monolayers of RASMCs in 96-well plates were pre-treated in antibiotic free full OptiDMEM with different concentrations DharmaFect2 for 60 minutes prior to activation. Cells were activated with a combination of LPS (100 µg/ml) and IFN- $\gamma$  (100 U/ml) in the absence and continued presence of DharmaFect2 for 24-hours. The stable NO metabolite, nitrite, present in the medium was analysed using the Greiss assay as described in the Methods (section 2.9). The data is presented as percentage of nitrite by activated cell without DharmaFect2 treatment (activated control). Data represent the **mean  $\pm$  S.E.M.** from three independent experiments. Statistical differences between means were determined using one-way analysis of variance (ANOVA) followed by Dunnett's multiple comparisons test of the normalized data.  $P > 0.05$  confirmed there was no significant difference when compared to non activated control.

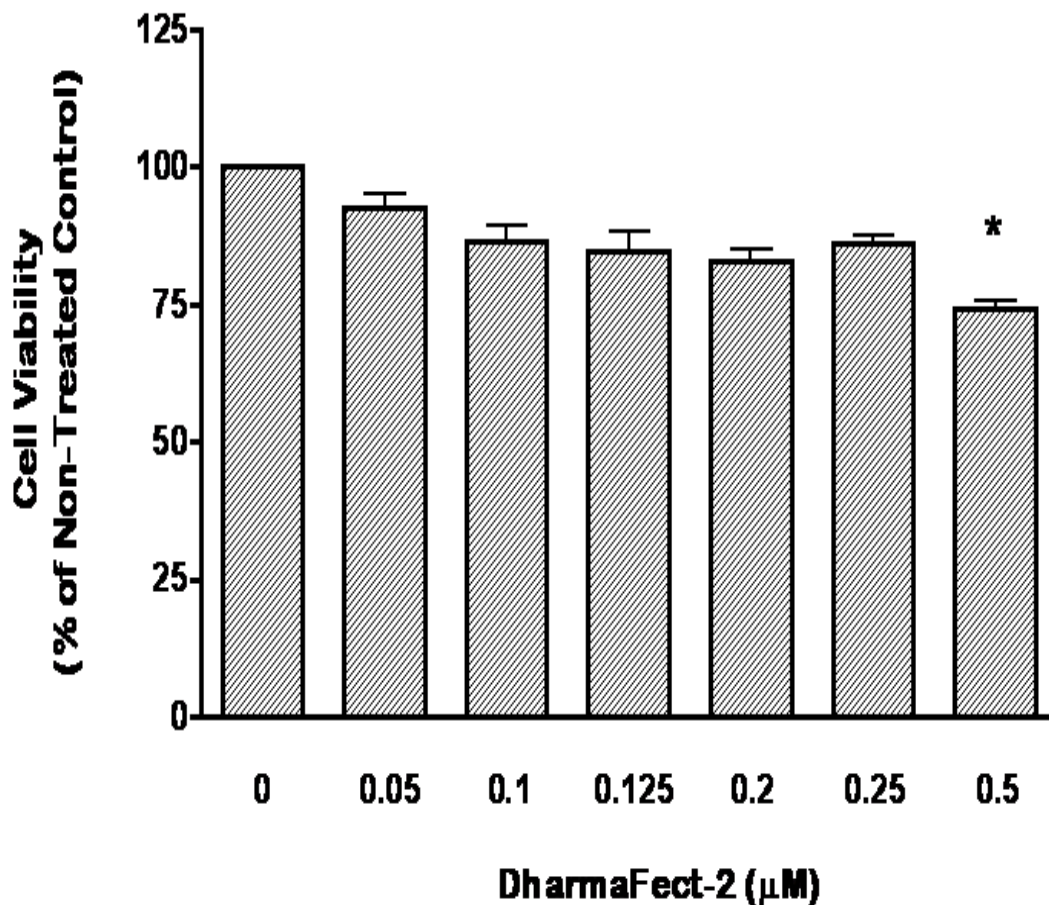


**Figure 4.3. Effects of DharmaFect2 on the viability of RASMCs**

Semi-confluent (90 %) monolayers of RASMCs in 96-well plates were pre-treated in antibiotic free full OptiDMEM with different concentrations DharmaFect2 for 60 minutes prior to activation. Cells were activated with a combination of LPS (100 µg/ml) and IFN- $\gamma$  (100 U/ml) in the absence and continued presence of DharmaFect2 for 24-hours. MTT metabolism by cells was determined colorimetrically as described in the Methods (Section 2.12). The data is presented as percentage in cell viability of activated cell without DharmaFect2 treatment (activated control). Data represent the **mean  $\pm$  S.E.M.** from three independent experiments, each with six replicates. Statistical differences between means were determined using one-way analysis of variance (ANOVA) followed by Dunnett's multiple comparisons test of the normalized data.  $P > 0.05$  confirmed there was no significant difference when compared to non activated control.

### **4.5.3 Optimization of siRNA delivery in RASMCs**

The successful and efficient delivery of siRNA into the nucleus is essential for effective knockdown of the targeted gene. To achieve this, experiments were initially conducted to optimise the efficiency of transfection of cells using the dye siGLO. As shown in Figure 4.1, treatment with siGLO together with the transfection agent *DharmaFect2* according to manufacturer's protocol resulted in high uptake and accumulation of siGLO in the nucleus of the cells (Figure 4.4C) which was not observed in the absence of *DharmaFect2*.

### **4.5.4 Assessment of knockdown of JAK2 following JAK2 siRNA treatment**

Having established that cells could be transfected efficiently with siGLO using *DharmaFect2* the next stage was to investigate whether the JAK2 siRNA could be successfully transfected into cells and whether depleted JAK2 protein expression and/or regulated iNOS expression and NO production. Because of time limitations, changes in L-arginine transport or in transporter expression were not investigated. These studies are however clearly needed and could form part of any future studies carried out by the group.

In the present studies, RASMCs were treated independently with the different JAK2 siRNA sequences (all at 100 nM final concentration) in the absence and presence of *DharmaFect2* at a concentration of 0.125 nM. As shown in Figure 4.5, JAK2 expression clearly detectable in control non-transfected cells was significantly attenuated in cells transfected with siRNA.

In order to assess knockdown we used western blot as a means to ascertain the effects of JAK2 down-regulation. Assessment of knockdown using target protein following SDS PAGE are influenced by a number of factors such as half-life of target protein, the role of constitutive protein expression versus transient protein expression. Following siRNA transfection, knockdown was expected to last for up about 72 hours.

Our western blot results as shown in Figure 4.7 and densitometrically illustrated in Figure 4.8 demonstrated that in untransfected cells (Lane 1, 2, 3 and 4) there was noticeably lack of any significant change in JAK2 expression. In addition, there was no change in JAK2 expression in cultured RASMCs induced with DharmaFect-2 mediated CYC siRNA as a positive control (i.e.Lane 4). In JAK2 siRNA treated cells however there were significant down-regulation in JAK2 protein expression in all the four sequences specific TargetPlus JAK2 siRNA tested but to varying extent. Densitometric analysis of our western blots bands as shown in Figure 4.8 demonstrated the following levels of down-regulation as listed below;

Lane 5 - JAK2 siRNA-[9] down regulated to  $31.33 \pm 4.49$  %

Lane 6 - JAK2 siRNA-[10] down regulated to  $12.11 \pm 2.99$  %

Lane 7 - JAK2 siRNA-[11] down regulated to  $21.94 \pm 4.37$  %

Lane 8 - JAK2 siRNA-[12] down regulated to  $38.52 \pm 8.44$  %

JAK2 siRNA-[12] was the least potent whiles JAK2 siRNA-[10] was the most potent in down regulating JAK2 protein expression.

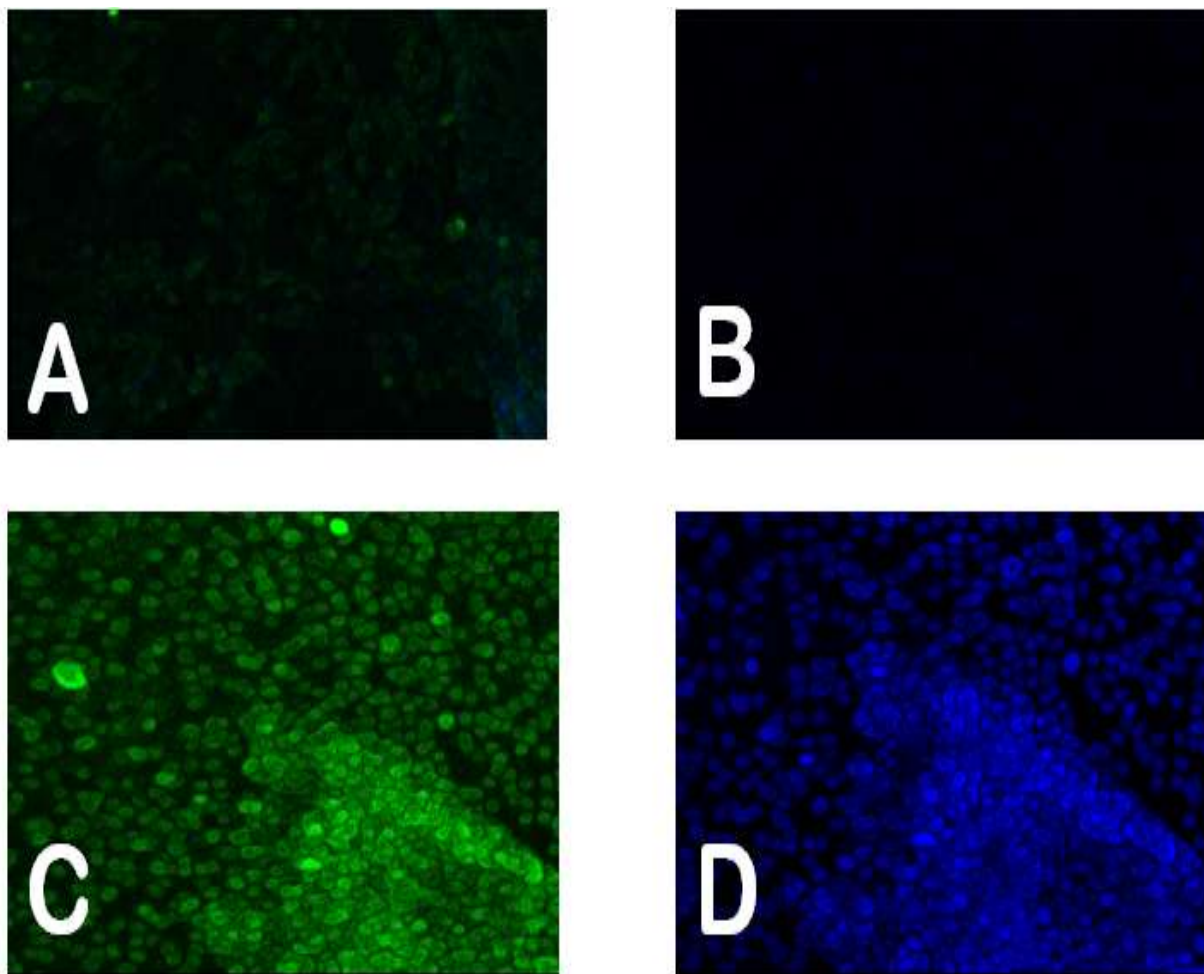


**Figure 4.4. Micrographs of RASMCs stained with siGLO in the absence and presence of DharmaFect 2.**

Cells were seeded at 2500 cells/well for at least 30 hours prior to transfection with 50 nM siGLO Green for a further 24 hours in the absence and presence of DharmaFect2 at final concentration of 0.125  $\mu$ g/ well. After 24 hours, cells were visualized under a confocal microscope. Figure **A** represents control where cells were treated with siGLO alone in the absence of DharmaFect2 and **B** are cells treated with siGLO and DAPI without DharmaFect2. Figure **C** show cells treated with siGLO together with DharmaFect 2 and **D** represent cells treated with DAPI and DharmaFect2. These results are representative of at least three independent experiments.

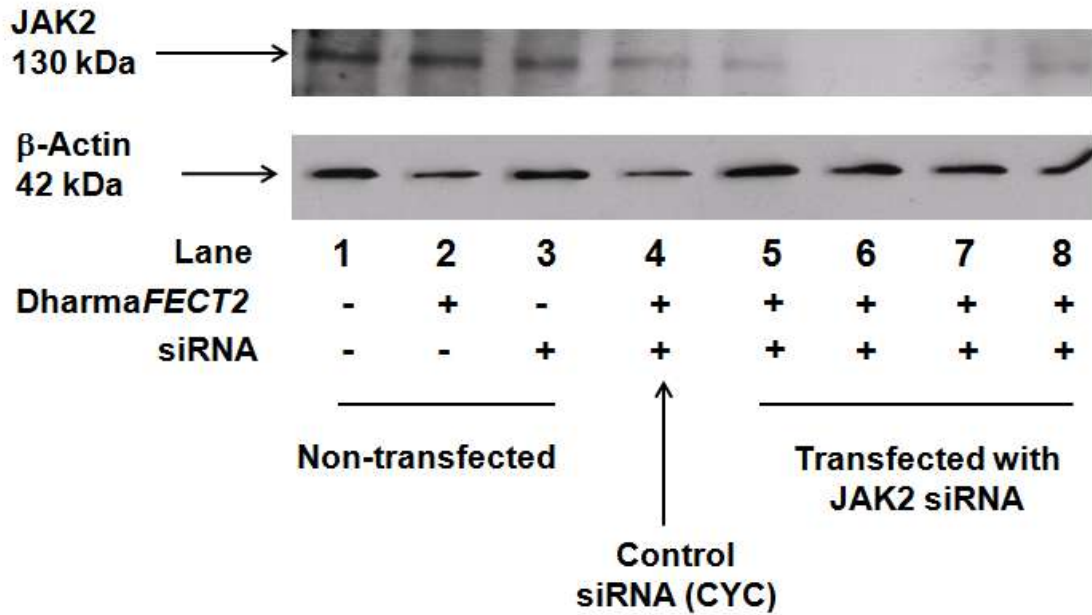


**Figure 4.5. Expression of JAK2 in both control and siRNA treated RASMCs.**

Semi-confluent monolayers of RASMCs in 12-well culture plates were cultured in either complete Opti-MEM alone (Lane 1), complete Opti-MEM + DharmaFect2 (Lane 2), complete Opti-MEM induced with siRNA targeting JAK2 gene (Lane 3), complete Opti-MEM induced with DharmaFect2 and control siRNA targeting CYC gene (Lane 4). Lanes 5 to 8 represent cells transfected with complete Opti-MEM induced with 4 different sequences specific TARGETplus siRNAs targeting different regions of JAK2 gene. Cells were harvested and 40  $\mu$ g of protein lysates resolved on SDS-PAGE gel. Western blotting was performed as described in Methods (Section 2.13). The blot is representative of three experiments. The bands at 42 kDa show expression levels of the  $\beta$ -actin to confirm equal loading.

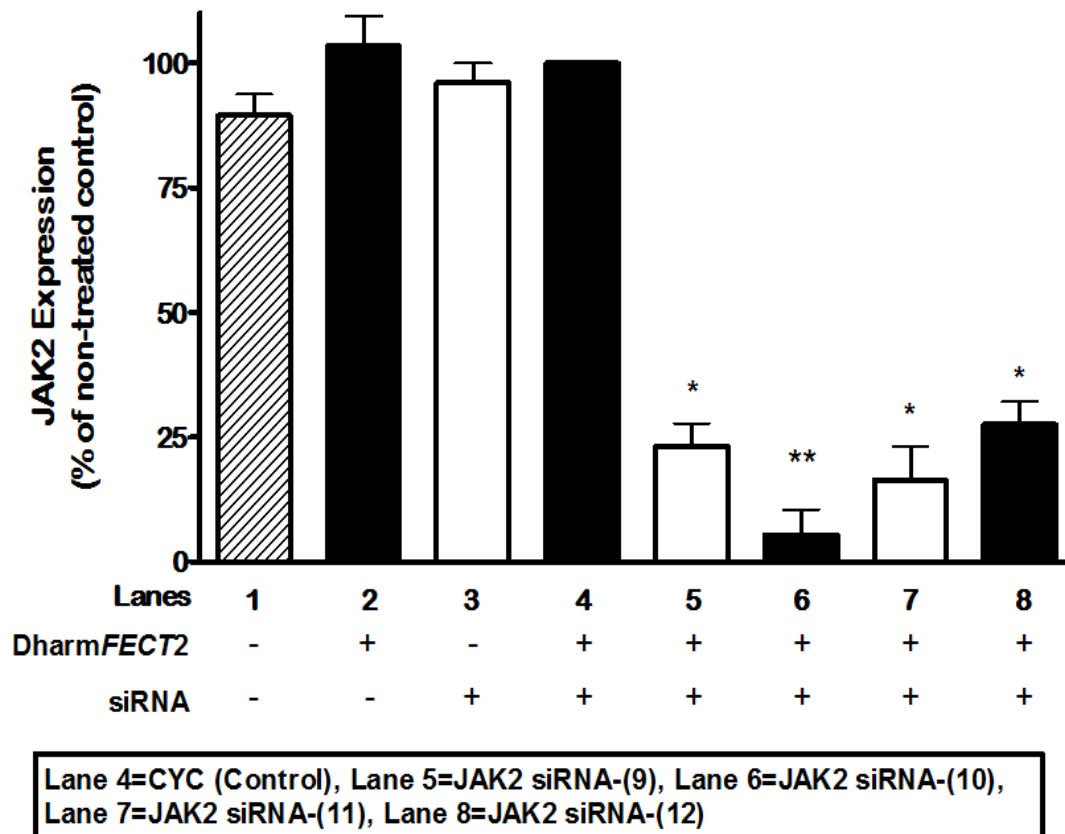


**Figure 4.6. Densitometry of JAK2 knockdown in both control and siRNA treated RASMCs.**

Densitometric quantification of JAK2 protein levels (obtained by western blotting) in siRNA transfected RASMCs in knockdown studies shown in Figure 4.5. Data are presented as a percentage of relative expression normalized to the  $\beta$ -Actin and compared to the positive control (as shown in lane 4). Data represent the **mean  $\pm$  S.E.M.** from three independent experiments. Statistical differences between means were determined using one-way analysis of variance (ANOVA) followed by Dunnett's multiple comparisons test of the normalized data. There was a very significant change in JAK2 protein expression in siRNA transfected RASMCs. \* & \*\* denotes  $P < 0.05$  and  $P < 0.01$  respectively when both are compared to positive control (bar 4).

#### **4.5.5 NO production in JAK2 knockdown RASMCs following siRNA treatment.**

Treatment of RASMCs with LPS (100 µg/ml) and IFN- $\gamma$  (100 u/ml) resulted in significant increases ( $p < 0.05$ ) in NO production. When untransfected cells were pre-treated with either DharmaFect-2 alone (Figure 4.9; Bar 2) or with siRNA targeting JAK2 gene alone (Figure 4.9 Bar 3) for 60 minutes prior to activation with both LPS and IFN- $\gamma$  and in complete absence of transfection reagent, there was no significant differences in the levels of nitrite produced. More importantly, treatment of cells with siRNA in the presence of the transfection reagent also failed to cause any significant change in basal or induced nitrite levels. This was indeed the case even when different siRNA oligonucleotides targeting different regions of the JAK2 gene were used.

In summary there was no significant difference in the levels of nitrite despite transfection mix containing siRNA targeting different regions of the JAK2 gene.

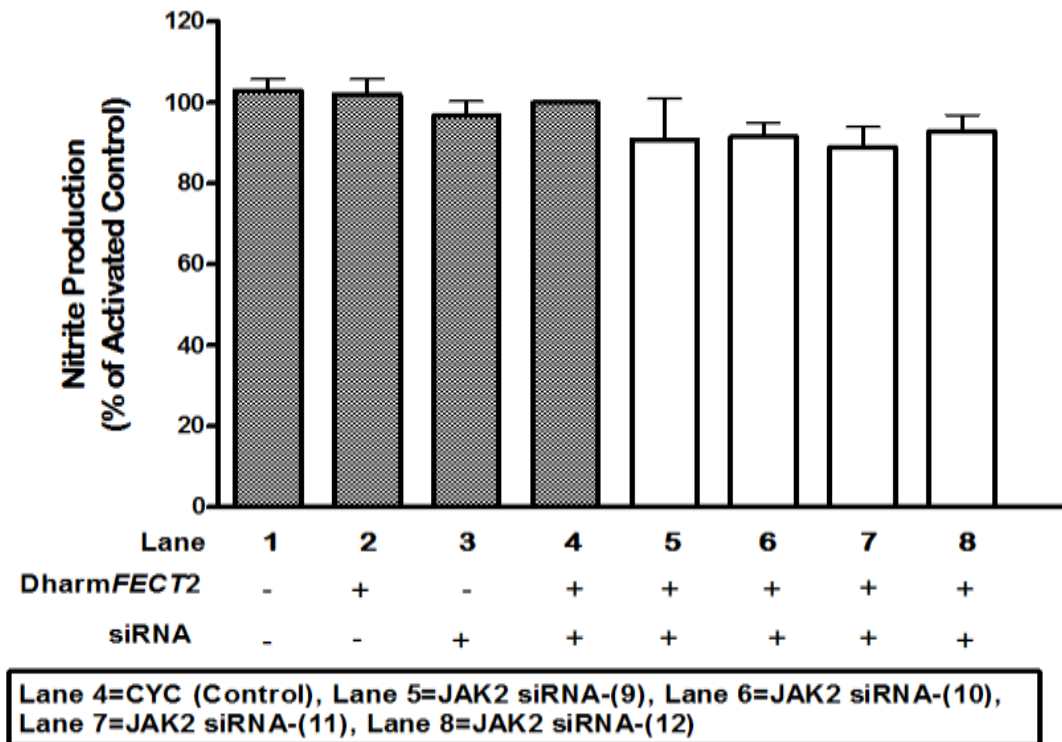


**Figure 4.7. Nitrite production in both control and siRNA treated RASMCs.**

Semi-confluent monolayer of RASMCs in 96 well plates, in the absence and presence of transfection mix containing siRNA targeting different regions of the JAK2 gene and DharmFect2 at final concentration of 0.125 µg/ well for 60 minutes prior to activation. Cells were activated with a combination of LPS (100 µg/ml) and IFN-γ (100 U/m) for a 24-hour incubation period. The stable NO metabolite, nitrite, present in the medium was analysed using the Greiss Assay as previously described in the Methods (Sections 2.9). The data is presented as percentage of nitrite production by activated control. Data represent the **mean ± S.E.M.** from three independent experiments, each performed with 6 replicates. Statistical differences between means were determined using one-way analysis of variance (ANOVA) followed by Dunnett's multiple comparisons test of the normalized data.  $P > 0.05$  confirmed there was no significant difference in nitrite production between siJAK2 transfected cells (i.e. bars 5, 6, 7 and 8) and positive control (bar 4).

## 4.6 DISCUSSION

In view of the findings in Chapter 3, further experiments were carried out using siRNA as a selective tool to unequivocally establish the role of JAK2 in the induction of iNOS in RASMCs.

As an evolving technology, the role of siRNA in RNA interference (RNAi) pathway is a fast emerging molecular approach to study gene function by specific inhibition of gene expression. Current application of gene knockdown involve the use of short (21 to 23 nucleotides) small interfering RNA (siRNA) (Moffat *et al.*, 2006; Shen, 2004; Zhou *et al.*, 2003). They are synthetic double stranded RNA duplexes designed to inhibit gene expression by inducing gene sequence-specific degradation of homologous mRNA (Elbashir *et al.*, 2001a; Fire *et al.*, 1998; Tuschl *et al.*, 1999). To date a number of studies have shown that siRNA can significantly suppress gene expression when delivered into mammalian cells in vitro (Elbashir *et al.*, 2001a; Fish *et al.*, 2004; McManus *et al.*, 2002).

In this thesis, sequences of pre-designed siRNA oligonucleotides were first examined by comparing their sequences to the entries of the rat GenBank database through the use of the BLASTN program which is available on the National Centre for Biotechnology Information web page (<http://www.ncbi.nlm.nih.gov/>)

The procedure for depleting genes such as JAK2 in cells is dependent on the sequence-specific, post transcriptional gene silencing of the JAK2 gene initiated by constructing, a 19-25 bp RNA duplex with complete sequence homology to the target (Shankar *et al.*, 2005). However the delivery of synthetic siRNA duplex into cells in general has been a major obstacle for its application (Zhang *et al.*, 2007). Earlier approaches of siRNA delivery into primary cells especially have largely proved unsuccessful due to cytotoxicity, size and nature of sequence (Whitehead *et al.*, 2009). In this thesis we set out, first and foremost to maximize siRNA delivery while minimizing cellular toxicity under miniaturized (96-well plate) format. We chose the lipid mediated transfection reagent DharmaFect2 on the basis of its previous use in rat derived cells including smooth muscle cell line (A7R5), rat fibroblast (RAT2), rat kidney fibroblast (NRK-49F) amongst others. Though the use of this transfection reagent represents the

most common approach, it is often associated with problems of cytotoxicity and its incompatibility with siRNA delivery into suspension and primary cells. We therefore optimized conditions for an effective delivery of a dose-dependent DharmaFect2 into our primary cells to enable high efficiency of siRNA delivery while still mindful of a low toxicity target. Other studies suggest that such delivery effects are likely to induce interferon response (Reynolds *et al.*, 2006) when not correctly used. Using DharmaFect2, we were able to confirm assessment of siRNA mediated knockdown following the introduction of the stable, fluorescent, non-targeting control siRNA with RISC-free modification, siGLO into the cells. As shown in our results when used in addition to DAPI stain, we demonstrated a high degree of efficiency which was not possible without this transfection reagent, thus confirming successful transfection of cells. Moreover, this was achieved with concentrations that caused little or no cytotoxicity to cells. In addition as with other reports (Elbashir *et al.*, 2001a; Lee *et al.*, 2002) we optimized and subsequently maintained siRNA concentration to about 1.25 nM and this did not alter the silencing effect, suggesting that siRNA by the nature of their design and sequence content were effective at concentrations several orders of magnitude below that of a conventional antisense gene-targeting experiment (Kehlenbach *et al.*, 1998).

To ensure that the experimental conditions did not interfere with the detection of nitrite produced, further controls were carried out including establishing the effects of different media on accumulated nitrite levels. The results obtained showed that using Opti-MEM in place of DMEM did not cause any significant change in nitrite levels, thus ruling out any artifacts resulting from the change in media conditions.

A critical observation from our results also showed that when primary RASMCs were treated separately with four sequence-specific siRNA for JAK2, there was suppression of JAK2 protein expression. In addition, the degree of the knockdown was very much dependent on the sequence specific designed construct delivered into the cells. To address the difference in level of knockdown we conducted a Basic Local Alignment Search Tool (BLAST) analysis (National Center for Biotechnology Information, NIH) for each of the four siRNA constructs. In order to identify the target region within the JAK2 gene, the BLAST tool enabled an alignment between homologous regions of both the target gene and each of the sequence specific siRNA constructs used. Each sequence

designed siRNA was aligned against the cDNA of the JAK2 gene, (1q52, Genomic Size: 58769 bp) **NM\_031514.1**. An alignment of the siRNA primers to JAK2 genome revealed regions targeted by each of the siRNA constructs used as shown in the schematic representation below (Figure 4.10).

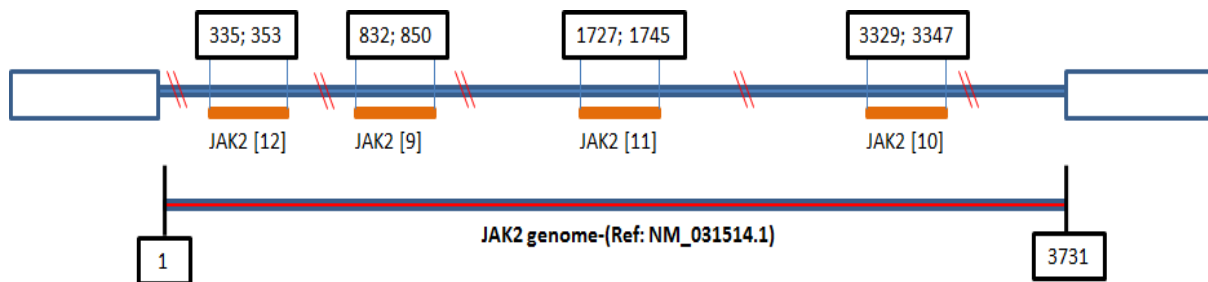


**Figure 4.10 JAK2 siRNA constructs in sequence-specific homology with JAK2 gene**

Schematic representation of JAK2 gene showing designated regions in the JAK2 Locus that were functionally inactivated by TARGETplus sequence-specific siRNA constructs (Dharmacon) that were transfected into RASMCs. JAK2 gene was functionally rendered inactive.

Western blotting analysis on lysates generated after 48 hours post transfection revealed clearly the expression of JAK2, thus suggesting this protein had a long half-life. Previous comparable experiments have found that measuring the mRNA of target genes were more reliable in assessing silencing efficacy compared to their protein levels. In addition it was significant to note that transfection of RASMCs with RNA duplexes as short as 19 bp could still cause detectable silencing as demonstrated in our results following western blot analysis. Our results are therefore consistent with other investigators that have used comparably much longer (22-25 bp) sequence specific siRNA targets with reported high efficiency and the added insignificant loss of potency. The much shorter duplex used in the thesis suggests that much of the effectiveness or potency of the silencing trigger might be attributed to the sequence specific design used.

We are the first to report JAK2 mediated siRNA knockdown in RASMCs in order to examine its role in JAK/STAT mediated iNOS expression. There is some consensus in acknowledging that effective gene silencing efficiency of siRNA is largely reliant on the local mRNA of the target region. Current strategies for effective silencing is still reliant on designing several siRNAs (more than three) against different regions of the same target gene of interest (Elbashir *et al.*, 2001a; Harborth *et al.*, 2001; Semizarov *et al.*, 2003).

We did not assess the efficacy of respective siRNAs provided but important parameters in assessing such knockdowns from reports have included the nature of secondary structure of the target mRNA in determining its accessibility (Luo *et al.*, 2004b; Zuker, 2003) to binding domains or receptors, duplex-end thermodynamic stability (Khvorova *et al.*, 2003; Schwarz *et al.*, 2003), sequence specific motifs (i.e. predominance of A or U bases in the 5' end of antisense) (Haley *et al.*, 2004; Ui-Tei *et al.*, 2004), 21mer targets, low GC-content and TT overhangs (Harborth *et al.*, 2003) to target sites. Results obtained in this study demonstrate how the variability in position of sequence specific siRNA site impacts on the efficacy in target degradation in our JAK2 model. Though we are unable to characterize the nature of each specific siRNA construct used in this thesis, our results showed variability in the knockdown effect. To date, strategies in designing effective siRNAs include the development of motif based algorithms (Pei *et al.*, 2006). Designing of such algorithms from previous studies (Amarzguioui *et al.*,

2004; Reynolds *et al.*, 2004) have included the use of low G-C content and secondary structure prediction in their design algorithms in assessing the efficacy of potential site for optimal siRNA/target sequence degradation. Other stringently applied criteria or parameters such as low internal stability on the sense strand at the 3' termini, lack of inverted repeats and specific positional sense strand base preference of construct in the design algorithm have all greatly improved efficacy of some selected and potent siRNAs (Reynolds *et al.*, 2004) by Dharmacon. Thus there may be other factors affecting RISC activity but these are yet to be discovered.

There was a high degree of efficiency in our transfected cells as demonstrated in our studies (Figure 4.1) with DharmaFect2. Also we were able to introduce siGLO and DAPI into cells with a high degree of efficiency which was not possible without this reagent, thus confirming successful transfection of cells. In addition this was achieved with concentrations that caused little or no cytotoxicity to cells. To ensure that the experimental conditions did not interfere with the detection of NO produced further controls were carried out including establishing the effects of different media on accumulated nitrite levels and the results obtained showed that using Opti-MEM in place of DMEM did not cause any significant change in nitrite levels thus ruling out any artefacts resulting from the experimental conditions.

To further address the role of JAK2 in cytokine mediated iNOS expression we successfully induced gene specific silencing by using four sequence specific siJAK2 constructs in transfecting RASMCs. When used, siRNA for JAK2 caused suppression of JAK2 protein expression but the degree of knockdown was very much dependent on the sequence construct used. Thus our results are consistent with previous publications (Jayasena, 2005; Zamore *et al.*, 2000) in confirming that different siRNA synthesized for various positions vary in their gene silencing effectiveness. Reasons for these differences as earlier highlighted varies but there is evidence to suggest that even though target recognition is highly sequence specific, the 5' end of the siRNA beginning with A-T pair, rather than a G-C pair with its complement is most effective in inducing cleavage compared to either the center or the 3' end of the target RNA (Elbashir *et al.*, 2001b). Aside from these parameters there is also the possibility of off-target effects or regulation. That is, siRNA may degrade or render ineffective other genes whose sequences are similar to that of the target gene. In designing the most effective siRNA

for specific targets, various authors (Takasaki, 2010; Xingang *et al.*, ; Yamada *et al.*, 2005) have designed predictive mathematical algorithms incorporating some of the above parameters and in addition including specific base preferences at certain locations within the siRNA duplex (Reynolds *et al.*, 2004).

Despite above 80 % average knockdown of JAK2, comparative analysis showed that there was still no significant change in nitrite production in RASMCs following stimulation with LPS and IFN- $\gamma$ , supporting the pharmacological data with AG490, that JAK2 may not be essential for iNOS expression. Since there was no significant change in nitrite levels (Figure 4.7) further studies examining iNOS protein expression was not conducted. We therefore conclude from these findings that despite the implication of JAK2 in other studies (Doi *et al.*, 2002; Kim *et al.*, 2007; Nishiya *et al.*, 1995) this kinase may not be directly relevant for iNOS expression at least in RASMCs under our experimental conditions. Several reports have shown that other pathways including p38 MAPK and the JNK may also be implicated iNOS expression (Chan *et al.*, 2001a; Da Silva *et al.*, 1997) but these were not investigated in this thesis. The lack of TYK2 specific inhibitors precludes verification of its role in this seemingly complex process.

In conclusion studies carried out in this thesis have further demonstrated that JAK2 may not be directly implicated in the signaling of cytokine stimulated NO production in both J774 macrophages and RASMCs. This is because prior treatment of two cell models with AG490, the specific JAK2 inhibitor did not completely inhibit cytokine-stimulated NO production in both cell models. In addition, transport studies also confirmed that JAK2 is unlikely to be a major mediator of cytokine-stimulated L-arginine transport in both models. Also the lack of phosphorylated JAK2 expression in the cytokine induced serum starved cells in both cell models further suggests a lack of any role for JAK2 in our studies. These conclusions however contrast with other investigators suggesting a positive role for this pathway in human epithelial-like colon carcinoma DLD-1 cells (Marrero *et al.*, 1998). In these cells, cytokine induction of iNOS is blocked by the JAK2-specific inhibitor, AG490 or tyrphostin B42. Also, JAK inhibitor I, which potently inhibits all four JAK family members (Thompson *et al.*, 2002) blocked the induction of iNOS and NO synthesis suggesting a role for a JAK in these processes. However our findings

suggest, under our experimental conditions, there was lack of a direct JAK2 effect on iNOS induction, NO production or L-arginine transporter activity.

**Chapter 5. Expression of phosphorylated STAT-1 and role of GTPases in the induction of the inducible L-arginine-NO pathway in J774 macrophages and rat cultured aortic smooth muscle cells**

## 5.1 INTRODUCTION

The findings discussed in Chapters 3 and 4 have strongly indicated that the JAKs and in particular JAK2 may not be required for the induction of iNOS and/or L-arginine transport in either RASMCs or J774 macrophages. This was based on observations from cells pre-treated with AG490 (an inhibitor routinely used as a potent JAK2 inhibitor (Meydan *et al.*, 1996) or with siRNA targeted at JAK2. In both cases, there were no significant modifications of induced NO synthesis or enhanced L-arginine transport rates in activated cells. As previously discussed, these results contrasted with other findings that have implicated JAK2 for iNOS induction (Cruz *et al.*, 1999; Nakashima *et al.*, 1999; Tsoyi *et al.*, 2008).

To confirm whether other components of the JAK/STAT pathway may be involved in our system, studies were conducted to examine whether STAT-1 was activated through phosphorylation in cells exposed to LPS alone or in combination with IFN- $\gamma$  in J774 macrophages and RASMCs respectively. In these experiments, changes in the expression profile of phosphorylated-STAT-1 (pSTAT-1) were determined by western blotting using a phospho-specific anti-STAT-1 antibody. Changes in expression of the activated (phosphorylated) protein were also determined in the absence and presence of AG490 or JAK inhibitor I and correlated with changes in nitrite production, iNOS expression and in L-arginine transport. More importantly, studies were also aimed at establishing whether STAT-1 may be activated directly and independently of the JAKs.

In this regard, it has been suggested that STAT-1 may be phosphorylated possibly by upstream GTPases (Pelletier *et al.*, 2003) and by nuclear pore targeting complex formation, independent of JAK mediated activation (Sekimoto *et al.*, 1997). Following from these observations parallel experiments were therefore conducted to examine whether inhibitors of GTPase signalling regulated iNOS expression and induced L-arginine transport. The studies were also extended by investigating whether STAT-1 could be activated directly by the small GTPase Rho and independently of the JAKs. These studies are relevant as it has been reported that STAT-1 can be phosphorylated directly by Rho, independent of JAK activation (Pelletier *et al.*, 2003). Additionally, some evidence has implicated Rho GTPase in modulating iNOS expression in airway

epithelial cells (Kraynack et al., 2002) and in smooth muscle cell (Yamamoto *et al.*, 2003) under inflammatory conditions.

To determine whether Rho plays any role in the induction of iNOS and/or L-arginine transport in RASMCs and J774 macrophages, additional experiments were carried out using atorvastatin, an HMG CoA inhibitor. The pleiotropic cellular effects for this class of statins on vascular endothelial and macrophages are usually direct (Takemoto *et al.*, 2001) and the mechanism is said to restrict or abrogate isoprenylation and farnesylation of small GTPases, particularly the Rho and Ras proteins. This reaction is known to down-regulate activities of the GTPases and thus modulate events further downstream (Liao *et al.*, 2005; Mason, 2003). Parallel studies were carried out using Y-27632, a prenyltransferase inhibitor reported to specifically inhibit Rho activity (Uehata *et al.*, 1997). These studies were conducted to determine whether STAT-1 phosphorylation was mediated through Rho signalling independent of the JAKs.

## **5.2 METHODS**

### **5.2.1 Experimental conditions**

#### **5.2.1.1 Cell culture**

Confluent monolayers of RASMCs or J774 macrophages in T-75 culture flasks were trypsinized as described in the methods and seeded into 96-well or 6-well plates for L-arginine transport measurement and Western blotting respectively. Cells were allowed to grow to between 80 to 90% confluent over 72 hours before being used in the experiments.

#### **5.2.1.2 Activation of cells**

To determine the time course of activation of STAT-1, initial experiments were carried out using cells in 6-well plates in which RASMCs were activated with LPS (100 µg/ml) in combination with IFN- $\gamma$  (100 U/ml) and J774 macrophages activated with LPS alone (1.0 µg/ml). Incubations were for 0, 5, 10, 15, 30, 60, 120 and 180 min. Cell lysates were separately generated for each cell type for western blotting as described in Methods (Section 2.9 and 2.11).

#### **5.2.2 Treating of cells with Rho-inhibitors**

Confluent monolayers of cells in 6 or 96-well plates were washed twice with PBS (X1) at 37 °C. This was immediately followed with incubation of cells with atorvastatin (1 to 100 µM) or with Y-27632 (0.01 to 10.0 µM) for 30 minutes prior to activating with LPS (100 µg/ml) in combination with IFN- $\gamma$  (100 U/ml) in RASMCs or LPS alone (1.0 µg/ml) in J774 macrophages. Cells were then incubated for a further 24 hours before determining levels of nitrite produced.

### **5.2.3 Determination of nitric oxide production**

Nitric oxide production was measured in the culture medium by the standard Greiss assay as described in Method (Section 2.9). Supernatant (100  $\mu$ l) from sub-confluent culture was mixed with an equal volume of Greiss reagent and absorbance was read at 540 nm.

### **5.2.4 Protein assay**

Protein content in cell lysates was determined using the BCA assay as described in the Methods (Section 2.11). Cell lysates (10  $\mu$ l) from sub-confluent cultures was mixed with 100  $\mu$ l of BCA reagent and absorbance read at 630 nm.

### **5.2.5 Western blot analysis**

Western blotting procedure was carried out as described in the Methods (Section 2.13). STAT-1 protein and its phosphorylated form in lysates were determined using rabbit polyclonal anti-STAT-1 or phosphor-STAT-1 antibody and a goat polyclonal antibody to rabbit IgG as a secondary antibody.

### **5.2.6 Cell cytotoxicity assay**

Changes in cell viability following exposure to the inhibitors were determined in parallel experiments where the medium was removed after 24 hr incubation for nitrite measurements and the cell monolayer incubated with 0.5 mg/ml MTT for 4 hours. Levels of formazan produced were determined as described in the Methods (Section 2.12).

### **5.3 STATISTICAL ANALYSIS**

All experiments were performed at least three times and data expressed as mean  $\pm$  SEM as reported. For multiple comparisons, statistical analysis was carried out with Graph Pad Prism (Graph Pad software, USA) using one-way ANOVA followed by Dunnett's test (in order to compare each treatment to control value). Where required, Student's t-tests were used for single comparisons between treated and control groups. Statistical significance was established at  $P < 0.05$ .

## **5.4 RESULTS**

### **5.4.1 Detection of phosphorylated STAT-1 protein in both RASMC and J774 macrophage cultures**

Prior to carrying out a detailed study of the phosphorylation of STAT-1, a pilot experiment was carried out to determine whether the phospho protein could be detected. The results as shown in Figures **5.1** and **5.2** indicate that in both RASMCs and J774 macrophages, pSTAT-1 protein was expressed when cells were respectively stimulated with a combination of LPS (100 µg) and IFN-γ (100 U/ml) or LPS (1.0 µg) alone. The level of phosphorylated protein expression was much higher in RASMCs than in J774 macrophages. There was however no phosphorylated STAT-1 expression in control non-activated cells.

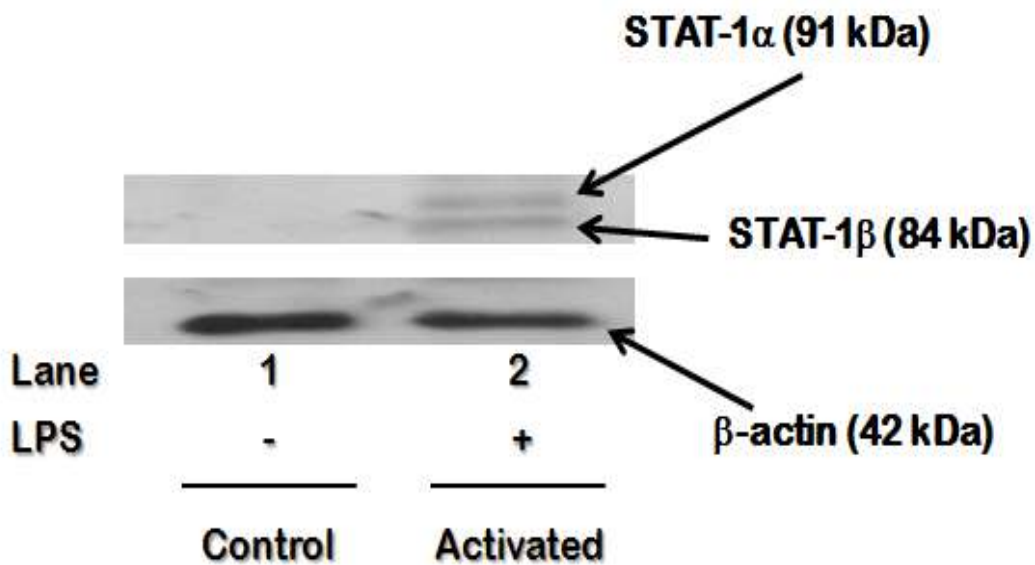


**Figure 5.1 STAT-1 $\alpha/\beta$  tyrosine phosphorylation in control and activated J774 macrophages.**

Confluent monolayers of J774 macrophages in 6-well plates were either incubated in DMEM alone or stimulated with LPS (1.0  $\mu\text{g/ml}$ ) in continued presence of complete DMEM for. Cell lysates were generated and equal quantities of protein (40  $\mu\text{g}$ ) subjected to western blotting as previously described in Methods (Section 2.13) using a pSTAT-1 specific antibody. The above Western blot insert is a representative of at least three independent experiments with bands showing STAT-1 as the target protein and  $\beta$ -actin as a loading control.

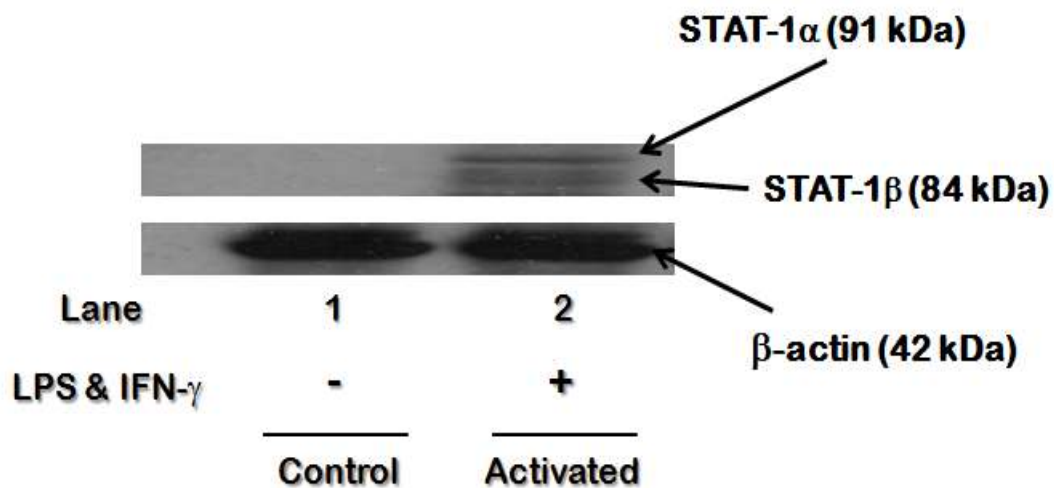


**Figure 5.2 STAT-1 $\alpha/\beta$  tyrosine phosphorylation expression in both control and activated expression in RASMCs**

Confluent monolayers of RASMCs in 6-well plates were cultured in complete DMEM alone or stimulated with both LPS (100  $\mu\text{g}/\text{ml}$ ) and IFN- $\gamma$  (100 U/ml) in continued presence of complete DMEM for. Cell lysates were generated and equal quantities of protein (40  $\mu\text{g}$ ) subjected to western blotting as previously described in Methods (Section 2.13) using a pSTAT-1 specific antibody. The above Western blot insert is a representative of at least three independent experiments with bands showing STAT-1 as the target protein and  $\beta$ -actin as a loading control.

#### **5.4.2 Time-dependent phosphorylation of STAT-1 in RASMCs and J774 macrophages**

Following the observations above further experiments were carried out to examine the time course of STAT-1 phosphorylation in the respective cells following exposure to LPS (J774 macrophages) or LPS and IFN- $\gamma$  (RASMCs). Since IFN- $\gamma$  has been reported to associate with the JAKs as its primary mode of signalling, we also further examined phosphorylation of STAT-1 in the presence of inhibitors, JAK-inhibitor-I and AG490.

Results from this time course study demonstrated that in RASMCs, there was a time-dependent increase in the expression of STAT-1 phosphorylation (Figure 5.3) following activation with a combination of IFN- $\gamma$  (100 U/ml) and LPS (100  $\mu$ g/ml). This was induced within 5 minutes of activation, reaching a peak after 30 minutes and was followed by a sharp decline thereafter. There were no expressions of phosphorylated STAT-1 in non-activated cells (Figure 5.3).

In contrast, results with J774 macrophages showed a different pattern of STAT-1 phosphorylation (Figure 5.4) following activation with LPS (1.0  $\mu$ g/ml). There was hardly any detectable phosphorylated protein within the first 30 minutes of activation. There was however marginal expression of phospho-STAT-1 at 60 minutes and the level of expression were sustained up to 120 minutes post activation. In addition there was very little change in intensity of expression over the stated period (see Figure 5.4).

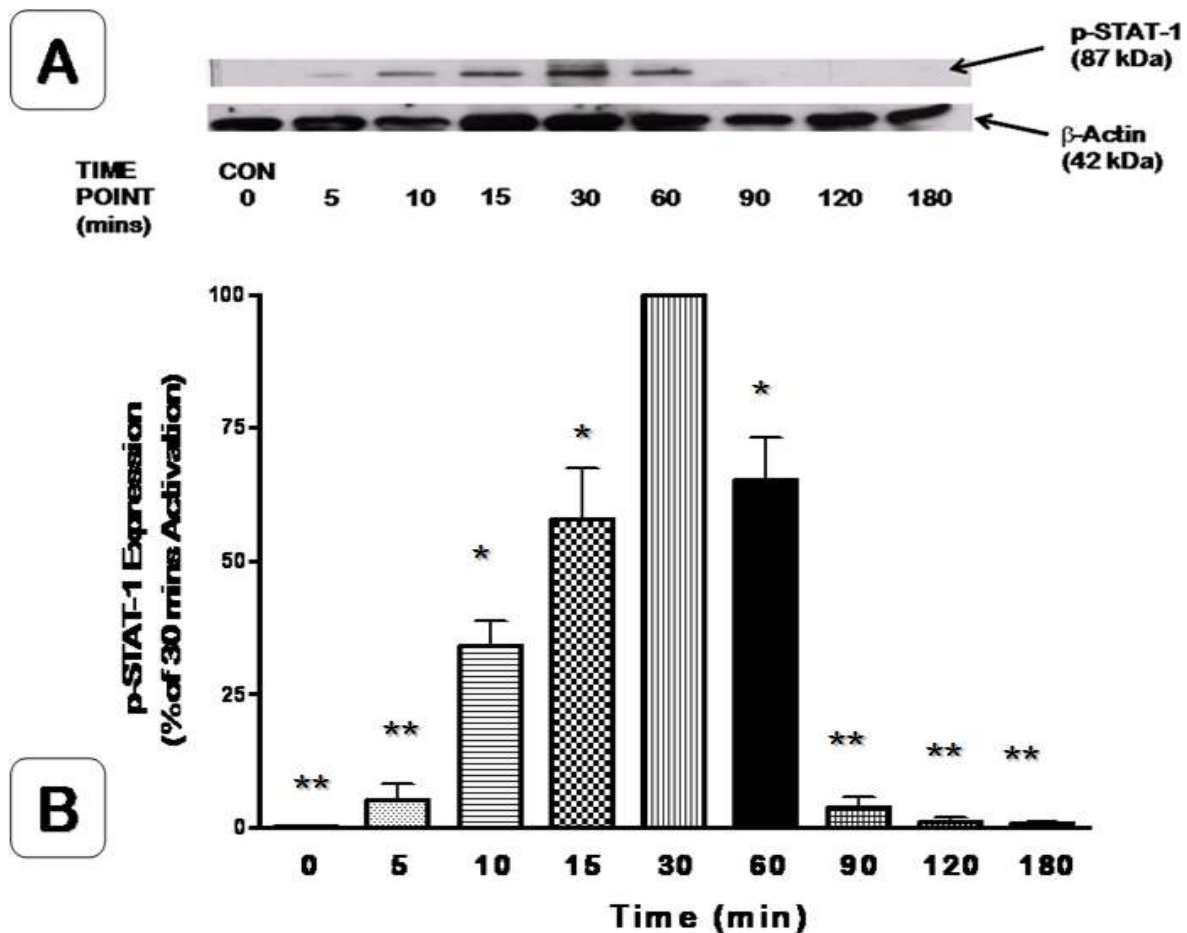


**Figure 5.3 Time-dependent phosphorylation of STAT-1 expression by a combined IFN- $\gamma$  (100 U/ml) and LPS (100  $\mu$ g/ml) in RASMCs**

Confluent monolayer of RASMCs in 6-well plates were incubated in complete DMEM alone (Control; Lane 1) or stimulated with both LPS (100  $\mu$ g/ml) and IFN- $\gamma$  (100 U/ml) in continuous presence of complete DMEM at the indicated time points. Cell lysates were generated and equal quantities of protein (40  $\mu$ g) were subjected to western blotting as previously described in Methods (Section 2.13) using a phospho-STAT-1 specific antibody. The above western blot (Figure A) is representative of at least three independent experiments. Intensity of protein bands were quantified by densitometric analysis and normalized to  $\beta$ -actin protein (Figure B). The data is expressed as a percentage of the value obtained from peak activated time (at time=30 min). A representative blot of at least three experiments is shown above. Data represents the **mean  $\pm$  SEM** from three independent experiments. Statistical differences between means were determined using one-way analysis of variance (ANOVA) followed by Dunnett's multiple comparisons test of the normalized data. \* & \*\* denotes  $P < 0.05$  and  $P < 0.01$  respectively when compared to untreated activated controls.

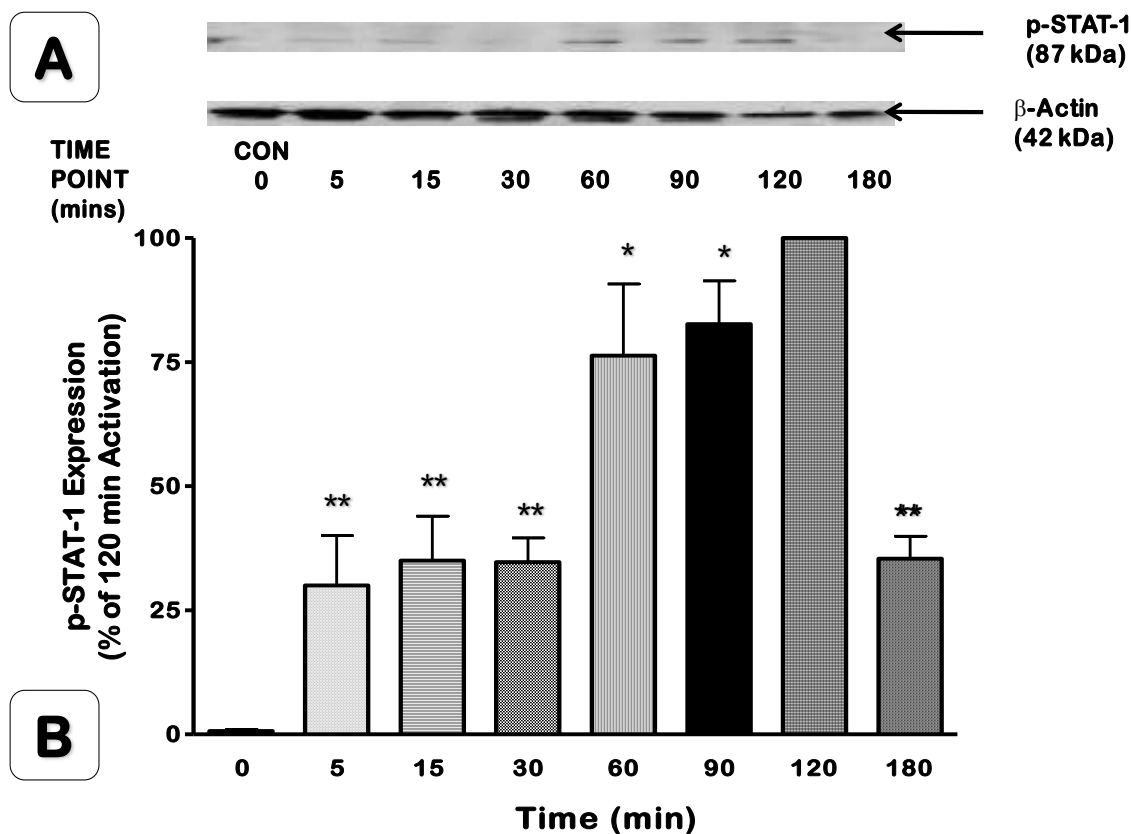


**Figure 5.4 Time-dependent phosphorylation of STAT-1 expression by LPS (1 µg/ml) activation of J774 macrophages**

Confluent monolayers of J774 macrophages in 6-well plates were incubated in complete DMEM alone (Control; Lane 1) or stimulated with LPS (1.0 µg/ml) in continuous presence of complete DMEM at the indicated time points. Cell lysates were generated and equal quantities of protein (40 µg) were subjected to western blotting as previously described in Methods (Section 2.13) using a phospho-STAT-1 specific antibody. The above western blot (Figure A) is representative of at least three independent experiments. Intensity of protein bands were quantified by densitometric analysis and normalized to β-actin protein (Figure B). The data is expressed as a percentage of the value obtained from peak activated time (at time=120 min). Data represent the **mean ± S.E.M.** from three independent experiments. Statistical differences between means were determined using one-way analysis of variance (ANOVA) followed by Dunnett's multiple comparisons test of the normalized data. \* & \*\* denotes  $P < 0.05$  and  $P < 0.01$  respectively when compared to the highest peaked activated time.

### 5.4.3 Effect of AG490 and JAK inhibitor I on STAT-1 phosphorylation

To evaluate the possible inhibitory effects of both AG490 and JAK inhibitor I on STAT-1 phosphorylation (pSTAT-1), cells were pre-treated with different concentrations of AG490 (0 to 10  $\mu$ M) or JAK inhibitor I (0 to 10  $\mu$ M) for 30 minutes prior to activation. Cells were then activated with LPS (1  $\mu$ g/ml) alone (for J774 macrophages) or with a combination of LPS (100  $\mu$ g/ml) and IFN- $\gamma$  (100 U/ml) (for RASMCs) in serum starved (0.1% FBS) DMEM for a further 24 hr.

The results obtained showed that JAK inhibitor I caused a concentration dependent decrease in pSTAT-1 expression in RASMCs (Figure 5.5). The decrease in expression was significant ( $p < 0.001$ ) with 10  $\mu$ M of the drug causing approximately about 80% reduction in p-STAT-1 expression over non treated activated control. Similarly in J774 macrophages, there was a much greater significant decrease in pSTAT-1 expression where, as shown in Figure 5.7, a 10  $\mu$ M of JAK-inhibitor I pre-treatment resulted in over 90 % reduction in p-STAT-1 expression over non treated activated control.

In contrast to JAK inhibitor I, pre-treatment of RASMCs with AG490 resulted in a very marginal decrease in pSTAT-1 expression but this was not statistically significant when compared to the non-drug treated cells (Figure 5.6). Similarly, in J774 macrophages there was no significant change in p-STAT-1 expression following pre-treatment with AG490 (Figure 5.8).

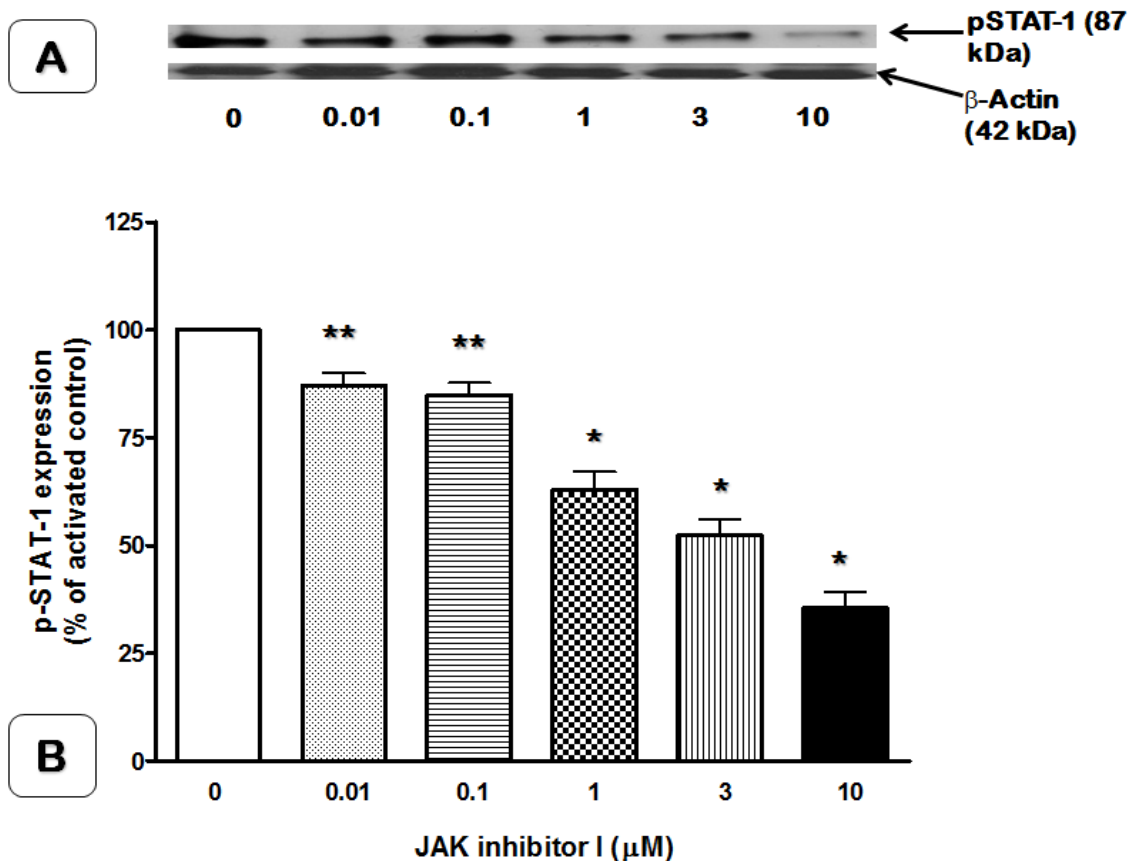


**Figure 5.5 Effect of JAK-inhibitor I on phosphorylated STAT-1 expression following activation in RASMCs.**

Confluent monolayers of RASMCs in 6-well plates were pre-treated with complete DMEM alone (Controls) and complete DMEM with different concentrations of JAK inhibitor I (0.01 to 10 μM) for 30 minutes prior to activation. Cells were activated with both LPS (100 μg/ml) and IFN-γ (100 U/ml) in the absence and continued presence of JAK inhibitor I. After 24 hours cell lysates were generated as previously described in the Methods (Section 2.13). Equal quantities of lysates (60 μg) were subjected to western blotting using a phospho-STAT-1 specific antibody. The above western blot (Figure A) is representative of at least three independent experiments. Respective protein band intensities were quantified by densitometric analysis and normalized to β-actin protein (Figure B). The data is presented as a percentage of relative intensity of phospho-STAT-1 protein expression in absence of inhibitor. Data represent the **mean ± S.E.M.** from three independent experiments. Statistical differences between means were determined using one-way analysis of variance (ANOVA) followed by Dunnett's multiple comparisons test of the normalized data. \* & \*\* denotes  $P < 0.01$  and  $P < 0.05$  respectively when compared to untreated activated control.

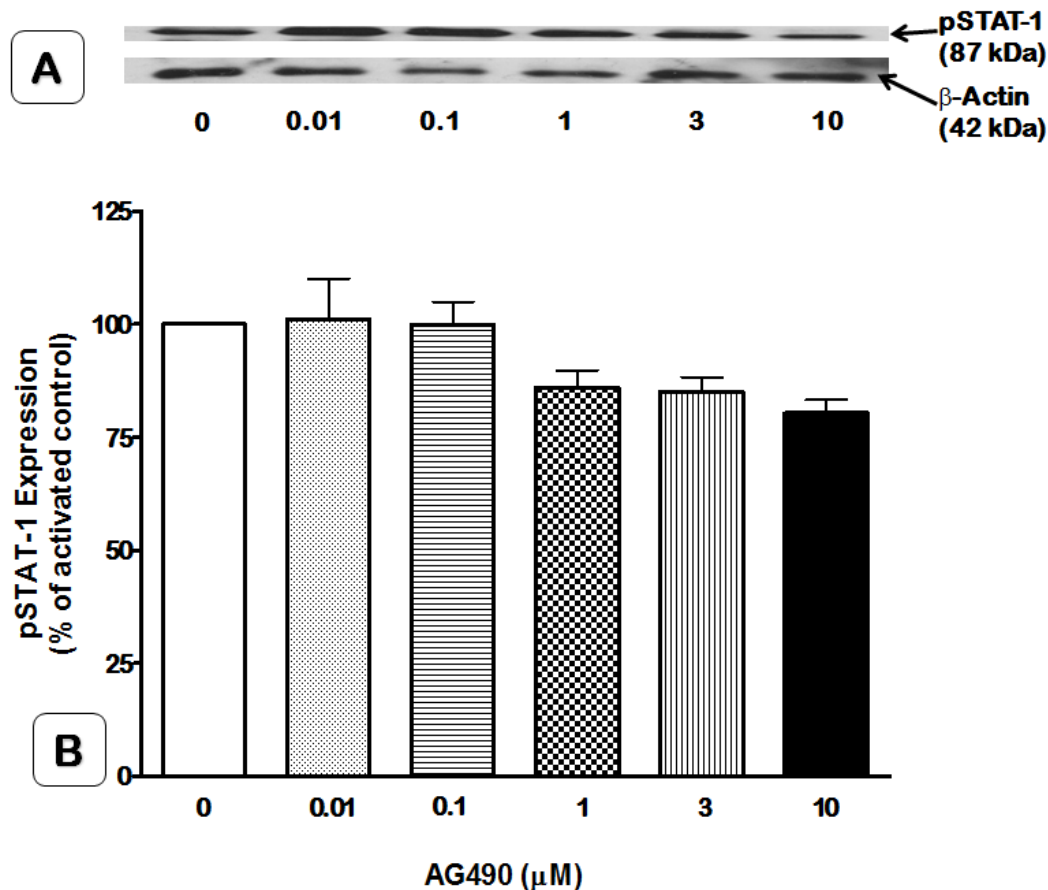


**Figure 5.6 Effect of AG490-inhibitor on expression of phosphorylated-STAT-1 expression following activation in RASMCs.**

Confluent monolayers of RASMCs in 6-well plates were pre-treated with complete DMEM alone (Controls) and complete DMEM with different concentrations of AG490 (0.01 to 10 μM) for 30 minutes prior to activation. Cells were activated with both LPS (100 μg/ml) and IFN-γ (100 U/ml) in the absence and continued presence of AG490. After 24 hours cell lysates were generated as previously described in the Methods (Section 2.13). Equal quantities of lysates (60 μg) were subjected to western blotting using a phospho-STAT-1 specific antibody. The above western blot (Figure A) is representative of at least three independent experiments. Respective protein band intensities were quantified by densitometric analysis and normalized to β-actin protein (Figure B). The data is presented as a percentage of relative intensity of phospho-STAT-1 protein expression in absence of inhibitor. Data represent the **mean ± S.E.M.** from three independent experiments. Statistical differences between means were determined using one-way analysis of variance (ANOVA) followed by Dunnett's multiple comparisons test of the normalized data.  $P > 0.05$  confirmed there was no significant difference when compared to untreated activated control.

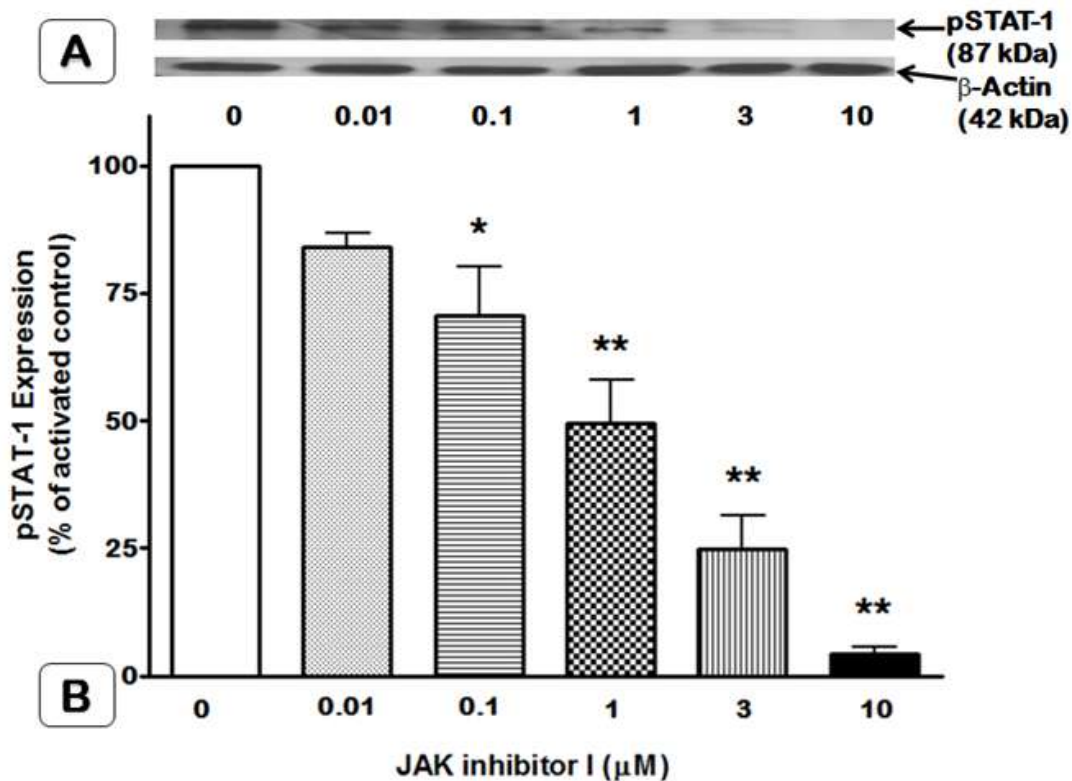


**Figure 5.7 Effect of JAK inhibitor I on phosphorylated-STAT-1 expression following activation in J774 macrophages.**

Confluent monolayers of J774 macrophages in 6-well plates were pre-treated with complete DMEM alone (Controls) and complete DMEM with different concentrations of JAK inhibitor I (0.01 to 10 μM) for 30 minutes prior to activation. Cells were activated with LPS (1.0 μg/ml) in the absence and continued presence of JAK inhibitor I. After 24 hours cell lysates were generated as previously described in the Methods (Section 2.13). Equal quantities of lysates (60 μg) were subjected to western blotting using a phospho-STAT-1 specific antibody. The above western blot (Figure A) is representative of at least three independent experiments. Respective protein band intensities were quantified by densitometric analysis and normalized to β-actin protein (Figure B). The data is presented as a percentage of relative intensity of phospho-STAT-1 protein expression in absence of inhibitor. Data represent the **mean ± S.E.M.** from three independent experiments. Statistical differences between means were determined using one-way analysis of variance (ANOVA) followed by Dunnett's multiple comparisons test of the normalized data. \* & \*\* denotes  $P < 0.05$  and  $P < 0.01$  respectively when compared to untreated activated control.

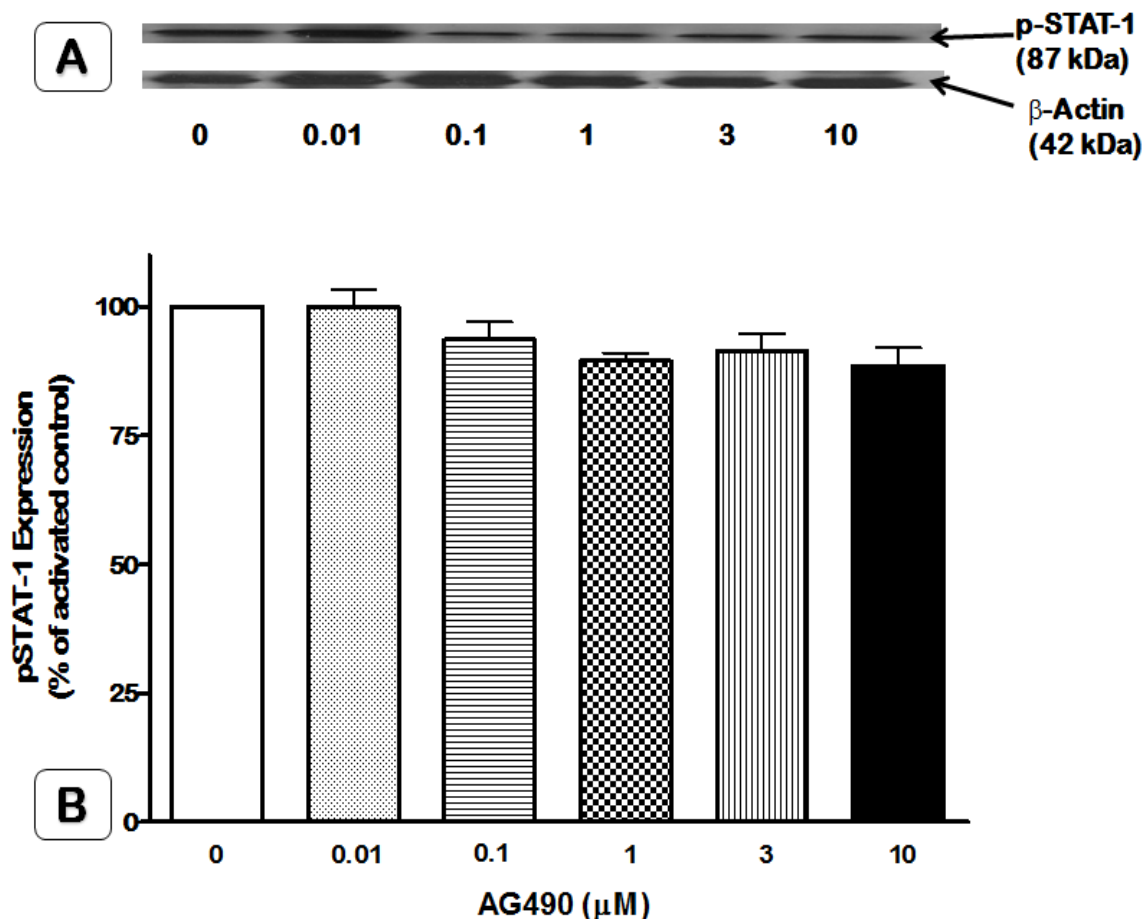


**Figure 5.8 Effect of AG490 inhibitor on phosphorylated-STAT-1 expression following activation in J774 macrophages.**

Confluent monolayers of J774 macrophages in 6-well plates were pre-treated with complete DMEM alone (Controls) and complete DMEM with different concentrations of AG490 (0.01 to 10 μM) for 30 minutes prior to activation. Cells were activated with LPS (1.0 μg/ml) in the absence and continued presence of AG490. After 24 hours cell lysates were generated as previously described in the Methods (Section 2.13). Equal quantities of lysates (60 μg) were subjected to western blotting using a phospho-STAT-1 specific antibody. The above western blot (Figure A) is representative of at least three independent experiments. Respective protein band intensities were quantified by densitometric analysis and normalized to β-actin protein (Figure B). The data is presented as a percentage of relative intensity of phospho-STAT-1 protein expression in absence of inhibitor. Data represent the **mean ± S.E.M.** from three independent experiments. Statistical differences between means were determined using one-way analysis of variance (ANOVA) followed by Dunnett's multiple comparisons test of the normalized data.  $P > 0.05$  confirmed there was no significant difference when compared to untreated activated control.

#### **5.4.4 Role of small GTPases in the induction of iNOS**

To determine whether Rho plays any role in the induction of iNOS and/or L-arginine transport in RASMCs and J774 macrophages, experiments were carried out using atorvastatin, a lipophilic HMG CoA inhibitor known to inhibit isoprenylation of small GTPases, particularly the Rho and Ras proteins and thus able to regulate their activity (Liao *et al.*, 2005; Mason, 2003). In addition, parallel studies were carried out using Y-27632, a prenyltransferase inhibitor reported to specifically inhibit Rho activity (Uehata *et al.*, 1997). These studies were conducted to determine whether STAT-1 phosphorylation could be mediated through Rho signalling independent of the JAKs.

#### **5.4.5 Effect of atorvastatin on nitrite production and inducible nitric oxide expression in RASMCs and J774 macrophages**

In RASMCs, the profile in nitrite production following pre-treatment with atorvastatin was biphasic. Low concentrations of atorvastatin (0.0 to 1.0  $\mu\text{M}$ ) had no significant effect ( $p > 0.05$ ) on accumulated nitrite levels when compared to activated control cells. In contrast, cells pre-treated with atorvastatin at 3  $\mu\text{M}$  and 10  $\mu\text{M}$  caused a significant ( $p < 0.05$ ) increase in nitrite production by  $72.6 \pm 9.3\%$  and  $144.3 \pm 12.1\%$  respectively above that induced in activated controls. Incubation of RASMCs with 30  $\mu\text{M}$  and 100  $\mu\text{M}$  atorvastatin however resulted in a concentration dependent decrease in nitrite production, resulting in an overall bell-shaped curve as shown in Figure 5.9. In addition atorvastatin did not cause any significant change in basal nitrite levels indicating that it acts to modulate the effects mediated by LPS and IFN- $\gamma$  and does not itself have any direct effect on the induction of NO production.

Production of nitrite in J774 macrophages also showed a biphasic profile (Figure 5.10). Nitrite production by activated cells showed an initial concentration dependent increase which peaked at 3.0  $\mu\text{M}$  of atorvastatin but declined thereafter. The change in nitrite production caused by atorvastatin was  $45.0 \pm 9.3\%$  higher than the activated control responses. As in RASMC controls, there was no significant change in nitrite production in non-activated J744 macrophages (Figure 5.10).



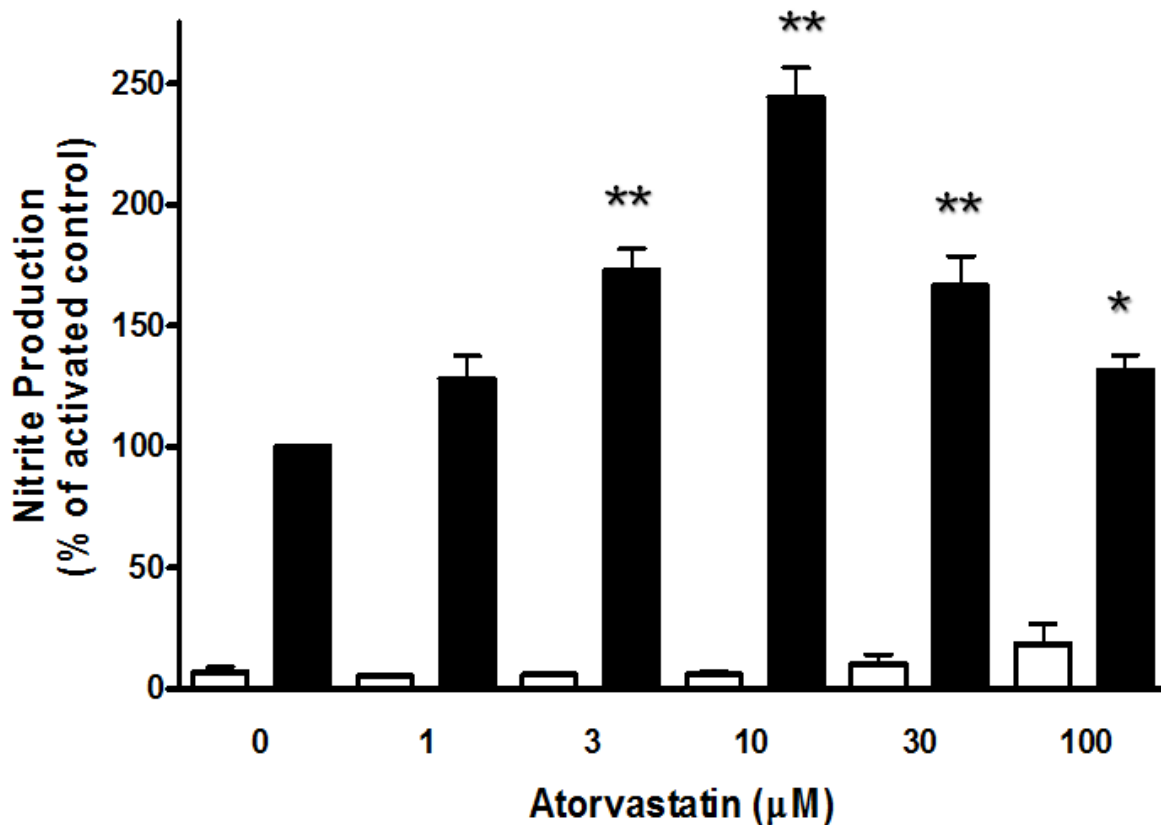


**Figure 5.9 Effects of atorvastatin on nitrite production in both control and activated RASMCs.**

Confluent monolayers of RASMCs in 96-well plates were pre-treated in complete DMEM alone (Controls) and in complete DMEM with different concentrations of atorvastatin (1 to 100 µM) for 30 min prior to activation. Cells were activated with both LPS (100 µg/ml) and IFN-γ (100 U/ml) for 24 hours. Nitrite accumulation in the culture medium was analyzed using the Greiss assay as previously described in the Method (Section 2.9). Open bars represent controls and black closed bars represent activated cells. Data represent the **mean ± S.E.M.** from three independent experiments with five replicates in each. Statistical differences between means were determined using one-way analysis of variance (ANOVA) followed by Dunnett's multiple comparisons test of the normalized data. \* & \*\* denotes  $P < 0.05$  and  $P < 0.01$  respectively when compared to untreated activated control.

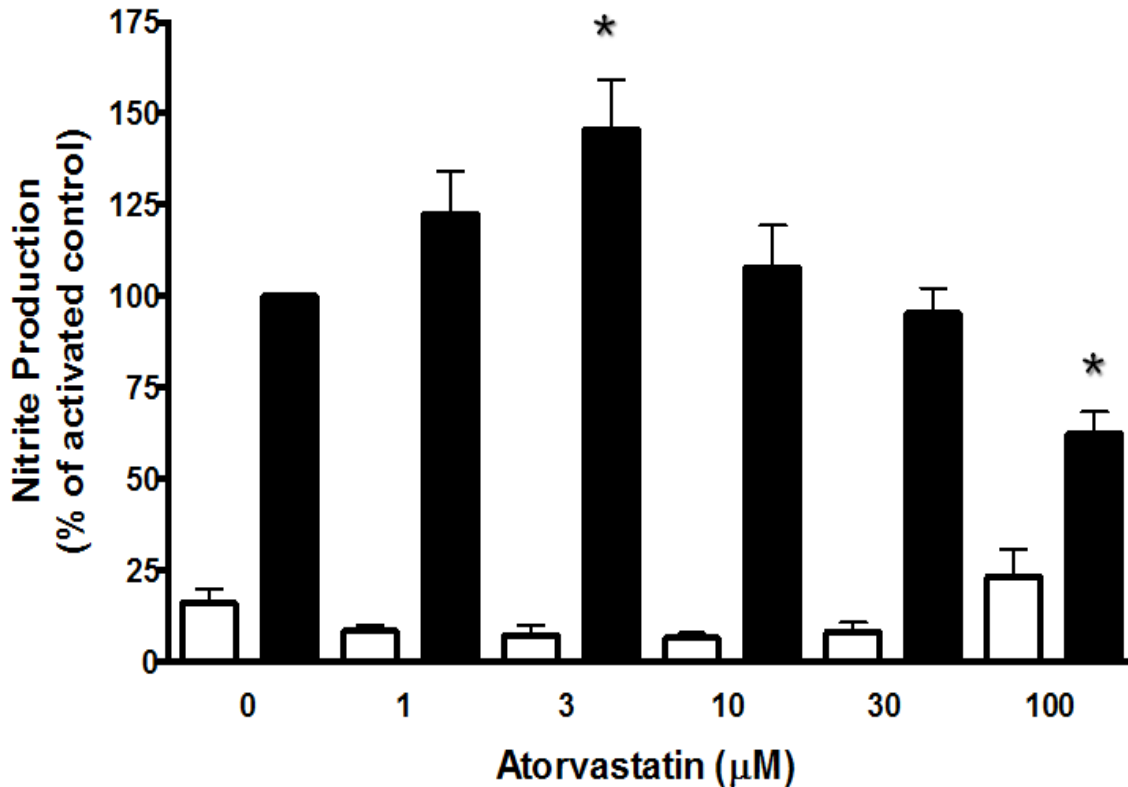


**Figure 5.10 Effects of atorvastatin on nitrite production in both control and activated murine J774 macrophages.**

Confluent monolayer of J774 macrophages in 96-well plates were pre-treated in complete DMEM alone (Controls) and in complete DMEM with different concentrations of atorvastatin (1 to 100 µM) for 30 min prior to activation. Cells were activated with LPS (1.0 µg/ml) for 24 hours. After a 24 hour incubation period, the stable NO metabolite, nitrite, present in the medium was analyzed using the Greiss Assay as previously described in Method (Section 2.9). Open bars represent controls and closed black bars represent activated cells. Data represent the **mean ± S.E.M.** from three independent experiments, each performed in five replicates. Statistical differences between means were determined using one-way analysis of variance (ANOVA) followed by Dunnett's multiple comparisons test of the normalized data. \* denotes  $P < 0.01$  when compared to untreated activated control.

#### **5.4.6 Effects of atorvastatin on iNOS protein expression in both RASMCs and J774 macrophages**

To determine whether atorvastatin affects iNOS expression, cells were pre-treated with different concentrations of the inhibitor for 30 min prior to activation. The results demonstrated that iNOS expression was not significantly altered by atorvastatin in either RASMCs (Figure **5.11**) or J774 macrophages (Figure **5.12**) despite the significant increase in NO production (as shown in Figures **5.9** and **5.10**).

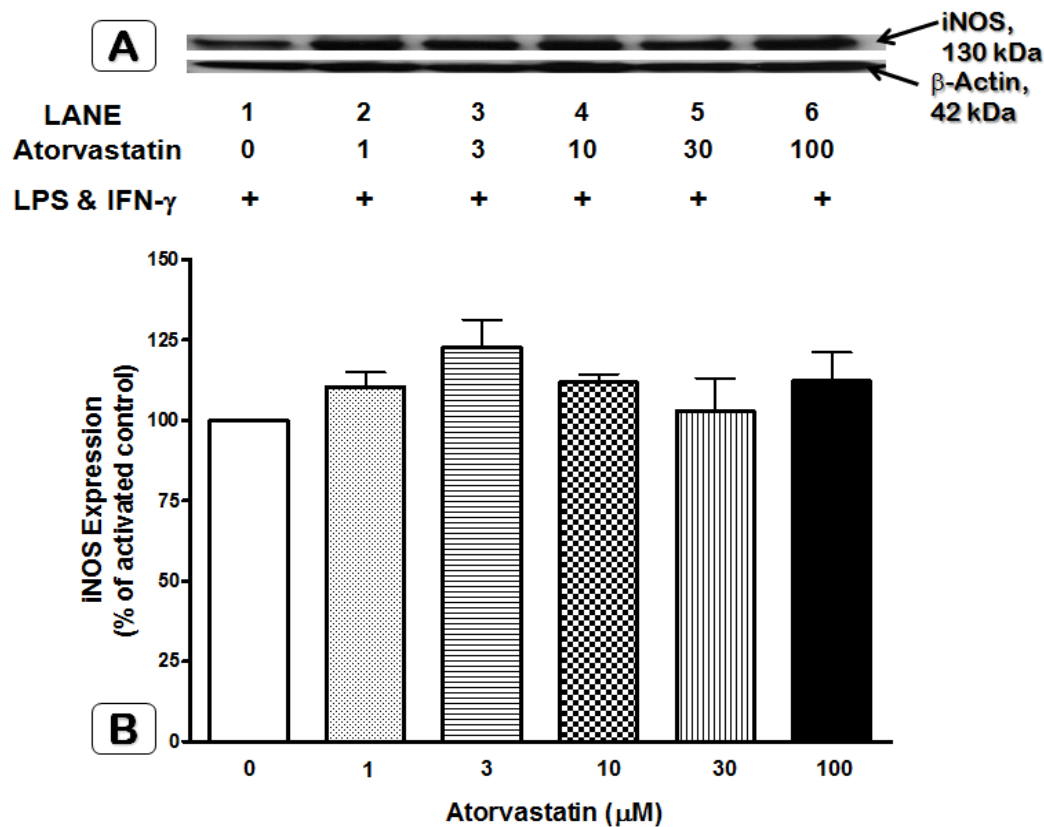


**Figure 5.11 Effect of Atorvastatin on iNOS protein expression in both control and activated RASMCs.**

Confluent monolayer of RASMCs in 6-well plates were pre-treated with either complete DMEM alone (Controls) and/ or complete DMEM with different concentrations of Atorvastatin (1 to 100  $\mu\text{M}$ ) for 30 minutes prior to activation. Cells were activated with LPS (100  $\mu\text{g/ml}$ ) and IFN- $\gamma$  (100 U/ml) in the absence and continued presence of Atorvastatin. After 24 hours cell lysates were generated and equal quantities of (60  $\mu\text{g}$ ) protein were subjected to western blotting using a specific anti-iNOS antibody as described in the Methods (Section 2.13). The above western blot (Figure A) is representative of at least three independent experiments. Respective protein band intensities were quantified by densitometric analysis and normalized to  $\beta$ -actin protein (Figure B). The data is presented as a percentage of relative intensity of iNOS protein expression compared to the control responses without atorvastatin treatment. Data represent the **mean  $\pm$  S.E.M.** from three independent experiments. Statistical differences between means were determined using one-way analysis of variance (ANOVA) followed by Dunnett's multiple comparisons test of the normalized data.  $P > 0.05$  confirmed there was no significant difference when compared to untreated activated control.

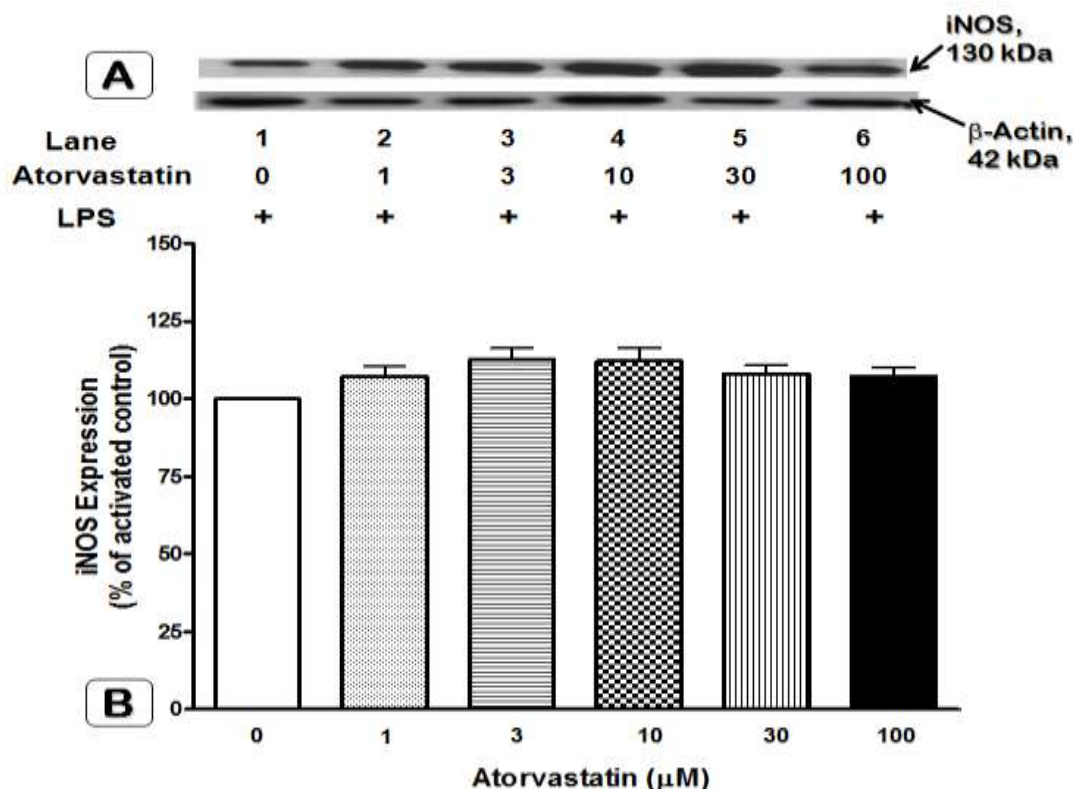


**Figure 5.12 Effect of Atorvastatin on iNOS protein expression in both control and activated J774 macrophages.**

Confluent monolayer of J774 macrophages in 6-well plates were pre-treated with either complete DMEM alone (Controls) and/ or complete DMEM with different concentrations of Atorvastatin (1 to 100 μM) for 30 minutes prior to activation. Cells were activated with LPS (1.0 μg/ml) in the absence and continued presence of Atorvastatin. After 24 hours cell lysates were generated and equal quantities of (60 μg) protein were subjected to western blotting using a specific anti-iNOS antibody as described in the Methods (Section 2.13). The above western blot (Figure A) is representative of at least three independent experiments. Respective protein band intensities were quantified by densitometric analysis and normalized to β-actin protein (Figure B). The data is presented as a percentage of relative intensity of iNOS protein expression compared to the control responses without atorvastatin. Data represent the **mean ± S.E.M.** from three independent experiments. Statistical differences between means were determined using one-way analysis of variance (ANOVA) followed by Dunnett's multiple comparisons test of the normalized data.  $P > 0.05$  confirmed there was no significant difference when compared to untreated activated control.

#### **5.4.7 Effects of atorvastatin on L-arginine transport in both RASMCs and J774 macrophages**

In order to examine the role of atorvastatin on transporter activity, cells were pre-treated with different concentrations of the drug for 30 min prior to activation with LPS (1.0 µg/ml) alone or a combination of LPS (100.0 µg/ml) and IFN-γ (100.0 U/ml) in J774 macrophages and RASMCs respectively. Confirmation of activation and protein content were assessed using Greiss and BCA assays after 24 hours as described in the Methods (Section 2.9 and 2.11 respectively).

Activation of RASMCs with LPS (100.0 µg/ml) and IFN-γ (100.0 U/ml) was able to enhance L-arginine transport and this was further potentiated in a concentration dependent manner when co-induced with atorvastatin. As shown in Figure 5.13, there was a 1.6 fold increase in transport ( $p < 0.01$ ) which peaked at 30 µM atorvastatin. Lower concentrations of 1.0 µM or below had no significant effect ( $p > 0.05$ ) despite the downward trend in profile. At the highest concentration of 100 µM, atorvastatin reduced L-arginine transport back to the levels shown in activated controls. There was no significant change in L-arginine transport in non activated controls.

In J774 macrophages, L-arginine transport following atorvastatin treatment also showed a biphasic or bell shaped response which peaked at 3 µM to about 2 fold over that in non treated activated control. This was followed by a concentration dependent decrease in L-arginine transport with increased atorvastatin concentration. At the highest administered atorvastatin concentration (100 µM) transport rate was reduced to about more than 40% of the untreated activated control values. Similarly, as demonstrated in RASMCs, the rate of L-arginine transport in control macrophages showed no significant change ( $P > 0.05$ ; Figure 5.14).

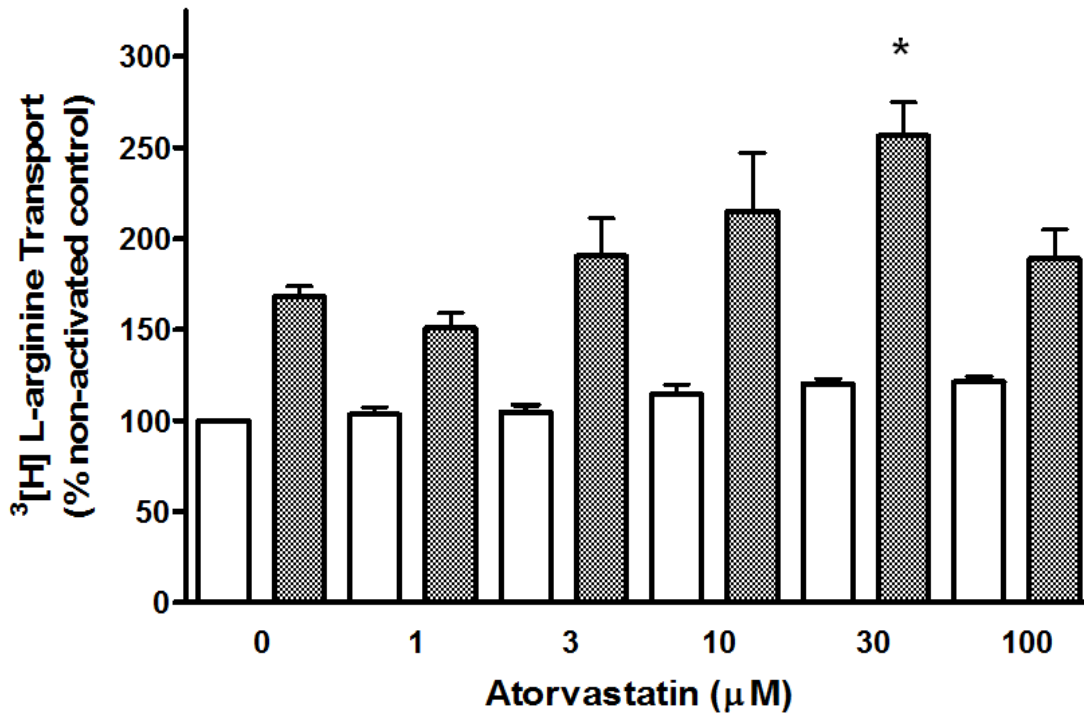


**Figure 5.13 Concentration dependent effect of atorvastatin on L-arginine transport in controls activated RASMCs.**

Confluent monolayers of RASMCs in 96-well plates was pre-treated in either complete DMEM alone (Controls) or in complete DMEM with different concentrations of atorvastatin (1 to 100 μM) for 30 min prior to activation. Cells were activated with both LPS (100.0 μg/ml) and IFN-γ (100.0 U/ml) in the absence (as control) and/or continued presence of atorvastatin. After 24 hour, nitrite and protein content in respective wells were assessed using the Greiss and BCA assays as described in the Methods (Section 2.9 & 2.11 respectively). Transport of <sup>3</sup>[H]-L-arginine was initiated and monitored over 2 min in both control and activated cells as described in the Methods (section 2.10). Open bars represent controls and closed grey bars represent activated cells. Data are presented as percentage of <sup>3</sup>[H] L-arginine transport by activated controls without inhibitor. Data represent the **mean ± S.E.M.** from three independent experiments, each with five replicates. Statistical differences between means were determined using one-way analysis of variance (ANOVA) followed by Dunnett's multiple comparisons test of the normalized data. \* denotes  $P < 0.01$  when compared to untreated activated controls.

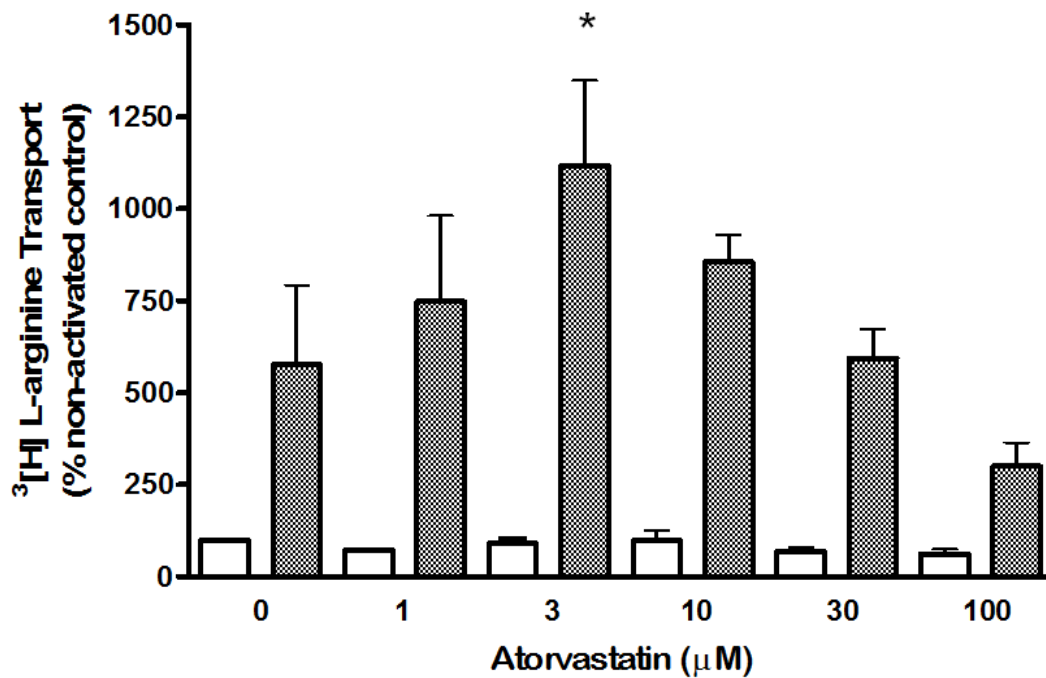


**Figure 5.14 Concentration dependent effect of atorvastatin on L-arginine transport in control and activated J774 macrophages.**

Confluent monolayer of J774 macrophages in 96-well plate was pre-treated in either complete DMEM alone (Controls) or in complete DMEM with different concentrations of atorvastatin (1 to 100 μM) for 30 min prior to activation. Cells were activated with LPS (1.0 μg/ml) in the absence (as control) and/or continued presence of atorvastatin. After 24 hour, nitrite and protein content in respective wells were assessed using the Greiss and BCA assays as described in the Methods (Section 2.9 & 2.11 respectively). Transport of  $^3\text{H}$ -L-arginine was initiated and monitored over 2 min in both control and activated cells as described in the Methods (section 2.10). Open bars represent controls and closed grey bars represent activated cells. Data are presented as percentage of  $^3\text{H}$  L-arginine transport by activated controls without inhibitor. Data represent the **mean  $\pm$  S.E.M.** from three independent experiments, each with five replicates. Statistical differences between means were determined using one-way analysis of variance (ANOVA) followed by Dunnett's multiple comparisons test of the normalized data. \* denotes  $P < 0.05$  when compared to untreated activated controls.

#### **5.4.8 Effects of atorvastatin on cell viability**

There was no significant difference in viability between control and activated RASMCs (Figure 5.15) or J774 macrophages (Figure 5.16) when exposed to atorvastatin at concentrations of 1.0, 10, 30 and 100  $\mu$ M. Although there was a very small decrease in MTT metabolism at the higher concentrations in both cell types, these differences were not statistically significant.

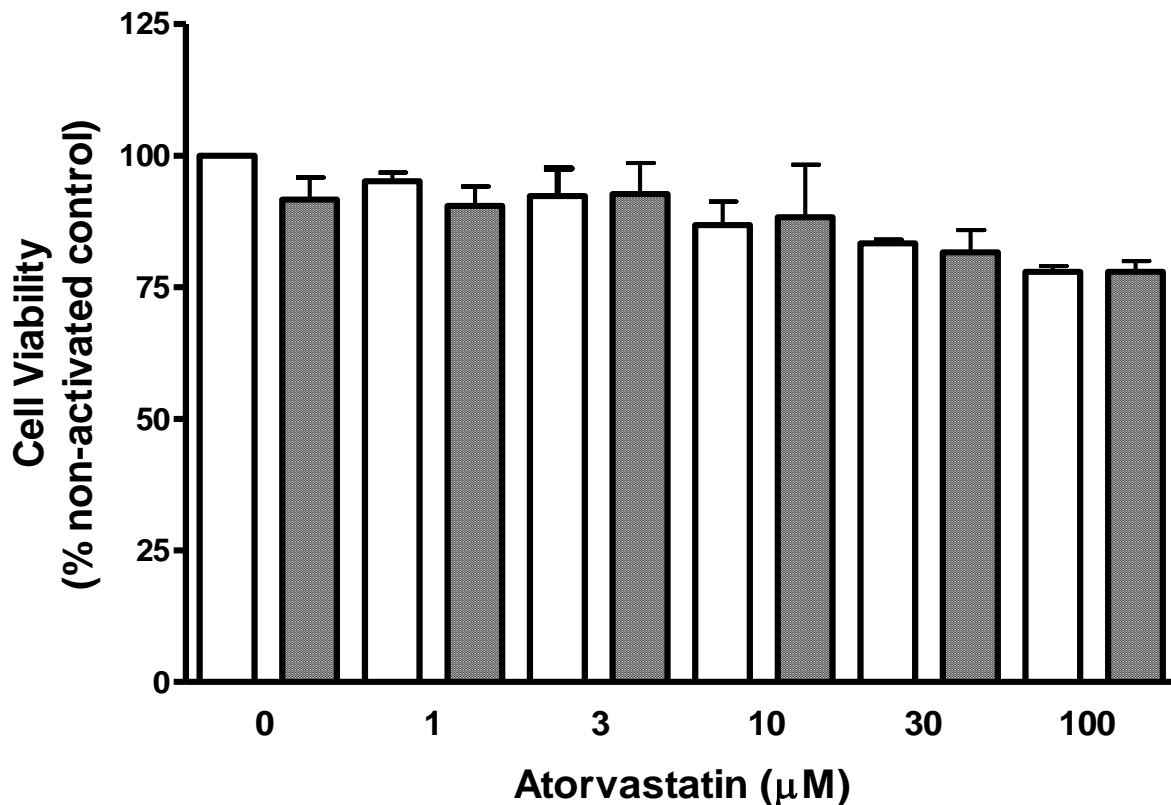


**Figure 5.15 Concentration dependent effects of atorvastatin on viability of both control and activated RASMCs**

Confluent monolayers of RASMCs in 96 well plate were pre-treated treated with either complete DMEM alone (Controls) or with different concentrations of treated with either complete DMEM alone (Controls) or with different concentrations of atorvastatin (1 to 100 μM) for 30 minutes prior to activation. Cells were activated with both LPS (100 μg/ml) and IFN-γ (100 U/ml) for a 24 hour in the continued presence of atorvastatin. MTT metabolism by cells was determined colorimetrically as described in the Methods (Section 2.12). Open bars represent controls and closed grey solid squares represent activated cells. The data is presented as the percentage of viable cell as compared to the control without atorvastatin treatment. Data represent the **mean ± S.E.M.** from three independent experiments, each with five replicates. Statistical differences between means were determined using one-way analysis of variance (ANOVA) followed by Dunnett's multiple comparisons test of the normalized data.  $P > 0.05$  confirmed there was no significant difference when compared to untreated controls

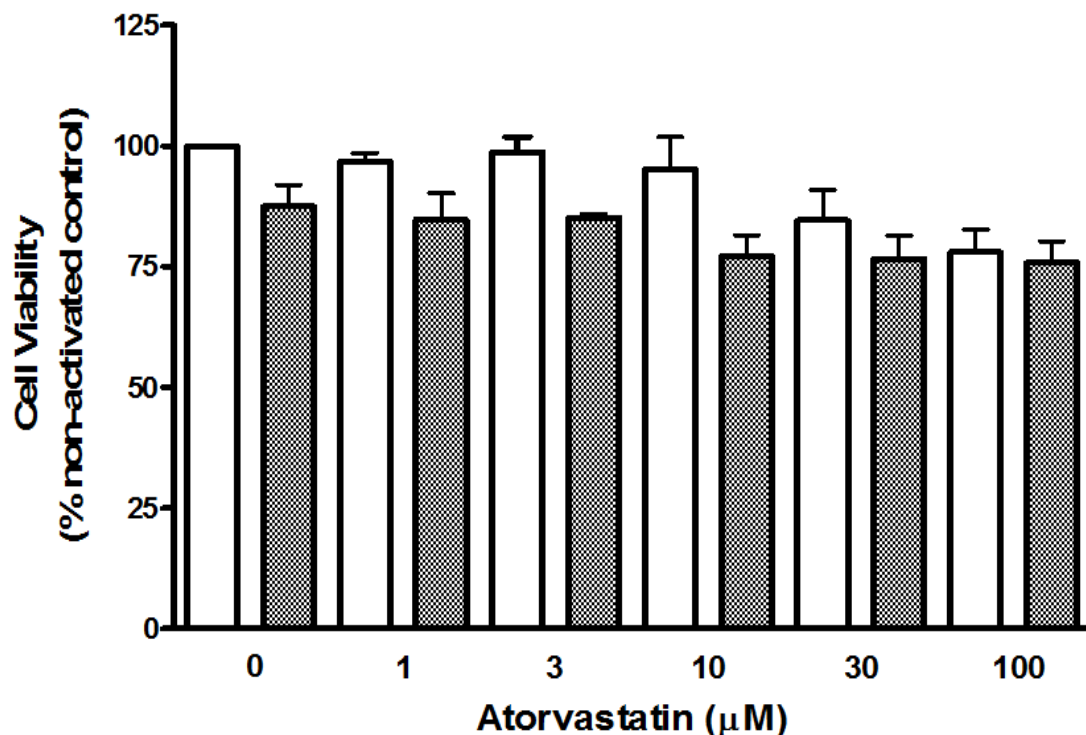


**Figure 5.16 Concentration dependent effects of atorvastatin on viability of both control and activated murine J774 macrophages.**

Confluent monolayer of J774 macrophages in 96 well plates were pre-treated treated with either complete DMEM alone (Controls) or with different concentrations of treated with either complete DMEM alone (Controls) or with different concentrations of atorvastatin (1 to 100 μM) for 30 minutes prior to activation. Cells were activated with LPS (1.0 μg/ml) for a 24 hour in the continued presence of atorvastatin. MTT metabolism by cells was determined colorimetrically as described in the Methods (Section 2.12). Open bars represent controls and closed grey solid squares represent activated cells. The data is presented as the percentage of viable cell as compared to the control without atorvastatin treatment. Data represent the **mean ± S.E.M.** from three independent experiments, each with five replicates. Statistical differences between means were determined using one-way analysis of variance (ANOVA) followed by Dunnett's multiple comparisons test of the normalized data.  $P > 0.05$  confirmed there was no significant difference when compared to untreated controls

#### **5.4.9 Effects of Y-27632 on nitrite production in RASMCs and J774 macrophages**

To further establish the role of Rho kinase additional experiments were carried out using Y-27632 inhibitor. The latter specifically targets ROCK by inactivating p160ROCK, a principal subunit of this kinase reported to regulate NO synthesis (Laufs et al., 2002).

As shown in Figures 5.17 and 5.18, there was the expected enhanced nitrite production in RASMCs activated with both LPS and IFN- $\gamma$  and in J774 macrophages activated with LPS alone for 24 hours at 37°C. A 30 min pre-incubation of cells with different concentrations of Y-27632 prior to activation, resulted in a concentration-dependent enhancement of induced nitrite accumulation which in RASMCs increased over the full concentration range of Y-27632 used (0.01  $\mu$ M to 10  $\mu$ M; Figure 5.17) while in J774 macrophages the increase peaked at 0.1  $\mu$ M, declining thereafter (Figure 5.18). The lower concentrations of the inhibitor caused no statistically significant change (all  $p > 0.05$ ) in nitrite production when compared to levels in non-drug treated activated control cells.

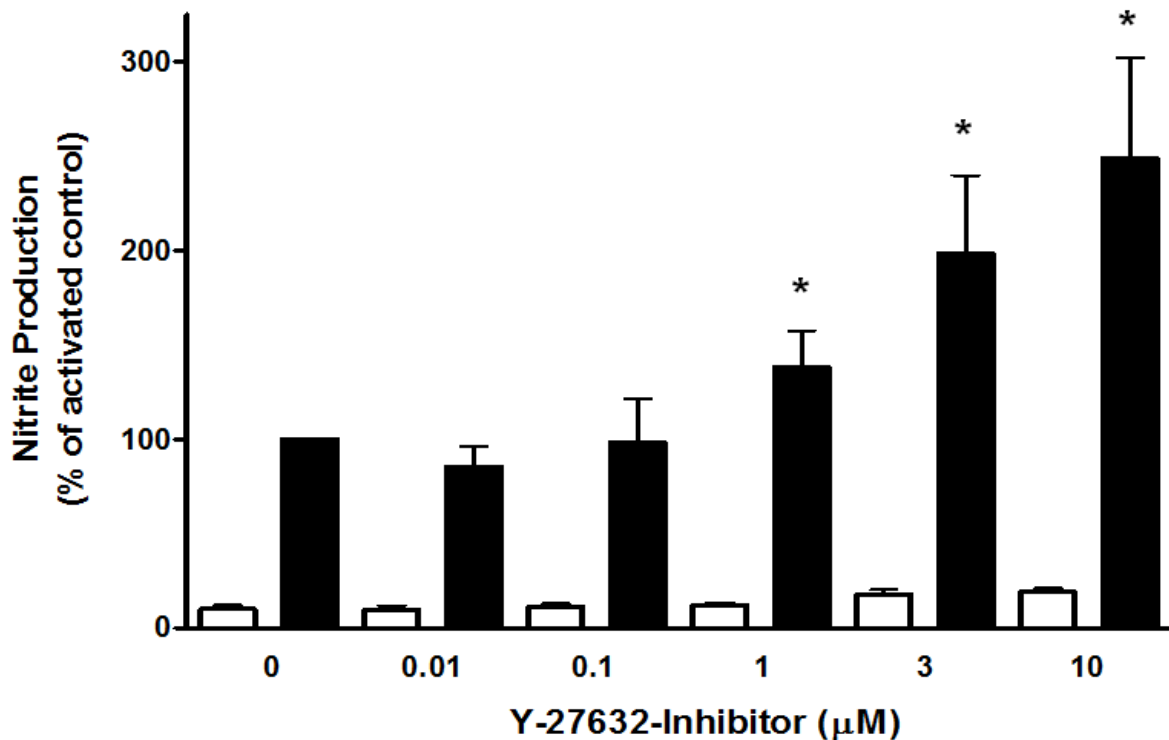


**Figure 5.17 Concentration dependent effect of Y-27632 inhibitor on nitrite production in both control and activated RASMCs.**

Confluent monolayer of RASMCs in a 96-well plate was pre-treated with different concentrations of Y-27632 inhibitor (0.01 to 10.0 µM) in complete DMEM for 30 min prior to activation. Cells were activated in the continued presence of Y-27632 inhibitor with both LPS (100 µg/ml) and IFN-γ (100 U/ml). After 24 hour incubation period, nitrite accumulation in the culture medium was analyzed using the Greiss assay as previously described in the Method (Section 2.9). Clear bars represent controls and closed black bars represent activated cells. Data indicates the percentage of viable cell as compared to controls without Y-27632 inhibitor treatment. Data represent the **mean ± S.E.M.** from three independent experiments, each with five replicates. Statistical differences between means were determined using one-way analysis of variance (ANOVA) followed by Dunnett's multiple comparisons test of the normalized data. \* denotes  $P < 0.01$  when compared to untreated controls.

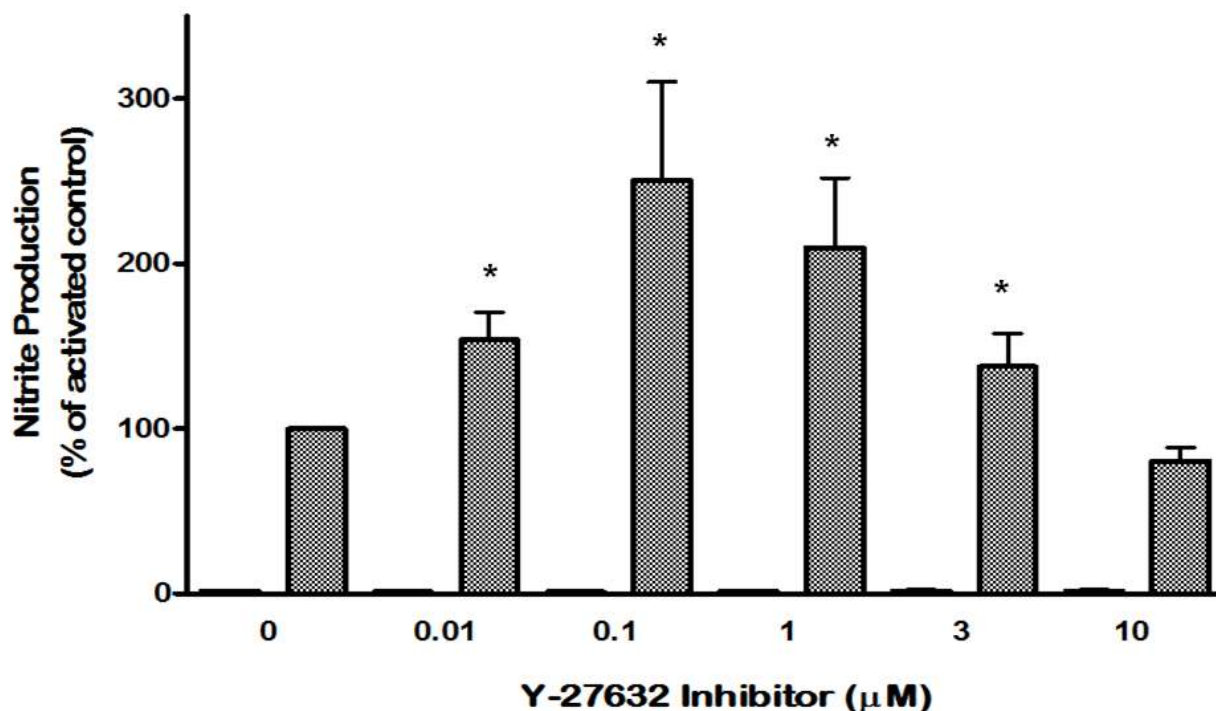


**Figure 5.18 Concentration dependent effect of Y-27632 inhibitor on nitrite production in both control and activated murine J774 macrophages.**

Confluent monolayer of J774 macrophages in a 96-well plate was pre-treated with different concentrations of Y-27632 inhibitor (0.01 to 10.0 µM) in complete DMEM for 30 min prior to activation. Cells were activated in the continued presence of Y-27632 inhibitor with LPS (1.0 µg/ml). After 24 hour incubation period, nitrite accumulation in the culture medium was analyzed using the Greiss assay as previously described in the Method (Section 2.9). Clear bars represent controls and closed grey bars represent activated cells. Data indicates the percentage of viable cell as compared to controls without Y-27632 inhibitor treatment. Data represent the **mean ± S.E.M.** from three independent experiments, each with five replicates. Statistical differences between means were determined using one-way analysis of variance (ANOVA) followed by Dunnett's multiple comparisons test of the normalized data.\* denotes  $P < 0.01$  when compared to untreated controls.

#### **5.4.10 Effect of Y-27632-inhibitor on L-arginine transport in both RASMCs and J774 macrophages**

Activation of RASMCs with a combination of LPS (100.0 µg/ml) and IFN-γ (100.0 U/ml) or J774 macrophages with LPS alone (1.0 µg/ml) was able to enhance L-arginine transport as shown in Figures 5.19 and 5.20 respectively. When pre-treated with Y-27632 prior to activation, there was a concentration-dependent increase in transport of L-arginine in both cell types. However the observed changes in RASMCs were less pronounced when compared to that in J774 macrophages. Moreover, responses in the latter cell type peaked at 0.01 µM to 1 µM and declined thereafter.

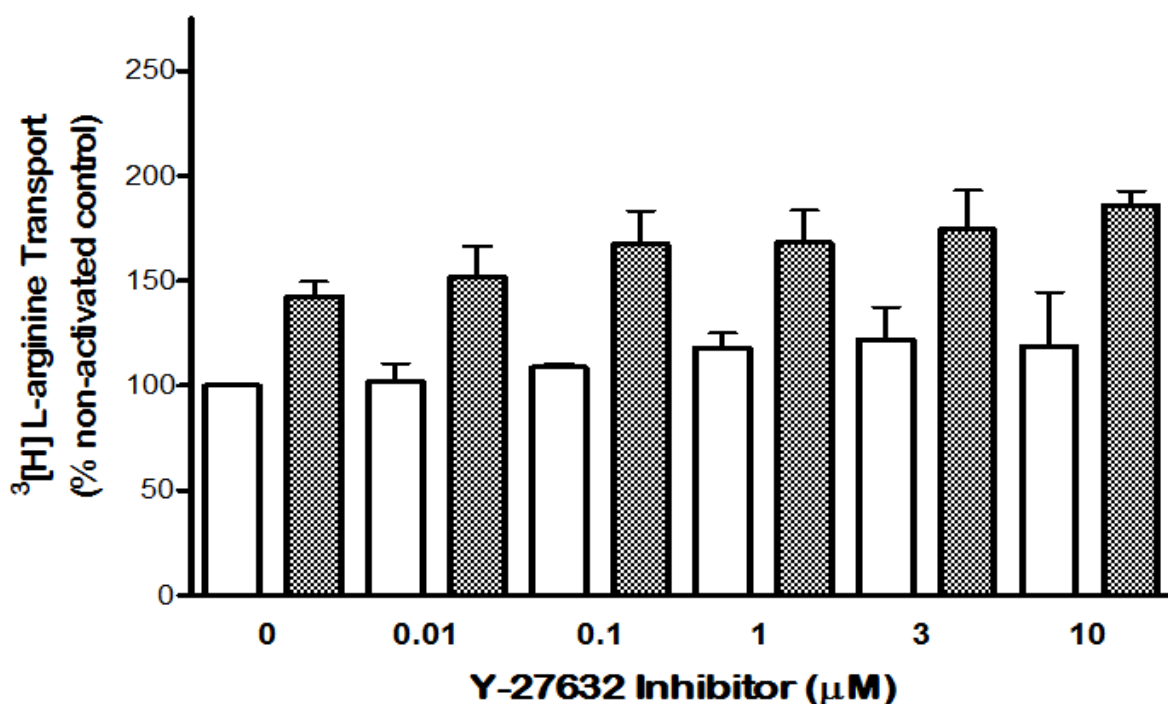


**Figure 5.19 Concentration dependent effect of Y-27632 inhibitor on L-arginine transport in both control and activated RASMCs.**

Confluent monolayer of RASMCs in 96-well plate was pre-treated in either complete DMEM alone (Controls) or in complete DMEM with different concentrations of Y-27632 inhibitor (0.01 to 10.0 μM) for 30 min prior to activation. Cells were activated with both LPS (100.0 μg/ml) and IFN-γ (100.0 U/ml) in the absence (as control) and/or continued presence of Y-27632 inhibitor. After 24 hour incubation period, nitrite and protein content of sample wells were assessed by the Greiss and BCA assays respectively as described in the Methods (Sections 2.9 and 2.11 respectively). Transport of  $^3\text{[H]}$  L-arginine was assessed over 2 min in both control and activated cells as described in the Methods (Section 2.10). Open bars represent controls and closed bars represent activated cells. Data are presented as percentage of  $^3\text{[H]}$  L-arginine transport by activated controls without inhibitor. Data represent the **mean ± S.E.M.** from three independent experiments, each with five replicates. Statistical differences between means were determined using one-way analysis of variance (ANOVA) followed by Dunnett's multiple comparisons test of the normalized data.  $P > 0.05$  confirmed there was no significant difference when compared to untreated controls.

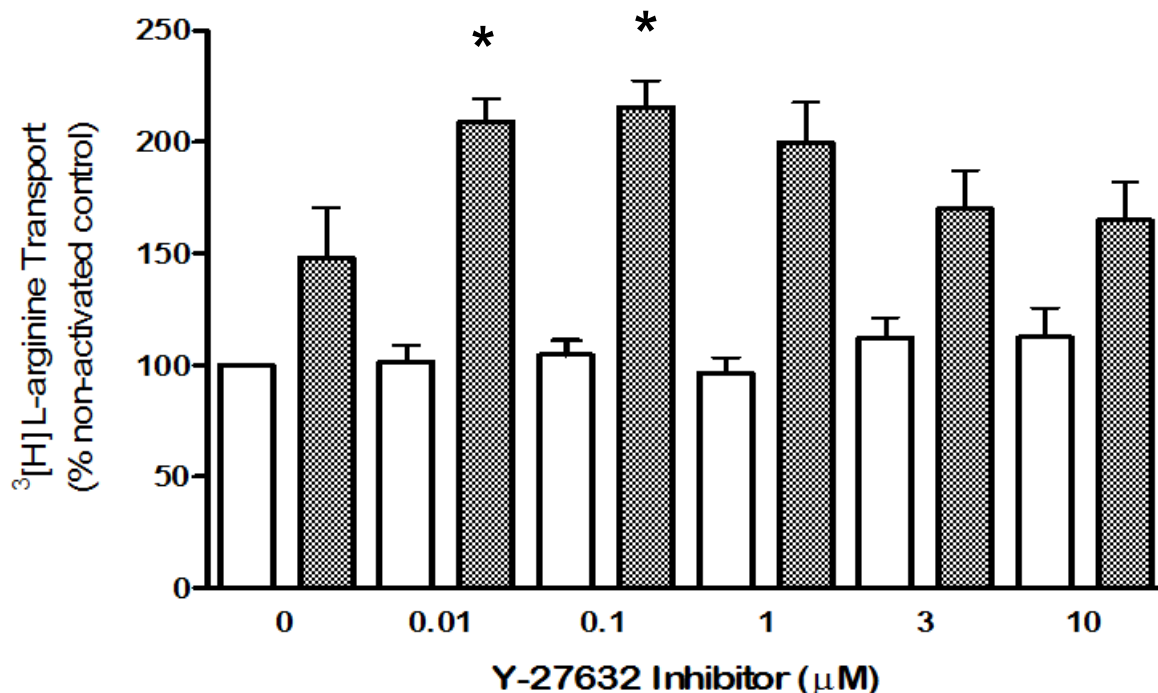


**Figure 5.20** Concentration dependent effect of Y-27632 inhibitor on L-arginine transport in both control and activated murine J774 macrophages.

Confluent monolayer of J774 macrophages in 96-well plate was pre-treated in either complete DMEM alone (Controls) or in complete DMEM with different concentrations of Y-27632 inhibitor (0.01 to 10.0 μM) for 30 min prior to activation. Cells were activated with LPS (1.0 μg/ml) in the absence (as control) and/or continued presence of Y-27632 inhibitor. After 24 hour incubation period, nitrite and protein content of sample wells were assessed by the Greiss and BCA assays respectively as described in the Methods (Sections 2.9 and 2.11 respectively). Transport of  $^3\text{[H]}$  L-arginine was assessed over 2 min in both control and activated cells as described in the Methods (Section 2.10). Open bars represent controls and closed bars represent activated cells. Data are presented as percentage of  $^3\text{[H]}$  L-arginine transport by activated controls without inhibitor. Data represent the **mean ± S.E.M.** from three independent experiments, each with five replicates. Statistical differences between means were determined using one-way analysis of variance (ANOVA) followed by Dunnett's multiple comparisons test of the normalized data. \* denotes  $P < 0.05$  when compared to untreated controls.

#### **5.4.11 Effect of Y-27632 inhibitor on cell viability**

The cytotoxic effects of Y-27632 inhibitor were assessed by measuring the mitochondrial dependent reduction of MTT to formazan as earlier described in Methods (Section 2.12). As shown in Figure 5.21, there was no significant difference in viability between control and activated RASMCs treated with up to 10.0  $\mu$ M Y-27632 inhibitor.

In J774 macrophages (Figure 5.22) there was no significant difference between control and activated cells across the concentration range under investigation. Treatment of macrophages with up to 10  $\mu$ M of Y-27632 did not cause any significant effect on cell viability in controls and activated cells.

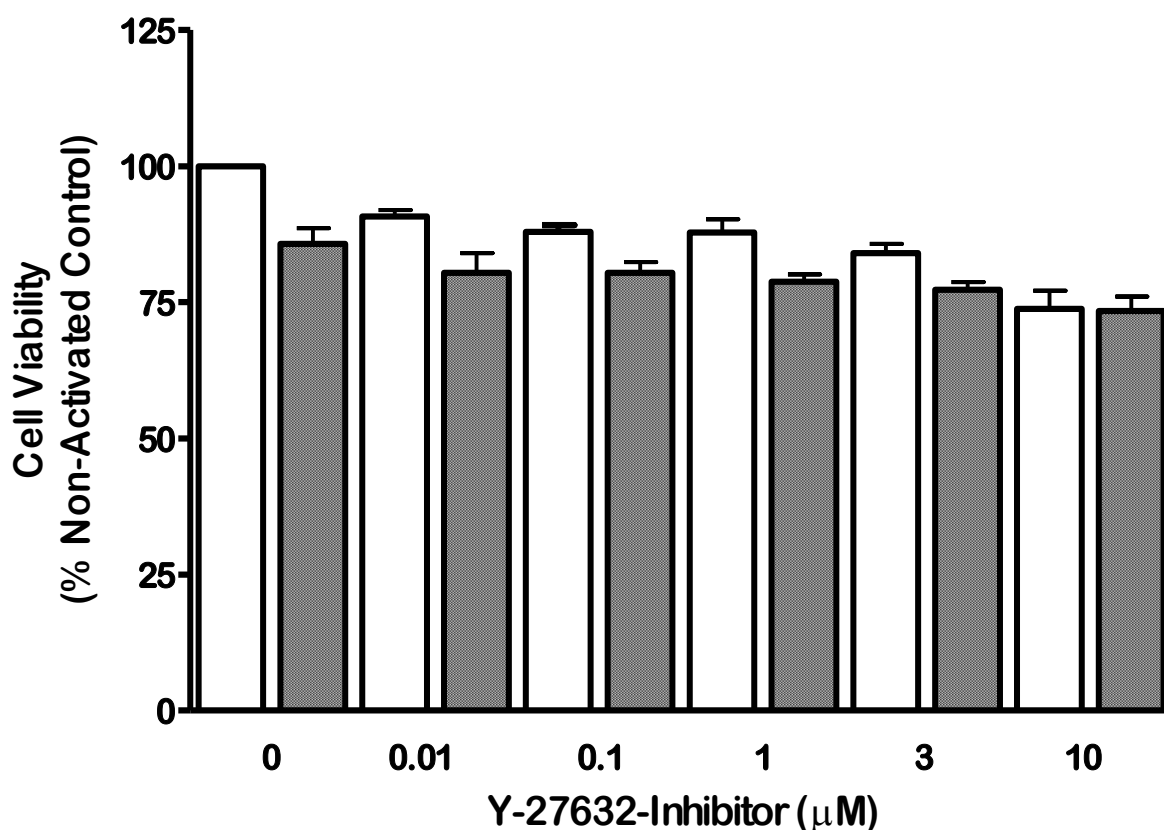


**Figure 5.21 Concentration dependent effect of Y-27632 inhibitor on viability of both control and activated RASMCs**

Confluent monolayer of RASMCs in 96 well plates was pre-treated in complete DMEM alone or with different concentrations of Y-27632 inhibitor (0.01 to 10.0 µM) for 30 minutes prior to activation. Cells were activated in the continued presence of Y-27632 inhibitor with LPS (100 µg/ml) and IFN-γ (100 U/ml) for 24 hours. MTT metabolism by cells was determined colorimetrically on a 96-well microtiter plate as described in the Methods (Section 2.12). Open bars represent controls and closed grey bars represent activated cells. Data represent the **mean ± S.E.M.** from three independent experiments, each with five replicates. Statistical differences between means were determined using one-way analysis of variance (ANOVA) followed by Dunnett's multiple comparisons test of the normalized data.  $P > 0.05$  confirmed there was no significant difference when compared to untreated controls.

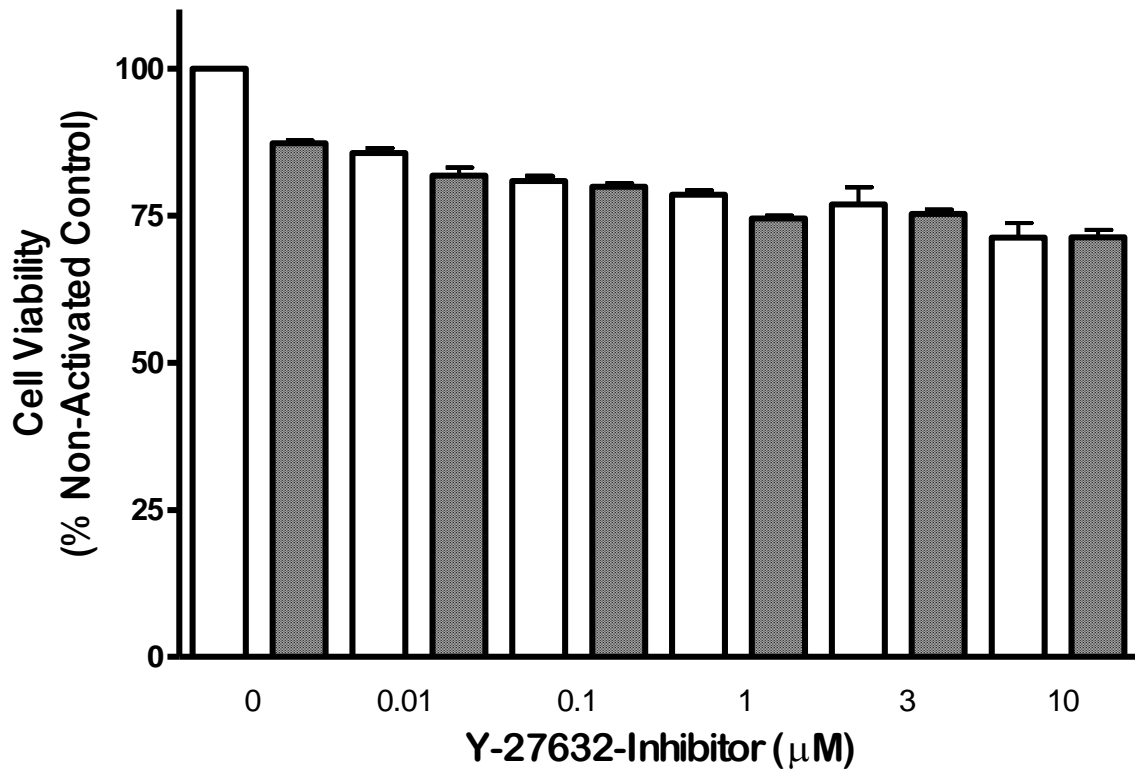


**Figure 5.22 Concentration dependent effect of Y-27632 inhibitor on viability of both control and activated J774 macrophages**

Confluent monolayer of J774 macrophages in 96 well plates were pre-treated in complete DMEM with different concentrations of Y-27632 inhibitor (0.01 to 10.0 µM) for 30 minutes prior to activation. Cells were activated in the continued presence of Y-27632 inhibitor with LPS (1.0 µg/ml) for a further 24 hour incubation period. MTT metabolism by cells was determined colorimetrically on a 96-well microtiter plate as described in the Methods (Section 2.12). Open bars represent controls and grey filled bars represent activated cells. Data represent the **mean ± S.E.M.** from three independent experiments, each with five replicates. Statistical differences between means were determined using one-way analysis of variance (ANOVA) followed by Dunnett's multiple comparisons test of the normalized data.  $P > 0.05$  confirmed there was no significant difference when compared to untreated controls.

## 5.5 DISCUSSION

To further confirm our findings in chapters 3 and 4 and the proposal that JAK2 may not be critical for the expression of the inducible L-arginine-NO pathway in RASMCs and J774 macrophages, we extended our studies by examining whether STAT-1 is indeed activated by LPS and IFN- $\gamma$  in RASMCs or by LPS alone in the macrophages. In addition, studies were also aimed at establishing whether the activation of STAT-1 is independent of or linked to the activation of the JAKs. This is because STAT-1 is a downstream target for IFN- $\gamma$  (Silvennoinen *et al.*, 1993; Watling *et al.*, 1993; Levy *et al.*, 1990). Originally identified to mediate actions of IFNs (Bromberg *et al.*, 1996; Darnell, 2007; Darnell, 1997) STATs are now reported to be involved in a diverse range of cellular activities including proliferation, differentiation, growth and apoptosis amongst others (Bromberg *et al.*, 2000; Ihle, 1996). Tyrosine phosphorylation on Tyr701 residue near to the carboxyl end (Meraz *et al.*, 1996) by JAKs results in STAT-1 activation (Ihle, 1996). However, STAT-1 activation and translocation is caused by independent tyrosine phosphorylation of the JAKs (Fukuzawa *et al.*, 2003; Schneider *et al.*, 2013). Additionally, there is evidence (Blanchette *et al.*, 2003b; Wen *et al.*, 1995; Zhang *et al.*, 1995) to suggest a requirement of a second phosphorylation event at Ser727 residue for maximum activation. Thus, apart from the JAKs other upstream mechanisms may activate STAT-1 resulting in gene transcription including that for iNOS and this will be discussed below.

The results obtained revealed that induction of RASMCs with LPS and IFN- $\gamma$  or J774 macrophages with LPS caused a time dependent phosphorylation of STAT-1. This result confirms that STAT-1 is indeed expressed in both cell types and can be activated by the stimuli used to induce iNOS and L-arginine transport. However, the time course was different between the two cell types. In RASMCs the optimum time course of STAT-1 activation peaked at 30 min while in J774 macrophages the phosphorylation of STAT-1 was comparatively delayed and prolonged after LPS stimulation. The reason for this observed trend is unclear but may reflect cell type differences or could be due to the different stimuli used and may suggest differences in the mechanisms that activate STAT-1. What is most significant and unexpected is the fact that phosphorylation of STAT-1 in either cell type was not blocked by AG490, the

potent JAK2 inhibitor. This is an interesting observation which confirms that activation of STAT-1 in our cell systems is not directly linked to JAK2 and can occur independently of the latter. This further supports the notion that JAK2 does not directly mediate the effects of IFN- $\gamma$  and/or LPS in inducing iNOS in our cell systems.

In contrast to AG490, results from studies with JAK inhibitor I showed a significant concentration dependent decrease in STAT-1 phosphorylation in both RASMCs and J774 macrophages. Since this inhibitor is effective against all JAK family members it is therefore likely that at least one of these kinases may mediate the actions of IFN- $\gamma$  and/or LPS in inducing iNOS. However, both current and previous data from our laboratory seem to rule out JAK2 based on data obtained with AG490. Similarly, JAK3 can also be discounted because AG490 has been shown to inhibit this isoform (Luo *et al.*, 2004a; Nielsen *et al.*, 1997; Wang *et al.*, 1999) but was without effect on iNOS expression, NO production of L-arginine transport. Thus, it is not unreasonable to suggest that neither JAK2 nor JAK3 may be critical for LPS-stimulated nitrite production in J774 macrophages. The other potential candidate JAK1 is susceptible to inhibition by JAK inhibitor I but a kinase-negative mutants of this protein can sustain IFN- $\gamma$ -inducible gene expression (Briscoe *et al.*, 1996) suggesting that it may not be required for IFN- $\gamma$  signalling. This however remains to be established in our cell system.

Based on the above process of elimination, the likely JAK family member that may be required is therefore TYK2. This kinase has been implicated in LPS signalling by several groups (Kamezaki *et al.*, 2004; Karaghiosoff *et al.*, 2003) and appears to be involved in the signalling pathway of autocrine/paracrine secreted IFN- $\beta$  (Colamonici *et al.*, 1994a; Colamonici *et al.*, 1994b; Domanski *et al.*, 1995) in macrophages treated with high levels of LPS (Fujihara *et al.*, 1994; Zhang *et al.*, 1994). It is not clear whether TYK2 itself can be activated directly by IFN- $\gamma$  and there is very little to suggest that it may be expressed in smooth muscle cells. Further studies were therefore carried out in Chapter 4 examining not only the expression but also the phosphorylation of TYK2 in both RASMCs and J774 macrophages. The data generated showed clearly that the protein is expressed under control conditions but does not seem susceptible to activation by either LPS alone or in combination with IFN- $\gamma$ . This conclusion is based on data showing that the phospho protein could not be detected by western blotting using

a selective phospho-specific antibody. Thus, the effects of JAK inhibitor I may be mediated by an action on another target protein other than the JAKs. At present it is not clear what the target is but it has been reported that STAT-1 can be phosphorylated by the GTPases independently of the JAKs (Gundogdu *et al.*, 2010). This is of relevance to this thesis and to confirm whether this might be the case, additional experiments were carried out investigating the effects of GTPase inhibitors on nitrite production and L-arginine transport. In these studies two GTPase inhibitors were used: atorvastatin and Y-27632, a specific Rho kinase inhibitor (Uehata *et al.*, 1997).

Atorvastatin is a synthetic HMG-CoA Reductase inhibitor commonly called statin and is used clinically in hypercholesterimic patients to reduce circulating cholesterol levels in the body. In addition, substantial outcomes from large clinical trials have demonstrated considerable improvements in both primary and secondary prevention of heart disease of patients following statin therapy. Also, statins have been reported to regulate eNOS expression although the majority of such effects have been attributed to statins acting as inhibitors of HMG-Co-A enzymes and lowering cholesterol biosynthesis (Laufs *et al.*, 2002). Statins have also been reported to cause alterations in tetrahydrobiopetrin synthesis (Hattori *et al.*, 2002), a cofactor in iNOS function. Such effects may involve regulating signaling pathways associated with the expression of iNOS. The pleiotropic actions of statins, mediated by antioxidant effects have been demonstrated in other studies (Laufs *et al.*, 2003; Takemoto *et al.*, 2001; Tanaka *et al.*, 2013) in which statins have also been reported to inhibit the activation of GTPases by inhibiting the synthesis of isoprenoids (farnesyl pyrophosphate and geranylgeranyl pyrophosphate) which are responsible for the post-translational modification of various proteins including small GTPases such as Rho and Ras. These drugs can therefore regulate downstream pathways which may feed into the nucleus to regulate iNOS expression. To confirm this, experiments were carried out examining the effects of atorvastatin on STAT-1 phosphorylation and on both NO production and L-arginine transport.

In these studies LPS plus IFN- $\gamma$  induction of RASMCs following atorvastatin pre-treatment caused a significant concentration dependent increase in NO production which peaked at 10  $\mu$ M. This trend was then followed by a decline thereafter suggesting a biphasic response to the drug. Interestingly, iNOS expression was not altered

suggesting that the actions of the statin were not a consequence of changes in iNOS protein expression. This would contrast with studies using MCF-7 cells which have demonstrated that statins inhibit geranylgeranylation of prenylated intermediates and thereby dose-dependently induce iNOS protein expression (Kotamraju *et al.*, 2007). In the present studies, atorvastatin may not regulate the GTPase pathway but could exert its effects by directly regulating NO production. One potential explanation for this effect is that because atorvastatin has anti-oxidant properties (Chen *et al.*, 2012; Wassmann *et al.*, 2002) it may be able to prevent the interaction of NO with superoxide radicals thus enhancing the levels which can be detected by the Griess assay. This however remains to be established to account for the present findings in this thesis.

In both cell systems, transport of L-arginine appeared to be enhanced by atorvastatin but only in activated cells. This effect was more pronounced in J774 macrophages and the pattern was also different between the two cell types in that the peak stimulation caused by atorvastatin in RASMCs was at 30  $\mu$ M while in J774 macrophages it was at 3  $\mu$ M. This may reflect subtle differences in the action of the drug which remains to be determined. Transport rates in controls however remained largely unaltered. Because of time limitations it was not possible to establish whether the increases were associated with changes in transporter gene expression as these studies remain critical. Similarly, westerns for changes in CAT protein expression could not be carried out because of lack of commercially available antibodies. However, it is likely that atorvastatin enhances L-arginine transport through changes in induction of the key carrier proteins. This is an interesting proposal that would be necessary to confirm in future studies.

Similar to atorvastatin, treatment of either RASMCs or J774 macrophages with Y-27632 prior to activation resulted in a concentration dependent increase in NO production with that in the macrophages declining above 1  $\mu$ M whilst peaking at 10  $\mu$ M in the RASMCs. The inducible NOS expression was not examined because of time limitations but studies on L-arginine transport confirmed a relatively similar trend to that seen with atorvastatin. Thus taken together, it would appear that both compounds may exert their effects via a similar mechanism which could involve inhibition of the GTPases but we cannot rule out that atorvastatin may also have the added anti-oxidant effects.

In summary, the results of this chapter have shed further light on the potential role of the JAK proteins or rather their lack of involvement in the induction of iNOS, NO production and L-arginine transport. Although further definitive studies may be needed we can speculate from the present findings that LPS either alone or together with IFN- $\gamma$  signal independently of the JAKs to induce the above processes. Whether this action is linked to the GTPases as was initially thought is debatable. This is because the data obtained for the latter suggests that GTPases suppress expression of the inducible L-arginine-NO pathway and their inhibition results in further stimulation. It is likely therefore that signaling through the GTPases is distinct from the signaling activated LPS and IFN- $\gamma$  for the induction of iNOS, NO and L-arginine. What is missing and could not be completed in time for submission of the thesis is whether the GTPases directly activate STAT-1. These experiments are critically needed.

**Chapter 6. Expression profile of Transporters in RASMCs and J774 macrophages**

## 6.1 INTRODUCTION

The use of both *in vitro* (Chen *et al.*, 1994) and *in vivo* (Allman *et al.*, 1996) animal models has further reinforced the suggestion that synthesis of NO by iNOS is predominantly dependent on extracellular L-arginine (Bogle *et al.*, 1992b). In addition, the main source of L-arginine is mainly acquired from diet and is reported to be actively transported into the cell through transporter carrier systems (Closs *et al.*, 2000; Closs *et al.*, 2004; Deves *et al.*, 1998c; Wileman *et al.*, 1995). The main transporter systems implicated include the SLC7 family which is further divided into two main subgroups; the cationic amino acid (CAT family – *SLC7A1 -A4*) and the glycoprotein-associated amino acid transporters (the gpaAT family (also called hetero-(di)-meric amino acid transporter family) – *SLC7A5 – SLC7A11*). The former are the high affinity carrier,  $y^+$  (CAT) system with secondary contributory role by the gpaAT system including  $y^+L$ ,  $b^+$  and  $b^{0,+}$  (Deves *et al.*, 1998a; Deves *et al.*, 1998b).

Results from our earlier experiments in this thesis and additionally by other investigators (Baydoun *et al.*, 1993a; Bogle *et al.*, 1992b; Durante *et al.*, 1995; Wileman *et al.*, 1995) have demonstrated that activation of RASMCs and J774 macrophages with pro-inflammatory mediators including LPS and cytokines (IFN- $\gamma$ ) cause an up-regulation of L-arginine transport which parallels the induction of iNOS. This observation has led to the proposal that transport of L-arginine may be critical for the activity of iNOS and makes the transporters potential targets for regulating the overproduction of NO. However, the expression profile of CATs may be tissue specific and the degree of participation of each carrier in mediating entry of L-arginine into cells is not completely understood especially under cytokine mediated inflammatory conditions. A clear understanding of the nature and cellular profile of expression of CATs is therefore essential. Thus, in this chapter, experiments were carried out to determine the profile of expression of CATs in RASMCs and in J774 macrophages and further to establish how these may be regulated by pro-inflammatory mediators.

The hetero-dimeric amino acid transporters (also called glycoprotein associated amino acid-(gpaAT)) are reported to participate in the transport of L-arginine and could therefore contribute to substrate supply for iNOS. The latter has however not been

addressed and there are few studies that have demonstrated the regulation of these carriers by pro-inflammatory mediators. This was therefore examined as part of the studies for this chapter. The investigated transporters included  $\gamma^+$ LAT1 (*SLC7A5*),  $\gamma^+$ LAT2 (*SLC7A6*) and  $b^{0,+}$  (*SLC7A9*).

## 6.2 METHODS

### 6.2.1 cDNA synthesis from extracted RNA

Separate flask containing 80-95 % confluent monolayers of RASMCs or J774 macrophages were respectively activated with a combination of LPS (100 µg/ml) and IFN- $\gamma$  (100 U/ml) or LPS (1.0 µg/ml). After 24 hour incubation, total RNA was extracted using RNeasy-60 as described in the Method (Chapter 2) and subsequently treated with Turbo DNase-free (Ambion, UK) following manufacturers' instructions to remove any contaminating DNA. The total RNA in all samples was quantified using a spectrophotometer (Biophotometer, Germany). The resulting purified RNA was reverse transcribed using the ImProm-II reverse transcription system (Promega, UK) by following the manufacturer's instructions. Briefly the RT step of priming the first-strand cDNA synthesis was carried out using the following reaction mixtures:

RNA (up to 1.0 µg/rxn)

Random (Hexamer) primer (up to 0.5 µg/ reaction)

Nuclease-free water

ImProm-II 5X Reaction Buffer

MgCl<sub>2</sub> (final concentration 1.5 – 8.0 mM)

dNTP mix (dGTP, dCTP, dATP and dTTP; each at a concentration of 500 µM)

RNasin Ribonuclease inhibitor (0.4 U/µl) - optional

ImProm-II reverse transcriptase ((up to 1.0 ug/20 µl-reaction)

Reverse transcription reactions in a final reaction volume of 20 µl containing the above were subjected to initial primer incubation (i.e. RNA and Hexamer random primer only) at 25 °C for 5 minutes, then at 42 °C for 60 minutes. A final reaction is a thermal inactivated step of the reverse transcriptase enzyme by incubating the reaction mixture at 70 °C for 15 minutes and cooled to 4 °C prior to storage at -80 °C.

## 6.2.2 Primer Design

The sequences of oligonucleotide primers (both Forward and Reverse) were designed to amplify the genes encoding the CATs,  $\gamma^+L$ ,  $b^{0+}$  and iNOS. Sequences of the investigated transcripts were retrieved from both murine and rat GenBank and Genome Browser databases. With the aid of both FASTPCR and Molecular Beacon primer design programmes, primers for the respective transporters, iNOS and two house keeping genes were designed as shown in Table 6.1. Other software programmes such as BLAST, Oligonucleotide calculator were used to aid in the design and selection of the most appropriate primers. Designed primer sequences were compared with those on GenBank using BLAST 2 sequences software and this showed that all designed primers had 100% identities with the GenBank database sequences as listed in Table 6.2. General primer design parameters were followed as described in the Methods (Section 2.17).

## 6.2.3 Reference gene Normalization

### 6.2.3.1 Internal control gene

Housekeeping genes (HKGs) are expressed in most cells under a wide range of conditions. Generally they are regarded as having ubiquitous expression in virtually all tissues with the primary role being to maintain normal but essential metabolic and cellular functions. Aside from this, it has been proposed that some HKGs may play a significant role in the regulation of important developmental pathways. In contrast, tissue specific genes carry out specific functions and are implicated in growth, differentiation, apoptosis and other developments (Butte *et al.*, 2001).

Gene expression assays require internal controls (Siebert *et al.*, 1992) that exhibit a constant basal level of expression to normalise with. Traditionally, glyceraldehyde 3-phosphate dehydrogenase (GAPDH) and  $\beta$ -actin (BACT) have been the most commonly used HKGs in normalising q-PCR experiments. Although under certain circumstances they may be superior to other HKGs, several publications have indicated that GAPDH (Deindl *et al.*, 2002; Glare *et al.*, 2002) and  $\beta$ -actin (Selvey *et al.*, 2001)

may vary considerably and are therefore unsuitable as HKG for gene expression studies. To this end, we examined the variability in expression profile of eight randomly chosen HKGs (see Table 6.1). These included several of those commonly used in both RASMCs and J774 macrophages. The analysis was carried out in one reaction to enable both the gene of interest (GOI) and housekeeping gene to be subjected to the same conditions and therefore achieve the main goal of identifying the ideal HKG for normalisation.

To identify the most stable expressed housekeeping genes under our experimental conditions, transcript expression for target genes were investigated under varying conditions in our cell models. In J774 macrophages three main treatment conditions were used; Control, LPS (1.0  $\mu\text{g/ml}$ ) or IFN- $\gamma$  (100 U/ml). In RASMCs, four conditions were used: Control, IFN- $\gamma$  (100 U/ml) only, LPS (100  $\mu\text{g/ml}$ ) only or a combination of both LPS (100  $\mu\text{g/ml}$ ) and IFN- $\gamma$  (100 U/ml). Two of the most stably expressed genes that were unaffected by the treatment conditions and could therefore be used for normalising target gene expression were chosen as HKGs.

**Table 6.1. Housekeeping genes analysed for use in normalising target gene expression**

Housekeeping Genes (HKGs)	Abbrev.	Gene Function	Reference(s)
Cyclophilin A (Peptidyl-prolyl isomerase A)	CYC A (PPIA)	Protein folding-serine/ threonine	(Luban <i>et al.</i> , 1993)
Tyrosine 3-monooxygenase/tryptophan 5-monooxygenase activation protein	YWHAZ	Protein kinase C inhibitor protein involved in protein domain specific binding	(Simsek-Duran <i>et al.</i> , 2004; Yaffe <i>et al.</i> , 1997)
Calnexin	CANX	Calcium binding protein	(Mueller <i>et al.</i> , 2008)
Ubiquitin C	UBC	Protein modifier-possibly protein catabolism	(Board <i>et al.</i> , 1992)
Ribosomal Protein L13A	RPL13A	Catalyst–protein synthesis	(Mazumder <i>et al.</i> , 2003)
$\beta$ -Actin	ACTB	Cytoskeletal structural protein	(Karakozova <i>et al.</i> , 2006; Kusner <i>et al.</i> , 2002)
$\S$ GAPDH	GAPDH	Glycolytic enzyme	(Burke <i>et al.</i> , 1996)
$\S\beta_2$ Microglobulin	B2M	Major Histocompatibility Complex (MHC)	(Arce-Gomez <i>et al.</i> , 1978)

$\S$  Primers designed in house (see primers). All other HKGs were provided by PrimerDesign (UK) Ltd.

**Table 6.2. Primers for transporter genes and HKGs evaluated**

GENES	GenBank (accession nos.)/ Chromosomal Band (Chr) MOUSE		GenBank (accession nos.)/ Chromosomal Band (Chr) RAT	
	<b>CAT-1 (SLC7A1)</b>	NM_007513.4	<b>5qG3</b>	NM_013111.2
<b>CAT2A (SLC7A2)</b>	NM_007514.3	<b>8qA4</b>	NM_001134686.1	<b>16q12.1</b>
<b>CAT2B (SLC7A2)</b>	NM_007514.3	<b>8qA4</b>	NM_001134686.1	<b>16q12.1</b>
<b>yLAT1 (SLC5A1)</b>	NM_011405.3	<b>14qC2</b>	NM_031341.1	<b>15p13</b>
<b>yLAT2 (SLC5A1)</b>	NM_178798.3	<b>8qD3</b>	NM_001107424.1	<b>19q12</b>
<b>b<sup>0</sup>AT1 (SLC5A9)</b>	NM_001199015.1	<b>7qB2</b>	NM_053929.1	<b>1q21</b>
<b>iNOS (or NOSII)</b>	NM_010927.3	<b>11qB5</b>	NM_012611	<b>10q25</b>
<b>GAPDH</b>	NM_008084	<b>6</b>	NM_017008	<b>4q42</b>
<b>β<sub>2</sub> Microglobulin</b>	NM_009735.3	<b>2</b>	NM_012512.2	<b>3q35</b>

## **6.2.4 Complementary DNA (cDNA) synthesis and real time; PCR analysis**

Prior to cDNA synthesis total RNA was treated with RNase-free DNase (Ambion, UK) according to manufacturers instruction to eliminate all traces of DNA. Complementary–DNA synthesis was carried out with purified RNA using the ImProm-II™ Reverse Transcription System (Promega, UK) kit by enabling annealing of first strand synthesis reaction of RNA and random hexamer primers at 25°C followed by an incubation step at 42°C for 60 minutes in the presence of 1 U/μl rRNasin ribonuclease Inhibitor and 4mM MgCl<sub>2</sub>. The reaction mixture was then subjected to thermal inactivation of the reverse transcriptase at 90°C for 5 min. The resulting 20 μl reaction mixture was diluted fivefold and stored at -70 °C until required in all subsequent q-PCR reactions.

Using Sybr Green q-PCR detection methodology, the transcriptional profiling of all eight HKGs and all transcripts for transporters in addition to that for iNOS were assessed. All Ct values generated from each assay run were determined at fixed threshold fluorescence value.

## **6.3 STATISTICAL ANALYSIS**

### **6.3.1 GeNORM Analysis**

The stability of the selected genes was analysed using the GeNorm software which provides a measure of gene stability by introducing two key parameters, an expression stability value, **M** and a mean pairwise variation, **V**.

Following q-PCR, CT values for the HKGs under investigation were transformed into relative quantification data using the delta CT method (Livak *et al.*, 2001). Replicates Ct values were first transformed into geNorm data followed by the determination of the arithmetic mean of the replicates. In geNorm, the measures of stability of the chosen HKGs were based on geometric averaging of expression levels. Using the geNorm analysis software, data were imported from the transformed Ct values

generated in Excel (with macros enabled). GeNorm charts were generated following importation of data into the programme. The first of three charts (see Figures **6.4** & **6.6** - J774 macrophages and RASMCs respectively) generated indicated the average stability value (**M**) of the HKG at each step during a stepwise exclusion of the least stable expressed HKG. The least stable HKG for J774 macrophages is shown on the left (B2M) with the most stable on the right (UBC & RPL13A) as illustrated in Figure **6.4**. Similarly, the least stable HKG for RASMCs is shown on the left (B2M) with the most stable on the right (CYC & RPL13A) as shown in Figure **6.6**.

The second chart (Figure **6.5** & **6.7**) following geNorm analysis was used as a guide for determining the optimal number of HKGs required in the assay. It therefore served as an illustration of the levels of variation in HKG stability and is known as the pairwise variation  $V$ , with an average score of 0.15 as the recommended ideal target. Standard curve were generated for each gene following serial dilution of the stock DNA against Ct of each gene. All the genes showed a linear correlation coefficient ( $R^2$ ) of 0.980 – 0.999 with efficiency of assay in the range of 96 – 104%. All Ct values of the respective genes were within the range of the Standard curve.

## 6.4 RESULTS

### 6.4.1 Confirmation of quantity and quality of RNA isolated

In order to ensure high quality RNA was used in the studies, the purity of isolated RNA samples was routinely checked using an agarose gel electrophoresis. The result as shown in Figure 6.1 demonstrated that the samples obtained from RASMCs were free of contaminants (mostly DNA) and were intact. This is based on the fact that there were clear 28S and 18S ribosomal RNA fragments identified with little or no smear. Similar blots were also obtained using total RNA isolates from J774 macrophages.

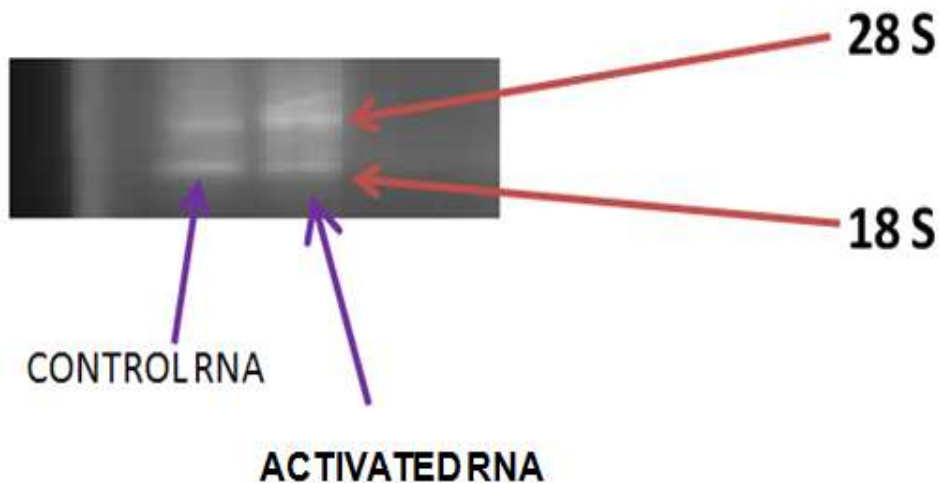


**Figure 6.1 A representative agarose gel electrophoresis of RNA isolated from both untreated (control) and activated RASMCs.**

Total RNA samples extracted from confluent untreated control or a combined LPS (100.0  $\mu\text{g/ml}$ ) and IFN- $\gamma$  (100.0 U/ml) stimulated RASMCs were mixed with bromophenol blue (1:1) and subjected to gel electrophoresis at 5 V/cm for approximately 45 minutes on a 1% agarose gel. The gel was transferred into a chamber with TBE buffer containing 10 $\mu\text{g/ml}$  ethidium bromide for 15 to 20 minutes. Gels were visualized under a transilluminator. The Figure above is a representative gel of at least three independent experiments showing 28s and 18s ribosomal bands with very little evidence of contamination in the samples.

#### **6.4.2 Expression patterns of HKGs in J774 Macrophages and RASMCs**

In J774 macrophages the eight chosen HKGs showed marked differences in their expression levels from the highest median Ct of 21.31 for Ubiquitin C (UBC) to the lowest median Ct of 14.54 for the ACTB gene (Figure 6.2). All but three HKG genes (CYC, UBC and RPL13A) had median Ct values above 20 while the remaining five genes (YWHAZ, CANX, ACTB, GAPDH and B2M) had median Ct values below 20. Similarly, in RASMCs there was a demonstrable wide range in expression of HKGs. As shown in Figure 6.3, all but two HKGs (CYC and YWHAZ) had median Ct values above 20 while the remaining six genes (CANX, UBC, RPL13A, ACTB, GAPDH and B2M) had median Ct values below 20.

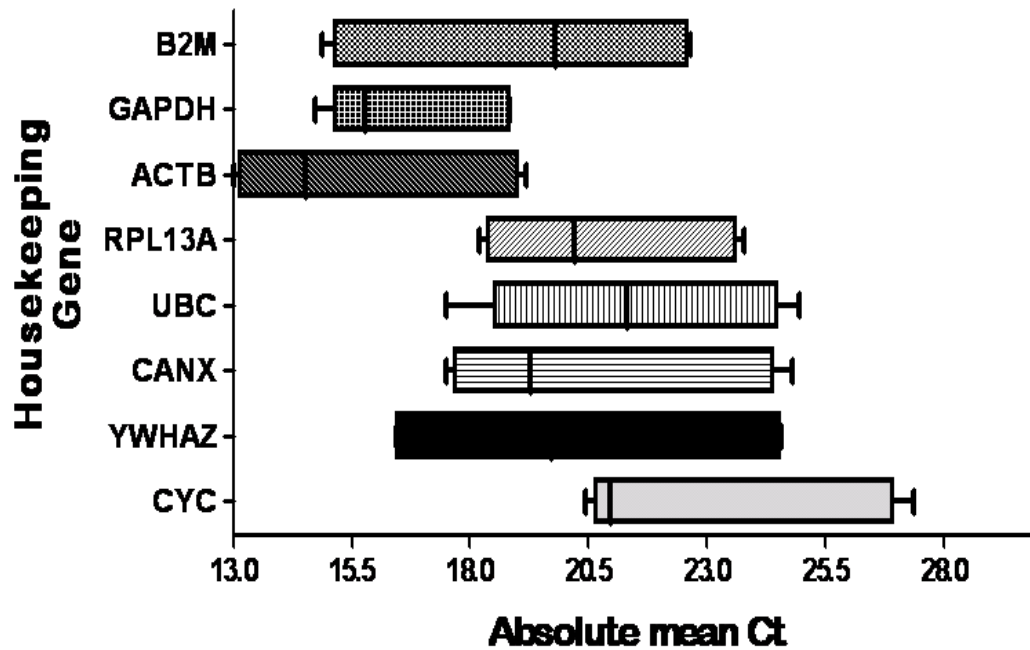


**Figure 6.2 Raw qualitative RT-PCR of Threshold cycle (Ct) for eight candidate HKGs in control and activated J774 macrophages**

Confluent monolayer of J774 macrophages were cultured in either complete DMEM alone (as Control) or stimulated with LPS (1  $\mu$ g/ml) in continued presence of complete DMEM. After 24 hour incubation period, nitrite content of the culture medium was assessed by the Greiss assay as described in the Methods (Section 2.9) to confirm activation of the cells. Total RNA was isolated from adherent cells and DNase treated. Purified RNA was then subsequently reversed transcribed to cDNA and real-time Sybr green based q-PCR analysis was performed as described in the Methods (Section 2.15 to 2.19). These results are the mean expression levels of transcripts in both activated and control cells and are representative of at least three independent experiments, each performed in triplicates. HKGs investigated include; **CYC**: Cyclophilin C; **YWHAZ**: Tyrosine 3-monooxygenase/tryptophan 5-monooxygenase activation protein, zeta polypeptide; **CANX**: Calnexin; **UBC**: Ubiquitin C; **RPL13A**: Ribosomal protein L13a; **ACTB**:  $\beta$ -Actin; **GAPDH**: Glyceraldehyde-3-phosphate dehydrogenase; **B2M**:  $\beta_2$ -Microglobulin

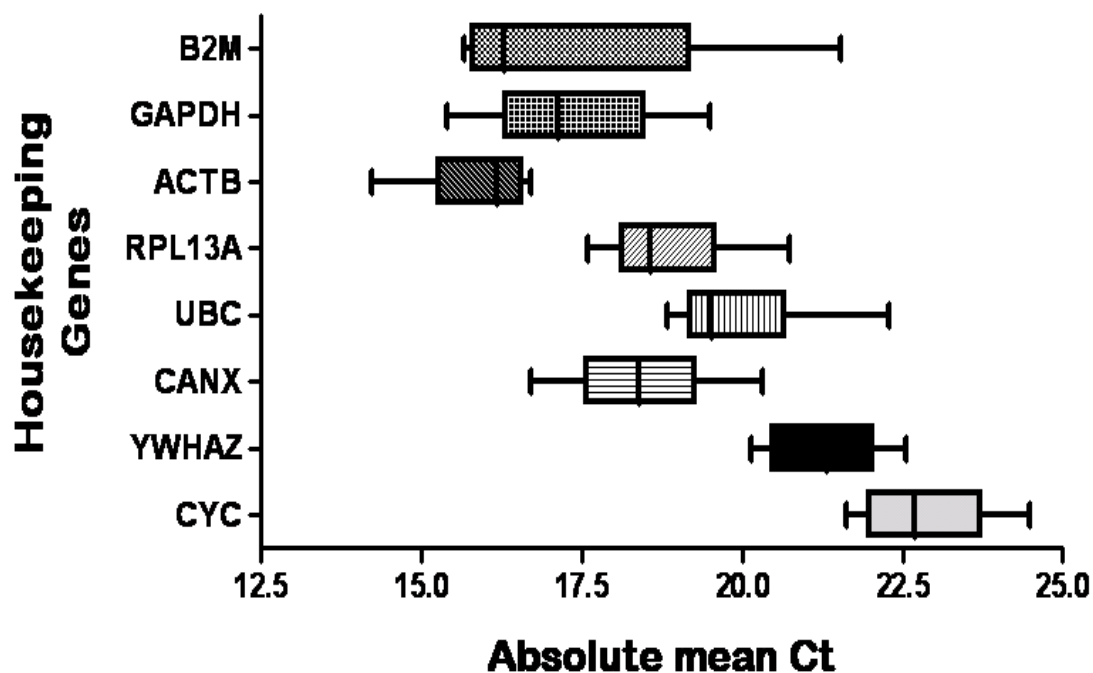


**Figure 6.3 Raw of Threshold cycle (Ct) for eight candidate HKGs in control and activated RASMCs.**

Confluent monolayer of RASMCs were cultured in either complete DMEM alone (as Control) or stimulated with both LPS (100.0  $\mu\text{g/ml}$ ) and IFN- $\gamma$  (100.0 U/ml) in continued presence of complete DMEM. After 24 hour incubation period, nitrite content of the culture medium was assessed by the Greiss assay as described in the Methods (Section 2.9) to confirm activation of the cells. Total RNA was isolated, DNase treated, purified before being reversed transcribed to cDNA and used in Sybr green based q-PCR reactions as described in Methods (Sections 2.15 to 2.19). These results are the mean expression levels of transcripts in both activated and control cells and are representative of at least three independent experiments, each performed in triplicates. HKGs investigated include; **CYC**: Cyclophilin C; **YWHAZ**: Tyrosine 3-monooxygenase/tryptophan 5-monooxygenase activation protein, zeta polypeptide; **CANX**: Calnexin; **UBC**: Ubiquitin C; **RPL13A**: Ribosomal protein L13a; **ACTB**:  $\beta$ -Actin; **GAPDH**: Glyceraldehyde-3-phosphate dehydrogenase; **B2M**:  $\beta_2$ -Microglobulin.

### 6.4.3 Optimisation and selection of the most stable HKG under experimental conditions

The amplification of each target HKG was carried out using the complementary DNA (cDNA). To ensure there was comparability between all the eight reference genes and the genes of interest, PCR efficiencies for all genes were undertaken. To evaluate the stability of the HKGs, geNorm (VBA) analysis software (Vandesompele *et al.*, 2002) was used with the incorporation of two key parameters which were an average expression stability value designated M and a pairwise variation, V. All reactions were performed in duplicates and a control using double distilled water was used for comparison. The threshold cycle (Ct) was automatically determined by using the Quansoft software (Techne).

Results from our q-PCR data showed varying ranges of stability for all the housekeeping genes examined in both control and in different activated conditions in RASMCs. Particularly, transcripts specific for CYC and RPL13A were the most stable, followed by CANX, GAPDH, YWHAZ, UBC and ACTB with B2M being the least stable. This trend in stability was determined by establishing the Ct value for each gene and normalising values in activated cells against controls (Table 6.1). The normalization factor produced was computed using the GeNorm analysis tool to determine the M values which were then plotted in Figure 6.4, clearly showing the trend in stability. Normally, M values of <1.5 indicate stable genes and in our screen all but one housekeeping gene fell below this with the most stable showing a M value of 0.152.

By comparison, the most stable genes in J774 macrophages were UBC and RPL13A with an M value of 0.026. The other stable genes in order of decreasing stability were: CANX, CYC, GAPDH, ACTB, YWHAC and B2M (as shown in Table 6.2 and in Figure 6.5).

**Table 6.3. Stability of housekeeping genes based on their respective Ct values in RASMCs**

Change Data	CYC	YWHAZ	CANX	UBC	RPL13A	ACTB	GAPDH	B2M	Normalisation Factor
S-1	1.43E-01	1.91E-01	1.15E-01	1.46E-01	1.30E-01	2.33E-01	6.93E-02	1.88E-02	0.3282
S-2	5.82E-01	4.12E-01	4.63E-01	9.73E-01	5.36E-01	4.34E-01	3.82E-01	1.00E+00	1.2226
S-3	1.00E+00	4.60E-01	2.3749						
S-4	4.48E-01	5.64E-01	3.38E-01	8.62E-01	5.11E-01	2.53E-01	3.46E-01	9.27E-01	1.0492
<b>M &lt; 1.5</b>	0.597	0.773	0.633	0.775	0.590	1.038	0.734	1.897	

ORDER OF INCREASING EXPRESSION STABILITY



**B2M, ACTB, UBC, YWHAZ, GAPDH, CANX, CYC, RPL13A**

This Table was generated by the geNorm analysis software which also generates a normalization factor required for the determination of **M** values for each gene. **S1** represents studies in control cells; **S2**, IFN- $\gamma$  treated cells; **S3**, LPS treated cells and **S4**, a combined LPS and IFN- $\gamma$  treated cells.

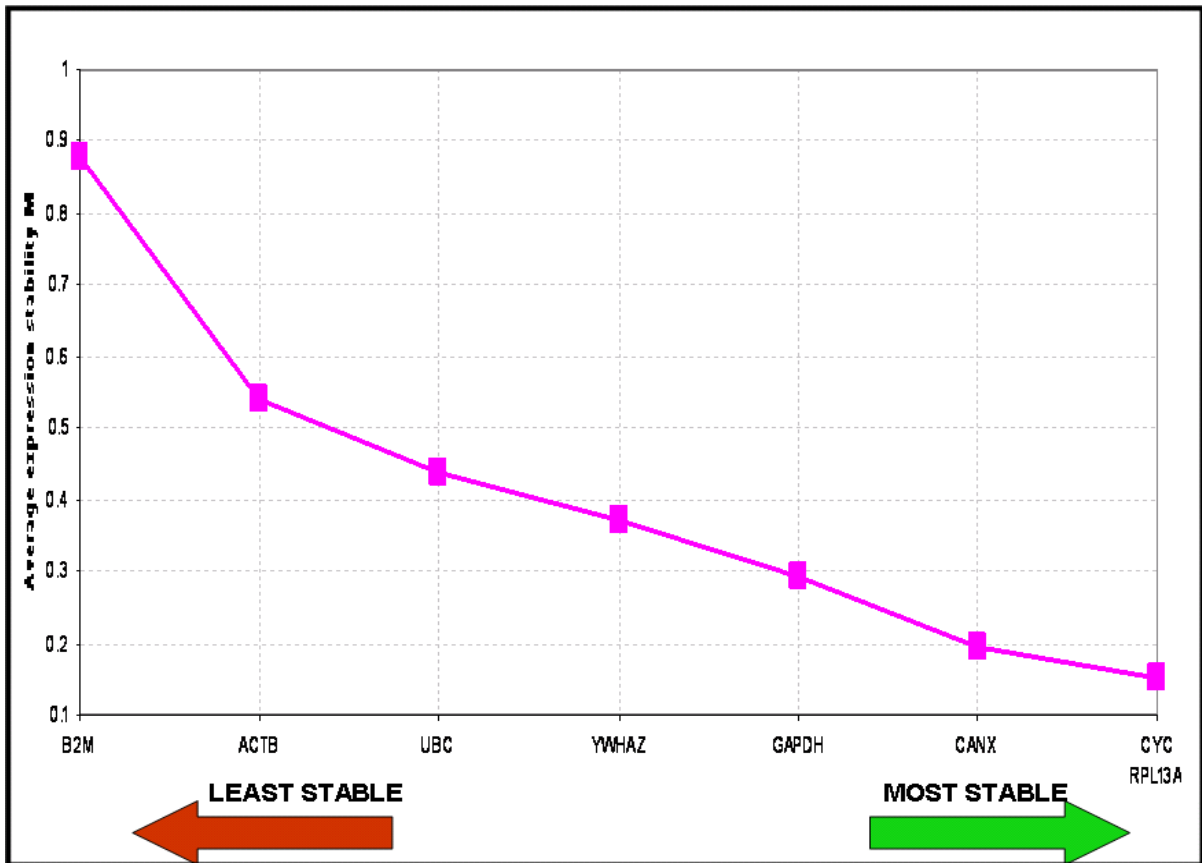


**Figure 6.4 Average expression stability values of various housekeeping genes in RASMCs.**

Confluent monolayer of RASMCs in T-25 flasks were cultured in complete DMEM alone (as Control) or stimulated with IFN- $\gamma$  (100 U/ml) or LPS (100  $\mu$ g/ml) or a combination of both IFN- $\gamma$  (100 U/ml) and LPS (100  $\mu$ g/ml) in continued presence of complete DMEM for 24 hours. Total RNA was isolated, DNase treated, purified before being reversed transcribed to cDNA and used in Sybr green based q-PCR reaction as described in Methods (Sections 2.15 to 2.19). Stability of the eight selected HKGs was undertaken to assess the most stable gene and assigned a stability value **M**, using the geNorm approach. Resulting data is plotted against the respective gene as shown above. This figure is representative of at least three independent experiments with both CYC and RPL13A having the lowest M value.

**Table 6.4. Stability of housekeeping genes based on their respective Ct values in J774 macrophages**

Change Data	CYC	YWHAZ	CANX	UBC	RPL13A	ACTB	GAPDH	B2M	Normalisation Factor
S-1	8.12E-01	1.04E-01	3.28E-01	2.89E-01	2.81E-01	9.79E-01	8.29E-01	3.96E-02	2.0881
S-2	1.00E+0 0	5.7846							
S-3	1.30E-02	3.70E-03	9.29E-03	2.65E-02	2.66E-02	2.74E-02	8.90E-02	5.76E-03	0.0828
	0.21915 1431	0.07279 5851	0.14492 0476	0.19705 4509	0.19569 3353	0.29936 9677	0.41947 7887	0.06107 2498	
M < 1.5	1.304	1.480	1.080	1.014	1.023	1.235	1.564	1.803	

ORDER OF INCREASING EXPRESSION STABILITY



B2M, YWHAZ, GAPDH, CYC, ACTB, CANX, RPL13A, UBC

This Table was generated by the geNorm analysis software which also generates a normalization factor required for the determination of M values for each gene. **S1** represents studies in control cells; **S2**, IFN- $\gamma$  treated cells and **S3** LPS treated cells.

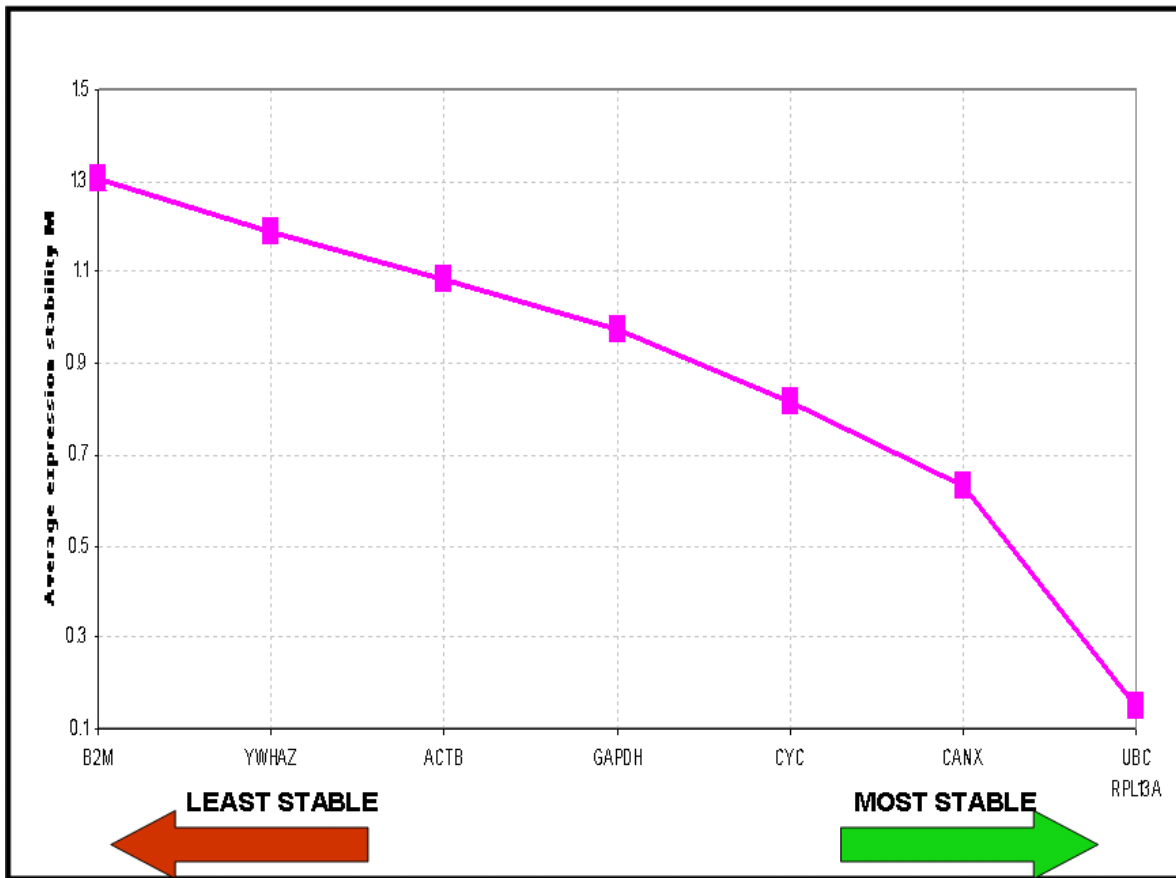


**Figure 6.5 Average expression stability (M) values of the HKGs in J774 macrophage using the geNorm program.**

Confluent monolayer of murine J774 macrophages in T-25 flasks were cultured in complete DMEM alone (as Control) or stimulated with IFN- $\gamma$  (10 U/ml) or LPS (1.0  $\mu$ g/ml) in continued presence of complete DMEM for 24 hours. Total RNA was isolated, DNase treated, purified before being reversed transcribed to cDNA and used in Sybr green based q-PCR reactions as described in Methods (Sections 2.15 to 2.19). Stability of the eight selected HKGs was undertaken to assess the most stable gene and assigned a stability value **M**, using the geNorm approach. Resulting data is plotted against the respective gene as shown above. This figure is representative of at least three independent experiments with both UBC and RPL13A having the lowest M value.

#### **6.4.4 Profile of L-arginine Transporter expression in RASMCs and J774 macrophages.**

As previously demonstrated (Baydoun *et al.*, 1993a; Baydoun *et al.*, 1994b; Kakuda *et al.*, 1999; Schott *et al.*, 1993b), L-arginine transport in this thesis increased in J774 macrophages following activation with LPS alone. Similarly, there was a comparative increase in L-arginine uptake in RASMCs when induced with both LPS (100 µg/ml) and IFN-γ (100U/ml). To determine which transporter may be critical for this change gene analysis of CAT expression was carried out comparing the relative expression of CAT transporters against the relevant housekeeping gene determined as described above. In RASMCs these were CYC and RPL13A and in J774 macrophages we used UBC and RPL13A. In addition, amplification of iNOS was also conducted and used for comparative purposes to determine how the induction of the enzyme correlates with the induction of CATs. This should help shed light on which CAT may be critical for substrate supply to iNOS by correlating profiles of increases with changes in function (ie NO production and L-arginine transport). A representative amplification plot of a ten-fold serially diluted iNOS cDNA showing a change in fluorescence ( $\Delta R_n$ ) as a function cycle numbers in iNOS transcript is shown in Figure 6.6 (RASMCs) and Figure 6.7 (J774 macrophages) below. This was first determined to basically establish that the reaction conditions resulted in efficient amplifications of the target gene.

In relation to CAT expression, primers of CAT genes had amplification slopes in the range of  $-3.19$  to  $-3.56$ , corresponding to amplification efficiencies of 93 to 105%. In RASMCs, all target genes achieved a correlation coefficient ( $R^2$ ) of between 0.965 – 0.999 (Data not shown). The average cycle threshold (AvCt) values indicate signals in single PCR reactions. Each Ct point represents an average of three replicates. Similarly, in J774 macrophages, target genes achieved a correlation coefficient ( $R^2$ ) of between 0.96 and 0.989 (Data not shown). The average cycle threshold (AvCt) values indicate signals in single PCR reactions. Each Ct point represents an average of three replicates.

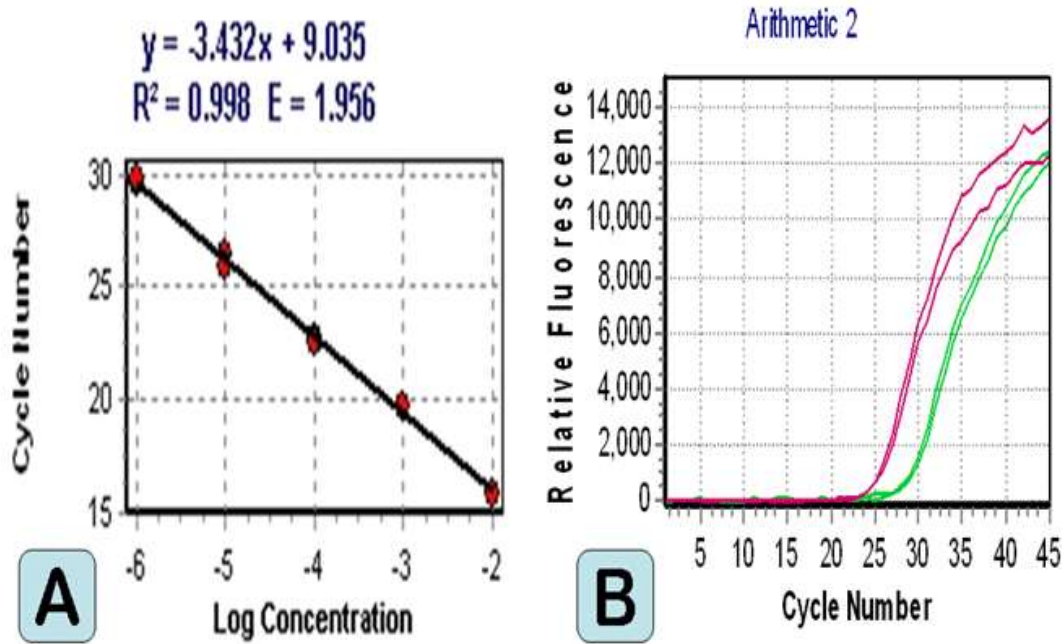


**Figure 6.6 Amplification curve of iNOS gene in RASMCs**

Confluent monolayer of RASMCs in T-25 flasks were cultured in complete DMEM alone (as Control) or stimulated with LPS (100.0  $\mu\text{g}/\text{ml}$ ) and IFN- $\gamma$  (100.0 U/ml) in continued presence of complete DMEM for 24 hours. Total RNA was isolated, DNase treated, purified before being reversed transcribed to cDNA and used in Sybr green based q-PCR reactions as described in Methods (Sections 2.15 to 2.19). A representative linear regression of the amplification plot of 10 fold serially diluted cDNA (in DNase free water) is shown in Figure A. Figure B is a representative amplification profile plot generated from the Quanta thermocycler software (Quansoft) with non-treated (green) and activated (red) serially diluted iNOS cDNA showing relative fluorescence ( $\Delta\text{Rn}$ ) as a function cycle numbers in the iNOS transcript.

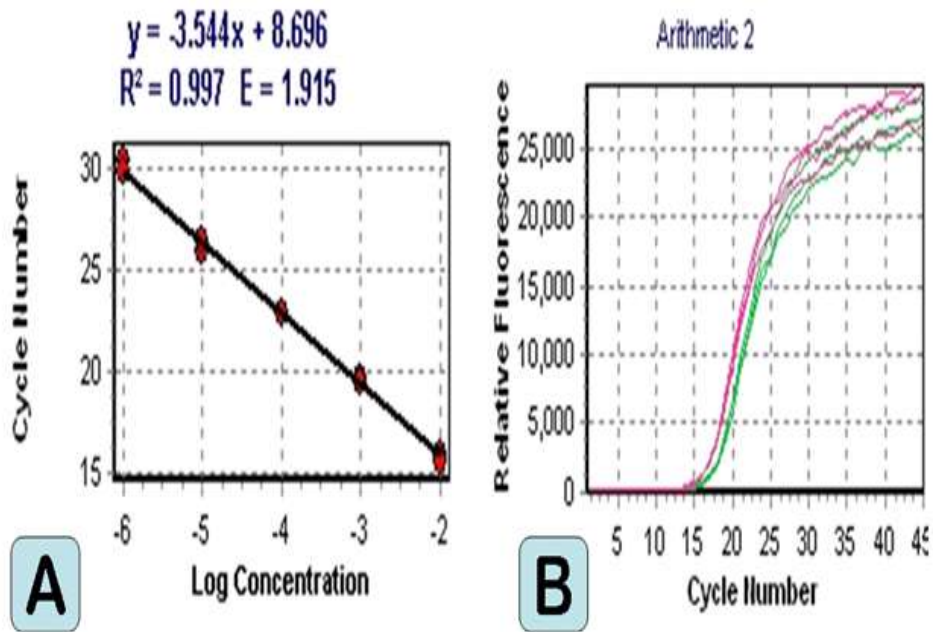


**Figure 6.7 Amplification curve of iNOS gene in J774 macrophages**

Confluent monolayer of J774 macrophages in T-25 flasks were cultured in complete DMEM alone (as Control) or stimulated with LPS (1.0  $\mu\text{g}/\text{ml}$ ) in continued presence of complete DMEM for 24 hours. Total RNA was isolated, DNase treated, purified before being reverse transcribed to cDNA and used in Sybr green based q-PCR reactions as described in Methods (Sections 2.15 to 2.19). A representative linear regression of the amplification plot of 10 fold serially diluted cDNA (in DNase free water) is shown above (Figure A). Figure B is a representative amplification profile plot generated from the Quantica thermocycler software (Quansoft) showing non-treated (green) and activated (red) serially diluted iNOS cDNA showing relative fluorescence ( $\Delta R_n$ ) as a function of cycle number in the iNOS transcript.

The presence of expected PCR products (transcript of transporter mRNA) was confirmed by melt-curves analysis which indicated amplification of a single product in the SYBR Green based q-PCR reaction assay. As shown in Figures **6.8** (RASMCs) and **6.9** (J774 macrophages) each of the targeted gene (i.e. CAT-1, CAT2A, CAT2B,  $\gamma^+$ LAT1,  $\gamma^+$ LAT2 and  $b^{0,+}$ ) had a single unique peak indicating a single product and thus confirming a successful reaction and target specificity. More importantly, basal expressions of these transporters were found in all cells in the absence of IFN- $\gamma$  and/or LPS. In control RASMCs, CAT-1 was the most highly expressed while CAT2A the least expressed transcript (Figure **6.10**). By comparison, CAT2B was the most highly expressed transcript in J774 macrophages with CAT2A again showing the least expression. Following induction RASMCs showed significantly enhanced expression of CAT2B ( $3.14 \pm 0.35$ ) while both CAT-1 and CAT2A were only moderately enhanced, showing 1.59 and 6.23 fold increases respectively. However neither of these increases were significantly different to control levels due to the large variations between experiments ( $p > 0.05$ ) (Figure **6.10**). In the macrophages, CAT2A did not appear to be induced and was in fact reduced by LPS ( $0.47 \pm 0.007$ ) but the large variations between experiments suggest the changes were not statistically different to control. Both CAT-1 and CAT2B were however significantly enhanced with the latter being the most predominant in LPS-activated cell (Figure **6.11**). The fold change in CAT2B expression was on average  $24.98 \pm 3.48$  and that of CAT-1 was  $10.9 \pm 1.3$ . These changes were much higher when compared to similar changes in RASMCs. In addition the expression of iNOS mRNA also increased very significantly to over  $3081 \pm 14.91$  fold compared to control cells.

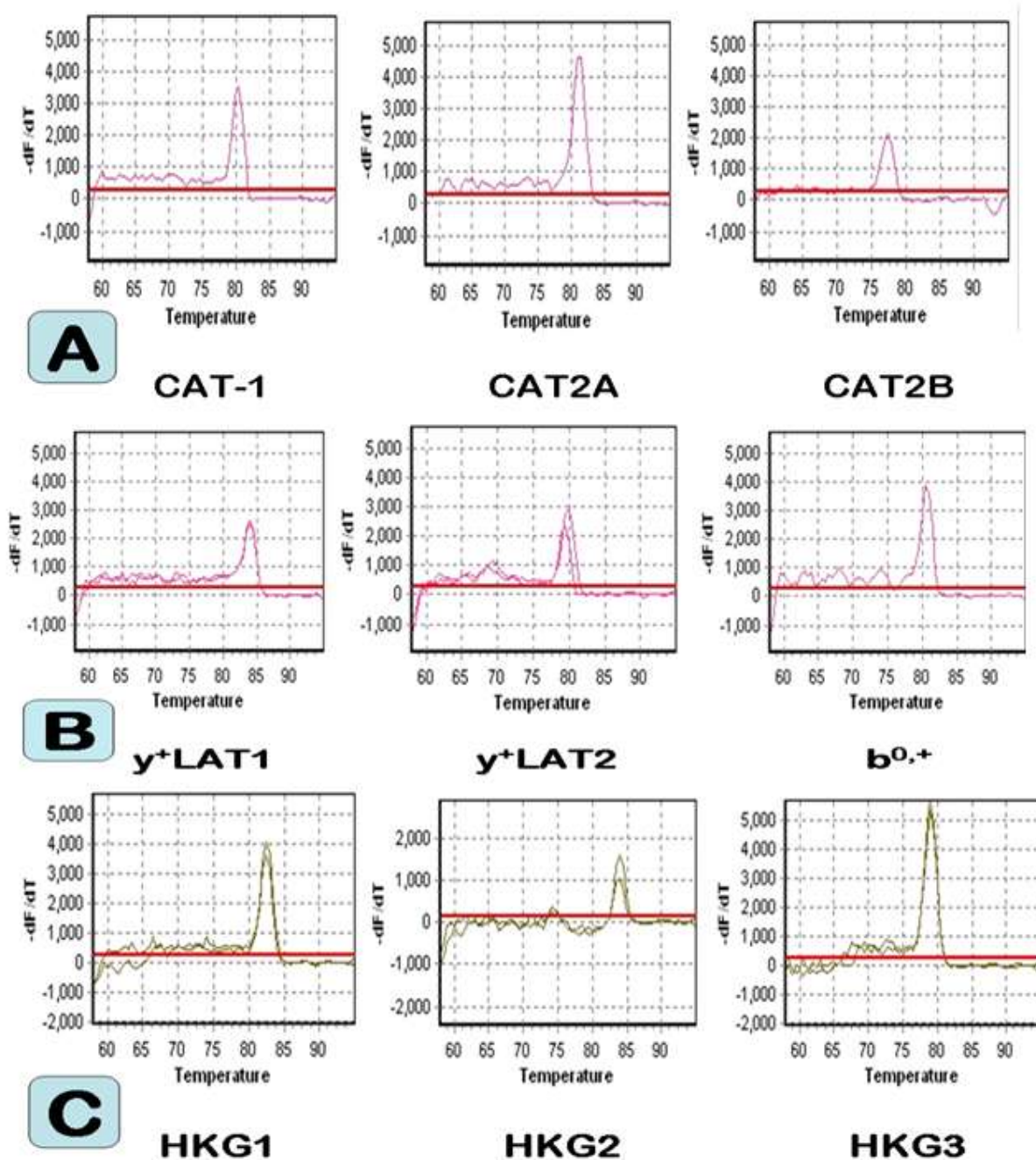


**Figure 6.8 Specificity of targeted gene expression in RASMCs**

Confluent monolayer of RASMCs in T-25 flasks were cultured in complete DMEM alone (as Control) or stimulated with both LPS (100  $\mu\text{g}/\text{ml}$ ) and IFN- $\gamma$  (100 U/ml) in continued presence of complete DMEM for 24 hours. Total RNA was isolated, DNase treated, purified before being reversed transcribed to cDNA and used in Sybr green based q-PCR reactions as described in Methods (Sections 2.15 to 2.19). Each Melting curve represents respective profile of the investigated carrier transport transcripts which includes CAT-1, CAT2A, CAT2B,  $y^+\text{LAT1}$ ,  $y^+\text{LAT2}$ ,  $b^{0+}$  and HKGs **CYC** (HKG1), **RPL13A** (HKG2) and **CANX** (HKG3).

## 6.4.5 Specificity in expression profile of CAT members in the murine J774 macrophages

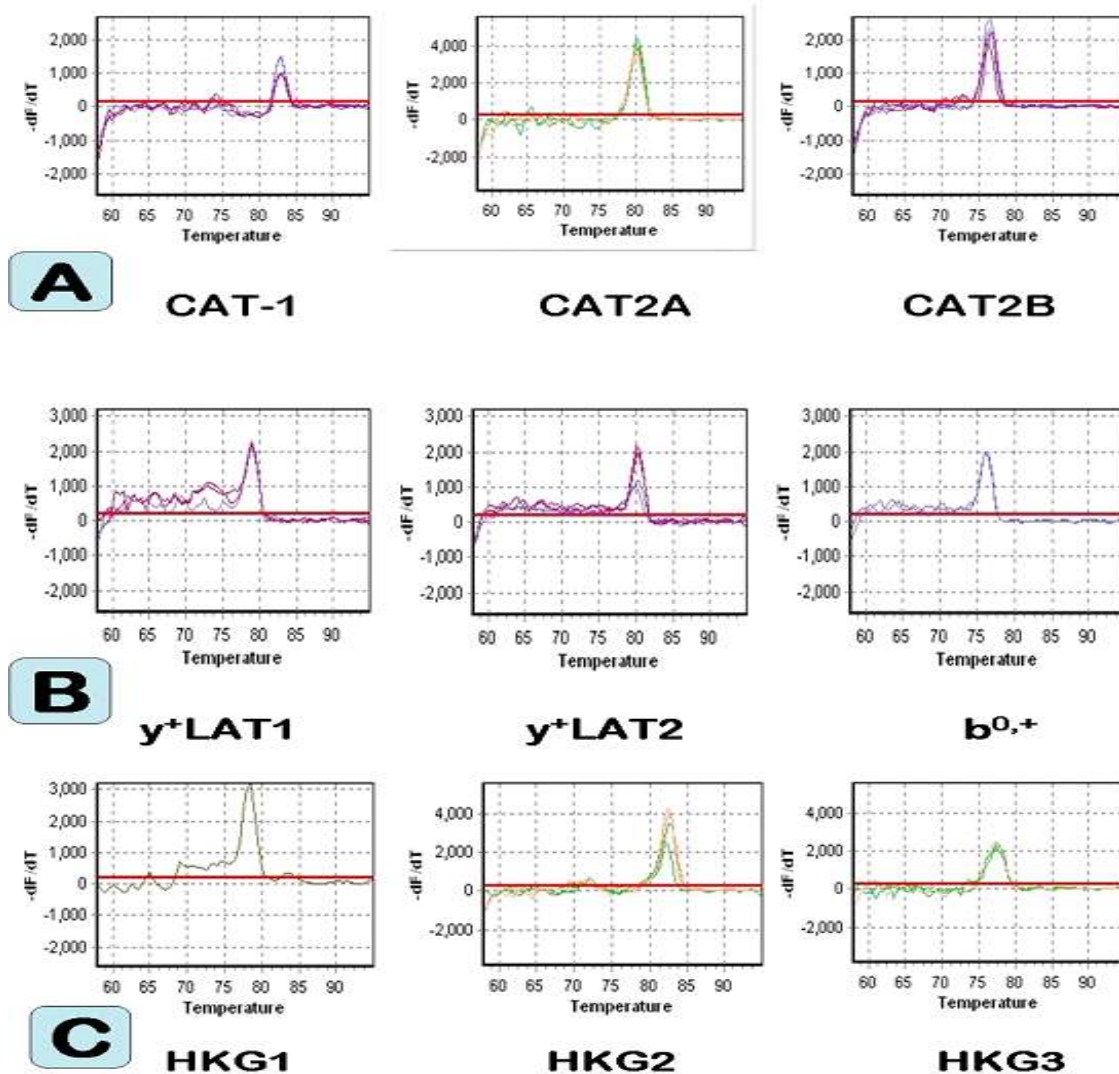


**Figure 6.9** Specificity of targeted gene expression in J774 macrophages

Confluent monolayer of J774 macrophages in T-25 flasks were cultured in complete DMEM alone (as Control) or stimulated with LPS (1.0  $\mu\text{g/ml}$ ) in continued presence of complete DMEM for 24 hours. Total RNA was isolated, DNase treated, purified before being reversed transcribed to cDNA and used in Sybr green based q-PCR reactions as described in Methods (Sections 2.15 to 2.19). Each Melting curve represents respective profile of the investigated carrier transport transcripts which includes CAT-1, CAT2A, CAT2B,  $y^+LAT1$ ,  $y^+LAT2$ ,  $b^{0,+}$  and HKGs UBC (**HKG1**), RPL13A (**HKG2**) and CANX (**HKG3**).

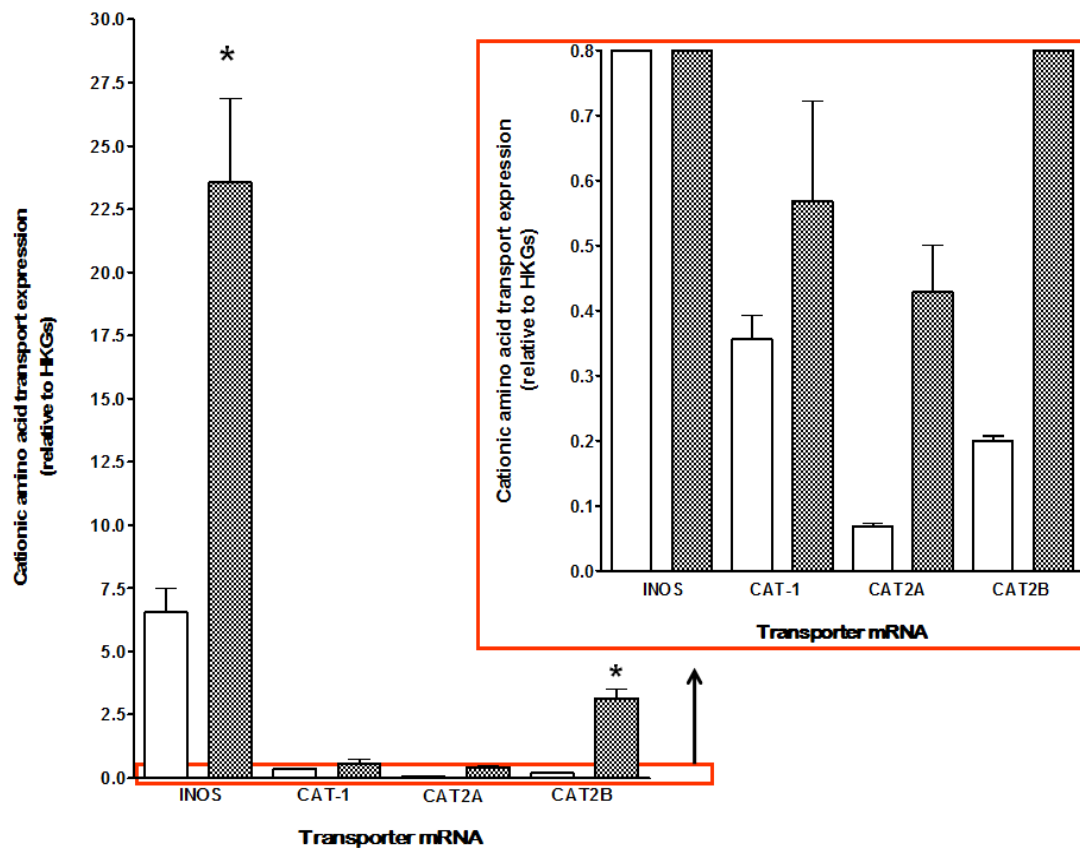


**Figure 6.10 Effect of IFN- $\gamma$  and LPS on the expression of CATs in RASMCs**

Confluent monolayer of RASMCs in T-25 flasks were cultured in complete DMEM alone (as Control) or stimulated with both LPS (100  $\mu\text{g}/\text{ml}$ ) and IFN- $\gamma$  (100 U/ml) in continued presence of complete DMEM for 24 hours. Total RNA was isolated, DNase treated, purified before being reversed transcribed to cDNA and used in Sybr green based q-PCR reactions as described in Methods (Sections 2.15 to 2.19). These results are mean expression levels of transcripts in both activated and non-activated cells normalized to HKGs, CYC and RPL13A. Open white bars represent controls and closed black filled bars represent activated cells. Data represent the **mean  $\pm$  S.E.M.** from three independent experiments, each performed in three replicates. Statistical differences between means were determined using one-way analysis of variance (ANOVA) followed by Dunnett's multiple comparisons test of the normalized data. \* denotes  $P < 0.01$  when compared to untreated controls. The highlighted insert is an adjusted normalized expression profile of data below 0.150 units in order to optimize visualization of lowly expressed transcripts.

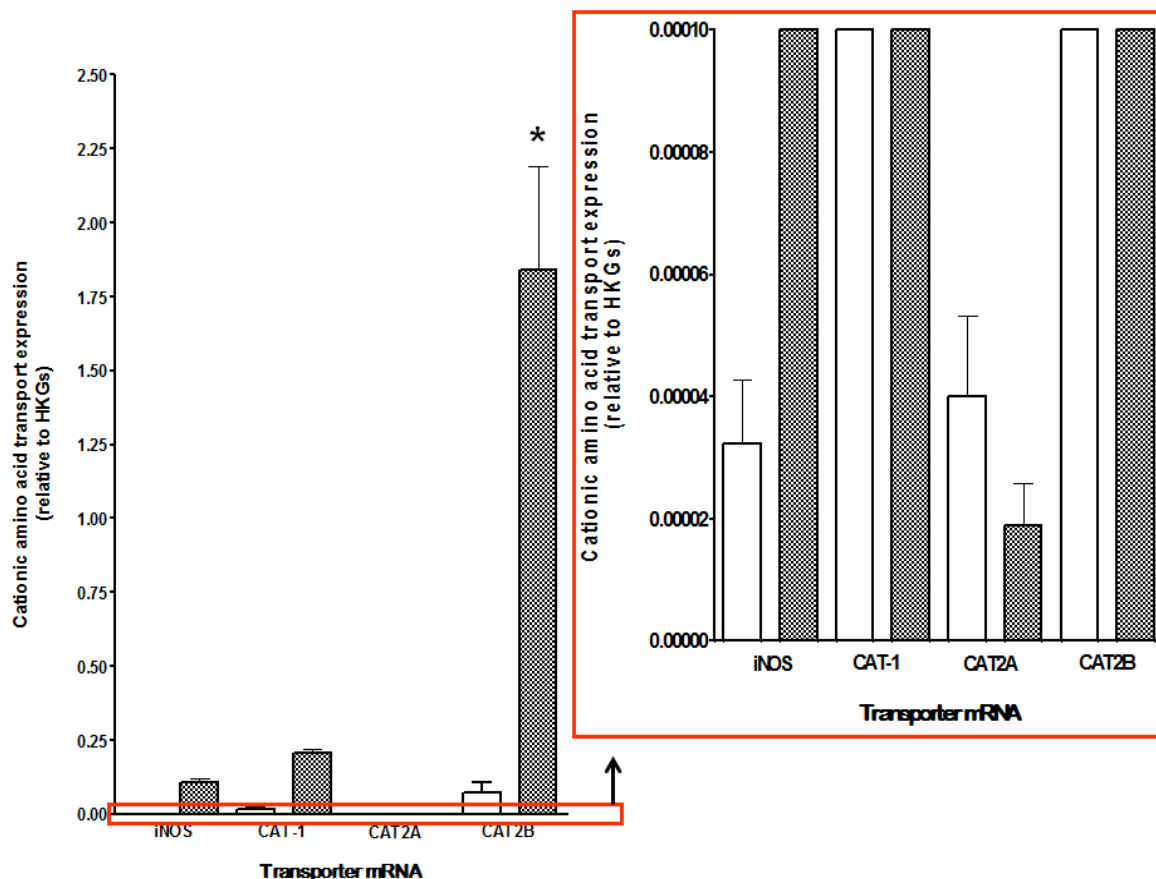


**Figure 6.11 Effect of LPS on the expression of CATs in J774 macrophages**

Confluent monolayer of J774 macrophages in T-25 flasks were cultured in complete DMEM alone (as Control) or stimulated with LPS (1.0  $\mu\text{g}/\text{ml}$ ) in continued presence of complete DMEM for 24 hours. Total RNA was isolated, DNase treated, purified before being reversed transcribed to cDNA and used in Sybr green based q-PCR reactions as described in Methods (Sections 2.15 to 2.19). These results are mean expression levels of transcripts in both activated and non-activated cells normalized to HKGs, CYC and RPL13A. Open white bars represent controls and closed black filled bars represent activated cells. Data represent the **mean  $\pm$  S.E.M.** from three independent experiments, each performed in three replicates. Statistical differences between means were determined using one-way analysis of variance (ANOVA) followed by Dunnett's multiple comparisons test of the normalized data. \* denotes  $P < 0.01$  when compared to untreated controls. The highlighted insert is an adjusted normalized expression profile of data below 0.150 units in order to optimize visualization of lowly expressed transcripts.

#### 6.4.6 Effect of Lipopolysaccharide and IFN- $\gamma$ on the expression of

heterodimeric amino acid transporter in cultured RASMCs and in murine

J774 macrophages

In parallel studies to the above, changes in the expression profile of  $y^+$ LAT1 (SLC7A5),  $y^+$ LAT2 (SLC7A6) and  $b^{0,+}$  (SLC7A9) were also examined. With the exception of  $b^{0,+}$  basal expression of each transporter was identified in both cell types in the absence of IFN- $\gamma$  and LPS. In RASMCs, all transcripts present in controls were moderately enhanced following activation; with  $y^+$ LAT1 and  $y^+$ LAT2 showing 3.17 and 2.21 fold increases respectively over control transcript levels (Figure 6.12). Although  $b^{0,+}$  was not expressed in controls, stimulation with both LPS and IFN- $\gamma$  resulted in detectable levels of expression albeit at very low levels. In J774 macrophages the results (Figure 6.13) showed increased expression in all three transcripts following stimulation with LPS. Increased expressions on  $y^+$ LAT1,  $y^+$ LAT2 and  $b^{0,+}$  were on average,  $44.4 \pm 0.02$ ,  $27.7 \pm 0.08$  and  $1.16 \pm 0.01$  fold respectively. As in RASMCs the expressions of transporters in control cells were very low.

A summary table of the changes in expression of all the transporters is shown in Table 6.5.

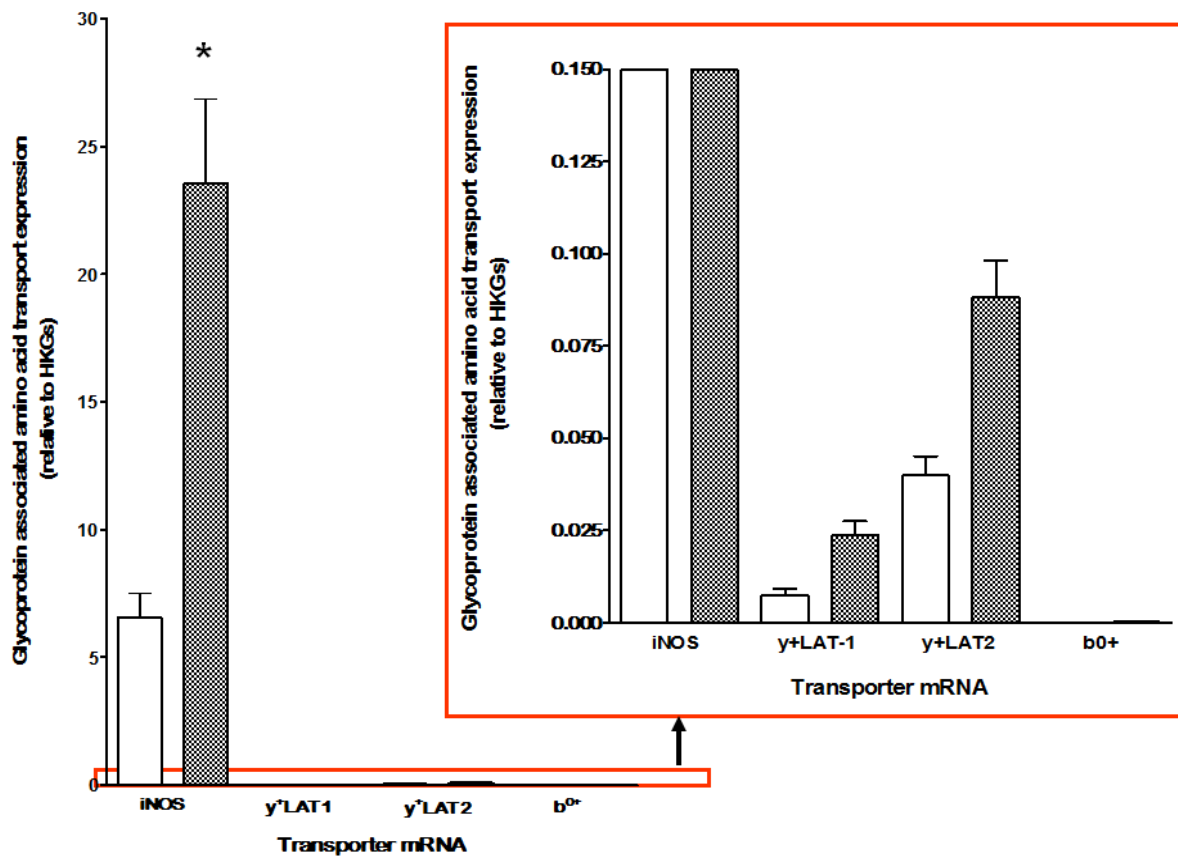


**Figure 6.12 Effect of IFN- $\gamma$  and LPS on the expression of glycoprotein associated amino acid transporters in RASMCs**

Confluent monolayer of RASMCs in T-25 flasks were cultured in complete DMEM alone (as Control) or stimulated with both LPS (100  $\mu$ g/ml) and IFN- $\gamma$  (100 U/ml) in continued presence of complete DMEM for 24 hours. Total RNA was isolated, DNase treated, purified before being reverse transcribed to cDNA and used in Sybr green based q-PCR reactions as described in Methods (Sections 2.15 to 2.19). These results are mean expression levels of transcripts in both activated and non-activated cells normalized to HKGs, CYC and RPL13A. Open white bars represent controls and closed black filled bars represent activated cells. Data represent the **mean  $\pm$  S.E.M.** from at least three independent experiments, each performed in three replicates. Statistical differences between means were carried out using one-way analysis of variance (ANOVA) followed by Dunnett's multiple comparisons test of the normalized data. \* denotes  $P < 0.01$  when compared to untreated controls. The highlighted insert is an adjusted normalized expression profile of data below 0.150 units in order to optimize visualization of lowly expressed transcripts.

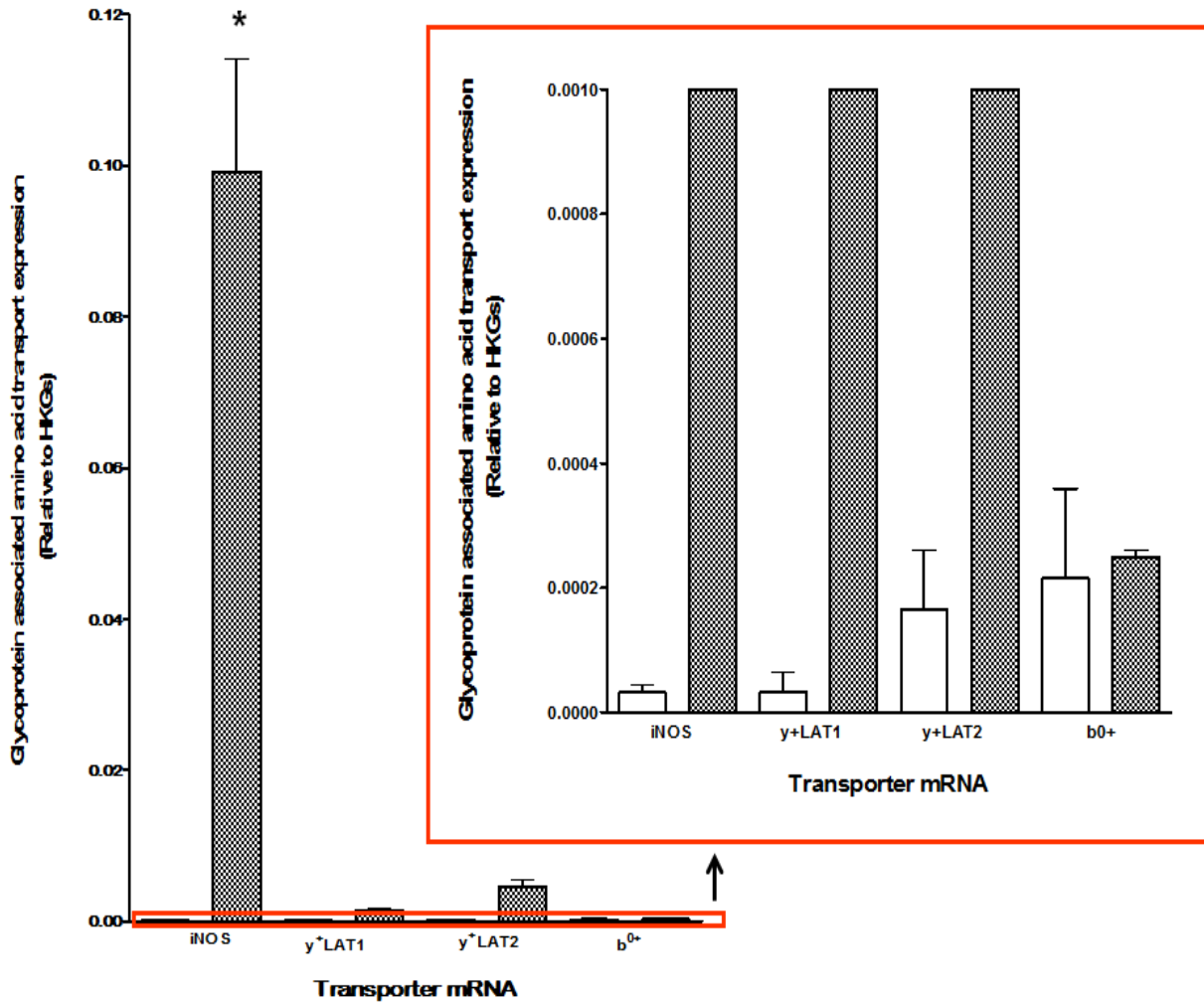


**Figure 6.13 Effect LPS on the expression of glycoprotein associated amino acid transporters in J774 macrophages**

Confluent monolayer of J774 macrophages T-25 flasks were cultured in complete DMEM alone (as Control) or stimulated with LPS (1.0  $\mu\text{g/ml}$ ) in continued presence of complete DMEM for 24 hours. Total RNA was isolated, DNase treated, purified before being reverse transcribed to cDNA and used in Sybr green based q-PCR reactions as described in Methods (Sections 2.15 to 2.19). These results are mean expression levels of transcripts in both activated and non-activated cells normalized to HKGs, UBC and RPL13A. Open white bars represent controls and closed black filled bars represent activated cells. Data represent the **mean  $\pm$  S.E.M.** from at least three independent experiments, each performed in three replicates. Statistical differences between means were determined using one-way analysis of variance (ANOVA) followed by Dunnett's multiple comparisons test of the normalized data. \* denotes  $P < 0.01$  when compared to untreated controls. The highlighted insert is an adjusted normalized expression profile of data below 0.001 units in order to optimize visualization of lowly expressed transcripts.

Table 6.5. Comparison of relative expression between levels of arginine transporters in RASMCs and J774 macrophages

HK GENES	RAT SMOOTH MUSCLE CELLS (RASMCs) FOLD EXPRESSION	MURINE J774 MACROPHAGES FOLD EXPRESSION
SLC7A1 (CAT-1)	1.59 ± 0.154	10.941 ± 1.252
SLC7A2 (CAT2A)	6.223 ± 0.072	0.473 ± 0.0068
SLC7A2 (CAT2B)	15.736 ± 0.347	24.980 ± 3.488
SLC7A7 (y+LAT1)	3.178 ± 0.0038	44.396 ± 0.0153
SLC7A6 (y+LAT2)	2.208 ± 0.01	27.709 ± 0.0835
SLC7A9 (b0+)	-	1.16 ± 0.0098
NOS2 (iNOS)	1.58 ± 0.332	3081.9 ± 14.91

## 6.5 DISCUSSION

### Housekeeping gene selection by assessing stability following gene expression

In comparing the levels of gene expression in different cell types or under different physiological conditions it is suggested that the housekeeping genes (HKGs, also called reference or normalizer) must be stable and specific in the profile they exhibit (Dheda *et al.*, 2004; Thellin *et al.*, 1999). Whether in gene micro-array which offers a high throughput or in q-PCR for sensitivity and precision, normalization is considered critical to compensate for the subtle changes in expression or variability in assays in order to allow accurate comparison of data between different samples and under varying condition. It is now widely recognized that there is not a single gene that is stable or suitable as a control under all experimental conditions (Bustin *et al.*, 2004). In this thesis we addressed these short comings by systematically analyzing the stability of a panel of HKGs prior to our target gene expression studies. Without these safe guards in place there could be misinterpretation of gene expression of target genes. Commonly used HKGs in expression studies have in the past included beta actin (ACTB), glyceraldeyde-3-phosphate dehydrogenase (GAPDH), beta-2-microglobulin (B2M), ribosome small subunit (18S) ribosomal RNA (rRNA), Ubiquitin C (UBC), hypoxanthine guanine phosphoribosyl transferase (HPRT), succinate dehydrogenase complex, subunit A (SDHA) and Tyrosine 3-monooxygenase/tryptophan 5-monooxygenase activation protein, zeta polypeptide (YWHAZ). Previous literature reported that genes such as GAPDH, beta-2-microglobulin, 28S RNA and  $\beta$ -Actin (ACTB) were widely used in many and past investigations and have presently been found to be very unstable under some experimental conditions (Deindl *et al.*, 2002; Goidin *et al.*, 2001;

Schmittgen *et al.*, 2000; Suzuki *et al.*, 2000) and therefore unreliable. The outcomes have therefore rendered such genes unsuitable as HKGs under the conditions reported (Dheda *et al.*, 2004; Thellin *et al.*, 1999; Zhong *et al.*, 1999). In view of the importance of identifying statistically significant data in this study we investigated a panel of 8 commonly used HKGs (as shown in **Table 2.**) in both RASMCs and J774 macrophages under both normal physiological and pathophysiological conditions. The pathophysiological conditions were induced using LPS alone or LPS+IFN- $\gamma$  or IFN- $\gamma$  alone.

Secondly the quality of the extracted RNA could impact on the accuracy of our data. All extracted RNA was routinely analyzed on both gel electrophoresis to detect 28s and 18s bands and additionally analyzed on the spectrophotometer for the 260/280 ratio (optimum range was between 1.78 and 2.08). These parameters were critical in validating our target gene expression studies. RNA quality, outside of these criteria was excluded from our final analysis and in addition to the presence of non-specific products or primer-dimers in our q-PCR assays. It is suggested that these artefacts do limit the dynamic range of the desired standard curve as a result of the apparent insufficient reaction components due to competition in the amplification cycle (Bustin *et al.*, 2004).

In monitoring the small changes in mRNA expression (Bustin, 2002), q-PCR assays combines the sensitivity, reproducibility and a wide quantification range of newly synthesized DNA in transcripts (Bustin, 2000). To this end we also demonstrated in this thesis the reliability of our q-PCR assays and amplification on the required genes being expressed by ensuring that each target gene had a representative product specific profile generated in our melt curve analysis after the amplification cycle. The melt curve is the first derivative of the plot which signifies the rate of change of fluorescence (Sybr Green assay) as a double-stranded PCR product melts in real time as a function of temperature (dF/dT). We further ensured that the product sizes of amplified transcripts in the real time PCR assays in this study were directly correlated with respective amplification

temperature ( $T_m$ ). All the target genes in this study had a unique peak as demonstrated in the melting curve profiles of all the carrier transporter transcripts being expressed using SYBR Green I.

Results from this study using the geNorm approach to select the most stable HKG identified RPL13A and UBC as the most stable HKG in J774 macrophages with both having geNorm (M) stability values of 0.026. In RASMCs however both CYC and RPL13A were shown to be the most stable HKG, both with slightly higher geNorm (M) stability values of 0.152. In addition results in this study demonstrated a wide range of stability in gene expression across the treatment conditions used. These suggest that there is species or even cell type specificity in stability of housekeeping genes depending on the treatment conditions.

Our results thus confirmed tissue specificity in expression variability of these genes. The geNorm analysis (Vandesompele *et al.*, 2002) approach to select the most appropriate HKG in both cell models incorporated two key parameter in our analysis; an average stability measure (M) and a pairwise variation (V). A low M value was indicative of stable expression and with minimum V cut-off value of 0.15 to require an additional gene in normalizing the gene of interest (GOI) (Vandesompele *et al.*, 2002). The selected genes also demonstrated very high expression profiles with comparatively reduced expression variability as required in current approaches to normalization (Galiveti *et al.*, 2010; Pfaffl *et al.*, 2004; Vandesompele *et al.*, 2002). In addition, data analysis from this study incorporated the geometric averaging of multiple control genes to improve on previous normalization strategies that were based on a single gene which led to erroneous results. We assessed the stability of the chosen genes by using the geNorm VBA applet (Vandesompele *et al.*, 2002). Although we only used the geNorm strategy in this study, similar analytical tools comparable to the geNorm approach of gene normalization have been reported. The 'Best Keeper' and 'NormFinder' (Andersen *et al.*, 2004; Pfaffl *et al.*, 2004) tools have been reported to achieve comparable results.

In summary, we have demonstrated in this study the reliability of the RPL13A and CYC in J774 macrophages and with RPL13A and UBC in RASMCS as stable HKGs to efficiently normalize gene expression studies in mouse and rat respectively. Several different investigations when normalizing HKGs have also found RPL13A to be a very reliable control gene though under different conditions (Curtis *et al.*, 2010; Quiroz *et al.*, 2010). It is however important to note that the selected genes could not account as appropriate normalizers for all experimental conditions associated with the respective cell models. They however represent adequate HKG targets in pro-inflammatory mediated conditions in view of their low gene expression variability amongst the HKGs so far examined in this thesis. Surprisingly, commonly used HKGs such as GAPDH, B2M and ACTB were inadequate HKGs under such pro-inflammatory mediated conditions and are therefore best avoided in any future experiments. The use of inappropriate HKG could lead to misinterpretation of gene expression pattern of the GOI. Given that gene stability is dependent on tissue or cell type specificity in addition to the physiological condition, it was imperative to validate chosen HKGs before embarking on any gene expression profiling. We have also demonstrated the ability of RT/ q-PCR as a platform for adequate assessment of gene stability without *priori* evidence. It is our hope that this study will identify novel genes relevant to pathophysiological processes as well as provide an insight into the complex regulatory system of iNOS induced nitrite production during inflammation.

## **Expression of Transporters responsible for L-arginine uptake:**

### **$y^+$ system of transporters**

Transporters of L-arginine are of particular importance not only as a source of essential amino acids but also as a key substrate for NO production in the vasculature by maintaining vascular tone, endothelial permeability, cell migration and proliferation. Moreover the cellular rate of nitrite production is principally dependent on L-arginine availability (Beasley *et al.*, 1991; Bogle *et al.*, 1992a; Iyengar *et al.*, 1987; Wileman *et al.*, 1995). Thus the fact that proinflammatory mediators also enhance L-arginine transport makes these carrier proteins potential targets for regulating induced NO synthesis.

To identify the carrier(s) responsible for substrate supply to iNOS it is important to examine the profile of expression of these proteins in different cell systems and this was examined in the RASMCs and J774 macrophages used in this thesis. In general, L-arginine transportation is mediated by a class of amino acid transporters largely characterized by their substrate specificity, relative affinity and ion dependency (Deves *et al.*, 1998b). To identify which may be expressed in the two cell systems, q-PCR gene expression analysis using the geNorm approach was carried out on total RNA isolated from each cell type. The data obtained has revealed, for the first time, the expression of transcript for all the sodium-independent transporters, (namely  $y^+$ ,  $y^+L$  and  $b^{0+}$ ) in both RASMCs and J774 macrophages. These observations are interesting because these carriers are thought to be selectively expressed in specific tissues. For instance, CAT-1 is ubiquitously expressed except in liver, and mediate high affinity ( $K_m$ : 0.1-0.2 mM) transport of L-arginine under normal physiological conditions (Kim *et al.*, 1991; Wang *et al.*, 1991). In contrast, CAT2A is thought to be more restricted in its expression and present predominantly in liver where it mediates low ( $K_m$ : 2.1-5.2 mM) affinity uptake of L-arginine (Closs *et al.*, 1993a; Kavanaugh *et al.*, 1994b) Because of this, CAT2A was thought to function only adequately at high

extracellular substrate concentrations and has led to the suggestion that it may not contribute significantly to L-arginine uptake into cells under normal physiological conditions. The present findings from this thesis however showed that this transporter is indeed expressed albeit at low mRNA level.

We are not able at present to establish whether the expressions of any of these transporters or indeed the increases observed reflect changes in functional activity of the respective proteins. It is therefore not clear from these studies as to what the significance is of the expression of any of the transporters identified. There is presently very little published literature on the regulation of the  $y^+$ LATs or  $b^{0,+}$  by inflammatory mediators and this is the first study to show their regulation by IFN- $\gamma$  and/or LPS. Further studies looking at the expression of each protein both at the transcript and protein levels and correlating with changes in iNOS activity are required. In the interim, it is worth noting that some of the findings support previous publications which have demonstrated enhanced CAT2B expressions in macrophages (Chen *et al.*, 2006; Hammermann *et al.*, 2000; Liu *et al.*, 2006), lung fibrosis (Niese *et al.*, 2010; Rothenberg *et al.*, 2006) and inflammatory induced endothelial cells (Visigalli *et al.*, 2010). The implication is that upregulation of this transporter under inflammatory conditions may facilitate enhanced substrate supply for sustained NO production in inflammation. This however needs further examination for the hypothesis to be substantiated unequivocally.

## **CONCLUSION**

Understanding the signaling pathways, as well as the molecular mechanism regulating iNOS expression is very important if novel therapeutic strategies are to be developed to modulate the excess production of NO and its deleterious consequences in disease states. Strides towards achieving this have been taken by many laboratories including ours where the focus has been to identify the key signalling mechanisms that mediate the induction by inflammatory mediators of both iNOS and L-arginine transport in cultured vascular cells and macrophages. In previous studies, the group's work has focused on the MAP kinases and has established a role of the p38 but not the p42/44 MAPKs in these processes (Baydoun et al., 1999). In this thesis the focus has been on the JAK/STAT pathway largely because of the lack of clarity in the role of the latter in the induction of iNOS. As already discussed earlier, there is conflicting data about the role of the JAKs in iNOS expression in different cell systems. This is highlighted by the fact that in previous studies in our group, they could not establish a critical role for JAK2 in the initiation of iNOS expression by LPS and IFN- $\gamma$  in smooth muscle cells (unpublished observations). As already mentioned this contrasts with other published literature and is puzzling since IFN- $\gamma$  is widely known to signal through JAKs.

The reasons for the discrepancies highlighted above are unclear but may simply reflect differences in cell systems or species. A clear approach using both molecular and pharmacological interventions was needed to unequivocally establish whether activation of the JAK/STAT pathway is indeed relevant for cells to express iNOS. Thus in this thesis a strategic approach was taken using two known pharmacological inhibitors of the JAKs as well as developing an siRNA protocol for knocking down JAK2. These two approaches together have helped confirm the group's preliminary findings and established clearly that activation of JAK2 is not a critical signaling protein for iNOS and indeed L-arginine transport. The studies were carried out in smooth muscle cells and in J774 macrophages. The rationale for working with these cell types is because smooth muscle cells have been reported to be the predominant cells within the vasculature that

express iNOS in inflammatory conditions such as septic shock (Liu *et al.*, 1997) and macrophages play a major role in host defense through production of NO (Kolyada *et al.*, 1996).

The results in this thesis have confirmed the effective and sustained induction of iNOS and L-arginine transport in RASMCs using a combination of LPS and IFN- $\gamma$  and in J774 macrophages, using LPS alone. These observations are consistent with the group's previous studies (Baydoun *et al.*, 1998; Baydoun *et al.*, 1993a) and demonstrates cell specific difference in their stimuli requirement for optimum iNOS induction and activity. RASMCs required both LPS and IFN- $\gamma$  exposure while J774 macrophages required LPS alone in order to induce iNOS protein expression, NO production and L-arginine transport. This induction pattern is consistent with the concept of cell type dependent specificity (Gao *et al.*, 1997; Kolyada *et al.*, 1996; Marrero *et al.*, 1998). Current molecular evidence from other studies suggests that IFN- $\gamma$  primes the induction of iNOS expression by stabilizing and thus prolonging the half-life of iNOS mRNA expression (Ozaki *et al.*, 2010). This may not be required in macrophages and as such LPS alone is sufficient to induce sustained expression of iNOS.

The induction of iNOS in both our cell systems was regulated differentially by the two JAK inhibitors used: JAK inhibitor I, a non specific tyrosine kinase inhibitor and the specific JAK2 inhibitor, AG490. Our results demonstrated significant reduction in iNOS protein expression, NO production and L-arginine transport with JAK inhibitor I but not with AG490 in both RASMCs and J774 macrophages. The inhibitions in the smooth muscle cells although dose dependent, were only partial suggesting that other pathways independent of that inhibited by JAK inhibitor I may also be involved. In addition these results suggest that the inducible L-arginine-NO pathway is induced by a complex network of more than one signaling transduction mechanisms. In contrast, in J774 macrophages the reductions following pre-treatment with JAK inhibitor I were much nearer to basal

levels in comparisons with that in RASMCs, suggesting that in these cells a JAK inhibitor I pathway may be exclusive for the induction of iNOS.

Since JAK inhibitor I is a known inhibitor of the JAKs, it is tempting to conclude from the data obtained that a JAK is involved in the actions of IFN- $\gamma$  and/or LPS in inducing both RASMCs and J774 macrophages. However, the consistent lack of effect demonstrated with AG490 would argue against a role for JAK2, the key JAK implicated by others as already explained. One hypothesis considered for the lack of action of AG490 is the possible lack of expression and/ or phosphorylation of JAK2 and TYK2 in RASMCs and J774 macrophages in response to IFN- $\gamma$  and/or LPS. We therefore next examined the expression of these two proteins and further examined whether these were phosphorylated following exposure of RASMCs to LPS and IFN- $\gamma$  or J774 macrophages to LPS alone. The data showed conclusively that both cell types expressed these JAKs albeit at different intensities in control cells. In the follow up study we could not demonstrate that either JAK2 or TYK2 was phosphorylated following induction of cells. These results suggest these JAKs were constitutively expressed in the respective cell types examined but not activated/phosphorylated. The reason for this unexpected finding is unclear but gives an insight, at least to why AG490 was without effect.

To have further evidence in eliminating JAK2 as a potential regulator of the expression of iNOS, studies were carried out using siRNA targeting knockdown of JAK2 in RASMCs. These studies unequivocally established that JAK2 was not required since siRNA mediated knockdown of this protein failed to significantly change iNOS expression or function. Although similar studies were not carried out in the J774 macrophages because of difficulties in transfecting these cells, it would not be unreasonable to speculate that the same may apply because of the lack of effects with AG490. This however will need to be confirmed in similar studies to those carried out in the RASMCs once suitable transfection strategies can be developed for macrophages.

Other than JAK2, there are three other proteins which are part of the JAK family and any one of these could potentially mediate the effects of the interferons. However as already argued in Chapter 3, a case could be made to eliminate JAK1, JAK3 and Tyk2. The argument given is that JAK3 is also susceptible to inhibition by AG490 which was without effect in our studies and JAK1 appears to be irrelevant for IFN- $\gamma$  signalling. TYK2 on the other hand appears to mediate IFN- $\alpha/\beta$  rather than IFN- $\gamma$  signalling (Karaghiosoff *et al.*, 2000). Thus, if none of the JAKs are involved, the question raised is what could be the target for JAK inhibitor I and are any other components of the JAK pathway such as the STATs involved? To answer these questions, the studies carried out were extended to investigate (i) the role of upstream signalling GTPases and (ii) whether STAT-1 was indeed activated through phosphorylation following exposure of cells to pro-inflammatory mediators. The latter study is critical because STAT-1 can be activated downstream of the JAKs but more importantly, in the context of our initial findings, can also be activated directly by GTPases and independently of the JAKs (Pelletier *et al.*, 2003). Such a mechanism could explain the JAK-independent induction of iNOS and L-arginine transport.

Western blotting initially carried out to detect STAT-1 expression and its activation revealed that this protein was indeed expressed in the cells and could be phosphorylated when cells were stimulated with their respective inducers. Interestingly, parallel studies carried out established that the expression of phospho-STAT-1 could be blocked by JAK inhibitor I but not by AG490 in both RASMCs and J774 macrophages. Thus the actions of JAK inhibitor I may be mediated via inhibition of STAT-1 activation which may involve inhibition of upstream signaling molecules independent of JAKs. At present the precise upstream targets for the JAK-independent activation of STAT-1 or indeed for JAK inhibitor I are not known and would require further studies in future to be able to determine what these are.

In terms of earlier signaling events that may feed through STAT-1 to induce the iNOS pathway the GTPases stand out as potential targets. The roles of these molecules were explored using atorvastatin, a 3 hydroxy 3-methylglutaryl CoA (HMG-CoA) reductase inhibitor. Statins reduce the geranylgeranylation and farnesylation of small GTPases, particularly the Rho and Ras proteins (Xiao *et al.*). These actions lead to down-regulation of their activities which has direct pleiotropic cellular actions, restricting or abrogating isoprenylation and thus modulation of events further downstream (Liao *et al.*, 2005; Mason, 2003). Parallel studies were also carried out using Y-27632, a prenyltransferase inhibitor which specifically inhibits Rho activity (Uehata *et al.*, 1997). These studies were initially conducted to determine whether STAT-1 phosphorylation was mediated through the GTPases independent of the JAKs. However, because of time constraints the experiments eventually carried out were restricted to establishing the effects of GTPase inhibitors on iNOS expression, NO production and L-arginine transport. The results obtained demonstrated that all three parameters were regulated by inhibitors of GTPases/Rho. In each case what was interesting was the observation that incubating cells with either Y-27632 or atorvastatin enhanced IFN- $\gamma$  and/or LPS induced effects. These observations suggest that GTPases/Rho may suppress the induction of the inducible L-arginine-NO pathway and their inhibition enhances the expression and/or function of the latter. This would however question whether GTPases in fact feed through STAT-1. Indeed western blots showed clearly that STAT-1 was phosphorylated by IFN- $\gamma$  and/or LPS which coincides with the induction of the inducible L-arginine-NO pathway. Moreover, treatment of cells with JAK inhibitor I blocked STAT-1 phosphorylation and subsequent expression of iNOS, NO production or enhanced L-arginine transport. Thus, if STAT-1 plays a role in our cell system, this would be to induce the L-arginine-NO pathway. Because the GTPases appear to suppress this process, it is unlikely that they do so by activating STAT-1. Of course they may inhibit the latter but this was not what we had hypothesized and would not be in line with other published literature. This is however an interesting point which will need further investigation in future studies.

In the case of atorvastatin, we cannot rule out that this compound may have other effects which directly affect the function of the induced proteins. This may be particularly true for iNOS since treatment of cells with the statin enhanced nitrite production without altering iNOS protein levels. Thus, in this case it is likely that atorvastatin regulated the function rather than the expression of iNOS. Atorvastatin is also known to have anti-oxidant properties and as a result could alternatively have had direct effects on the NO produced, thus preventing its interaction with superoxide radicals. In doing so, atorvastatin may be able to enhance the amount of nitrite detected even though there was no change in the levels of iNOS expressed. Further studies may however be required to fully understand the underlying mechanism(s) of action of atorvastatin under our experimental conditions.

Because of the critical role of L-arginine transporters may play in sustaining substrate supply to iNOS, some time was dedicated in this thesis to examine in more detail the intrinsic differences between the different transporters for L-arginine in both control and under cytokine mediated inflammatory conditions. As previously stated, transport of L-arginine into cells is mediated by several classes of CATs, characterized on the basis of ion dependency, substrate specificity and relative affinity (Deves *et al.*, 1998b). To address any subtle changes in the expression profiles in both cell types we used q-PCR, the most sensitive technique for gene expression. However, along with its sensitivity and wide dynamic range is the risk of data misinterpretation. This may result from inadequate sample preparation, inefficiencies in RNA extraction and RT procedures as well as amount and quality of RNA material. Other more intrinsic factors include poor primer design and inappropriate HKG selection. HKGs are used to normalize qPCRs in order to reduce possible sources of errors generated during the quantification of gene expression. The current MIQE guidelines (Bustin *et al.*, 2010; Bustin *et al.*, 2009) in addition to other independent

publications (Becker *et al.*, 2010; Taylor *et al.*, 2010) have been of enormous assistance to scientist.

Among the different normalisation strategies reported (Huggett *et al.*, 2005; Vandesompele *et al.*, 2002) we chose in this thesis the geNORM approach. Our results have identified RPL13A and UBC as the most stable HKGs in J774 macrophages with both having geNorm (M) stability values of 0.026. In RASMCs however both CYC and RPL13A were the most stable HKGs, both with slightly higher geNorm (M) stability values of 0.152. Thus even among different cell types, there are variations in the HKGs inspite of having the same experimental conditions. The most stable HKG across the cell types examined in this thesis is RPL13A.

We have also demonstrated that the  $y^+$  system of cationic amino acid transporters are constitutively expressed in both J774 macrophages and RASMCs. In addition in both LPS mediated activated J774 macrophages and LPS and IFN- $\gamma$  mediated activated RASMCs, the high affinity CAT2B mRNA expression was significantly enhanced. Up-regulation of CAT2B mRNA expressions in J774 macrophages was significantly much higher in comparison to that in RASMCs following activation. CAT2A mRNA expression are however down-regulated in J774 macrophages in contrast to its up-regulation in RASMCs which may demonstrate contrasting roles of transporters in substrate supply to iNOS. How variation in mRNA expression correlates with functional activity however remains to be established but only when suitable antibodies for each transporter becomes commercially available. At present we are unable to ascertain or determine whether the increased mRNA levels translate to increased protein levels.

Apart from the system  $y^+$  transporters other experiments examined expression of the  $y^+L$  and  $b^{0+}$  systems. As with the  $y^+$  carriers the results from q-PCR analysis

showed changes in both  $y^+L$  and  $b^{0+}$  expressions. The significance of these changes or indeed the expression profiles established will need further investigation if we are to determine the relevance of each carrier or system of carriers for substrate supply to iNOS for sustained NO synthesis. In the interim, it is important to appreciate that both vascular smooth muscle cells and macrophages express multiple transporter systems for L-arginine and each may be capable of supplying this amino acid into cells, thereby supporting NO synthesis. Moreover, these transporters can be upregulated and via signaling mechanisms which may overlap with those required for the induction of iNOS.

In conclusion, a series of detailed studies have been carried out as part of the programme of work for this thesis which has confirmed that the induction of iNOS and L-arginine transport occur in parallel in both smooth muscle cells and in macrophages. The induction of these processes appears to be independent of the JAKs but dependent on the phosphorylation of STAT-1, a potential downstream target for activation by JAKS. However, in our cell systems, it would appear that STAT-1 activation may occur independently of the JAKs. At present we have not been able to conclusively determine the upstream activator of STAT-1 but have established that its phosphorylation may be critical for the expression of the inducible L-arginine-NO pathway. In achieving this we have also demonstrated or at least given an indication that the so called selective JAK inhibitor, Jak inhibitor I, may have actions independent of inhibition of the JAKs. In addition, we have demonstrated that potential GTPase inhibitors, including the widely used atorvastatin may enhance NO synthesis and this could have implications in certain pathologies where it may be beneficial or harmful.

Although these findings and conclusions are supported by the data, it has to be acknowledged that power calculations were not carried out for the studies conducted and as such it may be possible that these were underpowered. Each study was however carried out in at least three independent experiments and in some cases with 6 replicates in each. Although the validity of the statistical tests

for underpowered studies may be limited, there is confidence that the trends obtained are indeed reproducible and consistent with both our previous work and with those of many other studies. Thus, the conclusions reached from the findings in this thesis would still be considered valid and indicative of the critical cellular events that regulate the induction, expression and function of the inducible L-arginine-NO pathways in the cell systems investigated. These pathways could be targeted in future therapeutic strategies to regulate iNOS expression and function and potentially the induction of L-arginine transport. Coupled to this, strategies could also be developed, targeting the LPS and/or cytokine receptors associated with the induction of these processes. Although there is some skepticism about the clinical efficacy of therapies targeting cytokines, there is emerging evidence that blockade of TNF- $\alpha$  is beneficial in a number of diseases including Rheumatoid Arthritis (Camussi *et al.*, 1998; Maini *et al.*, 1995; Reimold, 2003), ankylosing spondylitis (Braun *et al.*, 2002; Mathieu *et al.*, 2010), psoriasis (Tobin *et al.*, 2005; Woolacott *et al.*, 2006), and inflammatory bowel disease (Milia *et al.*, 2009; Perrier *et al.*, 2011). Furthermore, there is growing optimism that blockade of other cytokines such as IL-13, IL-9 or IL-4/13 receptors may be beneficial in asthmatics. These findings are beginning to set the trend for targeted cytokine/cytokine receptor therapy in disease treatment and it is likely that this can be extended to diseases associated with the induction of iNOS.

It however remains to be determined if targeting iNOS receptors as a therapeutic strategy is useful in the long term management of inflammation and sepsis in patients. This view is taken given the fact that iNOS induced nitrite production also serves a specific function in host defence against microbial infection and tumours. In addition, given the multiple and complex signalling cross-talk associated with iNOS induction, further investigations will be required and therapeutic strategy astutely devised and diligently evaluated in order to achieve a better outcome of disease.

## **FUTURE WORK**

The studies carried out in the thesis have generated data which has helped in shedding some light on the regulation of expression of the inducible L-arginine-NO pathway but at the same time raised some questions which will need addressing. Thus in developing this project in future the following is proposed:

The siRNA studies have demonstrated clearly that JAK2 may not be required for the induction of expression of the inducible L-arginine-NO pathway. Similar studies targeting TYK2 are now required to conclusively establish its role in this process.

In parallel with the above, additional studies using TYK2 specific pharmacological inhibitors could be used when these become commercially available. Such compounds could be used to investigate changes in iNOS expression, NO production, L-arginine transport and STAT-1 phosphorylation in both RASMCs and J774 macrophages.

Studies establishing whether atorvastatin or Y-27632 regulate GTPases and thus STAT-1 phosphorylation are also needed to confirm whether there is a direct link between these two targets. These studies could examine changes in STAT-1 phosphorylation by western blotting in both RASMCs and J774 macrophages treated with either atorvastatin or Y-27632.

The potentiation of nitrite levels by atorvastatin without any significant change in iNOS expression would suggest effects of the drug at the functional level or indeed through a direct antioxidant action on the NO generated. Studies are therefore needed to establish whether the atorvastatin effects are mediated through its antioxidant properties. These could include determining levels of reactive oxygen species (ROS) produced under each experimental condition and establishing whether ROS generation is altered by atorvastatin and whether this

correlates with changes in nitrite levels. Because of time limitations it was not possible to establish whether the increases in transport of L-arginine in both cell models following pre-treatment with atorvastatin were associated with changes in CAT transporter gene expression. These studies remain critical.

Since Y-27632 has been shown to enhance nitrite levels, experiments confirming whether this compound also alters iNOS expression are required. This is important since atorvastatin which produced similar effects on nitrite did not appear to alter levels of the enzyme. Though our result profile of CAT mRNA transporter expression in this thesis has also confirmed previous reports, the present lack of available antibodies for the respective transporters examined make it difficult to reconcile the changes in mRNA expression to protein expression and to functional activity. Further work will be required to address this when antibodies become available for these transporters. In addition, the implication of an enhanced CAT2B expression is up-regulation of this transporter under inflammatory conditions. This may facilitate enhanced substrate supply for sustained NO production in inflammation. This however needs further examination for the hypothesis to be substantiated unequivocally.

## REFERENCES

- Aaronson, DS, Horvath, CM (2002) A road map for those who don't know JAK-STAT. *Science (New York, N.Y)* **296**(5573): 1653-1655.
- Abramson, SB, Amin, AR, Clancy, RM, Attur, M (2001) The role of nitric oxide in tissue destruction. *Best Pract Res Clin Rheumatol* **15**(5): 831-845.
- Abu-Soud, HM, Wang, J, Rousseau, DL, Fukuto, JM, Ignarro, LJ, Stuehr, DJ (1995) Neuronal nitric oxide synthase self-inactivates by forming a ferrous-nitrosyl complex during aerobic catalysis. *The Journal of biological chemistry* **270**(39): 22997-23006.
- Adams, MR, McCredie, R, Jessup, W, Robinson, J, Sullivan, D, Celermajer, DS (1997) Oral L-arginine improves endothelium-dependent dilatation and reduces monocyte adhesion to endothelial cells in young men with coronary artery disease. *Atherosclerosis* **129**(2): 261-269.
- Adcock, IM, Shirasaki, H, Gelder, CM, Peters, MJ, Brown, CR, Barnes, PJ (1994) The effects of glucocorticoids on phorbol ester and cytokine stimulated transcription factor activation in human lung. *Life Sci* **55**(14): 1147-1153.
- Akira, S, Takeda, K (2004) Functions of toll-like receptors: lessons from KO mice. *C R Biol* **327**(6): 581-589.
- Albritton, LM, Tseng, L, Scadden, D, Cunningham, JM (1989) A putative murine ecotropic retrovirus receptor gene encodes a multiple membrane-spanning protein and confers susceptibility to virus infection. *Cell* **57**(4): 659-666.
- Alderton, WK, Cooper, CE, Knowles, RG (2001) Nitric oxide synthases: structure, function and inhibition. *The Biochemical journal* **357**(Pt 3): 593-615.
- Alheid, U, Frolich, JC, Forstermann, U (1987) Endothelium-derived relaxing factor from cultured human endothelial cells inhibits aggregation of human platelets. *Thromb Res.* **47**(5): 561-571.
- Allman, KG, Stoddart, AP, Kennedy, MM, Young, JD (1996) L-arginine augments nitric oxide production and mesenteric blood flow in ovine endotoxemia. *The American journal of physiology* **271**(4 Pt 2): H1296-1301.
- Amano, M, Chihara, K, Kimura, K, Fukata, Y, Nakamura, N, Matsuura, Y, Kaibuchi, K (1997) Formation of actin stress fibers and focal adhesions enhanced by Rho-kinase. *Science (New York, N.Y)* **275**(5304): 1308-1311.

Amarzguioui, M, Prydz, H (2004) An algorithm for selection of functional siRNA sequences. *Biochemical and biophysical research communications* **316**(4): 1050-1058.

Amir, S, English, AM (1991) An inhibitor of nitric oxide production, NG-nitro-L-arginine-methyl ester, improves survival in anaphylactic shock. *Eur J Pharmacol.* ;(): **203**(1): 125-127.

Andersen, CL, Jensen, JL, Orntoft, TF (2004) Normalization of real-time quantitative reverse transcription-PCR data: a model-based variance estimation approach to identify genes suited for normalization, applied to bladder and colon cancer data sets. *Cancer Res* **64**(15): 5245-5250.

Anderson, TJ (2003) Nitric Oxide, Atherosclerosis and the Clinical Relevance of Endothelial Dysfunction. *Heart Failure Reviews* **8**: 71-86.

Andoh, Y, Ogura, H, Satoh, M, Shimano, K, Okuno, H, Fujii, S, Ishimori, N, Eshima, K, Tamauchi, H, Otani, T, Nakai, Y, Van Kaer, L, Tsutsui, H, Onoe, K, Iwabuchi, K (2013) Natural killer T cells are required for lipopolysaccharide-mediated enhancement of atherosclerosis in apolipoprotein E-deficient mice. *Immunobiology* **218**(4): 561-569.

Andrew, PJ, Mayer, B (1999) Enzymatic function of nitric oxide synthases. *Cardiovascular Research* **43**(3): 521-531.

Annane, D, Sanquer, S, Sebille, V, Faye, A, Djuranovic, D, Raphael, JC, Gajdos, P, Bellissant, E (2000) Compartmentalised inducible nitric-oxide synthase activity in septic shock. *Lancet* **355**(9210): 1143-1148.

Argetsinger, LS, Campbell, GS, Yang, X, Witthuhn, BA, Silvennoinen, O, Ihle, JN, Carter-Su, C (1993) Identification of JAK2 as a growth hormone receptor-associated tyrosine kinase. *Cell* **74**(2): 237-244.

Arstall, MA, Sawyer, DB, Fukazawa, R, Kelly, RA (1999) Cytokine-mediated apoptosis in cardiac myocytes: the role of inducible nitric oxide synthase induction and peroxynitrite generation. *Circulation research* **85**(9): 829-840.

Asakura, H, Asamura, R, Ontachi, Y, Hayashi, T, Yamazaki, M, Morishita, E, Miyamoto, KI, Nakao, S (2005) Selective inducible nitric oxide synthase inhibition attenuates organ dysfunction and elevated endothelin levels in LPS-induced DIC model rats. *J Thromb Haemost* **3**(5): 1050-1055.

Aulak, KS, Liu, J, Wu, J, Hyatt, SL, Puppi, M, Henning, SJ, Hatzoglou, M (1996) Molecular sites of regulation of expression of the rat cationic amino acid transporter gene. *J Biol Chem* **271**(47): 29799-29806.

Axelsen, PH, Komatsu, H, Murray, IV (2011) Oxidative stress and cell membranes in the pathogenesis of Alzheimer's disease. *Physiology (Bethesda)* **26**(1): 54-69.

Bach, EA, Aguet, M, Schreiber, RD (1997) The IFN gamma receptor: a paradigm for cytokine receptor signaling. *Annual review of immunology* **15**: 563-591.

Bai, Y, Sanderson, MJ (2006) Modulation of the Ca<sup>2+</sup> sensitivity of airway smooth muscle cells in murine lung slices. *Am J Physiol Lung Cell Mol Physiol* **291**(2): L208-221.

Barbul, A (1986) Arginine: biochemistry, physiology, and therapeutic implications. *JPEN J Parenter Enteral Nutr* **10**(2): 227-238.

Baydoun, A, Morgan, D (1998) Inhibition of ornithine decarboxylase potentiates nitric oxide production in LPS-activated J774 cells. *British journal of pharmacology* **125**(7): 1511-1516.

Baydoun, AR, Bogle, RG, Pearson, JD, Mann, GE (1993a) Arginine uptake and metabolism in cultured murine macrophages. *Agents and actions* **38 Spec No**: C127-129.

Baydoun, AR, Bogle, RG, Pearson, JD, Mann, GE (1994a) Discrimination between citrulline and arginine transport in activated murine macrophages: inefficient synthesis of NO from recycling of citrulline to arginine. *British journal of pharmacology* **112**(2): 487-492.

Baydoun, AR, Emery, PW, Pearson, JD, Mann, GE (1990) Substrate-dependent regulation of intracellular amino acid concentrations in cultured bovine aortic endothelial cells. *Biochemical and biophysical research communications* **173**(3): 940-948.

Baydoun, AR, Foale, RD, Mann, GE (1993b) Bacterial endotoxin rapidly stimulates prolonged endothelium-dependent vasodilatation in the rat isolated perfused heart. *British journal of pharmacology* **109**(4): 987-991.

Baydoun, AR, Mann, GE (1994b) Selective targeting of nitric oxide synthase inhibitors to system  $\gamma^+$  in activated macrophages. *Biochemical and biophysical research communications* **200**(2): 726-731.

Baydoun, AR, Wileman, SM, Wheeler-Jones, CP, Marber, MS, Mann, GE, Pearson, JD, Closs, EI (1999) Transmembrane signalling mechanisms regulating expression of cationic amino acid transporters and inducible nitric oxide synthase in rat vascular smooth muscle cells. *The Biochemical journal* **344 Pt 1**: 265-272.

Beasley, D, Schwartz, JH, Brenner, BM (1991) Interleukin 1 induces prolonged L-arginine-dependent cyclic guanosine monophosphate and nitrite production in rat vascular smooth muscle cells. *J Clin Invest.* **87**(2): 602–608.

Beck, KF, Eberhardt, W, Walpen, S, Apel, M, Pfeilschifter, J (1998) Potentiation of nitric oxide synthase expression by superoxide in interleukin 1 beta-stimulated rat mesangial cells. *FEBS letters* **435**(1): 35-38.

Becker, C, Hammerle-Fickinger, A, Riedmaier, I, Pfaffl, MW (2010) mRNA and microRNA quality control for RT-qPCR analysis. *Methods* **50**(4): 237-243.

Beckman, JS (1991) The double-edged role of nitric oxide in brain function and superoxide-mediated injury. *J Dev Physiol.* **15**(1): 53-59.

Beckman, JS, Beckman, TW, Chen, J, Marshall, PA, Freeman, BA (1990) Apparent hydroxyl radical production by peroxynitrite: implications for endothelial injury from nitric oxide and superoxide. *Proceedings of the National Academy of Sciences of the United States of America* **87**(4): 1620-1624.

Behr-Roussel, D, Rupin, A, Simonet, S, Bonhomme, E, Coumailleau, S, Cordi, A, Serkiz, B, Fabiani, JN, Verbeuren, TJ (2000) Effect of chronic treatment with the inducible nitric oxide synthase inhibitor N-iminoethyl-L-lysine or with L-arginine on progression of coronary and aortic atherosclerosis in hypercholesterolemic rabbits. *Circulation* **102**(9): 1033-1038.

Bellmann, K, Burkart, V, Bruckhoff, J, Kolb, H, Landry, J (2000) p38-dependent enhancement of cytokine-induced nitric-oxide synthase gene expression by heat shock protein 70. *Journal of Biological Chemistry* **275**(24): 18172-18179.

Benjamin, N, Dutton, JA, Ritter, JM (1991) Human vascular smooth muscle cells inhibit platelet aggregation when incubated with glyceryl trinitrate: evidence for generation of nitric oxide. *Br J Pharmacol.* **102**(4): 847-850.

Benjamin, N, Vallance, P (1994) Plasma nitrite as a marker of nitric oxide production. *Lancet* **344**(8927): 960.

Bertran, J, Magagnin, S, Werner, A, Markovich, D, Biber, J, Testar, X, Zorzano, A, Kuhn, LC, Palacin, M, Murer, H (1992a) Stimulation of system y(+)-like amino acid transport by the heavy chain of human 4F2 surface antigen in *Xenopus laevis* oocytes. *Proceedings of the National Academy of Sciences of the United States of America* **89**(12): 5606-5610.

Bertran, J, Werner, A, Moore, ML, Stange, G, Markovich, D, Biber, J, Testar, X, Zorzano, A, Palacin, M, Murer, H (1992b) Expression cloning of a cDNA from rabbit kidney cortex that induces a single transport system for cystine and dibasic

and neutral amino acids. *Proceedings of the National Academy of Sciences of the United States of America* **89**(12): 5601-5605.

Bhat, GJ, Thekkumkara, TJ, Thomas, WG, Conrad, KM, Baker, KM (1994) Angiotensin II stimulates sis-inducing factor-like DNA binding activity. Evidence that the AT1A receptor activates transcription factor-Stat91 and/or a related protein. *The Journal of biological chemistry* **269**(50): 31443-31449.

Bhat, NR, Zhang, P, Bhat, AN (1999) Cytokine induction of inducible nitric oxide synthase in an oligodendrocyte cell line: role of p38 mitogen-activated protein kinase activation. *J Neurochem* **72**(2): 472-478.

Bhat, NR, Zhang, P, Lee, JC, Hogan, EL (1998) Extracellular signal-regulated kinase and p38 subgroups of mitogen-activated protein kinases regulate inducible nitric oxide synthase and tumor necrosis factor-alpha gene expression in endotoxin-stimulated primary glial cultures. *J Neurosci* **18**(5): 1633-1641.

Bhatt, KH, Pandey, RK, Dahiya, Y, Sodhi, A (2010) Protein kinase Cdelta and protein tyrosine kinase regulate peptidoglycan-induced nuclear factor-kappaB activation and inducible nitric oxide synthase expression in mouse peritoneal macrophages in vitro. *Mol Immunol* **47**(4): 861-870.

Blake, GJ, Ridker, PM (2002) Inflammatory bio-markers and cardiovascular risk prediction. *J Intern Med* **252**(4): 283-294.

Blanchette, J, Jaramillo, M, Olivier, M (2003a) Signalling events involved in interferon-gamma-inducible macrophage nitric oxide generation. *Immunology* **108**(4): 513-522.

Blanchette, J, Jaramillo, M, Olivier, M (2003b) Signalling events involved in interferon-gamma-inducible macrophage nitric oxide generation. *Immunology* **108**(4): 513-522.

Bode-Boger, SM, Scalera, F, Ignarro, LJ (2007) The L-arginine paradox: Importance of the L-arginine/asymmetrical dimethylarginine ratio. *Pharmacol Ther* **114**(3): 295-306.

Boehm, U, Klamp, T, Groot, M, Howard, JC (1997) Cellular responses to interferon-gamma. *Annual review of immunology* **15**: 749-795.

Bogle, RG, Baydoun, AR, Pearson, JD, Moncada, S, Mann, GE (1992a) L-Arginine Transport Is Increased in Macrophages Generating Nitric-Oxide. *Biochemical Journal* **284**: 15-18.

Bogle, RG, Baydoun, AR, Pearson, JD, Moncada, S, Mann, GE (1992b) L-arginine transport is increased in macrophages generating nitric oxide. *The Biochemical journal* **284 ( Pt 1)**: 15-18.

Boguski, MS, McCormick, F (1993) Proteins regulating Ras and its relatives. *Nature* **366(6456)**: 643-654.

Bohme, GA, Bon, C, Stutzmann, JM, Doble, A, Blanchard, JC (1991) Possible involvement of nitric oxide in long-term potentiation. *Eur J Pharmacol.* **199(3)**: 379-381.

Boissel, JP, Schwarz, PM, Forstermann, U (1998) Neuronal-type NO synthase: transcript diversity and expressional regulation. *Nitric Oxide* **2(5)**: 337-349.

Bolanos, JP, Almeida, A, Stewart, V, Peuchen, S, Land, JM, Clark, JB, Heales, SJ (1997) Nitric oxide-mediated mitochondrial damage in the brain: mechanisms and implications for neurodegenerative diseases. *J Neurochem* **68(6)**: 2227-2240.

Bowman, A, Gillespie, JS, Soares-da-Silva, P (1986) A comparison of the action of the endothelium-derived relaxant factor and the inhibitory factor from the bovine retractor penis on rabbit aortic smooth muscle. *Br J Pharmacol.* **87(1)**: 175-181.

Braun, J, Sieper, J, Breban, M, Collantes-Estevez, E, Davis, J, Inman, R, Marzo-Ortega, H, Mielants, H (2002) Anti-tumour necrosis factor alpha therapy for ankylosing spondylitis: international experience. *Ann Rheum Dis* **61 Suppl 3**: iii51-60.

Bredt, DS, Ferris, CD, Snyder, SH (1992) Nitric-Oxide Synthase Regulatory Sites - Phosphorylation by Cyclic Amp-Dependent Protein-Kinase, Protein-Kinase-C, and Calcium Calmodulin Protein-Kinase - Identification of Flavin and Calmodulin Binding-Sites. *Journal of Biological Chemistry* **267(16)**: 10976-10981.

Bredt, DS, Hwang, PM, Glatt, CE, Lowenstein, C, Reed, RR, Snyder, SH (1991) Cloned and expressed nitric oxide synthase structurally resembles cytochrome P-450 reductase. *Nature.* **351(6329)**: 714-718.

Bredt, DS, Snyder, SH (1989) Nitric oxide mediates glutamate-linked enhancement of cGMP levels in the cerebellum. *Proc Natl Acad Sci U S A.* **86(22)**: 9030-9033.

Breslow, MJ, Tobin, JR, Bredt, DS, Ferris, CD, Snyder, SH, Traystman, RJ (1992) Role of nitric oxide in adrenal medullary vasodilation during catecholamine secretion. *Eur J Pharmacol.* **210(1)**: 105-106.

Briscoe, J, Rogers, NC, Witthuhn, BA, Watling, D, Harpur, AG, Wilks, AF, Stark, GR, Ihle, JN, Kerr, IM (1996) Kinase-negative mutants of JAK1 can sustain interferon-gamma-inducible gene expression but not an antiviral state. *EMBO J* **15**(4): 799-809.

Bromberg, J, Darnell, JE, Jr. (2000) The role of STATs in transcriptional control and their impact on cellular function. *Oncogene* **19**(21): 2468-2473.

Bromberg, JF, Horvath, CM, Wen, Z, Schreiber, RD, Darnell, JE, Jr. (1996) Transcriptionally active Stat1 is required for the antiproliferative effects of both interferon alpha and interferon gamma. *Proceedings of the National Academy of Sciences of the United States of America* **93**(15): 7673-7678.

Brooks, SB, Lewis, MJ, Dickerson, RR (1993) Nitric-Oxide Emissions from the High-Temperature Viscous Boundary-Layers of Hypersonic Aircraft within the Stratosphere. *J. Geophys. Res.-Atmos.* **98**(D9): 16755-16760.

Budzinski, M, Misterek, K, Gumulka, W, Dorociak, A (2000) Inhibition of inducible nitric oxide synthase in persistent pain. *Life Sci* **66**(4): 301-305.

Buga, GM, Griscavage, JM, Rogers, NE, Ignarro, LJ (1993) Negative feedback regulation of endothelial cell function by nitric oxide. *Circulation research* **73**(5): 808-812.

Bult, H, Boeckstaens, GE, Pelckmans, PA, Jordaens, FH, Van Maercke, YM, Herman, AG (1990) Nitric oxide as an inhibitory non-adrenergic non-cholinergic neurotransmitter. *Nature*. **345**(6273): 346-347.

Bultinck, J, Sips, P, Vakaet, L, Brouckaert, P, Cauwels, A (2006) Systemic NO production during (septic) shock depends on parenchymal and not on hematopoietic cells: in vivo iNOS expression pattern in (septic) shock. *FASEB J* **20**(13): 2363-2365.

Busse, R, Mulsch, A (1990) Calcium-dependent nitric oxide synthesis in endothelial cytosol is mediated by calmodulin. *FEBS Lett* **265**(1-2): 133-136.

Bustin, SA (2000) Absolute quantification of mRNA using real-time reverse transcription polymerase chain reaction assays. *J Mol Endocrinol* **25**(2): 169-193.

Bustin, SA (2002) Quantification of mRNA using real-time reverse transcription PCR (RT-PCR): trends and problems. *J Mol Endocrinol* **29**(1): 23-39.

Bustin, SA, Beaulieu, JF, Huggett, J, Jaggi, R, Kibenge, FS, Olsvik, PA, Penning, LC, Toegel, S (2010) MIQE precis: Practical implementation of minimum standard guidelines for fluorescence-based quantitative real-time PCR experiments. *BMC Mol Biol* **11**: 74.

Bustin, SA, Benes, V, Garson, J, Hellemans, J, Huggett, J, Kubista, M, Mueller, R, Nolan, T, Pfaffl, MW, Shipley, G, Wittwer, CT, Schjerling, P, Day, PJ, Abreu, M, Aguado, B, Beaulieu, JF, Beckers, A, Bogaert, S, Browne, JA, Carrasco-Ramiro, F, Ceelen, L, Ciborowski, K, Cornillie, P, Coulon, S, Cuypers, A, De Brouwer, S, De Ceuninck, L, De Craene, J, De Naeyer, H, De Spiegelaere, W, Deckers, K, Dheedene, A, Durinck, K, Ferreira-Teixeira, M, Fieuw, A, Gallup, JM, Gonzalo-Flores, S, Goossens, K, Heindryckx, F, Herring, E, Hoenicka, H, Icardi, L, Jaggi, R, Javad, F, Karampelias, M, Kibenge, F, Kibenge, M, Kumps, C, Lambertz, I, Lammens, T, Markey, A, Messiaen, P, Mets, E, Morais, S, Mudarra-Rubio, A, Nakiwala, J, Nelis, H, Olsvik, PA, Perez-Novo, C, Plusquin, M, Remans, T, Rihani, A, Rodrigues-Santos, P, Rondou, P, Sanders, R, Schmidt-Bleek, K, Skovgaard, K, Smeets, K, Tabera, L, Toegel, S, Van Acker, T, Van den Broeck, W, Van der Meulen, J, Van Gele, M, Van Peer, G, Van Poucke, M, Van Roy, N, Vergult, S, Wauman, J, Tshuikina-Wiklander, M, Willems, E, Zaccara, S, Zeka, F, Vandesompele, J (2013) The need for transparency and good practices in the qPCR literature. *Nat Methods* **10**(11): 1063-1067.

Bustin, SA, Benes, V, Garson, JA, Hellemans, J, Huggett, J, Kubista, M, Mueller, R, Nolan, T, Pfaffl, MW, Shipley, GL, Vandesompele, J, Wittwer, CT (2009) The MIQE guidelines: minimum information for publication of quantitative real-time PCR experiments. *Clin Chem* **55**(4): 611-622.

Bustin, SA, Nolan, T (2004) Pitfalls of quantitative real-time reverse-transcription polymerase chain reaction. *J Biomol Tech* **15**(3): 155-166.

Butte, AJ, Dzau, VJ, Glueck, SB (2001) Further defining housekeeping, or "maintenance," genes Focus on "A compendium of gene expression in normal human tissues". *Physiol Genomics* **7**(2): 95-96.

Caivano, M (1998) Role of MAP kinase cascades in inducing arginine transporters and nitric oxide synthetase in RAW264 macrophages. *FEBS letters* **429**(3): 249-253.

Camussi, G, Lupia, E (1998) The future role of anti-tumour necrosis factor (TNF) products in the treatment of rheumatoid arthritis. *Drugs* **55**(5): 613-620.

Cao, Y, Gao, Z, Zhu, J, Wang, Q, Huang, Y, Chiu, C, Parker, B, Chu, P, Pant, WP (2008) Impacts of halogen additions on mercury oxidation, in a slipstream selective catalyst reduction (SCR), reactor when burning sub-bituminous coal. *Environ Sci Technol* **42**(1): 256-261.

Carley, AF, Rassias, S, Roberts, MW, Tang-Han, W (1979) Chemisorption of nitric oxide by nickel. *Surface Science* **84**(1).

Carr, GJ, Ferguson, SJ (1990) Nitric oxide formed by nitrite reductase of *Paracoccus denitrificans* is sufficiently stable to inhibit cytochrome oxidase activity and is reduced by its reductase under aerobic conditions. *Biochimica et biophysica acta* **1017**(1): 57-62.

Cauwels, A, Brouckaert, P (2011) Nitrite regulation of shock. *Cardiovascular research* **89**(3): 553-559.

Chan, ED, Morris, KR, Belisle, JT, Hill, P, Remigio, LK, Brennan, PJ, Riches, DW (2001a) Induction of inducible nitric oxide synthase-NO\* by lipoarabinomannan of *Mycobacterium tuberculosis* is mediated by MEK1-ERK, MKK7-JNK, and NF-kappaB signaling pathways. *Infect Immun* **69**(4): 2001-2010.

Chan, ED, Riches, DW (2001b) IFN-gamma + LPS induction of iNOS is modulated by ERK, JNK/SAPK, and p38(mapk) in a mouse macrophage cell line. *Am J Physiol Cell Physiol* **280**(3): C441-450.

Chan, ED, Riches, DW (1998) Potential role of the JNK/SAPK signal transduction pathway in the induction of iNOS by TNF-alpha. *Biochem Biophys Res Commun.* **253**(3): 790-796.

Chan, MM, Mattiacci, JA (2001c) Nitric oxide: actions and roles in arthritis and diabetes. *The Foot* **11**(1): 45-51.

Chang, EJ, Kundu, JK, Liu, L, Shin, JW, Surh, YJ (2011) Ultraviolet B radiation activates NF-kappaB and induces iNOS expression in HR-1 hairless mouse skin: role of IkappaB kinase-beta. *Mol Carcinog* **50**(4): 310-317.

Chen, CC, Lee, JJ, Tsai, PS, Lu, YT, Huang, CL, Huang, CJ (2006) Platonin attenuates LPS-induced CAT-2 and CAT-2B induction in stimulated murine macrophages. *Acta Anaesthesiol Scand* **50**(5): 604-612.

Chen, J, Baig, E, Fish, EN (2004) Diversity and relatedness among the type I interferons. *J Interferon Cytokine Res* **24**(12): 687-698.

Chen, J, Liu, B, Yuan, J, Yang, J, Zhang, J, An, Y, Tie, L, Pan, Y, Li, X (2012) Atorvastatin reduces vascular endothelial growth factor (VEGF) expression in human non-small cell lung carcinomas (NSCLCs) via inhibition of reactive oxygen species (ROS) production. *Mol Oncol* **6**(1): 62-72.

Chen, LC, Pace, JL, Russell, SW, Morrison, DC (1996) Altered regulation of inducible nitric oxide synthase expression in macrophages from senescent mice. *Infection and immunity* **64**(10): 4288-4298.

Chen, SJ, Wu, CC, Yen, MH (1994) Alterations of ex vivo vascular reactivity in intraperitoneal sepsis. *J Cardiovasc Pharmacol* **24**(5): 786-793.

Chin-Dusting, JP, Willems, L, Kaye, DM (2007) L-arginine transporters in cardiovascular disease: a novel therapeutic target. *Pharmacol Ther* **116**(3): 428-436.

Chin, JH, Azhar, S, Hoffman, BB (1992) Inactivation of endothelial derived relaxing factor by oxidized lipoproteins. *The Journal of clinical investigation* **89**(1): 10-18.

Cho, H, Xie, Q, Calaycay, J, Mumford, R, Swiderek, K, Lee, T, Nathan, C (1992) Calmodulin is a subunit of nitric oxide synthase from macrophages. *J. Exp. Med.* **176**(2): 599-604.

Christensen, HN (1990) Role of amino acid transport and countertransport in nutrition and metabolism. *Physiological reviews* **70**(1): 43-77.

Christensen, HN, Antonioli, JA (1969) Cationic Amino Acid Transport in the Rabbit Reticulocyte. Na<sup>+</sup>-dependent inhibition of Na<sup>+</sup>-independent transport. *J. Biol. Chem.* **244**(6): 1497-1504.

Christensen, HN, Handlogten, ME (1968) Modes of Mediated Exodus of Amino Acids from the Ehrlich Ascites Tumor Cell. *J. Biol. Chem.* **243**(20): 5428-5438.

Chu, SC, Marks-Konczalik, J, Wu, HP, Banks, TC, Moss, J (1998a) Analysis of the cytokine-stimulated human inducible nitric oxide synthase (iNOS) gene: characterization of differences between human and mouse iNOS promoters. *Biochem Biophys Res Commun* **248**(3): 871-878.

Chu, SC, Marks-Konczalik, J, Wu, HP, Banks, TC, Moss, J (1998b) Analysis of the cytokine-stimulated human inducible nitric oxide synthase (iNOS) gene: characterization of differences between human and mouse iNOS promoters. *Biochem Biophys Res Commun.* **248**(3): 871-878.

Closs, E, Albritton, L, Kim, J, Cunningham, J (1993a) Identification of a low affinity, high capacity transporter of cationic amino acids in mouse liver. *J. Biol. Chem.* **268**(10): 7538-7544.

Closs, E, Lyons, C, Kelly, C, Cunningham, J (1993b) Characterization of the third member of the MCAT family of cationic amino acid transporters. Identification of a domain that determines the transport properties of the MCAT proteins. *J. Biol. Chem.* **268**(28): 20796-20800.

Closs, EI, Albritton, LM, Kim, JW, Cunningham, JM (1993c) Identification of a low affinity, high capacity transporter of cationic amino acids in mouse liver. *The Journal of biological chemistry* **268**(10): 7538-7544.

Closs, EI, Graf, P, Habermeier, A, Cunningham, JM, Forstermann, U (1997) Human cationic amino acid transporters hCAT-1, hCAT-2A, and hCAT-2B: Three related carriers with distinct transport properties. *Biochemistry* **36**(21): 6462-6468.

Closs, EI, Scheld, JS, Sharafi, M, Forstermann, U (2000) Substrate supply for nitric-oxide synthase in macrophages and endothelial cells: role of cationic amino acid transporters. *Molecular pharmacology* **57**(1): 68-74.

Closs, EI, Simon, A, Vekony, N, Rotmann, A (2004) Plasma membrane transporters for arginine. *J Nutr* **134**(10 Suppl): 2752S-2759S; discussion 2765S-2767S.

Cochran, FR, Selph, J, Sherman, P (1996) Insights into the role of nitric oxide in inflammatory arthritis. *Med Res Rev* **16**(6): 547-563.

Cohen, J, Evans, TJ, Spink, J (1998) Cytokine regulation of inducible nitric oxide synthase in vascular smooth muscle cells. *Prog Clin Biol Res* **397**: 169-177.

Colamonici, O, Uyttendaele, H, Domanski, P, Yan, H, Krolewski, J (1994a) p135tyk2, an interferon-alpha-activated tyrosine kinase, is physically associated with an interferon-alpha receptor. *J. Biol. Chem.* **269**(5): 3518-3522.

Colamonici, O, Yan, H, Domanski, P, Handa, R, Smalley, D, Mullersman, J, Witte, M, Krishnan, K, Krolewski, J (1994b) Direct binding to and tyrosine phosphorylation of the alpha subunit of the type I interferon receptor by p135tyk2 tyrosine kinase. *Mol Cell Biol* **14**(12): 8133-8142.

Collarini, EJ, Oxender, DL (1987) Mechanisms of transport of amino acids across membranes. *Annual review of nutrition* **7**: 75-90.

Colton, CA, Czapiga, M, Snell-Callanan, J, Chernyshev, ON, Vitek, MP (2001) Apolipoprotein E acts to increase nitric oxide production in macrophages by stimulating arginine transport. *Biochimica et biophysica acta* **1535**(2): 134-144.

Cooke, JP, Dzau, VJ (1997) Nitric oxide synthase: role in the genesis of vascular disease. *Annu Rev Med* **48**: 489-509.

Crane, BR, Arvai, AS, Ghosh, DK, Wu, C, Getzoff, ED, Stuehr, DJ, Tainer, JA (1998) Structure of nitric oxide synthase oxygenase dimer with pterin and substrate. *Science*. **279**(5359): 2121-2126.

Crane, BR, Rosenfeld, RJ, Arvai, AS, Ghosh, DK, Ghosh, S, Tainer, JA, Stuehr, DJ, Getzoff, ED (1999) N-terminal domain swapping and metal ion binding in nitric oxide synthase dimerization. *EMBO J.* **18**(22): 6271-6281.

Cruz, MT, Duarte, CB, Goncalo, M, Carvalho, AP, Lopes, MC (1999) Involvement of JAK2 and MAPK on type II nitric oxide synthase expression in skin-derived dendritic cells. *The American journal of physiology* **277**(6 Pt 1): C1050-1057.

Cruz, MT, Duarte, CB, Goncalo, M, Carvalho, AP, Lopes, MC (2001) LPS induction of I kappa B-alpha degradation and iNOS expression in a skin dendritic cell line is prevented by the janus kinase 2 inhibitor, Tyrphostin b42. *Nitric Oxide* **5**(1): 53-61.

Cui, Z, Tuladhar, R, Hart, SL, Marber, MS, Pearson, JD, Baydoun, AR (2005) Rate of transport of L-arginine is independent of the expression of inducible nitric oxide synthase in HEK 293 cells. *Nitric Oxide* **12**(1): 21-30.

Curtis, KM, Gomez, LA, Rios, C, Garbayo, E, Raval, AP, Perez-Pinzon, MA, Schiller, PC (2010) EF1alpha and RPL13a represent normalization genes suitable for RT-qPCR analysis of bone marrow derived mesenchymal stem cells. *BMC Mol Biol* **11**: 61.

Da Silva, J, Pierrat, B, Mary, JL, Lesslauer, W (1997) Blockade of p38 mitogen-activated protein kinase pathway inhibits inducible nitric-oxide synthase expression in mouse astrocytes. *The Journal of biological chemistry* **272**(45): 28373-28380.

Darnell, JE, Jr. (2007) Interferon research: impact on understanding transcriptional control. *Curr Top Microbiol Immunol* **316**: 155-163.

Darnell, JE, Jr. (1997) STATs and gene regulation. *Science (New York, N.Y)* **277**(5332): 1630-1635.

Darnell, JE, Jr., Kerr, IM, Stark, GR (1994) Jak-STAT pathways and transcriptional activation in response to IFNs and other extracellular signaling proteins. *Science (New York, N.Y)* **264**(5164): 1415-1421.

Dawson, V, Dawson, T, London, E, Bredt, D, Snyder, S (1991) Nitric Oxide Mediates Glutamate Neurotoxicity in Primary Cortical Cultures. *PNAS* **88**(14): 6368-6371.

de Meirelles, LR, Mendes-Ribeiro, AC, Santoro, MM, Mendes, MA, da Silva, MN, Mann, GE, Brunini, TM (2007) Inhibitory effects of endogenous L-arginine analogues on nitric oxide synthesis in platelets: role in platelet hyperaggregability in hypertension. *Clin Exp Pharmacol Physiol* **34**(12): 1267-1271.

Decker, T, Kovarik, P (2000) Serine phosphorylation of STATs. *Oncogene* **19**(21): 2628-2637.

Deindl, E, Boengler, K, van Royen, N, Schaper, W (2002) Differential expression of GAPDH and beta3-actin in growing collateral arteries. *Mol Cell Biochem* **236**(1-2): 139-146.

Dell'Albani, P, Santangelo, R, Torrasi, L, Nicoletti, VG, de Vellis, J, Giuffrida Stella, AM (2001) JAK/STAT signaling pathway mediates cytokine-induced iNOS expression in primary astroglial cell cultures. *J Neurosci Res* **65**(5): 417-424.

Deshmukh, DR, Shope, TC (1983) Arginine requirement and ammonia toxicity in ferrets. *J Nutr.* **113**(8): 1664-1667.

Deves, R, Angelo, S, Rojas, AM (1998a) System y<sup>+</sup>L: the broad scope and cation modulated amino acid transporter. *Exp Physiol* **83**(2): 211-220.

Deves, R, Boyd, CA (1998b) Transporters for cationic amino acids in animal cells: discovery, structure, and function. *Physiological reviews* **78**(2): 487-545.

Deves, R, Boyd, CAR (1998c) Transporters for Cationic Amino Acids in Animal Cells: Discovery, Structure, and Function. *Physiol. Rev.* **78**(2): 487-545.

Dhanakoti, SN, Brosnan, JT, Herzberg, GR, Brosnan, ME (1990) Renal arginine synthesis: studies in vitro and in vivo. *The American journal of physiology* **259**(3 Pt 1): E437-442.

Dheda, K, Huggett, JF, Bustin, SA, Johnson, MA, Rook, G, Zumla, A (2004) Validation of housekeeping genes for normalizing RNA expression in real-time PCR. *Biotechniques* **37**(1): 112-114, 116, 118-119.

Diaz-Guerra, MJM, Castrillo, A, Martin-Sanz, P, Bosca, L (1999) Negative Regulation by Phosphatidylinositol 3-Kinase of Inducible Nitric Oxide Synthase Expression in Macrophages. *J Immunol* **162**(10): 6184-6190.

Dickhout, JG, Hossain, GS, Pozza, LM, Zhou, J, Lhotak, S, Austin, RC (2005) Peroxynitrite causes endoplasmic reticulum stress and apoptosis in human vascular endothelium: implications in atherogenesis. *Arteriosclerosis, thrombosis, and vascular biology* **25**(12): 2623-2629.

Doi, M, Shichiri, M, Katsuyama, K, Ishimaru, S, Hirata, Y (2002) Cytokine-activated Jak-2 is involved in inducible nitric oxide synthase expression independent from NF-kappaB activation in vascular smooth muscle cells. *Atherosclerosis* **160**(1): 123-132.

Doi, M, Shichiri, M, Katsuyama, K, Marumo, F, Hirata, Y (2000) Cytokine-activated p42/p44 MAP kinase is involved in inducible nitric oxide synthase gene expression independent from NF-kappaB activation in vascular smooth muscle cells. *Hypertens Res* **23**(6): 659-667.

Domanski, P, Yan, H, Witte, MM, Krolewski, J, Colamonici, OR (1995) Homodimerization and intermolecular tyrosine phosphorylation of the Tyk-2 tyrosine kinase. *FEBS Lett* **374**(3): 317-322.

Dubois-Rande, JL, Zelinsky, R, Roudot, F, Chabrier, PE, Castaigne, A, Geschwind, H, Adnot, S (1992) Effects of infusion of L-arginine into the left anterior descending coronary artery on acetylcholine-induced vasoconstriction of human atheromatous coronary arteries. *The American journal of cardiology* **70**(15): 1269-1275.

Durante, W, Liao, L, Schafer, AI (1995) Differential regulation of L-arginine transport and inducible NOS in cultured vascular smooth muscle cells. *Am J Physiol Heart Circ Physiol* **268**(3): H1158-1164.

Dykhuizen, RS, Frazer, R, Duncan, C, Smith, CC, Golden, M, Benjamin, N, Leifert, C (1996) Antimicrobial effect of acidified nitrite on gut pathogens: importance of dietary nitrate in host defense. *Antimicrob Agents Chemother* **40**(6): 1422-1425.

Elbashir, SM, Harborth, J, Lendeckel, W, Yalcin, A, Weber, K, Tuschl, T (2001a) Duplexes of 21-nucleotide RNAs mediate RNA interference in cultured mammalian cells. *Nature* **411**(6836): 494-498.

Elbashir, SM, Martinez, J, Patkaniowska, A, Lendeckel, W, Tuschl, T (2001b) Functional anatomy of siRNAs for mediating efficient RNAi in *Drosophila melanogaster* embryo lysate. *The EMBO journal* **20**(23): 6877-6888.

Elfering, SL, Sarkela, TM, Giulivi, C (2002) Biochemistry of Mitochondrial Nitric-oxide Synthase. *J. Biol. Chem.* **277**(41): 38079-38086.

Enkhbaatar, P, Murakami, K, Traber, LD, Cox, R, Parkinson, JF, Westphal, M, Esechie, A, Morita, N, Maybauer, MO, Maybauer, DM, Burke, AS, Schmalstieg, FC, Hawkins, HK, Herndon, DN, Traber, DL (2006) The inhibition of inducible nitric oxide synthase in ovine sepsis model. *Shock* **25**(5): 522-527.

Evora, PR, Simon, MR (2007) Role of nitric oxide production in anaphylaxis and its relevance for the treatment of anaphylactic hypotension with methylene blue. *Ann Allergy Asthma Immunol* **99**(4): 306-313.

Falk, E, Fernandez-Ortiz, A (1995) Role of thrombosis in atherosclerosis and its complications. *The American journal of cardiology* **75**(6): 3B-11B.

Fang, FC (2004) Antimicrobial reactive oxygen and nitrogen species: concepts and controversies. *Nat Rev Microbiol* **2**(10): 820-832.

Farrell, AJ, Blake, DR, Palmer, RM, Moncada, S (1992) Increased concentrations of nitrite in synovial fluid and serum samples suggest increased nitric oxide synthesis in rheumatic diseases. *Ann Rheum Dis*. **51**(11): 1219-1222.

Featherston, WR, Rogers, QR, Freedland, RA (1973) Relative importance of kidney and liver in synthesis of arginine by the rat. *The American journal of physiology* **224**(1): 127-129.

Feng, GJ, Goodridge, HS, Harnett, MM, Wei, XQ, Nikolaev, AV, Higson, AP, Liew, FY (1999) Extracellular signal-related kinase (ERK) and p38 mitogen-activated protein (MAP) kinases differentially regulate the lipopolysaccharide-mediated induction of inducible nitric oxide synthase and IL-12 in macrophages: *Leishmania phosphoglycans* subvert macrophage IL-12 production by targeting ERK MAP kinase. *J Immunol* **163**(12): 6403-6412.

Fernandez, J, Yaman, I, Mishra, R, Merrick, WC, Snider, MD, Lamers, WH, Hatzoglou, M (2001) Internal ribosome entry site-mediated translation of a mammalian mRNA is regulated by amino acid availability. *J Biol Chem* **276**(15): 12285-12291.

Finley, KD, Kakuda, DK, Barrieux, A, Kleeman, J, Huynh, PD, MacLeod, CL (1995) A mammalian arginine/lysine transporter uses multiple promoters. *Proc Natl Acad Sci U S A* **92**(20): 9378-9382.

Fire, A, Xu, S, Montgomery, MK, Kostas, SA, Driver, SE, Mello, CC (1998) Potent and specific genetic interference by double-stranded RNA in *Caenorhabditis elegans*. *Nature* **391**(6669): 806-811.

Fischmann, TO, Hruza, A, Niu, XD, Fossetta, JD, Lunn, CA, Dolphin, E, Prongay, AJ, Reichert, P, Lundell, DJ, Narula, SK, Weber, PC (1999) Structural characterization of nitric oxide synthase isoforms reveals striking active-site conservation. *Nature structural biology* **6**(3): 233-242.

Fish, RJ, Kruithof, EK (2004) Short-term cytotoxic effects and long-term instability of RNAi delivered using lentiviral vectors. *BMC Mol Biol* **5**: 9.

Fleming, I, Gray, GA, Schott, C, Stoclet, JC (1991) Inducible but not constitutive production of nitric oxide by vascular smooth muscle cells. *European journal of pharmacology* **200**(2-3): 375-376.

Flodstrom, M, Morris, SMJ, Eizirik, DL (1996) Role of the citrulline-nitric oxide cycle in the functional response of adult human and rodent pancreatic islets to cytokines. *Cytokine* **8**(8): 642-650.

Flodstrom, M, Niemann, A, Bedoya, F, Morris, S, Jr, Eizirik, D (1995) Expression of the citrulline-nitric oxide cycle in rodent and human pancreatic beta-cells:

induction of argininosuccinate synthetase by cytokines. *Endocrinology* **136**(8): 3200-3206.

Forstermann, U, Closs, EI, Pollock, JS, Nakane, M, Schwarz, P, Gath, I, Kleinert, H (1994) Nitric-Oxide Synthase Isozymes - Characterization, Purification, Molecular-Cloning, and Functions. *Hypertension* **23**(6): 1121-1131.

Forstermann, U, Gath, I, Schwarz, P, Closs, EI, Kleinert, H (1995a) Isoforms of Nitric-Oxide Synthase - Properties, Cellular- Distribution and Expressional Control. *Biochemical Pharmacology* **50**(9): 1321-1332.

Forstermann, U, Kleinert, H (1995b) Nitric-Oxide Synthase - Expression and Expressional Control of the 3 Isoforms. *Naunyn-Schmiedebergs Archives of Pharmacology* **352**(4): 351-364.

Frey, HC, Kim, K, Pang, SH, Rasdorf, WJ, Lewis, P (2008) Characterization of real-world activity, fuel use, and emissions for selected motor graders fueled with petroleum diesel and B20 biodiesel. *J Air Waste Manag Assoc* **58**(10): 1274-1287.

Fujihara, M, Ito, N, Pace, J, Watanabe, Y, Russell, S, Suzuki, T (1994) Role of endogenous interferon-beta in lipopolysaccharide-triggered activation of the inducible nitric-oxide synthase gene in a mouse macrophage cell line, J774. *J. Biol. Chem.* **269**(17): 12773-12778.

Fukuzawa, M, Abe, T, Williams, JG (2003) The Dictyostelium prestalk cell inducer DIF regulates nuclear accumulation of a STAT protein by controlling its rate of export from the nucleus. *Development* **130**(4): 797-804.

Furchgott, RF, Zawadzki, JV (1980) The obligatory role of endothelial cells in the relaxation of arterial smooth muscle by acetylcholine. *Nature.* **288**(5789): 373-376.

Furlong, B, Henderson, AH, Lewis, MJ, Smith, JA (1987) Endothelium-derived relaxing factor inhibits in vitro platelet aggregation. *Br J Pharmacol.* **90**(4): 687-692.

Galiveti, CR, Rozhdestvensky, TS, Brosius, J, Lehrach, H, Konthur, Z (2010) Application of housekeeping npcRNAs for quantitative expression analysis of human transcriptome by real-time PCR. *RNA* **16**(2): 450-461.

Gao, J, Morrison, DC, Parmely, TJ, Russell, SW, Murphy, WJ (1997) An interferon-gamma-activated site (GAS) is necessary for full expression of the mouse iNOS gene in response to interferon-gamma and lipopolysaccharide. *The Journal of biological chemistry* **272**(2): 1226-1230.

Gao, YT, Roman, LJ, Martasek, P, Panda, SP, Ishimura, Y, Masters, BS (2007) Oxygen metabolism by endothelial nitric-oxide synthase. *The Journal of biological chemistry* **282**(39): 28557-28565.

Garthwaite, J, Garthwaite, G, Palmer, RM, Moncada, S (1989) NMDA receptor activation induces nitric oxide synthesis from arginine in rat brain slices. *Eur J Pharmacol.* **172**(4-5): 413-416.

Geller, DA, Billiar, TR (1998) Molecular biology of nitric oxide synthases. *Cancer Metastasis Rev* **17**(1): 7-23.

Genc, K, Genc, S, Baskin, H, Semin, I (2006) Erythropoietin decreases cytotoxicity and nitric oxide formation induced by inflammatory stimuli in rat oligodendrocytes. *Physiol Res* **55**(1): 33-38.

Ghafourifar, P, Richter, C (1997) Nitric oxide synthase activity in mitochondria. *FEBS Lett.* ;(): **1**(418 (3)): 291-296.

Ghafourifar, P, Schenk, U, Klein, SD, Richter, C (1999) Mitochondrial Nitric-oxide Synthase Stimulation Causes Cytochrome c Release from Isolated Mitochondria. Evidence for intramitochondrial peroxynitrite formation. *J. Biol. Chem.* **274**(44): 31185-31188.

Ghosh, DK, Stuehr, DJ (1995) Macrophage NO synthase: characterization of isolated oxygenase and reductase domains reveals a head-to-head subunit interaction. *Biochemistry.* **34**(3): 801-807.

Gibson, A, Mirzazadeh, S, Hobbs, AJ, Moore, PK (1990) L-NG-monomethyl arginine and L-NG-nitro arginine inhibit non-adrenergic, non-cholinergic relaxation of the mouse anococcygeus muscle. *Br J Pharmacol.* **99**(3): 602-606.

Gillespie, JS, Liu, XR, Martin, W (1989) The effects of L-arginine and NG-monomethyl L-arginine on the response of the rat anococcygeus muscle to NANC nerve stimulation. *Br J Pharmacol.* **98**(4): 1080-1082.

Giulivi, C, Poderoso, JJ, Boveris, A (1998) Production of Nitric Oxide by Mitochondria. *J. Biol. Chem.* **273**(18): 11038-11043.

Glare, EM, Divjak, M, Bailey, MJ, Walters, EH (2002) beta-Actin and GAPDH housekeeping gene expression in asthmatic airways is variable and not suitable for normalising mRNA levels. *Thorax* **57**(9): 765-770.

Glusa, E, Markwardt, F, Sturzebecher, J (1974) Effects of sodium nitroprusside and other pentacyanonitrosyl complexes on platelet aggregation. *Haemostasis.* **3**(5-6): 249-256.

Goidin, D, Mamessier, A, Staquet, MJ, Schmitt, D, Berthier-Vergnes, O (2001) Ribosomal 18S RNA prevails over glyceraldehyde-3-phosphate dehydrogenase and beta-actin genes as internal standard for quantitative comparison of mRNA levels in invasive and noninvasive human melanoma cell subpopulations. *Anal Biochem* **295**(1): 17-21.

Goodman, MG, Chenoweth, DE, Weigle, WO (1982) Induction of interleukin 1 secretion and enhancement of humoral immunity by binding of human C5a to macrophage surface C5a receptors. *The Journal of experimental medicine* **156**(3): 912-917.

Granger, DL, Hibbs, JB, Jr., Perfect, JR, Durack, DT (1990) Metabolic fate of L-arginine in relation to microbiostatic capability of murine macrophages. *The Journal of clinical investigation* **85**(1): 264-273.

Granger, DL, Hibbs, JBJ, Perfect, JR, Durack, DT (1988) Specific amino acid (L-arginine) requirement for the microbiostatic activity of murine macrophages. *J Clin Invest.* **81**(4): 1129-1136.

Guha, M, Mackman, N (2002) The phosphatidylinositol 3-kinase-Akt pathway limits lipopolysaccharide activation of signaling pathways and expression of inflammatory mediators in human monocytic cells. *The Journal of biological chemistry* **277**(35): 32124-32132.

Gundogdu, MS, Liu, H, Metzdorf, D, Hildebrand, D, Aigner, M, Aktories, K, Heeg, K, Kubatzky, KF (2010) The haematopoietic GTPase RhoH modulates IL3 signalling through regulation of STAT activity and IL3 receptor expression. *Mol Cancer* **9**: 225.

Ha, YH, Milner, JA, Corbin, JE (1978) Arginine requirements in immature dogs. *J Nutr.* **108**(2): 203-210.

Habib, F, Dutka, D, Crossman, D, Oakley, CM, Cleland, JG (1994) Enhanced basal nitric oxide production in heart failure: another failed counter-regulatory vasodilator mechanism? *Lancet* **344**(8919): 371-373.

Haley, B, Zamore, PD (2004) Kinetic analysis of the RNAi enzyme complex. *Nat Struct Mol Biol* **11**(7): 599-606.

Hammermann, R, Brunn, G, Racke, K (2001) Analysis of the genomic organization of the human cationic amino acid transporters CAT-1, CAT-2 and CAT-4. *Amino Acids* **21**(2): 211-219.

Hammermann, R, Dreissig, MD, Mossner, J, Fuhrmann, M, Berrino, L, Gothert, M, Racke, K (2000) Nuclear factor-kappaB mediates simultaneous induction of inducible nitric-oxide synthase and Up-regulation of the cationic amino acid

transporter CAT-2B in rat alveolar macrophages. *Molecular pharmacology* **58**(6): 1294-1302.

Harari, OA, McHale, JF, Marshall, D, Ahmed, S, Brown, D, Askenase, PW, Haskard, DO (1999) Endothelial cell E- and P-selectin up-regulation in murine contact sensitivity is prolonged by distinct mechanisms occurring in sequence. *J Immunol* **163**(12): 6860-6866.

Harborth, J, Elbashir, SM, Bechert, K, Tuschl, T, Weber, K (2001) Identification of essential genes in cultured mammalian cells using small interfering RNAs. *Journal of cell science* **114**(Pt 24): 4557-4565.

Harborth, J, Elbashir, SM, Vandeburgh, K, Manninga, H, Scaringe, SA, Weber, K, Tuschl, T (2003) Sequence, chemical, and structural variation of small interfering RNAs and short hairpin RNAs and the effect on mammalian gene silencing. *Antisense Nucleic Acid Drug Dev* **13**(2): 83-105.

Hattori, Y, Campbell, E, Gross, S (1994) Argininosuccinate synthetase mRNA and activity are induced by immunostimulants in vascular smooth muscle. Role in the regeneration of arginine for nitric oxide synthesis. *J. Biol. Chem.* **269**(13): 9405-9408.

Hattori, Y, Kasai, K, Gross, SS (1999) Cationic amino acid transporter gene expression in cultured vascular smooth muscle cells and in rats. *Am J Physiol Heart Circ Physiol* **276**(6): H2020-2028.

Hattori, Y, Nakanishi, N, Kasai, K (2002) Statin enhances cytokine-mediated induction of nitric oxide synthesis in vascular smooth muscle cells. *Cardiovascular research* **54**(3): 649-658.

Heid, CA, Stevens, J, Livak, KJ, Williams, PM (1996) Real time quantitative PCR. *Genome research* **6**(10): 986-994.

Heiss, B, Frunzke, K, Zumft, WG (1989) Formation of the N-N bond from nitric oxide by a membrane-bound cytochrome bc complex of nitrate-respiring (denitrifying) *Pseudomonas stutzeri*. *Journal of bacteriology* **171**(6): 3288-3297.

Hellendall, RP, Ting, JP (1997) Differential regulation of cytokine-induced major histocompatibility complex class II expression and nitric oxide release in rat microglia and astrocytes by effectors of tyrosine kinase, protein kinase C, and cAMP. *J Neuroimmunol.* **74**(1-2): 19-29.

Hemmens, B, Goessler, W, Schmidt, K, Mayer, B (2000) Role of Bound Zinc in Dimer Stabilization but Not Enzyme Activity of Neuronal Nitric-oxide Synthase. *J. Biol. Chem.* **275**(46): 35786-35791.

Herrington, J, Smit, LS, Schwartz, J, Carter-Su, C (2000) The role of STAT proteins in growth hormone signaling. *Oncogene* **19**(21): 2585-2597.

Hibbs, J, Jr, Vavrin, Z, Taintor, R (1987) L-arginine is required for expression of the activated macrophage effector mechanism causing selective metabolic inhibition in target cells. *J Immunol* **138**(2): 550-565.

Hibbs, JB, Jr., Westenfelder, C, Taintor, R, Vavrin, Z, Kablitz, C, Baranowski, RL, Ward, JH, Menlove, RL, McMurry, MP, Kushner, JP, et al. (1992) Evidence for cytokine-inducible nitric oxide synthesis from L-arginine in patients receiving interleukin-2 therapy. *The Journal of clinical investigation* **89**(3): 867-877.

Higuchi, R, Fockler, C, Dollinger, G, Watson, R (1993) Kinetic PCR analysis: real-time monitoring of DNA amplification reactions. *Bio/technology (Nature Publishing Company)* **11**(9): 1026-1030.

Hirschfeld, M, Kirschning, CJ, Schwandner, R, Wesche, H, Weis, JH, Wooten, RM, Weis, JJ (1999) Cutting edge: inflammatory signaling by *Borrelia burgdorferi* lipoproteins is mediated by toll-like receptor 2. *J Immunol* **163**(5): 2382-2386.

Hon, WM, Khoo, HE, Mochhala, S (1998) Nitric oxide in septic shock: directions for future therapy? *Ann Acad Med Singapore* **27**(3): 414-421.

Horikoshi, T, Danenberg, KD, Stadlbauer, TH, Volkenandt, M, Shea, LC, Aigner, K, Gustavsson, B, Leichman, L, Frosing, R, Ray, M, et al. (1992) Quantitation of thymidylate synthase, dihydrofolate reductase, and DT-diaphorase gene expression in human tumors using the polymerase chain reaction. *Cancer Res* **52**(1): 108-116.

Hortelano, S, Genaro, AM, Bosca, L (1993) Phorbol Esters Induce Nitric-Oxide Synthase and Increase Arginine Influx in Cultured Peritoneal-Macrophages. *FEBS letters* **320**(2): 135-139.

Hosokawa, H, Sawamura, T, Kobayashi, S, Ninomiya, H, Miwa, S, Masaki, T (1997) Cloning and characterization of a brain-specific cationic amino acid transporter. *J Biol Chem* **272**(13): 8717-8722.

Hrabak, A, Idei, M, Temesi, A (1994) Arginine supply for nitric oxide synthesis and arginase is mainly exogenous in elicited murine and rat macrophages. *Life sciences* **55**(10): 797-805.

Hsiao, G, Shen, MY, Chang, WC, Cheng, YW, Pan, SL, Kuo, YH, Chen, TF, Sheu, JR (2003) A novel antioxidant, octyl caffeate, suppression of LPS/IFN-gamma-induced inducible nitric oxide synthase gene expression in rat aortic smooth muscle cells. *Biochem Pharmacol* **65**(8): 1383-1392.

Hu, X, Chen, J, Wang, L, Ivashkiv, LB (2007) Crosstalk among Jak-STAT, Toll-like receptor, and ITAM-dependent pathways in macrophage activation. *Journal of leukocyte biology* **82**(2): 237-243.

Huang, CJ, Tsai, PS, Lu, YT, Cheng, CR, Stevens, BR, Skimming, JW, Pan, WH (2004a) NF-kappaB involvement in the induction of high affinity CAT-2 in lipopolysaccharide-stimulated rat lungs. *Acta Anaesthesiol Scand* **48**(8): 992-1002.

Huang, H, Rose, JL, Hoyt, DG (2004b) p38 Mitogen-activated protein kinase mediates synergistic induction of inducible nitric-oxide synthase by lipopolysaccharide and interferon-gamma through signal transducer and activator of transcription 1 Ser727 phosphorylation in murine aortic endothelial cells. *Molecular pharmacology* **66**(2): 302-311.

Huggett, J, Dheda, K, Bustin, S, Zumla, A (2005) Real-time RT-PCR normalisation; strategies and considerations. *Genes Immun* **6**(4): 279-284.

Iadecola, C, Ross, ME (1997) Molecular pathology of cerebral ischemia: delayed gene expression and strategies for neuroprotection. *Annals of the New York Academy of Sciences* **835**: 203-217.

Iadecola, C, Zhang, F, Casey, R, Clark, HB, Ross, ME, Kukreja, RC (1996) Inducible Nitric Oxide Synthase Gene Expression in Vascular Cells After Transient Focal Cerebral Ischemia. *Stroke* **27**(8): 1373-1380.

Ialenti, A, Ianaro, A, Moncada, S, Di Rosa, M (1992) Modulation of acute inflammation by endogenous nitric oxide. *Eur J Pharmacol.* **211**(2): 177-182.

Igaz, P, Toth, S, Falus, A (2001) Biological and clinical significance of the JAK-STAT pathway; lessons from knockout mice. *Inflamm Res* **50**(9): 435-441.

Ignarro, L, Fukuto, J, Griscavage, J, Rogers, N, Byrns, R (1993) Oxidation of Nitric Oxide in Aqueous Solution to Nitrite but not Nitrate: Comparison with Enzymatically Formed Nitric Oxide From L-Arginine. *PNAS* **90**(17): 8103-8107.

Ignarro, LJ, Bush, PA, Buga, GM, Wood, KS, Fukuto, JM, J., R (1990) Nitric oxide and cyclic GMP formation upon electrical field stimulation cause relaxation of corpus cavernosum smooth muscle. *Biochem Biophys Res Commun.* **170**(2): 843-850.

Ignarro, LJ, Degnan, JN, Baricos, WH, Kadowitz, PJ, Wolin, MS (1982) Activation of purified guanylate cyclase by nitric oxide requires heme comparison of heme-deficient, heme-reconstituted and heme-containing forms of soluble enzyme from bovine lung. *Biochimica et Biophysica Acta (BBA) - General Subjects* **718**(1): 49-59.

- Ihle, JN (1995) Cytokine receptor signalling. *Nature* **377**(6550): 591-594.
- Ihle, JN (1996) STATs: signal transducers and activators of transcription. *Cell* **84**(3): 331-334.
- Ishizaki, T, Maekawa, M, Fujisawa, K, Okawa, K, Iwamatsu, A, Fujita, A, Watanabe, N, Saito, Y, Kakizuka, A, Morii, N, Narumiya, S (1996) The small GTP-binding protein Rho binds to and activates a 160 kDa Ser/Thr protein kinase homologous to myotonic dystrophy kinase. *The EMBO journal* **15**(8): 1885-1893.
- Ishizaki, T, Naito, M, Fujisawa, K, Maekawa, M, Watanabe, N, Saito, Y, Narumiya, S (1997) p160ROCK, a Rho-associated coiled-coil forming protein kinase, works downstream of Rho and induces focal adhesions. *FEBS letters* **404**(2-3): 118-124.
- Ivashkiv, LB, Hu, X (2004) Signaling by STATs. *Arthritis Res Ther* **6**(4): 159-168.
- Iyengar, R, Stuehr, DJ, Marletta, MA (1987) Macrophage synthesis of nitrite, nitrate, and N-nitrosamines: precursors and role of the respiratory burst. *Proceedings of the National Academy of Sciences of the United States of America* **84**(18): 6369-6373.
- Janssens, SP, Shimouchi, A, Quertermous, T, Bloch, DB, Bloch, KD (1992) Cloning and expression of a cDNA encoding human endothelium-derived relaxing factor/nitric oxide synthase. *J Biol Chem*. **267**(21): 14519-14522.
- Javanmard, SH, Nematbakhsh, M, Sanei, MH (2009) Early prevention by L-Arginine attenuates coronary atherosclerosis in a model of hypercholesterolemic animals; no positive results for treatment. *Nutr Metab (Lond)* **6**: 13.
- Jayasena, SD (2005) Designer siRNAs to overcome the challenges from the RNAi pathway. *J RNAi Gene Silencing* **2**(1): 109-117.
- Jorens, PG, Van Overveld, FJ, Bult, H, Vermeire, PA, Herman, AG (1991) L-arginine-dependent production of nitrogen oxides by rat pulmonary macrophages. *Eur J Pharmacol*. **200**(2-3): 205-209.
- Kakar, R, Kautz, B, Eklund, EA (2005) JAK2 is necessary and sufficient for interferon-gamma-induced transcription of the gene encoding gp91PHOX. *Journal of leukocyte biology* **77**(1): 120-127.
- Kakuda, DK, Sweet, MJ, MacLeod, CL, Hume, DA, Markovich, D (1999) CAT2-mediated L-arginine transport and nitric oxide production in activated macrophages. *The Biochemical journal* **340** ( Pt 2): 549-553.

Kamezaki, K, Shimoda, K, Numata, A, Matsuda, T, Nakayama, K-I, Harada, M (2004) The role of Tyk2, Stat1 and Stat4 in LPS-induced endotoxin signals. *Int. Immunol.* **16**(8): 1173-1179.

Kamijo, R, Harada, H, Matsuyama, T, Bosland, M, Gerecitano, J, Shapiro, D, Le, J, Koh, SI, Kimura, T, Green, SJ (1994) Requirement for transcription factor IRF-1 in NO synthase induction in macrophages. *Science.* **263**(5153): 1612-1615.

Kanai, A, Epperly, M, Pearce, L, Birder, L, Zeidel, M, Meyers, S, Greenberger, J, de Groat, W, Apodaca, G, Peterson, J (2004) Differing roles of mitochondrial nitric oxide synthase in cardiomyocytes and urothelial cells. *American journal of physiology* **286**(1): H13-21.

Kang, YJ, Koo, EB, Lee, YS, Yun-Choi, HS, Chang, KC (1999) Prevention of the expression of inducible nitric oxide synthase by a novel positive inotropic agent, YS 49, in rat vascular smooth muscle and RAW 264.7 macrophages. *British journal of pharmacology* **128**(2): 357-364.

Karaghiosoff, M, Neubauer, H, Lassnig, C, Kovarik, P, Schindler, H, Pircher, H, McCoy, B, Bogdan, C, Decker, T, Brem, G, Pfeffer, K, Muller, M (2000) Partial impairment of cytokine responses in Tyk2-deficient mice. *Immunity* **13**(4): 549-560.

Karaghiosoff, M, Steinborn, R, Kovarik, P, Kriegshauser, G, Baccarini, M, Donabauer, B, Reichart, U, Kolbe, T, Bogdan, C, Leanderson, T, Levy, D, Decker, T, Muller, M (2003) Central role for type I interferons and Tyk2 in lipopolysaccharide-induced endotoxin shock. *Nature Immunology* **4**(5): 471-477.

Karima, R, Matsumoto, S, Higashi, H, Matsushima, K (1999) The molecular pathogenesis of endotoxic shock and organ failure. *Mol Med Today* **5**(3): 123-132.

Kavanaugh, MP, Wang, H, Boyd, CA, North, RA, Kabat, D (1994a) Cell surface receptor for ecotropic host-range mouse retroviruses: a cationic amino acid transporter. *Arch Virol* **9**(Suppl): 485-494.

Kavanaugh, MP, Wang, H, Zhang, Z, Zhang, W, Wu, YN, Dechant, E, North, RA, Kabat, D (1994b) Control of cationic amino acid transport and retroviral receptor functions in a membrane protein family. *The Journal of biological chemistry* **269**(22): 15445-15450.

Kawahara, K, Gotoh, T, Oyadomari, S, Kajizono, M, Kuniyasu, A, Ohsawa, K, Imai, Y, Kohsaka, S, Nakayama, H, Mori, M (2001) Co-induction of argininosuccinate synthetase, cationic amino acid transporter-2, and nitric oxide synthase in activated murine microglial cells. *Brain Res Mol Brain Res* **90**(2): 165-173.

Kehlenbach, RH, Dickmanns, A, Gerace, L (1998) Nucleocytoplasmic shuttling factors including Ran and CRM1 mediate nuclear export of NFAT In vitro. *The Journal of cell biology* **141**(4): 863-874.

Kharitonov, SA, Yates, D, Robbins, RA, Logan-Sinclair, R, Shinebourne, EA, Barnes, PJ (1994) Increased nitric oxide in exhaled air of asthmatic patients. *Lancet*. **343**(8890): 133-135.

Khazaei, M, Mobarakeh, JI, Rahimi, AA, Razavi, MR (2012) Effect of chronic L-Arginine supplementation on aortic fatty streak formation and serum nitric oxide concentration in normal and high-cholesterol fed rabbits. *Acta Physiol Hung* **99**(1): 87-93.

Khvorova, A, Reynolds, A, Jayasena, SD (2003) Functional siRNAs and miRNAs exhibit strand bias. *Cell* **115**(2): 209-216.

Kilberg, MS, Stevens, BR, Novak, DA (1993) Recent advances in mammalian amino acid transport. *Annual review of nutrition* **13**: 137-165.

Kim, HJ, Tsoyi, K, Heo, JM, Kang, YJ, Park, MK, Lee, YS, Lee, JH, Seo, HG, Yun-Choi, HS, Chang, KC (2007) Regulation of lipopolysaccharide-induced inducible nitric-oxide synthase expression through the nuclear factor-kappaB pathway and interferon-beta/tyrosine kinase 2/Janus tyrosine kinase 2-signal transducer and activator of transcription-1 signaling cascades by 2-naphthylethyl-6,7-dihydroxy-1,2,3,4-tetrahydroisoquinoline (THI 53), a new synthetic isoquinoline alkaloid. *J Pharmacol Exp Ther* **320**(2): 782-789.

Kim, JW, Closs, EI, Albritton, LM, Cunningham, JM (1991) Transport of cationic amino acids by the mouse ecotropic retrovirus receptor. *Nature* **352**(6337): 725-728.

Kim, PK, Zamora, R, Petrosko, P, Billiar, TR (2001) The regulatory role of nitric oxide in apoptosis. *Int Immunopharmacol* **1**(8): 1421-1441.

Kimura, K, Ito, M, Amano, M, Chihara, K, Fukata, Y, Nakafuku, M, Yamamori, B, Feng, J, Nakano, T, Okawa, K, Iwamatsu, A, Kaibuchi, K (1996) Regulation of myosin phosphatase by Rho and Rho-associated kinase (Rho-kinase). *Science (New York, N.Y)* **273**(5272): 245-248.

Kinugawa, K-i, Shimizu, T, Yao, A, Kohmoto, O, Serizawa, T, Takahashi, T (1997) Transcriptional Regulation of Inducible Nitric Oxide Synthase in Cultured Neonatal Rat Cardiac Myocytes. *Circulation research* **81**(6): 911-921.

Kirk, SJ, Regan, MC, Barbul, A (1990) Cloned murine T lymphocytes synthesize a molecule with the biological characteristics of nitric oxide. *Biochem Biophys Res Commun.* **173**(2): 660-665.

Kirkeboen, KA, Strand, OA (1999) The role of nitric oxide in sepsis--an overview. *Acta Anaesthesiol Scand* **43**(3): 275-288.

Kirken, RA, Erwin, RA, Taub, D, Murphy, WJ, Behbod, F, Wang, L, Pericle, F, Farrar, WL (1999) Tyrphostin AG-490 inhibits cytokine-mediated JAK3/STAT5a/b signal transduction and cellular proliferation of antigen-activated human T cells. *Journal of leukocyte biology* **65**(6): 891-899.

Kitamura, Y, Takahashi, H, Nomura, Y, Taniguchi, T (1996) Possible involvement of Janus kinase Jak2 in interferon-gamma induction of nitric oxide synthase in rat glial cells. *European journal of pharmacology* **306**(1-3): 297-306.

Kjoller, L, Hall, A (1999) Signaling to Rho GTPases. *Experimental cell research* **253**(1): 166-179.

Klatt, P, Schmidt, K, Lehner, D, Glatter, O, Bachinger, HP, Mayer, B (1995) Structural analysis of porcine brain nitric oxide synthase reveals a role for tetrahydrobiopterin and L-arginine in the formation of an SDS-resistant dimer. *EMBO J.* **14**(15): 3687-3695.

Kleemann, R, Rothe, H, Kolb-Bachofen, V, Xie, QW, Nathan, C, Martin, S, Kolb, H (1993) Transcription and translation of inducible nitric oxide synthase in the pancreas of prediabetic BB rats. *FEBS letters* **328**(1-2): 9-12.

Kleinert, H, Euchenhofer, C, Fritz, G, Ihrig-Biedert, I, Forstermann, U (1998) Involvement of protein kinases in the induction of NO synthase II in human DLD-1 cells. *British journal of pharmacology* **123**(8): 1716-1722.

Kleinert, H, Pautz, A, Linker, K, Schwarz, PM (2004) Regulation of the expression of inducible nitric oxide synthase. *European journal of pharmacology* **500**(1-3): 255-266.

Knowles, RG, Moncada, S (1994) Nitric oxide synthases in mammals. *The Biochemical journal* **298 ( Pt 2)**: 249-258.

Knuefermann, P, Nemoto, S, Baumgarten, G, Misra, A, Sivasubramanian, N, Carabello, BA, Vallejo, JG (2002) Cardiac inflammation and innate immunity in septic shock: is there a role for toll-like receptors? *Chest* **121**(4): 1329-1336.

Kohnen, SL, Mouithys-Mickalad, AA, Deby-Dupont, GP, Deby, CM, Lamy, ML, Noels, AF (2001) Oxidation of tetrahydrobiopterin by peroxynitrite or oxoferryl species occurs by a radical pathway. *Free Radic Res* **35**(6): 709-721.

Kolyada, AY, Savikovsky, N, Madias, NE (1996) Transcriptional regulation of the human iNOS gene in vascular-smooth-muscle cells and macrophages: evidence for tissue specificity. *Biochemical and biophysical research communications* **220**(3): 600-605.

Kong, LY, McMillian, MK, Maronpot, R, Hong, JS (1996) Protein tyrosine kinase inhibitors suppress the production of nitric oxide in mixed glia, microglia-enriched or astrocyte-enriched cultures. *Brain Res.* **729**(1): 1996 Aug 1995.

Kotamraju, S, Williams, CL, Kalyanaraman, B (2007) Statin-induced breast cancer cell death: role of inducible nitric oxide and arginase-dependent pathways. *Cancer Res* **67**(15): 7386-7394.

Kovarik, P, Stoiber, D, Novy, M, Decker, T (1998) Stat1 combines signals derived from IFN-gamma and LPS receptors during macrophage activation. *The EMBO journal* **17**(13): 3660-3668.

Kroncke, KD, Brenner, HH, Rodriguez, ML, Etzkorn, K, Noack, EA, Kolb, H, Kolb-Bachofen, V (1993) Pancreatic islet cells are highly susceptible towards the cytotoxic effects of chemically generated nitric oxide. *Biochimica et biophysica acta* **1182**(2): 221-229.

Kubes, P, Suzuki, M, Granger, D (1991) Nitric Oxide: An Endogenous Modulator of Leukocyte Adhesion. *PNAS* **88**(11): 4651-4655.

Lamas, S, Michel, T, Collins, T, Brenner, BM, Marsden, PA (1992) Effects of interferon-gamma on nitric oxide synthase activity and endothelin-1 production by vascular endothelial cells. *J Clin Invest* **90**(3): 879-887.

Lancaster, JR, Jr. (1994) Simulation of the diffusion and reaction of endogenously produced nitric oxide. *Proceedings of the National Academy of Sciences of the United States of America* **91**(17): 8137-8141.

Laroux, FS, Pavlick, KP, Hines, IN, Kawachi, S, Harada, H, Bharwani, S, Hoffman, JM, Grisham, MB (2001) Role of nitric oxide in inflammation. *Acta Physiol. Scand.* **173**(1): 113-118.

Laufs, U, Kilter, H, Konkol, C, Wassmann, S, Bohm, M, Nickenig, G (2002) Impact of HMG CoA reductase inhibition on small GTPases in the heart. *Cardiovascular research* **53**(4): 911-920.

Laufs, U, Liao, JK (2003) Isoprenoid metabolism and the pleiotropic effects of statins. *Curr Atheroscler Rep* **5**(5): 372-378.

Laufs, U, Liao, JK (1998) Post-transcriptional regulation of endothelial nitric oxide synthase mRNA stability by Rho GTPase. *The Journal of biological chemistry* **273**(37): 24266-24271.

Lazaar, AL (2002) Airway smooth muscle: new targets for asthma pharmacotherapy. *Expert Opin Ther Targets* **6**(4): 447-459.

Lee, B, Kang, H, Pyun, K, Choi, I (1997) Roles of tyrosine kinases in the regulation of nitric oxide synthesis in murine liver cells: Modulation of NF- $\kappa$ B activity by tyrosine kinases. *Hepatology* **25**(4): 913-919.

Lee, NS, Dohjima, T, Bauer, G, Li, H, Li, MJ, Ehsani, A, Salvaterra, P, Rossi, J (2002) Expression of small interfering RNAs targeted against HIV-1 rev transcripts in human cells. *Nat Biotechnol* **20**(5): 500-505.

Leung, T, Chen, XQ, Manser, E, Lim, L (1996) The p160 RhoA-binding kinase ROK alpha is a member of a kinase family and is involved in the reorganization of the cytoskeleton. *Molecular and cellular biology* **16**(10): 5313-5327.

Leung, T, Manser, E, Tan, L, Lim, L (1995) A novel serine/threonine kinase binding the Ras-related RhoA GTPase which translocates the kinase to peripheral membranes. *The Journal of biological chemistry* **270**(49): 29051-29054.

Levitzki, A (1992) Tyrosine kinase blockers as novel antiproliferative agents and dissectors of signal transduction. *Faseb J* **6**(14): 3275-3282.

Li, H, Raman, CS, Glaser, CB, Blasko, E, Young, TA, Parkinson, JF, Whitlow, M, Poulos, TL (1999) Crystal Structures of Zinc-free and -bound Heme Domain of Human Inducible Nitric-oxide Synthase. IMPLICATIONS FOR DIMER STABILITY AND COMPARISON WITH ENDOTHELIAL NITRIC-OXIDE SYNTHASE. *J. Biol. Chem.* **274**(30): 21276-21284.

Li, J (2013) JAK-STAT and bone metabolism. *JAKSTAT* **2**(3): e23930.

Li, J, Li, W, Su, J, Liu, W, Altura, BT, Altura, BM (2004) Peroxynitrite induces apoptosis in rat aortic smooth muscle cells: possible relation to vascular diseases. *Exp Biol Med (Maywood)* **229**(3): 264-269.

Li, J, Su, J, Li, W, Liu, W, Altura, BT, Altura, BM (2003) Peroxynitrite induces apoptosis in canine cerebral vascular muscle cells: possible relation to neurodegenerative diseases and strokes. *Neurosci Lett* **350**(3): 173-177.

Liao, JK, Laufs, U (2005) Pleiotropic effects of statins. *Annu Rev Pharmacol Toxicol* **45**: 89-118.

Libby, P (2002) Inflammation in atherosclerosis. *Nature* **420**(6917): 868-874.

Liu, MC, Tsai, PS, Yang, CH, Liu, CH, Chen, CC, Huang, CJ (2006) Propofol significantly attenuates iNOS, CAT-2, and CAT-2B transcription in lipopolysaccharide-stimulated murine macrophages. *Acta Anaesthesiol Taiwan* **44**(2): 73-81.

Liu, R, Xu, N, Yi, W, Huang, K, Su, M (2012) Electroacupuncture effect on neurological behavior and tyrosine kinase-JAK 2 in rats with focal cerebral ischemia. *J Tradit Chin Med* **32**(3): 465-470.

Liu, SF, Ye, X, Malik, AB (1997) In vivo inhibition of nuclear factor-kappa B activation prevents inducible nitric oxide synthase expression and systemic hypotension in a rat model of septic shock. *J Immunol* **159**(8): 3976-3983.

Livak, KJ, Schmittgen, TD (2001) Analysis of relative gene expression data using real-time quantitative PCR and the 2(-Delta Delta C(T)) Method. *Methods* **25**(4): 402-408.

Lobo, V, Patil, A, Phatak, A, Chandra, N (2010) Free radicals, antioxidants and functional foods: Impact on human health. *Pharmacogn Rev* **4**(8): 118-126.

Lorsbach, RB, Murphy, WJ, Lowenstein, CJ, Snyder, SH, Russell, SW (1993) Expression of the nitric oxide synthase gene in mouse macrophages activated for tumor cell killing. Molecular basis for the synergy between interferon-gamma and lipopolysaccharide. *The Journal of biological chemistry* **268**(3): 1908-1913.

Lowenstein, C, Alley, E, Raval, P, Snowman, A, Snyder, S, Russell, S, Murphy, W (1993) Macrophage Nitric Oxide Synthase Gene: Two Upstream Regions Mediate Induction by Interferon {gamma} and Lipopolysaccharide. *PNAS* **90**(20): 9730-9734.

Lowenstein, C, Glatt, C, Bredt, D, Snyder, S (1992) Cloned and Expressed Macrophage Nitric Oxide Synthase Contrasts with the Brain Enzyme. *PNAS* **89**(15): 6711-6715.

Lu, SC, Wu, HW, Lin, YJ, Chang, SF (2009) The essential role of Oct-2 in LPS-induced expression of iNOS in RAW 264.7 macrophages and its regulation by trichostatin A. *Am J Physiol Cell Physiol* **296**(5): C1133-1139.

Luo, C, Laaja, P (2004a) Inhibitors of JAKs/STATs and the kinases: a possible new cluster of drugs. *Drug Discovery Today* **9**(6): 268-275.

Luo, KQ, Chang, DC (2004b) The gene-silencing efficiency of siRNA is strongly dependent on the local structure of mRNA at the targeted region. *Biochemical and biophysical research communications* **318**(1): 303-310.

Lyons, C, Orloff, G, Cunningham, J (1992) Molecular cloning and functional expression of an inducible nitric oxide synthase from a murine macrophage cell line. *J. Biol. Chem.* **267**(9): 6370-6374.

Maciejewski, JP, Selleri, C, Sato, T, Cho, HJ, Keefer, LK, Nathan, CF, Young, NS (1995) Nitric oxide suppression of human hematopoiesis in vitro. Contribution to inhibitory action of interferon-gamma and tumor necrosis factor-alpha. *J Clin Invest* **96**(2): 1085-1092.

MacLeod, CL, Finley, K, Kakuda, D, Kozak, CA, Wilkinson, MF (1990) *Molec. cell. Biol.* **10**: 3663-3674.

MacMicking, J, Xie, QW, Nathan, C (1997) Nitric oxide and macrophage function. *Annu Rev Immunol* **15**: 323-350.

Madamanchi, NR, Moon, SK, Hakim, ZS, Clark, S, Mehrizi, A, Patterson, C, Runge, MS (2005) Differential activation of mitogenic signaling pathways in aortic smooth muscle cells deficient in superoxide dismutase isoforms. *Arteriosclerosis, thrombosis, and vascular biology* **25**(5): 950-956.

Maini, RN, Elliott, MJ, Brennan, FM, Feldmann, M (1995) Beneficial effects of tumour necrosis factor-alpha (TNF-alpha) blockade in rheumatoid arthritis (RA). *Clin Exp Immunol* **101**(2): 207-212.

Manner, CK, Nicholson, B, MacLeod, CL (2003) CAT2 arginine transporter deficiency significantly reduces iNOS-mediated NO production in astrocytes. *J Neurochem* **85**(2): 476-482.

Marczin, N, Papapetropoulos, A, Jilling, T, Catravas, JD (1993) Prevention of Nitric oxide synthase induction in vascular smooth muscle cells by microtubule depolymerizing agents. *British Journal of Pharmacology* **109**: 603-605.

Marletta, MA, Yoon, PS, Iyengar, R, Leaf, CD, Wishnok, JS (1988) Macrophage oxidation of L-arginine to nitrite and nitrate: nitric oxide is an intermediate. *Biochemistry* **27**(24): 8706-8711.

Marrero, MB, Schieffer, B, Paxton, WG, Heerdt, L, Berk, BC, Delafontaine, P, Bernstein, KE (1995) Direct stimulation of Jak/STAT pathway by the angiotensin II AT1 receptor. *Nature* **375**(6528): 247-250.

Marrero, MB, Venema, VJ, He, H, Caldwell, RB, Venema, RC (1998) Inhibition by the JAK/STAT pathway of IFNgamma- and LPS-stimulated nitric oxide synthase induction in vascular smooth muscle cells. *Biochem Biophys Res Commun* **252**(2): 508-512.

Martin, E, Nathan, C, Xie, Q (1994) Role of interferon regulatory factor 1 in induction of nitric oxide synthase. *J. Exp. Med.* **180**(3): 977-984.

Mason, JC (2003) Statins and their role in vascular protection. *Clin Sci (Lond)* **105**(3): 251-266.

Mastronardi, ML, Mostefai, HA, Meziani, F, Martinez, MC, Asfar, P, Andriantsitohaina, R (2011) Circulating microparticles from septic shock patients exert differential tissue expression of enzymes related to inflammation and oxidative stress. *Critical care medicine* **39**(7): 1739-1748.

Mathieu, S, Dubost, JJ, Tournadre, A, Malochet-Guinamand, S, Ristori, JM, Soubrier, M (2010) Effects of 14 weeks of TNF alpha blockade treatment on lipid profile in ankylosing spondylitis. *Joint Bone Spine* **77**(1): 50-52.

McCartney-Francis, N, Allen, J, Mizel, D, Albina, J, Xie, Q, Nathan, C, Wahl, S (1993) Suppression of arthritis by an inhibitor of nitric oxide synthase. *J. Exp. Med.* **178**(2): 749-754.

McDonald, KK, Zharikov, S, Block, ER, Kilberg, MS (1997) A caveolar complex between the cationic amino acid transporter 1 and endothelial nitric-oxide synthase may explain the "arginine paradox". *The Journal of biological chemistry* **272**(50): 31213-31216.

McHale, JF, Harari, OA, Marshall, D, Haskard, DO (1999) Vascular endothelial cell expression of ICAM-1 and VCAM-1 at the onset of eliciting contact hypersensitivity in mice: evidence for a dominant role of TNF-alpha. *J Immunol* **162**(3): 1648-1655.

McManus, MT, Sharp, PA (2002) Gene silencing in mammals by small interfering RNAs. *Nat Rev Genet* **3**(10): 737-747.

McMillan, K, Bredt, D, Hirsch, D, Snyder, S, Clark, J, Masters, B (1992) Cloned, Expressed Rat Cerebellar Nitric Oxide Synthase Contains Stoichiometric Amounts of Heme, which Binds Carbon Monoxide. *PNAS* **89**(23): 11141-11145.

McWhinney, CD, Dostal, D, Baker, K (1998) Angiotensin II activates Stat5 through Jak2 kinase in cardiac myocytes. *Journal of molecular and cellular cardiology* **30**(4): 751-761.

Mellion, BT, Ignarro, LJ, Ohlstein, EH, Pontecorvo, EG, Hyman, AL, Kadowitz, PJ (1981) Evidence for the inhibitory role of guanosine 3', 5'-monophosphate in ADP-induced human platelet aggregation in the presence of nitric oxide and related vasodilators. *Blood.* **57**(5): 946-955.

Mellouk, S, Hoffman, SL, Liu, ZZ, de la Vega, P, Billiar, TR, Nussler, AK (1994) Nitric oxide-mediated antiplasmodial activity in human and murine hepatocytes induced by gamma interferon and the parasite itself: enhancement by exogenous tetrahydrobiopterin. *Infection and immunity* **62**(9): 4043-4046.

Mendes Ribeiro, AC, Hanssen, H, Kiessling, K, Roberts, NB, Mann, GE, Ellory, JC (1997) Transport of L-arginine and the nitric oxide inhibitor NG-monomethyl-L-arginine in human erythrocytes in chronic renal failure. *Clin Sci (Lond)* **93**(1): 57-64.

Meng, F, Lowell, CA (1997) Lipopolysaccharide (LPS)-induced macrophage activation and signal transduction in the absence of Src-family kinases Hck, Fgr, and Lyn. *The Journal of experimental medicine* **185**(9): 1661-1670.

Meraz, MA, White, JM, Sheehan, KC, Bach, EA, Rodig, SJ, Dighe, AS, Kaplan, DH, Riley, JK, Greenlund, AC, Campbell, D, Carver-Moore, K, DuBois, RN, Clark, R, Aguet, M, Schreiber, RD (1996) Targeted disruption of the Stat1 gene in mice reveals unexpected physiologic specificity in the JAK-STAT signaling pathway. *Cell* **84**(3): 431-442.

Mertz, ET, Beeson, WM, Jackson, HD (1952) Classification of essential amino acids for the weanling pig. *Arch Biochem Biophys* **38**: 121-128.

Meydan, N, Grunberger, T, Dadi, H, Shahar, M, Arpaia, E, Lapidot, Z, Leeder, JS, Freedman, M, Cohen, A, Gazit, A, Levitzki, A, Roifman, CM (1996) Inhibition of acute lymphoblastic leukaemia by a Jak-2 inhibitor. *Nature* **379**(6566): 645-648.

Middleton, SJ, Shorthouse, M, Hunter, JO (1993) Increased nitric oxide synthesis in ulcerative colitis. *Lancet*. **341**(8843): 465-466.

Mihm, MJ, Jing, L, Bauer, JA (2000) Nitrotyrosine causes selective vascular endothelial dysfunction and DNA damage. *J Cardiovasc Pharmacol* **36**(2): 182-187.

Milia, AF, Manetti, M, Generini, S, Polidori, L, Benelli, G, Cinelli, M, Messerini, L, Ibba-Manneschi, L, Matucci-Cerinic, M (2009) TNFalpha blockade prevents the development of inflammatory bowel disease in HLA-B27 transgenic rats. *J Cell Mol Med* **13**(1): 164-176.

Moffat, J, Sabatini, DM (2006) Building mammalian signalling pathways with RNAi screens. *Nat Rev Mol Cell Biol* **7**(3): 177-187.

Moncada, S, Higgs, A (1993) The L-arginine-nitric oxide pathway. *N Engl J Med* **329**(27): 2002-2012.

Moncada, S, Palmer, RM, Higgs, EA (1991) Nitric oxide: physiology, pathophysiology, and pharmacology. *Pharmacological reviews* **43**(2): 109-142.

Moran, MF, Koch, CA, Anderson, D, Ellis, C, England, L, Martin, GS, Pawson, T (1990) Src homology region 2 domains direct protein-protein interactions in signal transduction. *Proceedings of the National Academy of Sciences of the United States of America* **87**(21): 8622-8626.

Mori, M (2007) Regulation of nitric oxide synthesis and apoptosis by arginase and arginine recycling. *J Nutr* **137**(6 Suppl 2): 1616S-1620S.

Morikawa, A, Koide, N, Kato, Y, Sugiyama, T, Chakravorty, D, Yoshida, T, Yokochi, T (2000) Augmentation of nitric oxide production by gamma interferon in a mouse vascular endothelial cell line and its modulation by tumor necrosis factor alpha and lipopolysaccharide. *Infect Immun* **68**(11): 6209-6214.

Morris, JG, Rogers, QR (1978) Arginine: an essential amino acid for the cat. *J Nutr*. **108**(12): 1944-1953.

Muller, JM, Ziegler-Heitbrock, HW, Baeuerle, PA (1993) Nuclear factor kappa B, a mediator of lipopolysaccharide effects. *Immunobiology* **187**(3-5): 233-256.

Muniyappa, R, Xu, R, Ram, JL, Sowers, JR (2000) Inhibition of Rho protein stimulates iNOS expression in rat vascular smooth muscle cells. *American journal of physiology* **278**(6): H1762-1768.

Murphy, LD, Herzog, CE, Rudick, JB, Fojo, AT, Bates, SE (1990) Use of the polymerase chain reaction in the quantitation of mdr-1 gene expression. *Biochemistry* **29**(45): 10351-10356.

Murray, CJ, Lopez, AD (1997) Global mortality, disability, and the contribution of risk factors: Global Burden of Disease Study. *Lancet* **349**(9063): 1436-1442.

Muto, A, Fitzgerald, TN, Pimiento, JM, Maloney, SP, Teso, D, Paszkowiak, JJ, Westvik, TS, Kudo, FA, Nishibe, T, Dardik, A (2007) Smooth muscle cell signal transduction: implications of vascular biology for vascular surgeons. *J Vasc Surg* **45 Suppl A**: A15-24.

Nadler, JL, Velasco, JS, Horton, R (1983) Cigarette smoking inhibits prostacyclin formation. *Lancet* **1**(8336): 1248-1250.

Nagafuji, T, Matsui, T, Koide, T, Asano, T (1992) Blockade of nitric oxide formation by N omega-nitro-L-arginine mitigates ischemic brain edema and subsequent cerebral infarction in rats. *Neurosci Lett*. **147**(2): 159-162.

Nakai, M, Hojo, K, Taniguchi, T, Terashima, A, Kawamata, T, Hashimoto, T, Maeda, K, Tanaka, C (1998) PKC and tyrosine kinase involvement in amyloid beta (25-35)-induced chemotaxis of microglia. *Neuroreport* **9**(15): 3467-3470.

Nakane, M, Klinghofer, V, Kuk, JE, Donnelly, JL, Budzik, GP, Pollock, JS, Basha, F, Carter, GW (1995) Novel potent and selective inhibitors of inducible nitric oxide synthase. *Molecular pharmacology* **47**(4): 831-834.

Nakashima, O, Terada, Y, Inoshita, S, Kuwahara, M, Sasaki, S, Marumo, F (1999) Inducible nitric oxide synthase can be induced in the absence of active nuclear factor-kappaB in rat mesangial cells: involvement of the Janus kinase 2 signaling pathway. *J Am Soc Nephrol* **10**(4): 721-729.

Napoli, C, de Nigris, F, Williams-Ignarro, S, Pignalosa, O, Sica, V, Ignarro, LJ (2006) Nitric oxide and atherosclerosis: an update. *Nitric Oxide* **15**(4): 265-279.

Nathan, C (1992) Nitric oxide as a secretory product of mammalian cells. *Faseb J* **6**(12): 3051-3064.

Nathan, C, Calingasan, N, Nezezon, J, Ding, A, Lucia, MS, La Perle, K, Fuortes, M, Lin, M, Ehrt, S, Kwon, NS, Chen, J, Vodovotz, Y, Kipiani, K, Beal, MF (2005) Protection from Alzheimer's-like disease in the mouse by genetic ablation of inducible nitric oxide synthase. *The Journal of experimental medicine* **202**(9): 1163-1169.

Nathan, C, Xie, QW (1994) Regulation of biosynthesis of nitric oxide. *The Journal of biological chemistry* **269**(19): 13725-13728.

Nicholson, B, Manner, CK, Kleeman, J, MacLeod, CL (2001a) Sustained Nitric Oxide Production in Macrophages Requires the Arginine Transporter CAT2. *J. Biol. Chem.* **276**(19): 15881-15885.

Nicholson, B, Manner, CK, Kleeman, J, MacLeod, CL (2001b) Sustained nitric oxide production in macrophages requires the arginine transporter CAT2. *The Journal of biological chemistry* **276**(19): 15881-15885.

Nicoletti, VG, Caruso, A, Tendi, EA, Privitera, A, Console, A, Calabrese, V, Spadaro, F, Ravagna, A, Copani, A, Stella, AM (1998) Effect of nitric oxide synthase induction on the expression of mitochondrial respiratory chain enzyme subunits in mixed cortical and astroglial cell cultures. *Biochimie* **80**(10): 871-881.

Nielsen, M, Kaltoft, K, Nordahl, M, Ropke, C, Geisler, C, Mustelin, T, Dobson, P, Svejgaard, A, Odum, N (1997) Constitutive activation of a slowly migrating isoform of Stat3 in mycosis fungoides: Tyrphostin AG490 inhibits Stat3 activation and growth of mycosis fungoides tumor cell lines. *PNAS* **94**(13): 6764-6769.

Niese, KA, Chiaramonte, MG, Ellies, LG, Rothenberg, ME, Zimmermann, N (2010) The cationic amino acid transporter 2 is induced in inflammatory lung models and regulates lung fibrosis. *Respir Res* **11**: 87.

Nishida, K, Harrison, DG, Navas, JP, Fisher, AA, Dockery, SP, Uematsu, M, Nerem, RM, Alexander, RW, Murphy, TJ (1992) Molecular cloning and characterization of the constitutive bovine aortic endothelial cell nitric oxide synthase. *J Clin Invest.* **90**(5): 2092-2096.

Nishiya, T, Uehara, T, Edamatsu, H, Kaziro, Y, Itoh, H, Nomura, Y (1997) Activation of Stat1 and subsequent transcription of inducible nitric oxide synthase gene in C6 glioma cells is independent of interferon-gamma-induced MAPK activation that is mediated by p21ras. *FEBS Lett* **408**(1): 33-38.

Nishiya, T, Uehara, T, Nomura, Y (1995) Herbimycin A suppresses NF-kappa B activation and tyrosine phosphorylation of JAK2 and the subsequent induction of nitric oxide synthase in C6 glioma cells. *FEBS letters* **371**(3): 333-336.

Niwa, M, Kawai, Y, Nakamura, N, Futaki, S (1997) The structure of the promoter region for rat inducible nitric oxide synthase gene. *Life Sci.* **61**(5): PL 45-49.

Noris, M, Benigni, A, Boccardo, P, Aiello, S, Gaspari, F, Todeschini, M, Figliuzzi, M, Remuzzi, G (1993) Enhanced nitric oxide synthesis in uremia: implications for platelet dysfunction and dialysis hypotension. *Kidney international* **44**(2): 445-450.

Norris, K, Schrimpf, J, Flynn, J, Morris, S, Jr (1995) Enhancement of macrophage microbicidal activity: supplemental arginine and citrulline augment nitric oxide production in murine peritoneal macrophages and promote intracellular killing of *Trypanosoma cruzi*. *Infect. Immun.* **63**(7): 2793-2796.

Norris, PJ, Waldvogel, HJ, Faull, RL, Love, DR, Emson, PC (1996) Decreased neuronal nitric oxide synthase messenger RNA and somatostatin messenger RNA in the striatum of Huntington's disease. *Neuroscience.* **72**(4): 1037-1047.

Nowicki, JP, Duval, D, Poignet, H, Scatton, B (1991) Nitric oxide mediates neuronal death after focal cerebral ischemia in the mouse. *Eur J Pharmacol.* **204**(3): 339-340.

O'Brien, KD, McDonald, TO, Chait, A, Allen, MD, Alpers, CE (1996) Neovascular expression of E-selectin, intercellular adhesion molecule-1, and vascular cell adhesion molecule-1 in human atherosclerosis and their relation to intimal leukocyte content. *Circulation* **93**(4): 672-682.

O'Dell, T, Hawkins, R, Kandel, E, Arancio, O (1991) Tests of the Roles of Two Diffusible Substances in Long-Term Potentiation: Evidence for Nitric Oxide as a Possible Early Retrograde Messenger. *PNAS* **88**(24): 11285-11289.

O'Shea, JJ, Gadina, M, Schreiber, RD (2002) Cytokine signaling in 2002: new surprises in the Jak/Stat pathway. *Cell* **109** Suppl: S121-131.

Oda, T, So, Y, Sato, Y, Shimizu, N, Handa, H, Yasukochi, Y, Kasahara, T (2003) Inhibition by (+/-)-indenestrol A of interferon gamma-stimulated nitric oxide formation in murine macrophage RAW 264.7 cells. *Mutat Res* **534**(1-2): 187-195.

Ohmori, Y, Hamilton, TA (2001) Requirement for STAT1 in LPS-induced gene expression in macrophages. *Journal of leukocyte biology* **69**(4): 598-604.

Okugawa, S, Ota, Y, Kitazawa, T, Nakayama, K, Yanagimoto, S, Tsukada, K, Kawada, M, Kimura, S (2003) Janus kinase 2 is involved in lipopolysaccharide-induced activation of macrophages. *Am J Physiol Cell Physiol* **285**(2): C399-408.

Okusawa, S, Dinarello, CA, Yancey, KB, Endres, S, Lawley, TJ, Frank, MM, Burke, JF, Gelfand, JA (1987) C5a induction of human interleukin 1. Synergistic effect with endotoxin or interferon-gamma. *J Immunol* **139**(8): 2635-2640.

Okusawa, S, Yancey, KB, van der Meer, JW, Endres, S, Lonnemann, G, Heffer, K, Frank, MM, Burke, JF, Dinarello, CA, Gelfand, JA (1988) C5a stimulates secretion of tumor necrosis factor from human mononuclear cells in vitro. Comparison with secretion of interleukin 1 beta and interleukin 1 alpha. *The Journal of experimental medicine* **168**(1): 443-448.

Orlando, C, Pinzani, P, Pazzagli, M (1998) Developments in quantitative PCR. *Clin Chem Lab Med* **36**(5): 255-269.

Ozaki, T, Habara, K, Matsui, K, Kaibori, M, Kwon, AH, Ito, S, Nishizawa, M, Okumura, T (2010) Dexamethasone inhibits the induction of iNOS gene expression through destabilization of its mRNA in proinflammatory cytokine-stimulated hepatocytes. *Shock* **33**(1): 64-69.

Palacin, M, Estevez, R, Bertran, J, Zorzano, A (1998) Molecular biology of mammalian plasma membrane amino acid transporters. *Physiol Rev* **78**(4): 969-1054.

Palmer, RM, Ashton, DS, Moncada, S (1988a) Vascular endothelial cells synthesize nitric oxide from L-arginine. *Nature*. **333**(6174): 664-666.

Palmer, RM, Rees, DD, Ashton, DS, Moncada, S (1988b) L-arginine is the physiological precursor for the formation of nitric oxide in endothelium-dependent relaxation. *Biochem Biophys Res Commun*. **153**(3): 1251-1256.

Panaro, MA, Acquafredda, A, Lisi, S, Lofrumento, DD, Trotta, T, Satalino, R, Saccia, M, Mitolo, V, Brandonisio, O (1999) Inducible nitric oxide synthase and nitric oxide production in Leishmania infantum-infected human macrophages stimulated with interferon-gamma and bacterial lipopolysaccharide. *Int J Clin Lab Res* **29**(3): 122-127.

Panda, K, Rosenfeld, RJ, Ghosh, S, Meade, AL, Getzoff, ED, Stuehr, DJ (2002) Distinct Dimer Interaction and Regulation in Nitric-oxide Synthase Types I, II, and III. *J. Biol. Chem.* **277**(34): 31020-31030.

Papapetropoulos, A, Rudic, RD, Sessa, WC (1999) Molecular control of nitric oxide synthases in the cardiovascular system. *Cardiovascular Research* **43**(3): 509-520.

Park, YC, Lee, CH, Kang, HS, Chung, HT, Kim, HD (1997) Wortmannin, a Specific Inhibitor of Phosphatidylinositol-3-kinase, Enhances LPS-Induced NO Production from Murine Peritoneal Macrophages. *Biochemical and biophysical research communications* **240**(3): 692-696.

Paul, A, Doherty, K, Plevin, R (1997) Differential regulation by protein kinase C isoforms of nitric oxide synthase induction in RAW 264.7 macrophages and rat aortic smooth muscle cells. *Br J Pharmacol* **120**(5): 940-946.

Paul, A, Pendreigh, RH, Plevin, R (1995) Protein kinase C and tyrosine kinase pathways regulate lipopolysaccharide-induced nitric oxide synthase activity in RAW 264.7 murine macrophages. *Br J Pharmacol* **114**(2): 482-488.

Pedoto, A, Tassiopoulos, AK, Oler, A, McGraw, DJ, Hoffmann, SP, Camporesi, EM, Hakim, TS (1998) Treatment of septic shock in rats with nitric oxide synthase inhibitors and inhaled nitric oxide. *Crit Care Med* **26**(12): 2021-2028.

Pei, Y, Tuschl, T (2006) On the art of identifying effective and specific siRNAs. *Nat Methods* **3**(9): 670-676.

Pellegrini, S, Dusanter-Fourt, I (1997) The structure, regulation and function of the Janus kinases (JAKs) and the signal transducers and activators of transcription (STATs). *European journal of biochemistry / FEBS* **248**(3): 615-633.

Pelletier, S, Duhamel, F, Coulombe, P, Popoff, MR, Meloche, S (2003) Rho family GTPases are required for activation of Jak/STAT signaling by G protein-coupled receptors. *Molecular and cellular biology* **23**(4): 1316-1333.

Perrier, C, Rutgeerts, P (2011) Cytokine blockade in inflammatory bowel diseases. *Immunotherapy* **3**(11): 1341-1352.

Perrotta, I, Brunelli, E, Sciangula, A, Conforti, F, Perrotta, E, Tripepi, S, Donato, G, Cassese, M (2011) iNOS induction and PARP-1 activation in human atherosclerotic lesions: an immunohistochemical and ultrastructural approach. *Cardiovasc Pathol* **20**(4): 195-203.

Pestka, S, Krause, CD, Walter, MR (2004) Interferons, interferon-like cytokines, and their receptors. *Immunol Rev* **202**: 8-32.

Pestka, S, Langer, JA, Zoon, KC, Samuel, CE (1987) Interferons and their actions. *Annual review of biochemistry* **56**: 727-777.

Pfaffl, MW (2001) A new mathematical model for relative quantification in real-time RT-PCR. *Nucleic acids research* **29**(9): e45.

Pfaffl, MW, Tichopad, A, Prgomet, C, Neuvians, TP (2004) Determination of stable housekeeping genes, differentially regulated target genes and sample integrity: BestKeeper--Excel-based tool using pair-wise correlations. *Biotechnol Lett* **26**(6): 509-515.

Pfeffer, LM, Dinarello, CA, Herberman, RB, Williams, BR, Borden, EC, Bordens, R, Walter, MR, Nagabhushan, TL, Trotta, PP, Pestka, S (1998) Biological properties of recombinant alpha-interferons: 40th anniversary of the discovery of interferons. *Cancer Res* **58**(12): 2489-2499.

Poussin, C, Foti, M, Carpentier, JL, Pugin, J (1998) CD14-dependent endotoxin internalization via a macropinocytic pathway. *The Journal of biological chemistry* **273**(32): 20285-20291.

Prchal-Murphy, M, Semper, C, Lassnig, C, Wallner, B, Gausterer, C, Teppner-Klymiuk, I, Kobolak, J, Muller, S, Kolbe, T, Karaghiosoff, M, Dinnyes, A, Rulicke, T, Leitner, NR, Strobl, B, Muller, M (2012) TYK2 kinase activity is required for functional type I interferon responses in vivo. *PLoS One* **7**(6): e39141.

Pufahl, RA, Nanjappan, PG, Woodard, RW, Marletta, MA (1992) Mechanistic probes of N-hydroxylation of L-arginine by the inducible nitric oxide synthase from murine macrophages. *Biochemistry*. **31**(29): 6822-6828.

Qian, J, You, H, Zhu, Q, Ma, S, Zhou, Y, Zheng, Y, Liu, J, Kuang, D, Gu, Y, Hao, C, Ding, F (2013) Nitrotyrosine level was associated with mortality in patients with acute kidney injury. *PLoS One* **8**(11): e79962.

Quiroz, FG, Posada, OM, Gallego-Perez, D, Higuera-Castro, N, Sarassa, C, Hansford, DJ, Agudelo-Florez, P, Lopez, LE (2010) Housekeeping gene stability influences the quantification of osteogenic markers during stem cell differentiation to the osteogenic lineage. *Cytotechnology* **62**(2): 109-120.

Rabier, D, Narcy, C, Bardet, J, Parvy, P, Saudubray, JM, Kamoun, P (1991) Arginine remains an essential amino acid after liver transplantation in urea cycle enzyme deficiencies. *J Inherit Metab Dis* **14**(3): 277-280.

Radomski, MW, Palmer, RM, Moncada, S (1987) The role of nitric oxide and cGMP in platelet adhesion to vascular endothelium. *Biochem Biophys Res Commun* **148**(3): 1482-1489.

Raghavan, SA, Dikshit, M (2001) L-citrulline mediated relaxation in the control and lipopolysaccharide-treated rat aortic rings. *Eur J Pharmacol.* **431**(1): 61-69.

Ramagopal, MV, Leighton, HJ (1989) Analysis of the presence of postjunctional alpha-2 adrenoceptors in the rat anococcygeus muscle. *J Pharmacol Exp Ther.* **250**(2): 492-499.

Reade, MC, Clark, MF, Young, JD, Boyd, CA (2002) Increased cationic amino acid flux through a newly expressed transporter in cells overproducing nitric oxide from patients with septic shock. *Clin Sci (Lond)* **102**(6): 645-650.

Reddy, D, Lancaster, JRJ, Cornforth, DP (1983) Nitrite inhibition of Clostridium botulinum: electron spin resonance detection of iron-nitric oxide complexes. *Science* **221**(4612): 769-770.

Reif, A, Frohlich, LG, Kotsonis, P, Frey, A, Bommel, HM, Wink, DA, Pfeleiderer, W, Schmidt, HHHW (1999) Tetrahydrobiopterin Inhibits Monomerization and Is Consumed during Catalysis in Neuronal NO Synthase. *J. Biol. Chem.* **274**(35): 24921-24929.

Reimold, AM (2003) New indications for treatment of chronic inflammation by TNF-alpha blockade. *Am J Med Sci* **325**(2): 75-92.

Reynolds, A, Anderson, EM, Vermeulen, A, Fedorov, Y, Robinson, K, Leake, D, Karpilow, J, Marshall, WS, Khvorova, A (2006) Induction of the interferon response by siRNA is cell type- and duplex length-dependent. *RNA* **12**(6): 988-993.

Reynolds, A, Leake, D, Boese, Q, Scaringe, S, Marshall, WS, Khvorova, A (2004) Rational siRNA design for RNA interference. *Nat Biotechnol* **22**(3): 326-330.

Rimele, TJ, Sturm, RJ, Adams, LM, Henry, DE, Heaslip, RJ, Weichman, BM, Grimes, D (1988) Interaction of neutrophils with vascular smooth muscle: identification of a neutrophil-derived relaxing factor. *J Pharmacol Exp Ther.* **245**(1): 102-111.

Rodriguez-Linares, B, Watson, SP (1994) Phosphorylation of JAK2 in thrombin-stimulated human platelets. *FEBS letters* **352**(3): 335-338.

Romero-Bermejo, FJ, Ruiz-Bailen, M, Gil-Cebrian, J, Huertos-Ranchal, MJ (2011) Sepsis-induced cardiomyopathy. *Curr Cardiol Rev* **7**(3): 163-183.

Rose, WC, Haines, WJ, Warner, DT (1954) The amino acid requirements of man. V. The role of lysine, arginine, and tryptophan. *J Biol Chem.* ;(): **206**(1): 421-430.

Ross, R (1999) Atherosclerosis is an inflammatory disease. *American heart journal* **138**(5 Pt 2): S419-420.

Rothenberg, ME, Doepker, MP, Lewkowich, IP, Chiamonte, MG, Stringer, KF, Finkelman, FD, MacLeod, CL, Ellies, LG, Zimmermann, N (2006) Cationic amino acid transporter 2 regulates inflammatory homeostasis in the lung. *Proceedings of the National Academy of Sciences of the United States of America* **103**(40): 14895-14900.

Rotoli, BM, Bussolati, O, Sala, R, Barilli, A, Talarico, E, Gazzola, GC, Dall'Asta, V (2004) INF[gamma] stimulates arginine transport through system y+L in human monocytes. *FEBS letters* **571**(1-3): 177-181.

Roy, SK, Wachira, SJ, Weihua, X, Hu, J, Kalvakolanu, DV (2000) CCAAT/enhancer-binding protein-beta regulates interferon-induced transcription through a novel element. *The Journal of biological chemistry* **275**(17): 12626-12632.

Sahin-Toth, M, Kukor, Z, Toth, M (1997) Tetrahydrobiopterin preferentially stimulates activity and promotes subunit aggregation of membrane-bound calcium-dependent nitric oxide synthase in human placenta. *Mol. Hum. Reprod.* **3**(4): 293-298.

Salh, B, Wagey, R, Marotta, A, Tao, JS, Pelech, S (1998) Activation of Phosphatidylinositol 3-Kinase, Protein Kinase B, and p70 S6 Kinases in Lipopolysaccharide-Stimulated Raw 264.7 Cells: Differential Effects of Rapamycin, Ly294002, and Wortmannin on Nitric Oxide Production. *J Immunol* **161**(12): 6947-6954.

Sato, H, Fujiwara, M, Bannai, S (1992) Effect of lipopolysaccharide on transport and metabolism of arginine in mouse peritoneal macrophages. *J Leukoc Biol* **52**(2): 161-164.

Saura, M, Perez-Sala, D, Canada, F, Lamas, S (1996) Role of Tetrahydrobiopterin Availability in the Regulation of Nitric-oxide Synthase Expression in Human Mesangial Cells. *J. Biol. Chem.* **271**(24): 14290-14295.

Schindler, C, Darnell, JE, Jr. (1995) Transcriptional responses to polypeptide ligands: the JAK-STAT pathway. *Annual review of biochemistry* **64**: 621-651.

Schindler, CW (2002) Series introduction. JAK-STAT signaling in human disease. *The Journal of clinical investigation* **109**(9): 1133-1137.

Schmidlin, A, Wiesinger, H (1995) Stimulation of Arginine Transport and Nitric Oxide Production by Lipopolysaccharide Is Mediated by Different Signaling Pathways in Astrocytes. *J Neurochem* **65**(2): 590-594.

Schmidt, HH, Seifert, R, Bohme, E (1989) Formation and release of nitric oxide from human neutrophils and HL-60 cells induced by a chemotactic peptide, platelet activating factor and leukotriene B4. *FEBS letters* **244**(2): 357-360.

Schmittgen, TD, Zakrajsek, BA (2000) Effect of experimental treatment on housekeeping gene expression: validation by real-time, quantitative RT-PCR. *J Biochem Biophys Methods* **46**(1-2): 69-81.

Schneider, AG, Abi Abdallah, DS, Butcher, BA, Denkers, EY (2013) Toxoplasma gondii triggers phosphorylation and nuclear translocation of dendritic cell STAT1 while simultaneously blocking IFN $\gamma$ -induced STAT1 transcriptional activity. *PLoS One* **8**(3): e60215.

Schott, CA, Gray, GA, Stoclet, JC (1993a) Dependence of endotoxin-induced vascular hyporeactivity on extracellular L-arginine. *British journal of pharmacology* **108**(1): 38-43.

Schott, CA, Gray, GA, Stoclet, JC (1993b) Dependence of endotoxin-induced vascular hyporeactivity on extracellular L-arginine. *Br J Pharmacol.* **108**(1): 38-43.

Schott, CA, Vetrovsky, P, Stoclet, JC (1993c) Cationic amino acids inhibit the effects of L-arginine in rat aorta exposed to lipopolysaccharide. *European journal of pharmacology* **236**(1): 155-157.

Schulte, W, Bernhagen, J, Bucala, R (2013) Cytokines in sepsis: potent immunoregulators and potential therapeutic targets--an updated view. *Mediators Inflamm* **2013**: 165974.

Schumann, RR, Pfeil, D, Lamping, N, Kirschning, C, Scherzinger, G, Schlag, P, Karawajew, L, Herrmann, F (1996) Lipopolysaccharide induces the rapid tyrosine phosphorylation of the mitogen-activated protein kinases erk-1 and p38 in cultured human vascular endothelial cells requiring the presence of soluble CD14. *Blood* **87**(7): 2805-2814.

Schuster, A, Thakur, A, Wang, Z, Borowski, AG, Thomas, JD, Tang, WH (2012) Increased exhaled nitric oxide levels after exercise in patients with chronic systolic heart failure with pulmonary venous hypertension. *J Card Fail* **18**(10): 799-803.

Schwartz, IF, HersHKovitz, R, Iaina, A, Gnessin, E, Wollman, Y, Chernichowski, T, Blum, M, Levo, Y, Schwartz, D (2002) Garlic attenuates nitric oxide production in rat cardiac myocytes through inhibition of inducible nitric oxide synthase and the arginine transporter CAT-2 (cationic amino acid transporter-2). *Clin Sci (Lond)* **102**(5): 487-493.

Schwartz, IF, Schwartz, D, Wollman, Y, Chernichowski, T, Blum, M, Levo, Y, Iaina, A (2001) Tetrahydrobiopterin augments arginine transport in rat cardiac myocytes through modulation of CAT-2 mRNA. *J Lab Clin Med* **137**(5): 356-362.

Schwarz, DS, Hutvagner, G, Du, T, Xu, Z, Aronin, N, Zamore, PD (2003) Asymmetry in the assembly of the RNAi enzyme complex. *Cell* **115**(2): 199-208.

Scott-Burden, T, Elizondo, E, Ge, T, Boulanger, C, Vanhoutte, P (1994) Simultaneous activation of adenylyl cyclase and protein kinase C induces production of nitric oxide by vascular smooth muscle cells. *Mol Pharmacol* **46**(2): 274-282.

Seguin, MC, Klotz, FW, Schneider, I, Weir, JP, Goodbary, M, Slayter, M, Raney, JJ, Aniagolu, JU, Green, SJ (1994) Induction of nitric oxide synthase protects against malaria in mice exposed to irradiated Plasmodium berghei infected mosquitoes: involvement of interferon gamma and CD8+ T cells. *The Journal of experimental medicine* **180**(1): 353-358.

Selvey, S, Thompson, EW, Matthaei, K, Lea, RA, Irving, MG, Griffiths, LR (2001) Beta-actin--an unsuitable internal control for RT-PCR. *Mol Cell Probes* **15**(5): 307-311.

Semizarov, D, Frost, L, Sarthy, A, Kroeger, P, Halbert, DN, Fesik, SW (2003) Specificity of short interfering RNA determined through gene expression signatures. *Proceedings of the National Academy of Sciences of the United States of America* **100**(11): 6347-6352.

Sessa, W, Harrison, J, Barber, C, Zeng, D, Durieux, M, D'Angelo, D, Lynch, K, Peach, M (1992) Molecular cloning and expression of a cDNA encoding endothelial cell nitric oxide synthase. *J. Biol. Chem.* **267**(22): 15274-15276.

Shankar, P, Manjunath, N, Lieberman, J (2005) The prospect of silencing disease using RNA interference. *JAMA* **293**(11): 1367-1373.

Shen, WG (2004) RNA interference and its current application in mammals. *Chin Med J (Engl)* **117**(7): 1084-1091.

Sherman, MP, Griscavage, JM, Ignarro, LJ (1992) Nitric oxide-mediated neuronal injury in multiple sclerosis. *Medical Hypotheses* **39**(2): 143-146.

Sheta, EA, McMillan, K, Masters, BS (1994) Evidence for a bidomain structure of constitutive cerebellar nitric oxide synthase. *J Biol Chem.* **269**(21): 15147-15153.

Shibuki, K, Okada, D (1991) Endogenous nitric oxide release required for long-term synaptic depression in the cerebellum. *Nature.* **349**(6307): 326-328.

Shimoda, K, Tsutsui, H, Aoki, K, Kato, K, Matsuda, T, Numata, A, Takase, K, Yamamoto, T, Nukina, H, Hoshino, T, Asano, Y, Gondo, H, Okamura, T, Okamura, S, Nakayama, K, Nakanishi, K, Niho, Y, Harada, M (2002) Partial impairment of interleukin-12 (IL-12) and IL-18 signaling in Tyk2-deficient mice. *Blood* **99**(6): 2094-2099.

Siebert, PD, Larrick, JW (1992) Competitive PCR. *Nature* **359**(6395): 557-558.

Silva, CM, Lu, H, Weber, MJ, Thorner, MO (1994) Differential tyrosine phosphorylation of JAK1, JAK2, and STAT1 by growth hormone and interferon-gamma in IM-9 cells. *The Journal of biological chemistry* **269**(44): 27532-27539.

Silvennoinen, O, Ihle, JN, Schlessinger, J, Levy, DE (1993a) Interferon-induced nuclear signalling by Jak protein tyrosine kinases. *Nature* **366**(6455): 583-585.

Silvennoinen, O, Ihle, JN, Schlessinger, J, Levy, DE (1993b) Interferon-induced nuclear signalling by Jak protein tyrosine kinases. *Nature* **366**(6455): 583-585.

Simmons, WW, Closs, EI, Cunningham, JM, Smith, TW, Kelly, RA (1996) Cytokines and insulin induce cationic amino acid transporter (CAT) expression in cardiac myocytes. Regulation of L-arginine transport and no production by CAT-1, CAT-2A, and CAT-2B. *J Biol Chem* **271**(20): 11694-11702.

Singer, I, Kawka, D, Scott, S, Weidner, J, Mumford, R, Riehl, T, Stenson, W (1996) Expression of inducible nitric oxide synthase and nitrotyrosine in colonic epithelium in inflammatory bowel disease. *Gastroenterology* **111**(4): 871-885.

Skalli, O, Ropraz, P, Trzeciak, A, Benzonana, G, Gillissen, D, Gabbiani, G (1986) A monoclonal antibody against alpha-smooth muscle actin: a new probe for smooth muscle differentiation. *J. Cell Biol.* **103**(6): 2787-2796.

Slater, TF, Sawyer, B, Straeuli, U (1963) Studies on succinate-tetrazolium reductase systems. III. Points of coupling of four different tetrazolium salts. *Biochim Biophys Acta.* **77**: 383-393.

Sloan, JL, Mager, S (1999) Cloning and functional expression of a human Na(+) and Cl(-)-dependent neutral and cationic amino acid transporter B(0+). *The Journal of biological chemistry* **274**(34): 23740-23745.

Smith, MA, Richey Harris, PL, Sayre, LM, Beckman, JS, Perry, G (1997) Widespread peroxynitrite-mediated damage in Alzheimer's disease. *J Neurosci* **17**(8): 2653-2657.

Smith, PK, Krohn, RI, Hermanson, GT, Mallia, AK, Gartner, FH, Provenzano, MD, Fujimoto, EK, Goeke, NM, Olson, BJ, Klenk, DC (1985) Measurement of Protein Using Bicinchoninic Acid. *Analytical Biochemistry* **150**: 76-85.

Sneddon, JM, Vane, JR (1988) Endothelium-derived relaxing factor reduces platelet adhesion to bovine endothelial cells. *Proc Natl Acad Sci U S A.* **85**(8): 2800-2804.

Spink, J, Cohen, J, Evans, TJ (1995) The cytokine responsive vascular smooth muscle cell enhancer of inducible nitric oxide synthase. Activation by nuclear factor-kappa B. *The Journal of biological chemistry* **270**(49): 29541-29547.

Stark, GR, Kerr, IM, Williams, BR, Silverman, RH, Schreiber, RD (1998) How cells respond to interferons. *Annual review of biochemistry* **67**: 227-264.

Starr, R, Hilton, DJ (1999) Negative regulation of the JAK/STAT pathway. *Bioessays* **21**(1): 47-52.

Stathopoulos, PB, Lu, X, Shen, J, Scott, JA, Hammond, JR, McCormack, DG, Arnold, JM, Feng, Q (2001) Increased L-arginine uptake and inducible nitric oxide synthase activity in aortas of rats with heart failure. *American journal of physiology* **280**(2): H859-867.

Steffan, NM, Bren, GD, Frantz, B, Tocci, MJ, O'Neill, EA, Paya, CV (1995) Regulation of I $\kappa$ B alpha phosphorylation by PKC- and Ca(2+)-dependent signal transduction pathways. *J Immunol* **155**(10): 4685-4691.

Stempelj, M, Kedinger, M, Augenlicht, L, Klampfer, L (2007) Essential role of the JAK/STAT1 signaling pathway in the expression of inducible nitric-oxide synthase in intestinal epithelial cells and its regulation by butyrate. *The Journal of biological chemistry* **282**(13): 9797-9804.

Stevens, BR, Kakuda, DK, Yu, K, Waters, M, Vo, CB, Raizada, MK (1996) Induced nitric oxide synthesis is dependent on induced alternatively spliced CAT-2 encoding L-arginine transport in brain astrocytes. *The Journal of biological chemistry* **271**(39): 24017-24022.

Strobl, B, Stoiber, D, Sexl, V, Mueller, M (2011) Tyrosine kinase 2 (TYK2) in cytokine signalling and host immunity. *Front Biosci* **16**: 3214-3232.

Suzuki, T, Higgins, PJ, Crawford, DR (2000) Control selection for RNA quantitation. *Biotechniques* **29**(2): 332-337.

Szabo, C, Mitchell, JA, Thiemermann, C, Vane, JR (1993) Nitric oxide-mediated hyporeactivity to noradrenaline precedes the induction of nitric oxide synthase in endotoxin shock. *British journal of pharmacology* **108**(3): 786-792.

Tachado, SD, Zhang, J, Zhu, J, Patel, N, Koziel, H (2005) HIV impairs TNF-alpha release in response to Toll-like receptor 4 stimulation in human macrophages in vitro. *American journal of respiratory cell and molecular biology* **33**(6): 610-621.

Takasaki, S (2010) Efficient prediction methods for selecting effective siRNA sequences. *Comput Biol Med* **40**(2): 149-158.

Takemoto, M, Liao, JK (2001) Pleiotropic effects of 3-hydroxy-3-methylglutaryl coenzyme a reductase inhibitors. *Arteriosclerosis, thrombosis, and vascular biology* **21**(11): 1712-1719.

Tanaka, S, Fukumoto, Y, Nochioka, K, Minami, T, Kudo, S, Shiba, N, Takai, Y, Williams, CL, Liao, JK, Shimokawa, H (2013) Statins Exert the Pleiotropic Effects Through Small GTP-Binding Protein Dissociation Stimulator Upregulation With a Resultant Rac1 Degradation. *Arteriosclerosis, thrombosis, and vascular biology* **33**(7): 1591-1600.

Taniguchi, T (1995) Cytokine signaling through nonreceptor protein tyrosine kinases. *Science (New York, N. Y)* **268**(5208): 251-255.

Tate, SS, Yan, N, Udenfriend, S (1992) Expression cloning of a Na(+)-independent neutral amino acid transporter from rat kidney. *Proceedings of the National Academy of Sciences of the United States of America* **89**(1): 1-5.

Taylor, BS, de Vera, ME, Ganster, RW, Wang, Q, Shapiro, RA, Morris Jr., SM, Billiar, TR, Geller, DA (1998) Multiple NF-kappa B Enhancer Elements Regulate Cytokine Induction of the Human Inducible Nitric Oxide Synthase Gene. *J. Biol. Chem.* **273**(24): 15148-15156.

Taylor, S, Wakem, M, Dijkman, G, Alsarraj, M, Nguyen, M (2010) A practical approach to RT-qPCR-Publishing data that conform to the MIQE guidelines. *Methods* **50**(4): S1-5.

Tentolouris, C, Tousoulis, D, Stefanadis, C (2004) L-arginine "paradox" in coronary atherosclerosis. *Circulation* **110**(7): e71.

Thellin, O, Zorzi, W, Lakaye, B, De Borman, B, Coumans, B, Hennen, G, Grisar, T, Igout, A, Heinen, E (1999) Housekeeping genes as internal standards: use and limits. *J Biotechnol* **75**(2-3): 291-295.

Thiemermann, C, Szabo, C, Mitchell, JA, Vane, JR (1993) Vascular hyporeactivity to vasoconstrictor agents and hemodynamic decompensation in hemorrhagic shock is mediated by nitric oxide. *Proc Natl Acad Sci U S A.* **90**(1): 267-271.

Thiemermann, C, Vane, J (1990) Inhibition of nitric oxide synthesis reduces the hypotension induced by bacterial lipopolysaccharides in the rat in vivo. *European journal of pharmacology* **182**(3): 591-595.

Thompson, JE, Cubbon, RM, Cummings, RT, Wicker, LS, Frankshun, R, Cunningham, BR, Cameron, PM, Meinke, PT, Liverton, N, Weng, Y, DeMartino, JA (2002) Photochemical preparation of a pyridone containing tetracycle: a Jak protein kinase inhibitor. *Bioorg Med Chem Lett* **12**(8): 1219-1223.

Titheradge, MA (1999) Nitric oxide in septic shock. *Biochim Biophys Acta* **1411**(2-3): 437-455.

Tobin, AM, Kirby, B (2005) TNF alpha inhibitors in the treatment of psoriasis and psoriatic arthritis. *BioDrugs* **19**(1): 47-57.

Toda, N, Tanabe, S, Nakanishi, S (2011) Nitric oxide-mediated coronary flow regulation in patients with coronary artery disease: recent advances. *Int J Angiol* **20**(3): 121-134.

Tousoulis, D, Tentolouris, C, Crake, T, Katsimaglis, G, Stefanadis, C, Toutouzas, P, Davies, GJ (1999) Effects of L- and D-arginine on the basal tone of human diseased coronary arteries and their responses to substance P. *Heart (British Cardiac Society)* **81**(5): 505-511.

Tsoyi, K, Kim, HJ, Shin, JS, Kim, DH, Cho, HJ, Lee, SS, Ahn, SK, Yun-Choi, HS, Lee, JH, Seo, HG, Chang, KC (2008) HO-1 and JAK-2/STAT-1 signals are involved in preferential inhibition of iNOS over COX-2 gene expression by newly synthesized tetrahydroisoquinoline alkaloid, CKD712, in cells activated with lipopolysacchride. *Cell Signal* **20**(10): 1839-1847.

Tuschl, T, Zamore, PD, Lehmann, R, Bartel, DP, Sharp, PA (1999) Targeted mRNA degradation by double-stranded RNA in vitro. *Genes & development* **13**(24): 3191-3197.

Uehata, M, Ishizaki, T, Satoh, H, Ono, T, Kawahara, T, Morishita, T, Tamakawa, H, Yamagami, K, Inui, J, Maekawa, M, Narumiya, S (1997) Calcium sensitization

of smooth muscle mediated by a Rho-associated protein kinase in hypertension. *Nature* **389**(6654): 990-994.

Ui-Tei, K, Naito, Y, Takahashi, F, Haraguchi, T, Ohki-Hamazaki, H, Juni, A, Ueda, R, Saigo, K (2004) Guidelines for the selection of highly effective siRNA sequences for mammalian and chick RNA interference. *Nucleic acids research* **32**(3): 936-948.

Ulhaq, S, Chinje, EC, Naylor, MA, Jaffar, M, Stratford, IJ, Threadgill, MD (1999) Heterocyclic analogues of L-citrulline as inhibitors of the isoforms of nitric oxide synthase (NOS) and identification of N(delta)-(4,5-dihydrothiazol-2-yl)ornithine as a potent inhibitor. *Bioorg Med Chem* **7**(9): 1787-1796.

Ullrich, R, Scherrer-Crosbie, M, Bloch, KD, Ichinose, F, Nakajima, H, Picard, MH, Zapol, WM, Quezado, ZM (2000) Congenital deficiency of nitric oxide synthase 2 protects against endotoxin-induced myocardial dysfunction in mice. *Circulation* **102**(12): 1440-1446.

Uze, G, Lutfalla, G, Mogensen, KE (1995) Alpha and beta interferons and their receptor and their friends and relations. *J Interferon Cytokine Res* **15**(1): 3-26.

Vadiveloo, PK, Vairo, G, Hertzog, P, Kola, I, Hamilton, JA (2000) Role of type I interferons during macrophage activation by lipopolysaccharide. *Cytokine* **12**(11): 1639-1646.

Vallance, P, Moncada, S (1993) Role of endogenous nitric oxide in septic shock. *New Horiz* **1**(1): 77-86.

van der Wal, AC, Becker, AE, van der Loos, CM, Das, PK (1994) Site of intimal rupture or erosion of thrombosed coronary atherosclerotic plaques is characterized by an inflammatory process irrespective of the dominant plaque morphology. *Circulation* **89**(1): 36-44.

Vanderkooi, JM, Wright, WW, Erecinska, M (1994) Nitric oxide diffusion coefficients in solutions, proteins and membranes determined by phosphorescence. *Biochimica et biophysica acta* **1207**(2): 249-254.

Vandesompele, J, De Preter, K, Pattyn, F, Poppe, B, Van Roy, N, De Paepe, A, Speleman, F (2002) Accurate normalization of real-time quantitative RT-PCR data by geometric averaging of multiple internal control genes. *Genome biology* **3**(7): RESEARCH0034.

Vasdev, S, Gill, V (2008) The antihypertensive effect of arginine. *Int J Angiol* **17**(1): 7-22.

Velazquez, L, Fellous, M, Stark, GR, Pellegrini, S (1992) A protein tyrosine kinase in the interferon alpha/beta signaling pathway. *Cell* **70**(2): 313-322.

Verrey, F, Closs, EI, Wagner, CA, Palacin, M, Endou, H, Kanai, Y (2004) CATs and HATs: the SLC7 family of amino acid transporters. *Pflugers Arch* **447**(5): 532-542.

Visigalli, R, Barilli, A, Bussolati, O, Sala, R, Gazzola, GC, Parolari, A, Tremoli, E, Simon, A, Closs, EI, Dall'Asta, V (2007) Rapamycin stimulates arginine influx through CAT2 transporters in human endothelial cells. *Biochimica et biophysica acta* **1768**(6): 1479-1487.

Visigalli, R, Barilli, A, Parolari, A, Sala, R, Rotoli, BM, Bussolati, O, Gazzola, GC, Dall'Asta, V (2010) Regulation of arginine transport and metabolism by protein kinase Calpha in endothelial cells: stimulation of CAT2 transporters and arginase activity. *Journal of molecular and cellular cardiology* **49**(2): 260-270.

Vital, AL, Goncalo, M, Cruz, MT, Figueiredo, A, Duarte, CB, Lopes, MC (2003) Dexamethasone prevents granulocyte-macrophage colony-stimulating factor-induced nuclear factor-kappaB activation, inducible nitric oxide synthase expression and nitric oxide production in a skin dendritic cell line. *Mediators Inflamm* **12**(2): 71-78.

Wallace, RB, Johnson, MJ, Hirose, T, Miyake, T, Kawashima, EH, Itakura, K (1981) The use of synthetic oligonucleotides as hybridization probes. II. Hybridization of oligonucleotides of mixed sequence to rabbit beta-globin DNA. *Nucleic acids research* **9**(4): 879-894.

Wang, H, Kavanaugh, MP, North, RA, Kabat, D (1991) Cell-surface receptor for ecotropic murine retroviruses is a basic amino-acid transporter. *Nature* **352**(6337): 729-731.

Wang, LH, Kirken, RA, Erwin, RA, Yu, C-R, Farrar, WL (1999) JAK3, STAT, and MAPK Signaling Pathways as Novel Molecular Targets for the Tyrphostin AG-490 Regulation of IL-2-Mediated T Cell Response. *J Immunol* **162**(7): 3897-3904.

Wang, Z, Yang, H, Tachado, SD, Capo-Aponte, JE, Bildin, VN, Koziel, H, Reinach, PS (2006) Phosphatase-mediated crosstalk control of ERK and p38 MAPK signaling in corneal epithelial cells. *Investigative ophthalmology & visual science* **47**(12): 5267-5275.

Wassmann, S, Laufs, U, Muller, K, Konkol, C, Ahlbory, K, Baumer, AT, Linz, W, Bohm, M, Nickenig, G (2002) Cellular antioxidant effects of atorvastatin in vitro and in vivo. *Arteriosclerosis, thrombosis, and vascular biology* **22**(2): 300-305.

- Watling, D, Guschin, D, Muller, M, Silvennoinen, O, Witthuhn, BA, Quelle, FW, Rogers, NC, Schindler, C, Stark, GR, Ihle, JN, et al. (1993) Complementation by the protein tyrosine kinase JAK2 of a mutant cell line defective in the interferon-gamma signal transduction pathway. *Nature* **366**(6451): 166-170.
- Wei, CC, Wang, ZQ, Tejero, J, Yang, YP, Hemann, C, Hille, R, Stuehr, DJ (2008) Catalytic reduction of a tetrahydrobiopterin radical within nitric-oxide synthase. *The Journal of biological chemistry* **283**(17): 11734-11742.
- Weisz, A, Oguchi, S, Cicatiello, L, Esumi, H (1994) Dual mechanism for the control of inducible-type NO synthase gene expression in macrophages during activation by interferon-gamma and bacterial lipopolysaccharide. Transcriptional and post-transcriptional regulation. *The Journal of biological chemistry* **269**(11): 8324-8333.
- Wells, RG, Lee, WS, Kanai, Y, Leiden, JM, Hediger, MA (1992) The 4F2 antigen heavy chain induces uptake of neutral and dibasic amino acids in *Xenopus* oocytes. *The Journal of biological chemistry* **267**(22): 15285-15288.
- Wen, Z, Zhong, Z, Darnell, JE, Jr. (1995) Maximal activation of transcription by Stat1 and Stat3 requires both tyrosine and serine phosphorylation. *Cell* **82**(2): 241-250.
- Westenberger, U, Thanner, S, Ruf, HH, Gersonde, K, Sutter, G, Trentz, O (1990) Formation of free radicals and nitric oxide derivative of hemoglobin in rats during shock syndrome. *Free Radic Res Commun.* **11**(1-3): 167-178.
- White, M, Gazzola, G, Christensen, H (1982) Cationic amino acid transport into cultured animal cells. I. Influx into cultured human fibroblasts. *J. Biol. Chem.* **257**(8): 4443-4449.
- Whitehead, KA, Langer, R, Anderson, DG (2009) Knocking down barriers: advances in siRNA delivery. *Nat Rev Drug Discov* **8**(2): 129-138.
- Wileman, S, Mann, G, Baydoun, A (1995) Induction of L-arginine transport and nitric oxide synthase in vascular smooth muscle cells: synergistic actions of pro-inflammatory cytokines and bacterial lipopolysaccharide. *Br J Pharmacol* **116**(8): 3243-3250.
- Wileman, SM, Mann, GE, Pearson, JD, Baydoun, AR (2003) Role of L-citrulline transport in nitric oxide synthesis in rat aortic smooth muscle cells activated with LPS and interferon-gamma. *British journal of pharmacology* **140**(1): 179-185.
- Wilks, AF, Harpur, AG, Kurban, RR, Ralph, SJ, Zurcher, G, Ziemiecki, A (1991) Two novel protein-tyrosine kinases, each with a second phosphotransferase-

related catalytic domain, define a new class of protein kinase. *Molecular and cellular biology* **11**(4): 2057-2065.

Wink, DA, Osawa, Y, Darbyshire, JF, Jones, CR, Eshenaur, SC, Nims, RW (1993) Inhibition of cytochromes P450 by nitric oxide and a nitric oxide-releasing agent. *Arch Biochem Biophys* **300**(1): 115-123.

Winlaw, DS, Smythe, GA, Keogh, AM, Schyvens, CG, Spratt, PM, Macdonald, PS (1994) Increased nitric oxide production in heart failure. *Lancet* **344**(8919): 373-374.

Witthuhn, BA, Quelle, FW, Silvennoinen, O, Yi, T, Tang, B, Miura, O, Ihle, JN (1993) JAK2 associates with the erythropoietin receptor and is tyrosine phosphorylated and activated following stimulation with erythropoietin. *Cell* **74**(2): 227-236.

Wolf, S, Janzen, A, Vekony, N, Martine, U, Strand, D, Closs, EI (2002) Expression of solute carrier 7A4 (SLC7A4) in the plasma membrane is not sufficient to mediate amino acid transport activity. *The Biochemical journal* **364**(Pt 3): 767-775.

Woodard, MH, Dunn, WA, Laine, RO, Malandro, M, McMahon, R, Simell, O, Block, ER, Kilberg, MS (1994) Plasma membrane clustering of system y<sup>+</sup> (CAT-1) amino acid transporter as detected by immunohistochemistry. *The American journal of physiology* **266**(5 Pt 1): E817-824.

Woolacott, N, Bravo Vergel, Y, Hawkins, N, Kainth, A, Khadjesari, Z, Misso, K, Light, K, Asseburg, C, Palmer, S, Claxton, K, Bruce, I, Sculpher, M, Riemsma, R (2006) Etanercept and infliximab for the treatment of psoriatic arthritis: a systematic review and economic evaluation. *Health technology assessment (Winchester, England)* **10**(31): iii-iv, xiii-xvi, 1-239.

Woolf, N (1990) Pathology of atherosclerosis. *British medical bulletin* **46**(4): 960-985.

Wright, SD, Ramos, RA, Tobias, PS, Ulevitch, RJ, Mathison, JC (1990) CD14, a receptor for complexes of lipopolysaccharide (LPS) and LPS binding protein. *Science (New York, N.Y)* **249**(4975): 1431-1433.

Wu, G, Meininger, CJ (2002) Regulation of nitric oxide synthesis by dietary factors. *Annual review of nutrition* **22**: 61-86.

Wu, GY, Brosnan, JT (1992) Macrophages can convert citrulline into arginine. *Biochem J.* **281**(Pt 1): 45-48.

Wu, JY, Robinson, D, Kung, HJ, Hatzoglou, M (1994) Hormonal regulation of the gene for the type C ecotropic retrovirus receptor in rat liver cells. *J Virol.* **68**(3): 1615-1623.

Xiao, H, Qin, X, Ping, D, Zuo, K Inhibition of Rho and Rac geranylgeranylation by atorvastatin is critical for preservation of endothelial junction integrity. *PLoS One* **8**(3): e59233.

Xie, QW, Kashiwabara, Y, Nathan, C (1994) Role of transcription factor NF-kappa B/Rel in induction of nitric oxide synthase. *The Journal of biological chemistry* **269**(7): 4705-4708.

Xie, QW, Whisnant, R, Nathan, C (1993) Promoter of the mouse gene encoding calcium-independent nitric oxide synthase confers inducibility by interferon gamma and bacterial lipopolysaccharide. *The Journal of experimental medicine* **177**(6): 1779-1784.

Xingang, J, Lu, Z, Han, Q Mini-clusters with mean probabilities for identifying effective siRNAs. *BMC Res Notes* **5**: 512.

Xu, J, Xie, Z, Reece, R, Pimental, D, Zou, MH (2006) Uncoupling of endothelial nitric oxidase synthase by hypochlorous acid: role of NAD(P)H oxidase-derived superoxide and peroxynitrite. *Arteriosclerosis, thrombosis, and vascular biology* **26**(12): 2688-2695.

Xu, W, Liu, LZ, Loizidou, M, Ahmed, M, Charles, IG (2002) The role of nitric oxide in cancer. *Cell Res* **12**(5-6): 311-320.

Yamada, T, Morishita, S (2005) Accelerated off-target search algorithm for siRNA. *Bioinformatics* **21**(8): 1316-1324.

Yamakado, T, Nishikawa, M, Hidaka, H (1982) Stimulation of human platelet guanylate cyclase by nitroso compounds. *Thromb Res.* **26**(2): 135-140.

Yamamoto, T, Takeda, K, Harada, S, Nakata, T, Azuma, A, Sasaki, S, Nakagawa, M (2003) HMG-CoA reductase inhibitor enhances inducible nitric oxide synthase expression in rat vascular smooth muscle cells; involvement of the Rho/Rho kinase pathway. *Atherosclerosis* **166**(2): 213-222.

Yan, ZQ, Yokota, T, Zhang, W, Hansson, GK (1996) Expression of inducible nitric oxide synthase inhibits platelet adhesion and restores blood flow in the injured artery. *Circulation research* **79**(1): 38-44.

Yang, CH, Tsai, PS, Lee, JJ, Huang, CH, Huang, CJ (2005) NF-kappaB inhibitors stabilize the mRNA of high-affinity type-2 cationic amino acid transporter in LPS-stimulated rat liver. *Acta Anaesthesiol Scand* **49**(4): 468-476.

Yang, RB, Mark, MR, Gray, A, Huang, A, Xie, MH, Zhang, M, Goddard, A, Wood, WI, Gurney, AL, Godowski, PJ (1998) Toll-like receptor-2 mediates lipopolysaccharide-induced cellular signalling. *Nature* **395**(6699): 284-288.

Yang, Z, Harrison, CM, Chuang, GC, Ballinger, SW (2007) The role of tobacco smoke induced mitochondrial damage in vascular dysfunction and atherosclerosis. *Mutat Res* **621**(1-2): 61-74.

Yeh, TC, Pellegrini, S (1999) The Janus kinase family of protein tyrosine kinases and their role in signaling. *Cell Mol Life Sci* **55**(12): 1523-1534.

Yoon, HJ, Jun, CD, Kim, JM, Rim, GN, Kim, HM, Chung, HT (1994) Phorbol ester synergistically increases interferon-gamma-induced nitric oxide synthesis in murine microglial cells. *Neuroimmunomodulation* **1**(6): 377-382.

Yu, H, Liu, Z, Zhou, H, Dai, W, Chen, S, Shu, Y, Feng, J (2012) JAK-STAT pathway modulates the roles of iNOS and COX-2 in the cytoprotection of early phase of hydrogen peroxide preconditioning against apoptosis induced by oxidative stress. *Neurosci Lett* **529**(2): 166-171.

Yui, Y, Hattori, R, Kosuga, K, Eizawa, H, Hiki, K, Kawai, C (1991) Purification of nitric oxide synthase from rat macrophages. *J. Biol. Chem.* **266**(19): 12544-12547.

Zafiriou, O, Hanley, Q, Snyder, G (1989) Nitric oxide and nitrous oxide production and cycling during dissimilatory nitrite reduction by *Pseudomonas perfectomarina*. *J. Biol. Chem.* **264**(10): 5694-5699.

Zamore, PD, Tuschl, T, Sharp, PA, Bartel, DP (2000) RNAi: double-stranded RNA directs the ATP-dependent cleavage of mRNA at 21 to 23 nucleotide intervals. *Cell* **101**(1): 25-33.

Zembowicz, A, Hecker, M, Macarthur, H, Sessa, W, Vane, J (1991) Nitric Oxide and Another Potent Vasodilator are Formed from NG-Hydroxy- L-Arginine by Cultured Endothelial Cells. *PNAS* **88**(24): 11172-11176.

Zhang, F, Iadecola, C (1998a) Temporal characteristics of the protective effect of aminoguanidine on cerebral ischemic damage. *Brain Res* **802**(1-2): 104-110.

Zhang, H, Chen, X, Teng, X, Snead, C, Catravas, JD (1998b) Molecular cloning and analysis of the rat inducible nitric oxide synthase gene promoter in aortic smooth muscle cells. *Biochem Pharmacol* **55**(11): 1873-1880.

Zhang, H, Snead, C, Catravas, JD (2001) Nitric oxide differentially regulates induction of type II nitric oxide synthase in rat vascular smooth muscle cells

versus macrophages. *Arteriosclerosis, thrombosis, and vascular biology* **21**(4): 529-535.

Zhang, S, Zhao, B, Jiang, H, Wang, B, Ma, B (2007) Cationic lipids and polymers mediated vectors for delivery of siRNA. *J Control Release* **123**(1): 1-10.

Zhang, X, Alley, EW, Russell, SW, Morrison, DC (1994) Necessity and sufficiency of beta interferon for nitric oxide production in mouse peritoneal macrophages. *Infect Immun.* **62**(1): 33-40.

Zhang, X, Blenis, J, Li, HC, Schindler, C, Chen-Kiang, S (1995) Requirement of serine phosphorylation for formation of STAT-promoter complexes. *Science (New York, N.Y)* **267**(5206): 1990-1994.

Zhang, X, Laubach, VE, Alley, EW, Edwards, KA, Sherman, PA, Russell, SW, Murphy, WJ (1996) Transcriptional basis for hyporesponsiveness of the human inducible nitric oxide synthase gene to lipopolysaccharide/interferon-gamma. *J Leukoc Biol* **59**(4): 575-585.

Zheng, Y, Qin, H, Frank, SJ, Deng, L, Litchfield, DW, Tefferi, A, Pardanani, A, Lin, FT, Li, J, Sha, B, Benveniste, EN (2011) A CK2-dependent mechanism for activation of the JAK-STAT signaling pathway. *Blood* **118**(1): 156-166.

Zhong, H, Simons, JW (1999) Direct comparison of GAPDH, beta-actin, cyclophilin, and 28S rRNA as internal standards for quantifying RNA levels under hypoxia. *Biochemical and biophysical research communications* **259**(3): 523-526.

Zhou, HJ, Tsai, SY, Tsai, MJ (2003) RNAi technology and its use in studying the function of nuclear receptors and coregulators. *Nucl Recept Signal* **1**: e008.

Zhou, R, Zheng, SX, Tang, W, He, PL, Li, XY, Yang, YF, Li, YC, Geng, JG, Zuo, JP (2006) Inhibition of inducible nitric-oxide synthase expression by (5R)-5-hydroxytryptolide in interferon-gamma- and bacterial lipopolysaccharide-stimulated macrophages. *J Pharmacol Exp Ther* **316**(1): 121-128.

Zhu, Y, Nikolic, D, Van Breemen, RB, Silverman, RB (2005) Mechanism of inactivation of inducible nitric oxide synthase by amidines. Irreversible enzyme inactivation without inactivator modification. *J Am Chem Soc* **127**(3): 858-868.

Zhu, ZG, Jin, H, Yu, PJ, Tian, YX, Zhang, JJ, Wu, SG (2013) Mollugin inhibits the inflammatory response in lipopolysaccharide-stimulated RAW264.7 macrophages by blocking the Janus kinase-signal transducers and activators of transcription signaling pathway. *Biol Pharm Bull* **36**(3): 399-406.

Zuker, M (2003) Mfold web server for nucleic acid folding and hybridization prediction. *Nucleic acids research* **31**(13): 3406-3415.

